DISSERTATION ZUR ERLANGUNG DES DOKTORGRADES
DER FAKULTÄT FÜR CHEMIE UND PHARMAZIE
DER LUDWIG-MAXIMILIANS-UNIVERSITÄT MÜNCHEN

A functional characterisation of the dimerisation motif in fibronectin, *in vivo* and *in vitro*

Josefine Gibson

aus Gladsaxe, Dänemark

2014

ERKLÄRUNG

Diese Dissertation wurde im Sinne von § 7 der Promotionsordnung vom 28. November 2011 von Herrn Prof. Dr. med. Reinhard Fässler betreut.

EIDESSTATTLICHE VERSICHERUNG

Diese Dissertation wurde eigenständig und ohne unerlaubte Hilfe erarbeitet.

München, 10. januar 2014

Josefine Gibson

Dissertation eingereicht am: 10. Januar 2014

1. Gutachterin/Gutachter: Prof. Dr. Reinhard Fässler
2. Gutachterin/Gutachter: Prof. Dr. Angelika Vollmar

Mundliche Prüfung am: 3. Juli 2014

The work presented in this thesis was conducted under the supervision of Prof. Dr. Reinhard Fässler at the Max Planck Institute of Biochemistry between June 2009 and December 2013.

1 TABLE OF CONTENTS

2 LIST OF ABBREVIATIONS

A	
aa	Amino acid
α	alpha
ALK	Activin receptor-like kinase
B	
β	beta
BCA	Bicinchoninic acid
BM	Basement membrane
bp/kpb	Base pairs / kilo base pairs
BSA	Bovine serum albumin
C	
C	Cysteine
Ca^{2+}	Calcium ion
Cas	Crk-associated substrate
Cdc42	Cell division cycle 42 homologue
cDNA	Complementary DNA
CHO	Chinese hamster ovary
cf.	Compare with
cFN	Cellular FN
Crk	Chicken Tumor Virus 10 regulator of kinase
D	
Da/kDa	Daltons / kilo Daltons
DAB	3-3' diaminobenzidine
DAPI	4', 6-Diamidin-2-phenylindol-dihydrochloride
DMEM	Dulbecco's Modified Eagle Medium
DNA	Deoxyribonucleic acid
DOC	Deoxycholate
Dock180	180 kDa protein downstream of Crk
E	
E	Embryonic day
ECM	Extracellular matrix
EIIIA/B	Extra fibronectin type III domain A or B
EDTA	Ethylenediaminetetraacetic acid
e.g.	For example
ERK	Extracellular signal-regulated kinase
ES cell	Embryonic stem cell
EtOH	Ethanol
F	
FACS	Fluorescence activated cell sorting
F-actin	Filamentous actin
FAK	Focal adhesion kinase
FBS	Fetal bovine serum
FGF	Fibroblast growth factor
FGFR	FGF receptor
FN	Fibronectin
FNI, II, III	Fibronectin type 1, 2 and 3 repeasts
G	
GAG	Glycosaminoglycan
GAP	GTPase activating proteins
GEF	Guanine nucleotide exchange factors
GDI	Guanine nucleotide-dissociation inhibitors
GFR	Growth factor receptor
GTP	Guanine triphosphate
H	
H&E	Hematoxylin and eosin
HLH	Helix-loop-helix
HRP	Horse radish peroxidase
I	
ICAM	Intercellular adhesion molecule
Id1	Inhibitor of DNA 1
i.e.	That is
IF	Immunofluorescence
ILK	Integrin-linked kinase
IP	Immunoprecipitation
L	
LAP	Latency-associated peptide
LTBP	Latent TGF-β binding protein
LLC	Large latent complex
M	
M	Molar
MadCAM	Mucosal vascular addressin cell adhesion molecules
MAPK	Mitogen-activated protein kinase
MLEC	Mink lunk epithelial cell
mM	Millimolar
mm	Millimetre
μm	Micrometre
MeOH	Methanol
mg	Milligram
Mg^{2+}	Magnesium ion
MEF	Murine embryonic fibroblast
MLC2	Myosin light chain 2
MT-MMP	Trans-membrane matrix metalloproteinase
mTOR(c)	Mammalian target of rapamycin (complex)
N	
nm	Nanometre
NMII	Non-muscle myosin II
P	
Pa/kPa	Pascals / kilo Pascals
PAK	p21-activated kinase 1
PAI-1	Plasminogen activator inhibitor 1
Par3	Partitioning defective 3
PBS	Phosphate-buffered saline
PCR	Polymerase chain reaction
PDGF-BB	Platelet-derived growth factor BB
PDGFR	PDGF receptor
PECAM-1	Platelet/endothelial cell adhesion molecule 1
PFA	Paraformaldehyde
pFN	Plasma FN
PH	Pleckstrin homology
PI3K	Phosphoinositide 3-kinase
pI:C	Polyinosinic:polycytidylic acid
PIP_2	Phosphatidylinositol (4,5)-bisphosphate
PIP_3	Phosphatidylinositol (3,4,5)-trisphosphate
PMSF	Phenylmethylsulfonyl fluoride
PODXL	Podocalyxin
PSHRN	Pro-Ser-His-Arg-Asn
PTEN	Phosphatase and tensin homolog
pY	Phosphorylated tyrosine residue
R	
Rac	Ras-related C3 botulinum substrate
RGD	Arg-Gly-Asp
RIPA	Radio Immuno Precipitation Assay
RNA	Ribonucleic acid
ROCK	Rho kinase
S	
S	Serine
SDS	Sodium dodecyl sulfate
SDS-PAGE	SDS-polyacrylamide gel electrophoresis
SFK	Src family kinase
SLC	Small latent complex
T	
Taq	*Thermophilus aquaticus*
TBS	Tris-buffered saline
TGF-β	Transforming growth factor-β
TGF-βR	TGF-β receptor
Tris	Tris/hydroxymethyl) aminomethane
V	
VCAM	Vascular cell adhesion molecule
VE-cadherin	Vascular endothelial cadherin
VEGF-A	Vascular endothelial growth factor A
VEGFR	VEGF receptor
v-region	Variable region
vSMC	Vascular smooth muscle cell
W	
WT	Wild type

3 SUMMARY

Fibronectin (FN) is a vertebrate-specific high-molecular-weight glycoprotein that is deposited into the extracellular matrix by virtually all cell types and is secreted into the blood plasma by hepatocytes. Effectively all FN is secreted as globular and dimerised molecules. Dimerisation of FN molecules is mediated by disulfide bonds between two pairs of C-terminal cysteine residues; this pair of cysteines constitutes the FN dimerisation motif. Cells adhere to FN through integrin cell surface receptors. The main FN-binding integrins are integrins $\alpha5\beta1$ and $\alpha V\beta3$. The ability of integrins to bind specific integrin-binding motifs in FN not only facilitates cell-anchorage to a FN substrate, but also facilitates a fundamental step in the conversion of soluble, globular FN into an insoluble, fibrillar matrix. FN fibrillogenesis, the assembly of a fibrillar fibronectin matrix, is crucial because the fibrillar form of FN is the biologically active form that allows FN to serve as a master scaffolding protein among the extracellular matrix proteins and to regulate growth factor bioavailability. A dogma of FN fibrillogenesis, originating from early studies of FN fibrillogenesis examined *in vitro* (Schwarzbauer, 1991), dictates that FN dimerisation is an absolute requirement for FN fibrillogenesis and hence FN function.

The aim of this PhD project was to characterise the function of the FN dimerisation motif *in vivo*. The strategy was to address the requirement for FN dimerisation with a mouse model carrying mutant FN alleles in which the two critical cysteine residues of the dimerisation motif were mutatated to serine residues ($FN^{CC>SS/CC>SS}$).

The main findings of this study are (1) the $FN^{CC>SS}$ knock-in mutation causes recessive embryonic lethality in mice, (2) $FN^{CC>SS/CC>SS}$ mouse embryos die between E9.5 and E11.5, (3) embryonic lethality is most prominently associated with severe remodelling defects of the cardiovascular system, affecting both embryo proper and extraembryonic tissue and (4) monomerised $FN^{CC>SS}$ is assembled into a fibrillar extracellular matrix, which is, however, macroscopically distorted and compromises the mechanical properties of the associated extracellular matrix. However, neither integrin signalling nor migration speed of fibroblasts on ECM platforms are affected by the presence of $FN^{CC>SS}$ matrix. Furthermore, (5) $FN^{CC>SS}$ disrupts the fibrillar morphology, but not the protein level, of latent TGF-β binding protein 1 deposited in the extracellular matrix, but (6) does not affect the storage capacity of the extracellular matrix transforming growth factor-β storage or the abilty of integrin $\alpha V\beta6$ to release transforming growth factor-β from the extracellular matrix, and, finally, (7) neither does $FN^{CC>SS}$ affect the levels of vascular endothelial growth factor receptor signalling in embryonic tissue.

With this study, I demonstrate that monomerised $FN^{CC>SS}$ is assembled into a fibrillar matrix both *in vivo* and *in vitro*, but that this monomerised $FN^{CC>SS}$ matrix retains partial functionality of dimeric FN *in vivo*. Dimerisation of FN is required to establish robust structural and mechanical features of the resulting fibrillar matrix. Although cardiovascular remodelling defects suggest malfunction of integrin function and/or growth factor bio-unavailability, these features of the $FN^{CC>SS}$ matrix do not appear to affect integrin function or the ability of the ECM to regulate growth factor bioavailability.

4 INTRODUCTION

4.1 Cell adhesion and the extracellular matrix

The ability of cells to adhere to each other and to their immediate environment is a fundamental aspect of multi-cellular organisation and order among the Metazoa. With the evolution of complex multicellular organisms, individual cells were required to specialise in function. As part of a coordinated effort to propagate the survival of the organism, individual cells had to both create and interact with a specialised microenvironment of other cells and non-cellular components. Cell adhesion to each other and the extracellular matrix (ECM) are fundamental to basic cellular and tissue function. These processes guide cellular migration, regulate differentiation and define the spatial dimensions and physical limits of higher-order structures. Equally important for the benefit of the multicellular organism is strict adherence to a developmental programme that avoids dysplastic growth. For example, the survival of many cell types depends critically on contacts they make with each other and the (ECM), and without anchorage, these cell types undergo anoikis (Frisch and Francis, 1994). Thus, cell adhesion is fundamental to the propagation and protection of multicellular organisms.

The mechanical integrity of tissues is crucial to its homeostasis and is established through the interconnection of cytoskeletal networks and ECM through cell-cell junctions and cell-matrix adhesions. By providing a highly interconnected extracellular scaffold, the ECM is responsible for much of this mechanical integration. The ECM is an acellular, insoluble protein- and carbohydrate-based microenvironment, in which composition, supramolecular organisation and degree of intramolecular and intermolecular crosslinking create the properties that provide physical cues to cells and structural integrity to tissues. Importantly, cells create their own ECM by secreting and coordinating the deposition and arrangement of all components of the ECM. While most cells types express ECM proteins, the types and amounts of ECM typically relate to the function of the cell and tissue. Each of the various components of the ECM, including glycoproteins, proteoglycans and, in the case of bone, mineral deposits, confers a specific property to the ECM. The fibrous ECM proteins, including collagen, elastin, fibronectin and laminin, form highly fibrillar and cross-linked matrices that confer tensile strength and flexibility to tissues, but also have adhesive functions. The proteoglycans and their respective glycosaminoglycan chains represent a second major class of ECM components that are higly hydrated, fill cell-free spaces and resist compressive forces. In addition to structural and mechanical integrity, the ECM provides instructive information. Many ECM glycoproteins are recognised by cell surface receptors and allow cells to adhere to and move directionally along ECM. Also, both glycoproteins and proteoglycans within the ECM bind specific paracrine growth factors, such as fibroblast growth factor (FGF), vascular endothelial growth factor A (VEGF-A) and transforming growth factor β (TGF-β), and thereby regulate their bioavailability in space and time. All these functions make the ECM an important regulator of developmental and regenerative processes. The ECM is a dynamic compartment, as the proteins and carbohydrates within are continuously

remodelled, both in response to developmental signals and mechanical stimuli, and this dynamic behaviour is fundamental to developing, shaping and maintaining tissue (Aszódi et al., 2006).

Whether a sponge or a mammal, the ability of a cell to adhere to the ECM relies on cell surface receptors that allow cells to recognise, bind, manipulate and respond to the ECM. Therefore, in addition to composition, quantity and architecture of ECM components, the profile of cell surface receptors that bind ECM proteins are fate-determining factors in cell-ECM adhesion, cell behaviour and tissue homeostasis.

4.2 The integrin family of adhesion receptors

The integrin family of adhesion receptors represents a major class of metazoan cell surface receptors involved in cellular adhesion to the ECM, and in certain cases in vertebrates, to each other (Hynes, 2002b). In doing so, integrins play key roles in fundamental biological processes by integrating cell migration, differentiation, growth and apoptosis. Consequently, integrins are important regulators of diverse biological processes, such as development, the immune response, leukocyte trafficking and hemostasis, but are also implicated in diseases including artherosclerosis, autoimmune diseases and cancer.

4.2.1 The integrins and their ligands

Integrins are heterodimeric type I transmembrane proteins that arise through non-covalent association of integrin α and β subunits. These integrin α and β subunits are modular proteins, each of which has a large extracellular domain, a single transmembrane α-helix and a short (10-70 amino acid) cytoplasmic domain (this is true for all subunits except the β4 subunit, which has large cytoplasmic domain of 1072 residues). The mammalian genome encodes eighteen α subunits and eight β subunits, which combine into twenty-four distinct αβ heterodimeric integrins (Hynes, 2002b). Alternative splicing of integrin transcripts and their tissue-specific expression patterns add further complexity to the map of integrins. The combination of α and β chain determines both ligand and signalling specificity of the integrin. However, while some integrins are specific in their recognition of ligands, others are promiscuous; hence there exists significant redundancy in ligand-recognition, i.e. various integrins will recognise the same ligand, and some integrins recognise more than one ligand.

Generally, integrins are classified into four clusters with respect to ligand-specificity (fig 1). Three of these clusters represent ECM-binding integrins: (i) the collagen-binding integrins, (ii) the laminin-binding integrins and (iii) the integrins that recognise ECM molecules that contain and display an arginine-glycine-aspartate (RDG) motif, such as fibronectin, vitronectin, LAP-TGF-β, tenascin, osteopontin and thrombospondin in vertebrates (Humphries, 2006) and tiggrin in *Drosophila* (Hynes, 2002b). The fourth cluster of integrins does not interact with ECM molecules, but recognises cellular counter receptors and thus participates in cell-cell adhesion. These are leukocyte-specific integrins, that bind intercellular adhesion molecules (ICAMs), vascular cell-adhesion molecules (VCAMs) and mucosal vascular addressin cell adhesion molecules (MadCAMs) and are thereby paramount to cell-cell interactions in the hematopoetic system.

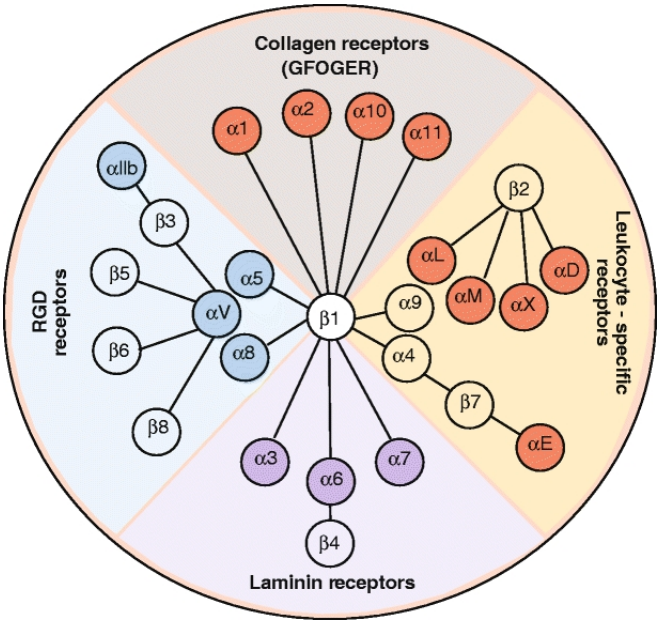

Figure 4.1. The mammalian family of integrin adhesion receptor heterodimers. Adapted from (Barczyk et al., 2009).

4.2.2 Integrin activation

Integrins are inserted into the plasma membrane in an inactive state that have low affinity for extracellular ligands and are thus unable to bind ECM or cellular counter-receptors. Integrins are rendered inactive by a closed structural conformation that is enforced by (1) the clasping of the α and β subunit tails through both electrostatic and hydrophobic interactions (Vinogradova et al., 2000; Vinogradova et al., 2002), (2) a coiled-coil interaction between transmembrane domains of both α and β subunits (Gottschalk, 2005) and (3) the bending of the extracellular domains (Xiong et al., 2001) (fig. 4.2). Upon activation, integrins signal bidirectionally across the plasma membrane. An extracellular stimulus, such as the binding of an extracellular ligand to integrins, induces intracellular signalling (outside-in signalling), while intracellular signals induced by integrin-independent events can also promote signalling cascades that alter the ligand-binding activity of integrins and cause extracellular changes (inside-out signalling). Hence, the determining events of integrin activation are conformational changes induced by the binding of either an extracellular ligand (outside-in signalling) or cytoplasmic proteins (inside-out signalling) and generally involve unclasping of the α and β integrin cytoplasmic tails (Kim et al., 2003) and extension of the integrin extracellular domains (Zhu et al., 2007) (fig. 4.2).

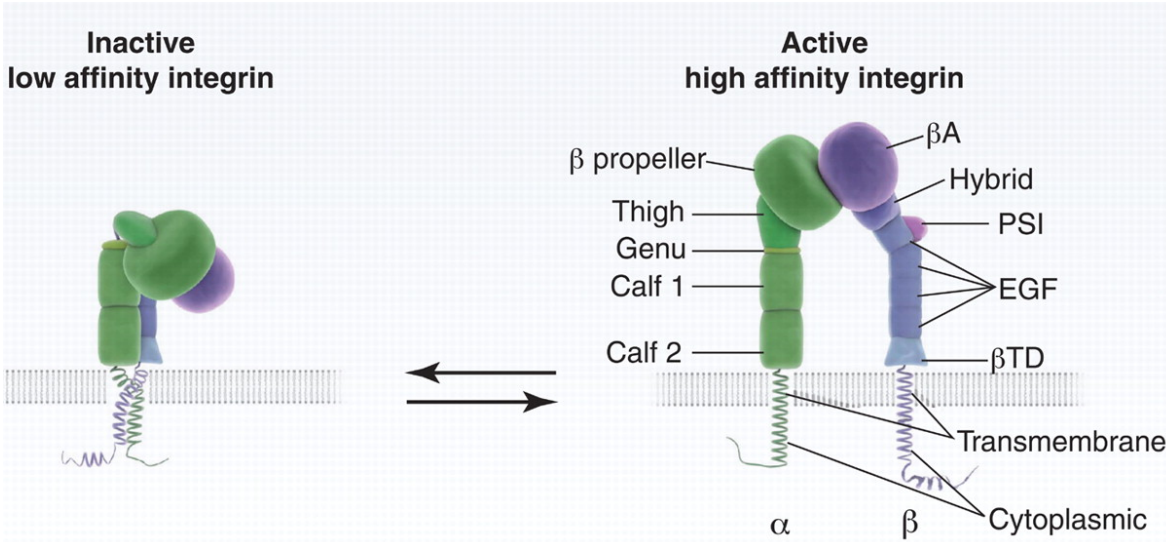

Figure 4.2. Diagrammatic representation of the integrin heterodimer the conformational changes that are associated with integrin activation. The α integrin subunit is shown in green and the β is shown in purple. The integrin heterodomer consists of a ligand-binding head domain formed of the β propeller of the α integrin subunit and the hybrid and βA domains of the β integrin subunit. The βA domain contains Mg^{2+} and Ca^{2+} binding sites essential for ligand binding. The ligand-binding head domain rests on both α and β integrin subunit ectodomains. Specific contacts between the ectodomains, transmembrane domain and cytoplasmic domains keep the integrin in a bent conformation, which is inactive. Integrin activation occurs with the separation of the ectodomains, transmembrane and cytoplasmic domains and an extension of the integrin conformation. Adapted from (Moser et al., 2009b).

The talins and kindlins are key intracellular integrin activators. Inside-out signalling promotes the translocation of talin and kindlin to integrin complexes where they drive integrin activation by binding the β integrin cytoplasmic tails at membrane-proximal and -distal NPxY motifs, respectively, and by promoting the unclasping of the α and β integrin cytoplasmic tails (Calderwood et al., 2002; Jiang et al., 2003; Shi et al., 2007; Ma et al., 2008; Montanez et al., 2008; Moser et al., 2008; Ussar et al., 2008; Moser et al., 2009a). Kindlins are proposed to aid talin in inducing conformational changes that switch the integrins from a bent, inactive and low-affinity state to an extended, active and high-affinity state that exposes the ligand-binding site (Xiao et al., 2004; Luo et al., 2007; Montanez et al., 2008; Moser et al., 2008) (not sure if these references actually show that kindling promotes this conformational change; Shi and Ma demonstrate that it activates integrins. The effect of talin and kindlin on integrin activation relies on their ability to interact with phosphoinositides (this might be an exaggeration, PIP binding is not necessary for integrin activation) in the plasma membrane (Saltel et al., 2009; Qu et al., 2011; Liu et al., 2011). Local increases in phosphatidylinositol (4,5)-bisphosphate (PIP_2) synthesis at the leading edge of cells or within focal complexes creates PIP_2-rich lipid rafts that serve as docking sites for talin and kindlin, which, upon binding PIP_2, undergo conformational changes that allow them to bind β integrin tails and capture both vinculin and F-actin filaments (Humphries et al., 2007; Goksoy et al., 2008; Saltel et al., 2009; Legate et al., 2011) (nb PI binding is required for kindlins to activate integrins, but there is no evidence that PIPs induce conformational changes in kindlin. PIPs most likely disrupt the autoinhibitory interaction between the talin head and rod). An additional possibility is that activators are needed to displace inhibitors of integrin activation, such as sharpin (Rantala et al., 2011) and integrin cytoplasmic domain-associated protein-1 (ICAP-1) (Bouvard et al.,

2003; Shattil et al., 2010) (nb latter ref is review). However, the crosstalk mechanisms between talin and kindlin is still an active field of investigation, and it remains unclear if talin and kindlin function sequentially or simultaneously (Moser et al., 2009b) (fig. 4.3), although recent work shows that both adaptor proteins can bind the β integrin tail simultaneously (Bledzka et al., 2012) (nb because they don't bind the same sequence). A recent report addressing the role of phosphoinositides in integrin activation shows that kindlin accumulates at newly forming focal adhesions at a higher rate than talin (Legate et al., 2011), which suggests that kindlin is either always associated with the plasma membrane or arrives at focal adhesions first and is followed by talin, although neither talin nor kindlin play a direct role in the recruitment of the other partner (Kahner et al., 2012; Bledzka et al., 2012).

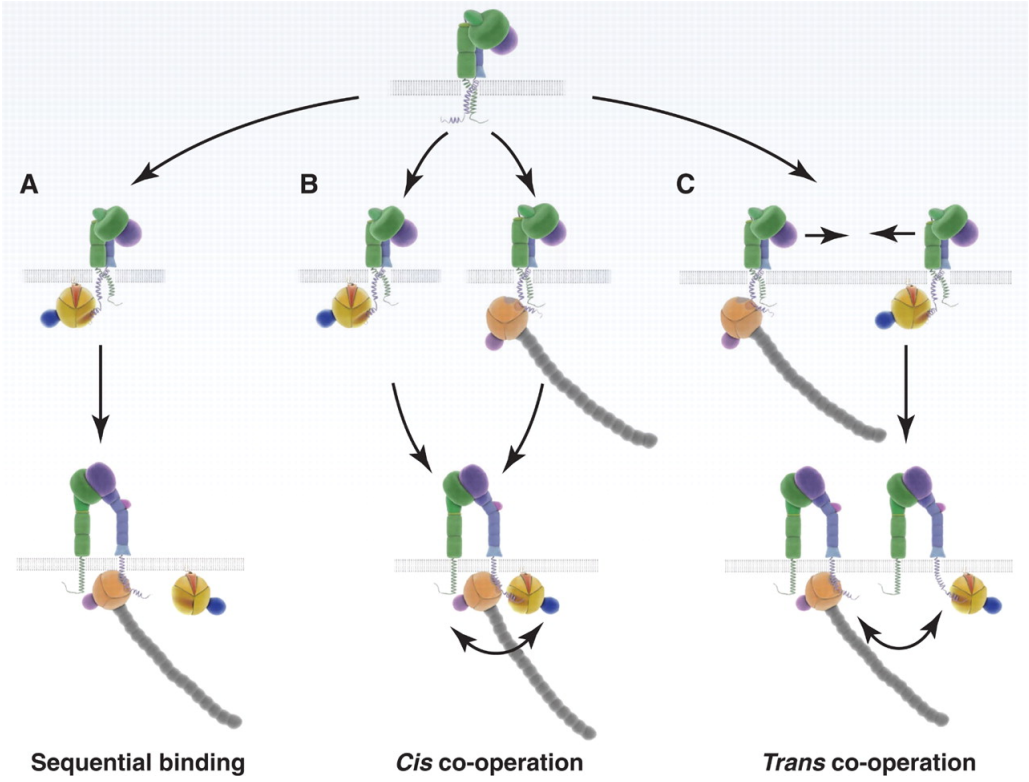

Figure 4.3. Three possible modes of integrin activation by talin and kindlin. (A) In the model for sequential binding, kindlin binding to the membrane distal NxxY motif in β integrin subunit tails facilitates talin binding to the same membrane proximal NPxY and concomitant displacement of kindlin and integrin activation. (B) Simultaneous binding in cis of kindlin to the membrane distal NxxY motif and binding of talin to the membrane proximal NPxY motif in β integrin subunit tails could facilitate integrin activation. (C) Cooperation of kindlin and talin bound to β integrin subunit tails in trans is speculated as a means of seeding integrin clusters. Adapted from (Moser et al., 2009b).

The initial contact between an active integrin and an extracellular ligand, such as FN, leads to the formation of nascent adhesions. Nascent adhesions form in the lammelipodium, which is a zone of membrane protrusion at the leading edge of the cell that is projected forward by the continuous creation of new mesh-like actin networks (Alexandrova et al., 2008; Choi et al., 2008) (fig. 4.5). These early integrin complexes are inherently unstable and transient structures. To persist, the integrin-ECM bond must be reinforced and the integrin adhesion complex must undergo further maturation. Upon activation, integrins undergo conformational changes that expose docking sites within the β integrin tail that allow the allosteric recruitment of cytoplasmic proteins. Almost all β integrin tails contain two

conserved docking sites consisting of a membrane-proximal NPxY motif and a membrane-distal NxxY motif (where x represents any amino acid), which serve as docking sites for phosphotyrosine-binding domain-containing adaptor proteins, such as talin (Calderwood et al., 2003; Legate and Fässler, 2009). Unlike the integrins themselves, these newly recruited adaptor proteins have scaffolding, enzymatic or F-actin-binding and -regulating activity. Together, these adaptor proteins build adhesion structures that function both as biochemical signalling hubs and mechanical links between the ECM and the cytoskeleton.

A distinctive feature of integrins in cell-ECM complexes is their tendency to cluster and assemble in a hierarchical manner (Miyamoto et al., 1995; Carman and Springer, 2003; Zaidel-Bar et al., 2004). Through the progressive clustering of hundreds or even thousands of activated integrins, adaptor proteins and actin filaments, collectively referred to as the integrin "adhesome" (Zaidel-Bar et al., 2007), integrin adhesion complexes mature into large and powerful adhesome-associated signalling hubs, referred to as focal adhesions. Focal adhesions exist in various sizes and stages of maturation. Despite the continuum of maturation stages, the ultrastructural architecture of all focal adhesions is uniform; an approximatly fourty nanometre thick core of focal adhesion proteins arrange vertically between the membrane-bound integrin and the actin stress fibre, forming distinct functional layers of signalling proteins, force-transducing proteins and actin-regulating proteins (Kanchanawong et al., 2010) (fig. 4.4).

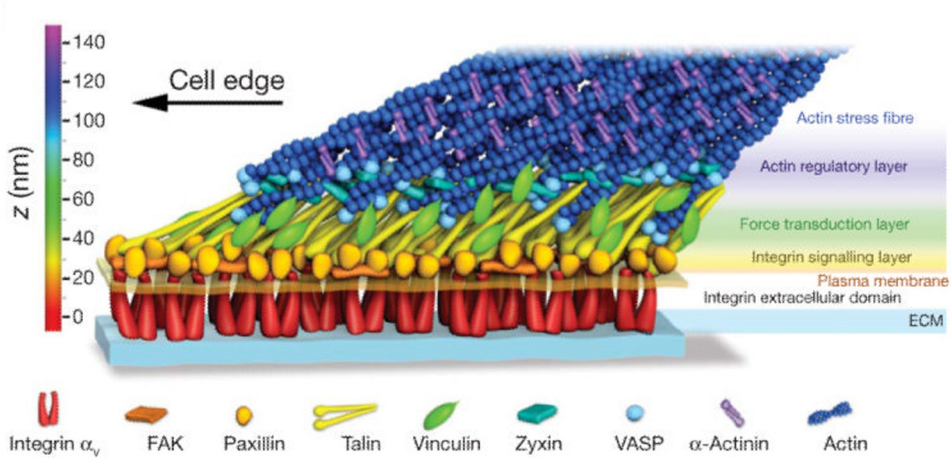

Figure 4.4. The nanoscale architecture of focal adhesions. The protein positions, but not the protein stoichiometry, in this model were experimentally determined. Adapted from (Kanchanawong et al., 2010).

Mechanical coupling of integrins, such as integrin α5β1, to the actin cytoskeleton is a key step in reinforcing the integrin adhesion complex (Friedland et al., 2009) and enables the cell to perform work on its extracellular environment (Li et al., 2005a; Legate et al., 2009). The earliest points of mechanical coupling between the integrins, the actin cytoskeleton and extracellular ligand are within focal complexes that develop from nascent adhesions at the transition zone between the lamellipodium and the lamellum (Choi et al., 2008) (fig. 4.5). The initial link between integrins and the cytoskeleton following integrin activation relies on the adaptor function of talin to form a slip bond between the integrin β tail and F-actin, which allows the very first application of cytoskeleton-generated force to the

extracellular ligand (Jiang et al., 2003). Vinculin binds both talin and actin and thereby cross-links and stabilises the talin–actin interaction (Gallant, 2005; Humphries et al., 2007) nb! not sure why Gallant was added here, while the presence of the large paxillin molecule provides an assembly platform for subsequent waves of focal adhesion adaptor proteins (Laukaitis et al., 2001; Digman et al., 2008) Zaidel-Bar 2007 phospho-paxillin study would have been good to add here. Incorporation of α-actinin into the integrin adhesion complex promotes the organisation, stabilisation and strengthening of the link between integrins and the cytoskeleton by cross-linking F-actin filaments (Brown et al., 2006; Choi et al., 2008). A core scaffolding ternary protein complex consisting of integrin-linked kinase (ILK), PINCH and parvin (termed the IPP complex) assists in the mechanical coupling of integrins to the actin cytoskeleton in effect of ILK binding integrins β tails directly and parvin interacting with F-actin (Legate et al., 2006; Wickström et al., 2010). The kindlins also participate in the mechanical coupling of integrins to the actin cytoskeleton through their direct binding to integrin β tails (β1 and β3) and by interacting with F-actin either through the IPP complex or through a complex of migfilin and filamin (Tu et al., 2003; Moser et al., 2008; Montanez et al., 2008; Ussar et al., 2008). Fine-tuning the stability of the integrin-actin linkage within focal complexes is in part achieved by focal adhesion kinase (FAK) (Ilić et al., 2004), which has both scaffolding and signalling functions.

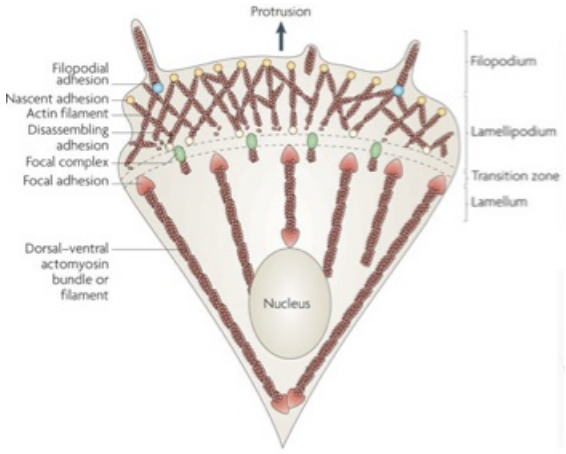

Figure 4.5. A schematic representation of the adhesion structures in a migrating cell. Nascent adhesions form in filopodial and lamellipodial protrusions at the cell front. Maturation of nascent adhesions to focal complexes and focal adhesions occurs in the transition zone between the lamellipodium and lamellum and with the mechanical coupling of integrins to cross-linked actin filaments. Focal adhesions are stabilised and grow upon contractile force exerted on integrins by actomyosin filaments. Adapted from (Parsons et al., 2010).

Filaments of F-actin connected to adhesion complexes are under tension in effect of pulling by non-muscle myosin II (NMII) molecular motors that associate with the actin cytoskeleton (actomyosin) and are as such referred to as stress fibres. Along with α-actinin, NMII plays an important role in the maturation of focal adhesions and the stability of actomyosin stress fibres that become connected to focal adhesions (Even-Ram et al., 2007; Choi et al., 2008) (fig. 4.5). The dynamic behaviour of the actomyosin machinery is regulated by the RhoA GTPase family and its effectors (Chrzanowska-Wodnicka and Burridge, 1996). In the context of actin cytoskeleton dynamics, the prominent members of the Rho GTPases family are RhoA, Rac1 and Cdc42, as they are general

regulators of actin cytoskeleton remodelling in response to mechanical stimuli. As a GTPase, each member cycles between an active, GTP-bound state and an inactive, GDP-bound state (fig. 4.6). This cycle is regulated through the joint effort of guanine nucleotide exchange factors (GEFs), GTPase-activating proteins (GAPs) and guanine nucleotide-dissociation inhibitors (GDIs). GEFs and GAPs of RhoA family proteins are among the many proteins that are recruited to and activated at focal adhesions (Jaffe and Hall, 2005).

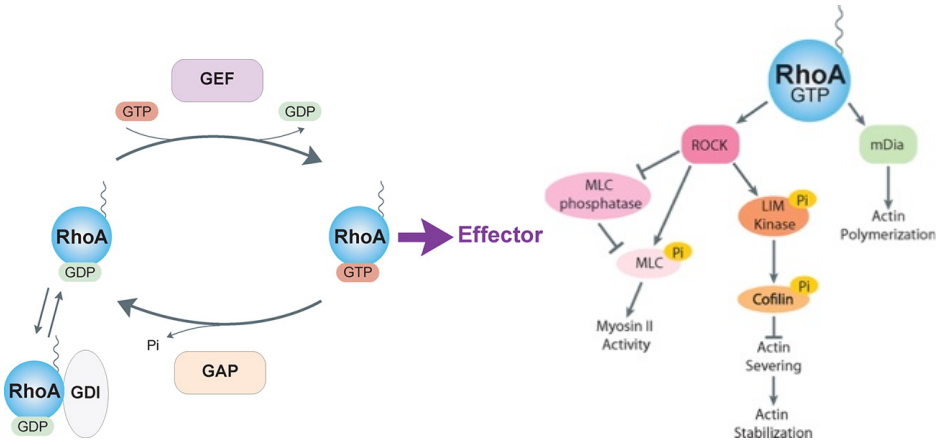

Figure 4.6. Schematic representation of the RhoA cycle and RhoA effector signalling. Left: As a GTPase, RhoA cycles between an inactive GDP-bound form and an active GTP-bound form. The exchange of GDP for GTP, i.e. activation, is catalysed by the GEFs, while the GAPs stimulate intrinsic GTPase activity and thereby inactivate RhoA. The GDIs sequester RhoA in its GDP-bound state and prevents RhoA activation. Right: In its active form, RhoA interacts with multiple cytoplasmic effectors that promote actomyosin contractility and actin polymer stability. Adapted from (Lessey et al., 2012).

In its active state, RhoA interacts with a number of effectors, one of which is the Rho kinase (ROCK1 and ROCK2 in mammals) (fig. 4.6). ROCK enhances NMII activity by promoting phosphorylation of the regulatory light chain of NMII, both by (i) directly phosphorylating and activating the regulatory myosin light chain subunit of NMII (MLC, also known as myosin regulatory light chain) (Amano et al., 1996) and (ii) phosphorylating and inactivating MLC phosphatase (Kimura et al., 1996; Totsukawa et al., 2000) (nb – Totsukawa shows that MLCK in the cell periphery phosphorylates MLC. Phosphorylation of MLC at serine 19 has an activating effect on the ability of NMII to interact with actin and thereby contract and bundle F-actin stress fibres. ROCK also stabilises F-actin filaments by phosphorylating and thereby activating LIM kinase, which in turn phosphorylates and inactivates the actin-severing activity of cofilin (Maekawa, 1999; Ohashi, 2000). An additional effector of RhoA is the mDia1 formin, an actin nucleation factor that cooperates with ROCK to build stress fibres (Watanabe et al., 1999; Li and Higgs, 2003) (fig. 4.6). In response to biochemical signals from the focal adhesion through the RhoA/ROCK axis, NMII and α-actinin cross-link and bundle F-actin filaments and thereby promote the clustering of both actin-binding adhesion components and integrins. Hence, biochemical signals through the RhoA/ROCK axis changes the dynamics of the contractile actinmyosin in response to new sites of adhesion, generating mechanical forces that will allow the cell to stabilise its adhesion sites, migrate in a polarised fashion and, as I shall describe in a subsequent chapter, modulate the fibrillar architecture of the ECM (Yoneda et al., 2005; Yoneda et al., 2007) inappropriate to use yoneda 2005 – talks only bout functional diff betw rock 1 and 2.

While the generation of contractile force by NMII is not required for nascent adhesion formation, the transmission of mechanical force through integrins may drive the maturation of the integrin adhesion complex (Stricker et al., 2013). For example, the interaction dynamics of integrin α5β1 integrins with FN is based on catch bond behaviour, which implies that the lifetime of the integrin-FN interaction is increased with the application of force to the bond (in the force range of 10–30 pN)(Kong et al., 2009). Also, integrin α5β1 is known to transition from a relaxed to a tensioned state in response to force transduction, inducing a molecular switch in the integrin-FN interface that allows the α5 integrin subunit to engage with the synergy motif in FN and strengthen the integrin-FN interaction (Friedland et al., 2009). NMII-dependent tension also brings about dramatic changes in the protein profile of the integrin adhesion complex, which serves to mature the adhesion complex (Kuo et al., 2011; Schiller and Fässler, 2013). However, the attachment of integrins to F-actin cytoskeleton is not only critical to the formation of focal adhesions. By virtue of this association with the actin cytoskeleton, integrin-based adhesions can confer to the cell both biochemical, physical and topographical information about the immediate microenvironment (Geiger et al., 2009). Given the dynamic and highly responsive nature of the actin cytoskeleton in terms of polymerisation and actomyosin contraction, environmental sensing by integrins gives the cell the ability to rapidly adjust its cytoskeletal organisation, and hence its shape and motility, which is the basis by which integrins facilitate cell adhesion, spreading and migration.

Even after integrins have reached full activation within a focal adhesion, adhesion complexes remain highly dynamic in structure and molecular composition. Some cell types, like fibroblasts, have very dynamic cell-matrix adhesion complexes, and when anchored to two-dimensional substrates, integrin α5β1-containing focal adhesions are remodelled into a structurally and functionally distinct class of cell-matrix adhesions called fibrillar adhesions (Katz et al., 2000; Pankov et al., 2000; Zamir et al., 2000). Fibrillar adhesions differ from focal adhesions in their location and morphology; rather than dots at the cell periphery, which is typical for focal adhesions, fibrillar adhesions are elongated fibrils or arrays of dots distributed in more central areas under the cells.

The formation of fibrillar adhesions was originally described using pulse-chase experiments with antibodies targeting the active conformations of integrins (Pankov et al., 2000). Yamada and colleagues demonstrated that once a cell anchors to an ECM substrate and the αVβ3- and α5β1-containing focal adhesions have matured, integrin α5β1 segregates from the medial end of a mature focal adhesion and translocates centripetally from the lamellae towards the cell body, forming the streak-like adhesion complexes that were termed fibrillar adhesions (Pankov et al., 2000). These fibrillar adhesions are devoid of focal adhesion components such as vinculin and paxillin, and instead acquire tensin (Zaidel-Bar et al., 2003) nb this reference is inappropriate. Tensin couples integrins to actin via minimum two actin-binding domains in the N-terminus and acts as a cross-linker between these integrins and actin during during translocation (Lo et al., 1994). Although the rate of translocation differs depending on cell type (Pankov et al., 2000; Zamir et al., 2000), the translocation of integrin α5β1 is always driven by stress fibre contractility generated by the same actomyosin machinery that was required to stabilise focal adhesions (Pankov et al., 2000; Zamir et al., 2000). It will become clear in subsequent chapters

that the formation of fibrillar adhesions is a particularly interesting phase of adhesion complex maturation and dynamics because it involves FN organisation and remodelling (Pankov et al., 2000).

4.2.3 Integrin signalling

In the context of cell adhesion, integrins are just as important as signal transduction receptors as they are adhesion receptors. Integrin cell-matrix adhesions are highly active signalling hubs, and importantly, integrin signalling does not occur in isolation, but crosstalks with growth factor receptor (GFR)-induced signalling pathways to fine-tune the chemical and mechanical integration of the cell within their extracellular milieu.

Important examples of integrin-GFR crosstalk are the integrin-mediated transactivation of receptor tyrosine kinases such as FGF receptor (FGFR), epithelial growth factor (EGFR), platelet-derived growth factor (PDGFR) and VEGF receptor (VEGFR), which, in turn, are known to amplify an integrin signal (Sundberg and Rubin, 1996; Moro et al., 1998; Zou et al., 2012). For example, the simultaneous activation of integrins and GFR, such as EGFR and PDGFR, prolongs and intensifies the activation of extracellular signal-regulated kinase (ERK) within the mitogen-activated protein kinase (MAPK) signalling pathway, to an extent that is not seen with GFR activation alone (Miyamoto et al., 1996; Roovers et al., 1999). Also VEGF receptor (VEGFR) signalling in endothelial cells is most potent when integrins are activated (Soldi et al., 1999).

Receptor crosstalk is facilitated by the transient complex formation between integrins, GFR and their respective adaptor scaffolding proteins and signalling kinases. For example, at early stages of integrin-mediated adhesion of EGF-stimulated fibroblasts, macromolecular complexes form between integrins, EGFR, the adaptor protein p130 Crk-associated substrate (p130Cas) and the c-Src kinase (Moro et al., 2002). Studies like this suggest that a substantial part of integrin-mediated signal tranduction actually could be mediated by integrin-transactivated GFR, as exemplified by the requirement for EGFR activation for integrin-mediated cell adhesion (Marcoux and Vuori, 2003).

At the very early stages of integrin activation, Src and FAK cooperate to initiate a variety of biochemical signal transduction pathways. Src is a member of the Src family kinase (SFK) non-receptor tyrosine kinases, whose kinase activity is regulated by phosphorylation of a number of internal tyrosines and are recruited to and activated at nascent adhesions. FAK is an early component of the integrin adhesion complex, acting both as a scaffolding protein and a signalling protein (Kim and Kim, 2008) (this reference seems inappropriate, it's about dynamics of FAK phosphoryl.). FAK responds to activated integrins by auto-phosphorylating a tyrosine residue (Tyr 397), which creates a docking site for SH2 domains in Src, allowing Src to bind FAK and phosphorylate additional tyrosine residues, which overall serve to enhance the signalling potential of the Src-FAK complex (Schaller et al., 1994; Schlaepfer et al., 1994; Calalb et al., 1995; Calalb et al., 1996; Thomas et al., 1998).

The Ras-MEK-MAPK pathway is a significant signal transduction pathway downstream of the activated Src-FAK complex and is necessary for cellular responses to both activated GFRs and integrins. There are multiple points of convergence between GFR/RTK and integrin signalling. One point of intersection between activated integrins and EGFR occurs at the level of Raf1, the

phosphorylation of which is required for downstream phosphorylation of ERK (Edin and Juliano, 2005). Another point of convergence occurs at p21-activated kinase 1 (PAK1), which phosphorylates MEK and thereby drives the Ras-MEK-MAPK signalling pathway (Slack-Davis et al., 2003). ERK phosphorylation modulates focal adhesion dynamics through MLCK-mediated stress fiber organisation, but is also necessary for protein synthesis, cell cyle progression and cell proliferation (Treisman, 1996; Webb et al., 2004; Walker et al., 2005).

A second signalling pathway that is regulated by the Src-FAK complex, and which is of major importance to the pro-survival effects of integrin activation, involves the serine-threonine kinase Akt (also known as protein kinase B, PKB). Upon integrin activation, the autophosphorylation of FAK (at Tyr 397) provides a docking site for the SH2 domain of the p85-regulatory subunit of phosphoinositide 3-kinase (PI3K) and thereby recruits PI3K to focal adhesions (Chen et al., 1996). PI3K catalyses the deposition of phosphoinositide-3,4,5-P3 (PIP_3) lipids into the plasma membrane surrounding focal adhesions. This local increase in PIP_3 concentration recruits proteins with plekstrin-homology (PH) domains to the focal adhesion, and among these proteins are the PIP_3-dependent kinase 1 (PDK1) and Akt. Bringing Akt and PDK1 within close proximity of each other allows PDK1 to phosphorylate and activate Akt (King et al., 1997; Vanhaesebroeck and Alessi, 2000). Complete activation and substrate specificity of Akt requires further phosphorylation by mammalian target of rapamycin (mTOR) kinase as part of the mTOR complex 2 (mTORC2) (Guertin et al., 2006; Ikenoue et al., 2008). It is possible that mTOR is brought to the focal adhesion by ILK (McDonald et al., 2008). Akt activation affects a number of cellular responses, and one major consequence of Akt activation is the suppression of apoptosis pathways (Kennedy et al., 1997; Downward, 1998; Brunet et al., 1999). PI3K has also been shown to be required for the activation of the Ras-Raf1-MEK-MAPK signalling pathway, most probably downstream of Ras and upstream of Raf1 (King 1997).

Within focal adhesions, FAK also regulates focal adhesion turnover and cell migration by recruiting and phosphorylating p130Cas (Cary et al., 1998). This initiates the recruitment of a series of adaptor proteins (involving adaptor protein Crk (Chicken Tumor Virus 10 regulator of kinase) and the Rac GEF Dock180 (180 kDa protein downstream of Crk)) that lead to the activation of the small GTPase Rac1 at the plasma membrane to promote actin cytoskeletal rearrangements and focal adhesion turnover in preparation for cellular adhesion and migration (Kiyokawa et al., 1998) (nb this ref doesn't refer to ELMO). FAK also associates with p190RhoGEF to stimulate RhoA activity and promote actin cytoskeleton contractility (Zhai et al., 2003).

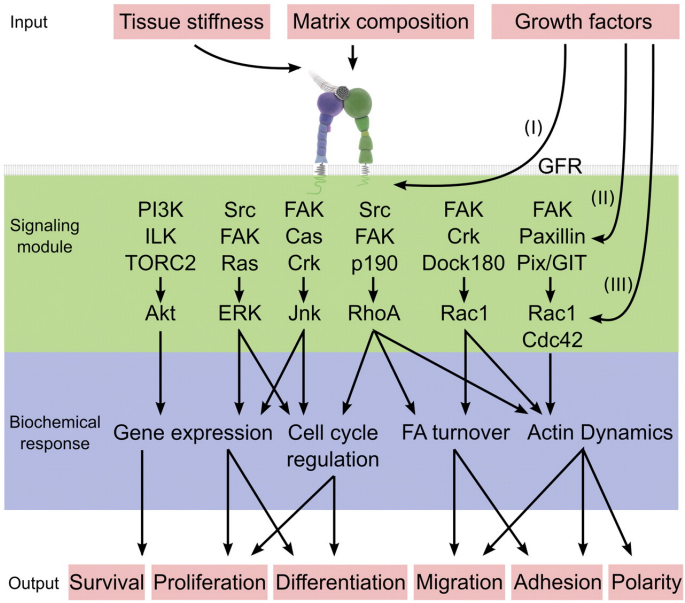

Figure 4.7. Integrin outside-in signalling elicits multiple biochemical signalling pathways that ultimately lead to changes in gene expression. Integrin outside-in signals are generated in response to extracellular mechanical properties and biochemical composition. These integrin-mediated signals are integrated with growth factor-mediated signals to fine-tune the cellular response to microenvironmental cues. Adapted from (Legate et al., 2009).

The composition of integrin-bound proteins affects the signalling properties of the integrin complex. As outlined above, some biochemical signalling pathways downstream of integrin adhesions have been characterised. Given that integrins interact with hundreds of different molecules, the adhesome signalling network becomes very complex. Biochemical signals emanating from the integrin adhesome feed into complex signalling pathways that ultimately regulate gene expression, cell cycle progression, focal adhesion turnover and actin dynamics. Collectively, this elicits a plethora of fundamental, yet diverse cellular outputs such as survival, proliferation, differentiation, migration, adhesion and cell polarity (Legate et al., 2009) (fig. 4.7).

4.2.4 Integrins in mouse development

Mouse genetic tools have contributed enormously to the wealth of knowledge on the roles that integrins play in mouse development as well as their contribution to adult tissue homeostasis and regenerative processes. The genetic ablation of integrin genes leads to a variety of phenotypes, ranging from apparently normal mice to early embryonic lethality. The diversity of integrin mutant phenotypes reflects the many specialised functions of integrins during the development or maintainance of tissue integrity.

Targeting single α and β integrin subunits has been important in elucidating their respective functional contributions of specific integrin heterodimers. For example, the genetic disruption of integrin β1 essentially ablates the entire subfamily of β1 integrins and results in peri-implantation lethality (Fässler and Meyer, 1995; Stephens et al., 1995). However, among the integrin α subunits that are known partners of β1 integrin, only the deletion of specific integrin α subunits cause embryonic lethality, and none of these α subunit knockout mice show the same degree of severity as integrin β1 knock out, suggesting a level of functional compensation.

To provide an overview of integrin function in mouse development, I have summarised the phenotypes for single integrin α or β subunit knockout mice (table 4.1). In subsequent chapters of this introduction, I shall describe in greater detail the phenotypes of the FN-binding integrin knockout mice in the context of FN function. A large proportion of these constitutive integrin subunit genetic manipulations cause recessive embryonic lethality. The study of integrin function in processes related to integrin cell adhesion and signalling, but which would normally occur after the time of lethality, is grately facilitated by the use of conditional, tissue-specific integrin subunit knockout mouse models. I will return to such tissue-specific ablation of FN-binding integrins in subsequent chapters.

Table 4.1. Phenotypes of single-integrin-knockout mice. Adapted from (Bouvard et al., 2013).

Integrin subunit	Phenotype	Effect of loss	Reference
α1	Viable, fertile	Defects in collagen synthesis, skin thickening, reduced tumour vascularisation.	(Gardner et al., 1999) (Pozzi et al., 2000)
α2	Viable, fertile	Defects in platelet adhesion and response to collagen, diminished mammary gland branching morphogenesis.	(Holtkötter et al., 2002) (Chen et al., 2002)
α3	Perinatal lethal	Defects in kidney and lung development, skin blistering, disorganised basement membrane.	(Kreidberg et al., 1996) (DiPersio et al., 1997)
α4	Embryonic lethal	Defects in placenta formation, cardiac development and abnormal development of hematopoietic lineages in fetal liver.	(Yang et al., 1995) (Arroyo et al., 1999) (Sengbusch et al., 2002)
α5	Embryonic lethal	Defects in mesoderm-derived tissues and in neural crest cell survival.	(Yang et al., 1993) (Goh et al., 1997)
α6	Embryonic or perinatal lethal	Vascular hemorrhaging, abnormal vascular smooth muscle. Absent hemidesmosomes and skin blistering.	(Flintoff-Dye et al., 2005) (Georges-Labouesse et al., 1996)
α7	Perinatal lethal	Muscular dystrophy.	(Mayer et al., 1997)
α8	Perinatal lethal	Defects in kidney morphogenesis, inner ear stereocilia defects.	(Müller et al., 1997)
α9	Perinatal lethal	Defects in lymphatic valve formation and in the development of the lymphatic system, chylothorax.	(Huang et al., 2000b) (Bazigou et al., 2009) (Danussi et al., 2013)
α10	Viable, fertile	Dwarfism, abnormal chondrocyte behaviour, defects in growth plate morphogenesis and function.	(Bengtsson et al., 2005)
α11	Viable, fertile	Dwarfism, increased mortality, most likely due to failed incisor eruption.	(Popova et al., 2007)
αv	Embryonic or perinatal lethal	Deficient placentation, distended blood vessels, intracerebral and intestinal hemorrhage, cleft palate.	(Bader et al., 1998)
αx	Viable, fertile	Monocyte recruitment and atherosclerosis development.	(Wu et al., 2009)
αD	Viable, fertile	T cell defects, reduced immuned response to bacterial infections.	(Wu et al., 2004)
αL	Viable, fertile	Impaired immune response, failed tumour rejection.	(Schmits et al., 1996) (Shier et al., 1996)
αM	Viable, fertile	Impaired phagocytosis and neutrophil apoptosis.	(Coxon et al., 1996)
αE	Viable, fertile	Reduced lymphocyte numbers, inflammatory skin lesions.	(Schön et al., 1999)
αIIb	Viable, fertile	Impaired blood clot formation, platelet abnormalities.	(Tronik-Le Roux et al., 2000)
β1	Embryonic lethal	Inner cell mass deterioration, peri-implantation defect E5.5, defective BM assembly.	(Fässler and Meyer, 1995) (Stephens et al., 1995)
β2	Viable, fertile	Impaired leucocyte migration, skin infections.	(Scharffetter-Kochanek et al., 1998)
β3	Viable, fertile	Impaired blood clot formation, platelet abnormalities, enhanced pathological angiogenesis, bone defects.	(Hodivala-Dilke et al., 1999) (Reynolds et al., 2002)(McHugh et al., 2000)
β4	Perinatal lethal	Skin blistering.	(Dowling et al., 1996) (van der Neut et al., 1996)
β5	Viable, fertile	No apparent phenotype.	(Huang et al., 2000a)
β6	Viable, fertile	Inflammation in skin and lungs, TGF-β activation defect.	(Huang et al., 1996) (Munger et al., 1999)
β7	Viable, fertile	Impaired T cell migration to Peyer's patches, reduced lymphocyte number associated with gut epithelia.	(Wagner et al., 1996)
β8	Embryonic or perinatal lethal	Defects in vascular morphogenesis placenta, yolk sac, central nervous system and gastrointestinal system, cleft palate.	(Zhu et al., 2002)

4.3 Fibronectin (FN)

FN is a prominent constituent of the vertebrate connective tissue ECM, basal laminae and plasma. As a ligand of multiple integrin heterodimers and a binding partner of various ECM components, FN plays versatile roles in regulating cellular function. As an integrin ligand, a core function of FN is to support cell adhesion and migration of mesenchymal (and hematopoietic) cells. Yet with its many extracellular interaction partners, FN supports important biological processes during development and in adult physiology. As one of the earliest proteins to assemble within the extracellular space, FN is believed to coordinate the assembly of other matrix proteins and can be thought of as a "master organiser" of the ECM (Dallas et al., 2006; Schwarzbauer and DeSimone, 2011). FN is also involved in the propagation of diseases like cancer, fibrosis and artherosclerosis, and is considered a diagnostic marker for various pathologies.

The fibrillar form of FN is the principal biologically functional form of FN. Yet, cells secrete FN as inert globular units, which must undergo fibrillogenesis to become multi-functional supra-molecular fibrillar structures. FN fibrillogenesis is a complex, cell-driven assembly process that is initiated and governed by integrins and thermodynamics (Singh et al., 2010). The assembly of FN into a fibrillar matrix will be described in subsequent chapters, but first I shall introduce the important structural features of FN that are required for FN assembly and function.

4.3.1 Modular composition and alternative splice forms of FN

FN is a complex glycoprotein with a molecular weight of about 250 kDa and a carbohydrate content of 4-10% O-linked and N-linked glycosylation units (Choi and Hynes, 1979; Fibronectin, 1989; Hynes, 1990). FN is composed of three types of repeating, but structurally and functionally defined modules (FNI, FNII and FNIII) arranged in an array along the length of the protein and essentially integrating multiple functions into one molecule (Petersen et al., 1983; Hynes, 1990). More specifically, FN consists of twelve FNI repeats ($FNI_{1\text{-}12}$), two FNII repeats ($FNII_{1\text{-}2}$) and fifteen FNIII repeats ($FNIII_{1\text{-}15}$) (fig. 4.8). Despite FN being an exclusively vertebrate protein, the FNIII module is an ancient domain that is found in both intracellular and extracellular proteins expressed by both animals (as cell surface receptors and cell adhesion molecules, such as tenascin), plants and bacteria (Bork and Doolittle, 1992; Tsyguelnaia and Doolittle, 1998).

FN is encoded by a single gene, *Fn1*, that gives rise to significant protein heterogeneity through alternative splicing of the *Fn1* mRNA transcript. Alternative splicing of the *Fn1* transcript shows cell-type specific and species-specific patterns, which are regulated throughout development, but always targets three regions of the *Fn1* mRNA transcript, resulting in isoforms with complete or partial excision of individual modules; this gives rise to at least twelve isoforms in mouse and twenty isoforms in humans (Schwarzbauer et al., 1983; Kornblihtt et al., 1984; Kornblihtt et al., 1985; Schwarzbauer et al., 1987; Hynes, 1990). Alternative splicing activity within the polynucleotide array of $FNIII_{1\text{-}15}$ determines the presence or absence of exons encoding extra FN type III domain B (EIIIB, between $FNIII_{7\text{-}8}$) and EIIIA (between $FNIII_{11\text{-}12}$) as well as subdivisions of the variable (V) region (also

known as IIICS, between $FNIII_{14-15}$). Whereas regulated alternative splicing of EIIIA and EIIIB either includes or excludes these single extra FN type III-encoding exons, splicing within the V region either removes the entire V sequence (V0) or generates segments of varying lengths (generally termed V+ and include V64, V89, V95 and V120, where numbers denote the number of amino acids included in the V region, and the two latter forms are exclusively found in human). EIIIA- and EIIIB-containing FN are predominantly expressed during embryonic development, but are subsequently lost at postnatal stages (Pagani et al., 1991; Chauhan et al., 2004) (Ref Chauhan not really relevant). Although the expression of these extra FNIII domains is lost in normal adult tissue, they seem to play an essential part in the developing embryo; when both alternatively spliced segments are excised from the mouse genome by genetic recombination (FN $EIIIA^{-/-}/EIIIB^{-/-}$ double null), mice die during embryonic development with multiple severe cardiovascular defects (Astrof et al., 2007). However, mice expressing FN that lacks either EIIIA or EIIIB show only mild defects, but are otherwise viable and fertile (Fukuda et al., 2002; Muro et al., 2003; Tan et al., 2004). It is peculiar that EIIIA and EIIIB isoforms become reexpressed under pathological circumstances such as wound healing (Ffrench-Constant et al., 1989; Muro et al., 2003; Kilian et al., 2008), cancers (Koukoulis et al., 1993; Villa et al., 2008), artherosclerosis (Tan et al., 2004; Babaev et al., 2008), thrombosis (Chauhan et al., 2008), lung fibrosis (Muro et al., 2008) and kidney disease (Van Vliet et al., 2001). Alternatively spliced forms of FN carrying the V region are expressed both during embryogenesis and in adult tissue (Ffrench-Constant et al., 1989; Oyama et al., 1989).

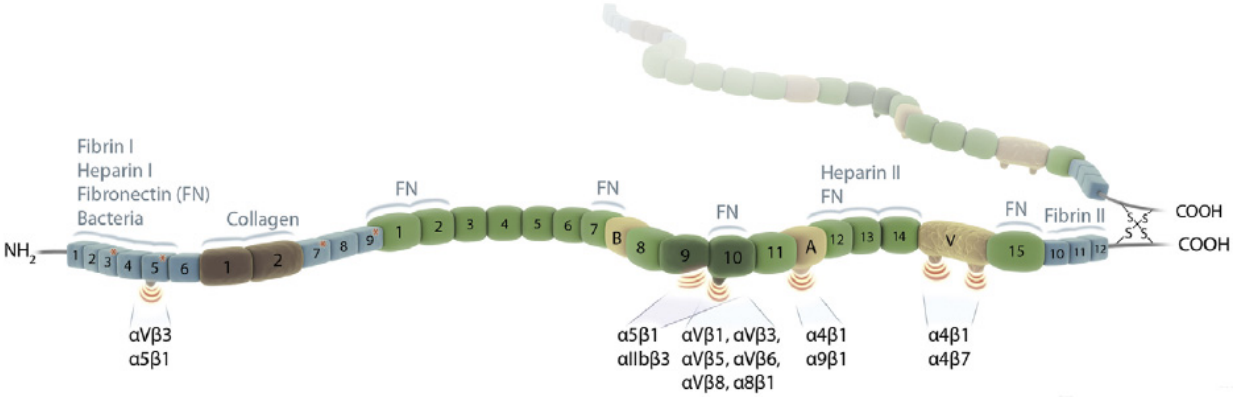

Figure 4.8. A diagrammatic representation of the modular structure of dimeric FN. FNI repeats are indicated in blue, FNII in brown, FNIII in green and the alternatively spliced extra FNIII repeats, EIIIA, EIIIB and the V-region are indicated in sand. Prominent binding partners of FN to other ECM proteins are indicated above the molecule, while integrin heterodimers and their recognition sites in FN are denoted below. Note the dimerisation motif mediated by C^{2458} and C^{2462} at the C-terminal of FN. Adapted from (Leiss et al., 2008).

Several features of FN are critical for its biological function. FN segregates into two functionally distinct pools on the basis of solubility and fibrillity. So-called cellular FN (cFN) is a ubiquitously expressed form of FN that becomes converted into an insoluble and fibrillar constituent of the ECM or basal laminae of most mesenchymal and epithelial cell types. Hepatocytes, on the other hand, secrete large amounts of so-called plasma FN (pFN) into the plasma, reaching concentrations of about 300 μg/ml. pFN circulates in plasma in a globular and soluble state until converted into an insoluble and fibrillar form by activated integrins, typically upon vascular injury or lesions, where fibrillar FN

supports the growth and stability of platelet thrombi during haemostasis (Ni et al., 2003; Cho and Mosher, 2006). cFN-type isoforms of FN include both EIIIA- and EIIIB-containing FN, whereas pFN has no extra domains. pFN isoforms are heterogenous in that FN dimers tend to carry one V0 subunit and one V+ subunit (V0/V+), whereas cFN is almost always found to contain either full-length or shortened stretches of the V region (Hynes, 1990).

As will become clear in subsequent chapters, the conversion of soluble FN into a fibrillar matrix is a cell-driven, integrin-dependent process. Indeed, the segregation of cFN and pFN in time and space is largely a consequence of the temporal and spatial regulation of integrin activation. Cells depositing FN into the ECM or basal lamina constitutively express active forms of integrins that will convert globular FN into a fibrillar form. However, haematopoetic cells circultating in the blood, where they are constantly exposed to pFN, must temporally restrict the conversion of soluble FN into a fibrillar form to times when blood clots are needed to prevent bleeding. By maintaining their repertoire of surface integrins in an inactive state and only shifting to an active state in response to signals emanating from vascular injury, heamatopoietic cells ensure that pFN is converted into a fibrillar matrix only at the right time and place. While pFN plays an important part in blood clotting, it is also implicated in artherosclerosis and liver fibrosis. It is also noteworthy that pFN and cFN are not fully separated in space; pFN has been found to leak into tissues from the blood and become integrated into the cell-associated fibrillar matrix (Moretti et al., 2007).

A crucial feature of FN is its dimerisation. Dimerisation is allegedly required for the *de novo* assembly of a fibrillar FN matrix and thus FN function (Schwarzbauer, 1991). Dimerisation of FN is achieved in the endoplasmic reticulum by inter-chain disulfide bond formation between two pairs of cysteine residues (C^{2458} and C^{2462}) in the extreme C-terminus of two FN molecules (Choi and Hynes, 1979). The dimeric form of FN is by far the most prevalent form in tissues. However, naturally occurring single-chain isoforms do exist. In cartilage, a unique pattern of alternative splicing creates a FN isoform that lacks the entire V region along with the $FNIII_{15}$ and FNI_{10} repeats [termed (V+C)-] (MacLeod et al., 1996). Although this FN splice variant retains the two C-terminal cysteine residues essential for dimerisation, cellular and/or structural constraints appear to impair the ability to dimerise, and as such this FN isoform exists not only as a homodimer but also in an unusual monomeric configuration (Burton-Wurster et al., 1999). The tissue-specific expression pattern of this fibronectin isoform suggests that it may have an important function in the matrix organisation of cartilage, but the contribution of a single-chain form of FN to the properties of the ECM are still unknown. Zebrafish express a truncated form of FN (FN2) that lacks the two cysteines that are usually involved in the formation of interchain disulfide bonds (Zhao et al., 2001). This single-chain isoform must retain important biological activity as it is expressed throughout zebrafish development and supports cell adhesion and spreading of fish embryonic cells.

4.3.2 FN-binding integrins

FN is an integrin ligand and provides a platform for cell adhesion and migration. While eleven integrins have been shown to interact with FN *in vitro* (Humphries, 2006; Leiss et al., 2008), four of

these integrins (α5β1, αVβ3, α4β1 and αIIbβ3) interact with FN to the extent that they regulate FN fibril assembly. However, the binding specificity of this group of FN-binding integrins is not always limited to FN. A variety of ECM proteins contain an asparagine-glycine-aspartate (RGD) tripeptide motif that is recognised by integrins, but the ease by which an integrin can structurally accommodate the RDG sequence in a given ECM protein determines relative affinities of the integrin for its various ligands. It is also noteworthy that the ability of FN to serve as an adhesive substrate to cells is not strictly dependent on integrins; FN binding is also promoted by the interaction of heparin-binding domain in $FNIII_{13-14}$ with heparin or heparan sulphate proteoglycans, such as the syndecans, that are expressed on cell membranes (Saunders and Bernfield, 1988; Barkalow and Schwarzbauer, 1991; Barkalow and Schwarzbauer, 1994; Couchman, 2010). The interaction between FN and syndecans is significant in that it has been shown to synergise with integrin-FN binding in promoting adhesion-dependent processes such as integrin-based focal adhesion formation and cell spreading (Woods and Couchman, 1998; Woods and Couchman, 2001; Klass et al., 2000; Couchman, 2010; Morgan et al., 2007). I will now focus exclusively on the interaction of FN with integrins.

Integrins interact with FN at one of two main central "cell-binding sites" to promote cell adhesion and FN fibrillogenesis. One central cell-binding domain is represented by the RGD tripeptide motif in $FNIII_{10}$ (Pierschbacher and Ruoslahti, 1984a). Crystal structures of $FNIII_{10}$ have revealed that the RGD motif is on a conformationally flexible loop between two β strands and becomes exposed and available for binding by integrins when FN is absorbed to a surface (such as cell culture glass or plastic) (Baron et al., 1992; Leahy et al., 1992; Main et al., 1992) then how to thrombin-stimulated, activated platelets bind globular FN. The RGD motif in FN is recognised by integrins α5β1, αVβ1, αVβ3, αVβ6, α8β1, α9β1 and αIIbβ3 (Humphries, 2006; Leiss et al., 2008) (fig. 4.8) The specificity and importance of the interaction between integrins and the RGD motif is demonstrated by the ability of RGD motif-containing peptides to support fibroblast attachment to an RGD peptide-coated surface, and, when administered in soluble form, to inhibit adhesion of both freshly seeded fibroblasts and thrombin-stimulated platelets to FN (Pierschbacher et al., 1983; Pierschbacher and Ruoslahti, 1984a; Pierschbacher and Ruoslahti, 1984b; Ginsberg et al., 1985). Furthermore, the addition of RGD motif-containing peptides to adherent cells abolishes the ability of cells to assemble FN fibrils (Plow et al., 1985). Deletion of genes in the mouse encoding integrins α5 and αV causes embryonic lethality and is associated with a complete failure to assemble a fibrillar FN matrix (Yang et al., 1999). The importance of the integrin interaction with the RGD motif is made even more clear by the phenotype of the mouse expressing FN in which the aspartic acid residue in the RGD motif was mutated to glutamic acid (FN^{RGE}); here, the FN integrins that rely on RGD motif can no longer interact with $FNIII_{10}$ and embryos die with mesodermal and vascular defects, reminiscent of the embryonic lethal phenotype of the integrin α5 knock-out mouse (Yang et al., 1993; Takahashi et al., 2007). However, the findings that both $FN^{RGE/RGE}$ embryos and integrin α5 knock-out mouse embryos show nearly equal quantities of fibrillar FN in the anterior trunk tissue suggested that αV integrins in this tissue were able to interact with FN and induce its assembly in an RGD motif-independent manner. This led to the discovery of new αV integrin-binding sites at the N-terminus of FN; in FNI_5, an asparagine-glycine-arginine (NGR)

sequence becomes a high-affinity binding site for integrin αVβ3 through the deamidation of the asparagine residue, possibly catalysed by protein l-isoaspartyl methyltransferase, which thereby creates a spatially accessible iso-DGR sequence that is recognised by RGD-binding integrin αVβ3 (Curnis et al., 2006; Leiss et al., 2008) Leiss 08 is the wrong reference. Use Takahashi 07. Although FN deamidation has not been demonstrated *in vivo*, it presents a plausible mechanism of αV-dependent and α5β1-independent FN fibril assembly (in a way it is still RGD dependent because it depends on deamindation of the asparagine to arspartic acid) in the embryo anterior trunk (Takahashi et al., 2007).

Some FN-binding integrins, most notably integrin α5β1 and αIIbβ3 require an additional binding motif in FN, called the synergy motif, to maximise binding affinity of the FN-integrin interaction (Bowditch et al., 1994; Danen et al., 1995; Chada et al., 2006). The synergy motif comprises the (at least) minimal peptide sequence Pro-His-Ser-Arg-Asn (PHSRN) within the centre of $FNIII_9$, and is thus placed in the vicinity of the RGD motif in $FNIII_{10}$ (Nagai et al., 1991; Aota et al., 1994; Bowditch et al., 1994; Redick et al., 2000; Chada et al., 2006) (fig 4.9). The synergy motif was once proposed to exert its positive effect only when the RGD and the synergy motifs were simultaneously bound by integrin β1 and α5 subunits, respectively, but more recent studies have shown that the synergy motif does not engage integrins directly, but exerts a positive, indirect effect on the affinity of integrins for the RGD motif by (a) optimally orienting the loop containing the RGD motif for integrin binding or, alternatively, (b) by so-called long range electrostatic steering whereby electrostatic repulsion between negative charges within $FNIII_{7-10}$ and its binding pocket in the integrin α5 subunit becomes neutralised by basic residues within the synergy motif (Takagi et al., 2003). Despite the substantial contribution of the synergy motif to overall binding affinity and a report claiming that the synergy motif is essential for α5β1-mediated *de novo* accumulation of a FN matrix (Sechler et al., 1997), it is intriguing that a mouse model engineered to express a knock-in mutation that disrupts the synergy motif shows no obvious developmental or adult physiological defects (Dr Mercedes Costell, unpublished observation).

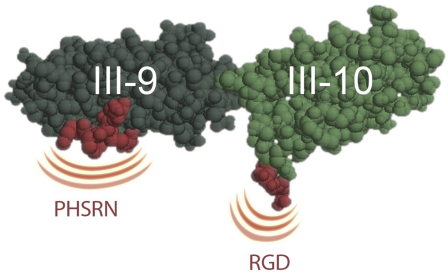

Figure 4.9. A schematic depiction of $FNIII_{9-10}$. These two adjacent type III modules contain the synergy motif (PHSRN) and the cell-binding RGD motif (both highlighted in red). Although probably not in contact with integrin α5β1, the synergy motif is thought to increase the binding affinity of integrin α5β1 for the RGD motif. Adapted from (Leiss et al., 2008).

As described above, the expression of alternatively spliced FN isoforms is spatially and temporally regulated during development and disease. This suggests that the various FN isoforms have unique functions during both physiological and pathological tissue remodelling. Interestingly, all three major sites of alternative splicing flank domains that allow FN to interact with integrins. EIIIA- and EIIIB-

containing isoforms of cFN are particularly interesting in this respect because they flank the cell-binding domains in $FNIII_{9-10}$ and could modulate the ability of integrins to regulate FN fibrillogenesis and/or cell adhesion. Alternative splicing could give rise to FN isoforms with different cell-adhesive, ligand-binding and solubility properties that allow cells to alter the chemical composition and mechanical properties of the ECM in a developmental and tissue-specific manner. Some cell types require the presence of EIIIA-containing FN for integrin-mediated adhesion (Manabe et al., 1997); for example, EIIIA contains a EDGIHEL sequence that is recognised by integrins α4β1 and α9β1 (Liao et al., 2002; Shinde et al., 2008). The contribution of each extra domain to FN fibrillogenesis has also been tested in cell culture experiments. These showed that fibroblasts cultured in the presence of recombinant FN fragments containing either EIIIA or EIIIB domains would enhance the incorporation of the recombinant FN into a pre-existing matrix (Guan et al., 1990). Another study showed that EIIIB-/- mouse embryonic fibroblasts (MEFs) tend to deposit less FN into cell-derived ECM (Fukuda et al., 2002). Structural studies support the notion that the presence of EIIIB stabilises macromolecular fibril formation and integrin clustering (Schiefner et al., 2012). Interestingly, MEFs expressing $FN^{EIIIA-/-/EIIIB-/-}$ deposit FN into a fibrillar state in the ECM (Astrof et al., 2007), but such an $FN^{EIIIA-/-/EIIIB-/-}$ matrix must contain qualitative distortions that account for the embryonic lethality of $FN^{EIIIA-/EIIIB-}$ mice, perhaps by modulating the ability of integrins to interact with FN.

V+ FN isoforms could also have a role in regulating cell adhesion. The V120 isoform of FN, which contains the peptide sequence spanning the Heparin-II (HepII) binding domain and the type III connecting segment (IIICS), includes the minimal sequences REDV, which are functionally related to the RGD motif, and LDV. Various cell types specifically attach to FN through integrins α4β1 and α4β7 by recognition of these sequences (Wayner et al., 1989; Guan and Hynes, 1990; Nojima et al., 1990; Mould et al., 1991). Other cell types use α4 integrins to bind the V-region (IIICS) of FN and thereby initiate FN fibril assembly (Sechler et al., 2000).

4.3.3 The assembly of a fibrillar FN matrix

At physiological pH and salt concentration, the native conformation of FN is compact and globular due to intramolecular ionic interactions between the two arms of the dimeric FN molecule (Johnson et al., 1999), and remains soluble as long as there is no encounter with cells expressing active integrins. Activated integrins will bind soluble FN and initiate an elaborate conversion of FN into a highly fibrillar and organised form that is chemically cross-linked to a degree that resists solubilisation in sodium deoxycholate detergent. In its fibrillar form, FN provides a platform for cell attachment, cell migration and tissue organisation as well as a depot to store growth factors. Essentially, FN acquires all its functionality once in a fibrillar form, and therefore it is crucial to understand the mechanism underlying this conversion. FN fibrillogenesis is the process by which soluble FN transitions into to a fibrillar form, and I shall now provide a detailed account of this mechanism.

4.3.3.1 Integrins initiate FN fibrillogenesis

While a number of integrins have been found to interact with FN (Zhang et al., 1993), the integrin α5β1 is considered the prime integrin responsible for promoting FN fibril assembly. This was

demonstrated in early experiments where chinese hamster ovary (CHO) cells transfected with integrin α5 showed an enhanced ability to assemble FN fibrils (Giancotti and Ruoslahti, 1990), and in other experiments where blocking antibodies against α5 or β1 integrins prevented FN matrix assembly (Akiyama et al., 1989; Fogerty et al., 1990). Even small fragments of FN containing the RGD motif (i.e. an integrin cell-binding site) will inhibit the assembly of FN fibrils by cells (McDonald et al., 1987), and experimental work with chimeric β1 integrins, rendered incapable of binding an ECM ligand, inhibit FN fibril assembly (LaFlamme, 1994). However, some cell types lacking α5 integrins will initiate FN fibrillogenesis using the αV integrins, which bind FN through either the RGD motif or peptide sequences within FNI_{1-5} (Wennerberg et al., 1996; Wu et al., 1996; Takahashi et al., 2007). The employment of αV integrins could account for the FN fibrillogenesis that has been shown to occur in α5 knockout mice or in cultures of α5 knockout MEFs (Yang et al., 1993; Yang and Hynes, 1996). However, it is widely accepted that integrin α5β1 is superior over integrin αVβ3 in driving *de novo* fibrillogenesis. Firstly, integrin αVβ3 cannot bind soluble FN, whereas α5β1 can (Huveneers et al., 2008). The RGD motif is not exposed in soluble FN, but the ability of integrin α5β1 to bind the synergy motif could stabilise a particular orientation of the RGD motif within $FNIII_{10}$ that favours its ligation to integrin α5β1 (Altroff, 2004). Although integrin α5β1 will bind to FN lacking the synergy motif, both the RGD and synergy motifs are necessary for integrin α5β1 to induce fibrillogenesis (Danen et al., 1995; Sechler et al., 1997). Secondly, the ability of integrin α5β1 to engage the synergy motif in response to tension strengthens the integrin-FN bond, and this could distinguish integrin α5β1 from integrin αVβ3 in terms of ability to initiate adhesion and FN fibrillogenesis (Friedland et al., 2009). Third, integrin α5β1 is known to stimulate higher levels of RhoA-GTP loading than integrin αVβ3 and thereby generate a different degree of tension to allow the process of fibrillar adhesion formation and concomitant FN fibrillogenesis (Danen et al., 2002) These differences could explain why fibroblasts performing αV integrin-mediated FN assembly creates, at best, a network of stunted fibrils. *In vivo*, however, it is most likely that the two integrin heterodimers cooperate within the same focal adhesion to regulate FN fibril architecture. The platelet-specific integrin αIIbβ3 will also assemble fibrillar FN matrix upon stimulation (Wu et al., 1995; Olorundare et al., 2001), and this process is an important part of thrombus formation.

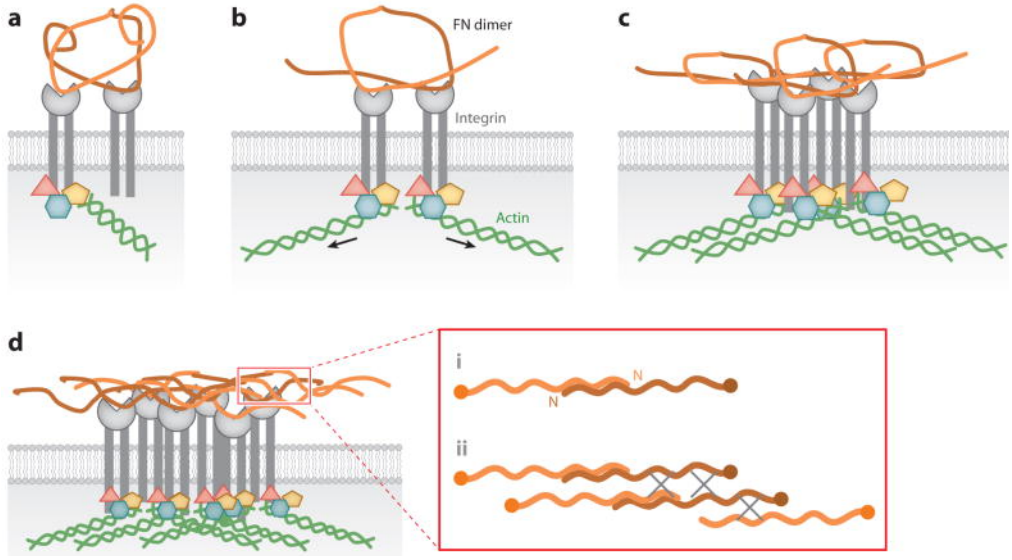

Figure 4.10. Schematic representation of the major steps in FN fibrillogenesis. (A) Integrin α5β1 (grey) capture globular FN dimers (orange/brown) in the extracellular matrix. (B) Recruitment of signalling and actin-binding cytoplasmic proteins (pink, blue, yellow) to the integrin cytoplasmic tail ensures the mechanical coupling of integrins to the contractile actomyosin machinery (green). Biochemical signals emanating from integrin signalling platforms lead to the generation of contractile force by the actomyosin machinery, which, when transduced through integrins, induces conformational changes in FN. (C) Integrin clustering and FN-FN interactions promote the build-up of stretches of FN fibrils. (D) The presence of multiple FN-binding sites in the FN dimer allows a high degree of intramolecular cross-linking in FN, which stabilises the formation of supramolecular (DOC-insoluble) structures of FN in a fibrillar matrix. Adapted from (Singh et al., 2010).

The early events of FN fibrillogenesis require the mechanical coupling of the extracellular ligand to the contractile actin cytoskeleton via integrins (fig. 4.10 A). This was demonstrated by early experiments where cells expressing a recombinant truncated form of integrin β1 cytoplasmic domain failed to assemble a FN matrix (Wu et al., 1995) and where the pharmacological interruption of the actin cytoskeleton inhibited FN fibrillogenesis (Ali and Hynes, 1977; Christopher et al., 1997). FN fibrillogenesis is coupled to the maturation of integrin adhesions into fibrillar adhesions (Pankov et al., 2000; Yamada et al., 2003). FN is first seen as punctate structures associated with integrins within maturing focal adhesions in the lamellae. FN follows the same centripetal segregation pattern as integrin α5β1, transitioning into structurally compact fibrils *en route* that align with stretches of integrin α5β1, actin stress fibres and adhesion-associated signalling molecules, such as tensin. Here the role of integrins as mechanotransducers is paramount to FN fibrillogenesis; binding of FN by integrins stimulates the generation of mechanical force by the contractile actin cytoskeleton, leading to a build-up of mechanical tension across the ligand-bound integrin, which, when transduced to the bound FN, stretches the globular FN molecule. This stretching overcomes intramolecular forces holding the FN dimer in a compact globule and pries apart the two arms of the dimer (Baneyx et al., 2002; Smith et al., 2007) (fig. 4.10 B and 4.11). As will become apparent in the following chapter, FN harbours hidden hydrophobic domains that represent cryptic FN-binding sites. The unravelling of these cryptic FN-binding sites upon integrin binding allows intermolecular FN-FN interactions to drive the propagation of a polymerisation reaction that transforms FN into fibrils.

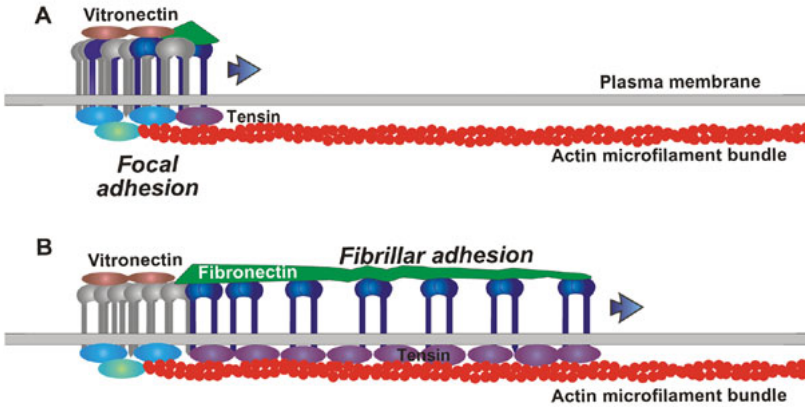

Figure 4.11. FN extension within fibrillar adhesions. Transition of integrin α5β1 (blue) from focal adhesions at the cell periphery along stress fibres towards the cell body (arrow) forms fibrillar adhesions that pull on bound FN (green) and thereby manipulate FN into a fibrillar matrix. This transition involves the acquisition of tensin and loss of other focal adhesion components such as paxillin and vinculin. Adapted from (Yamada et al., 2003).

A number of focal adhesion components are directly involved in the processes of fibrillar adhesion formation and FN fibrillogenesis. Talin is one of the earliest activators of β1 integrins, and if prevented from binding the intracellular domain of integrin β1, both integrin activation and FN fibril formation is diminished (Green et al., 2009). Cells lacking FAK in focal adhesions fail to translocate integrin-bound FN and other focal adhesion proteins along the actin fibres in fibrillar adhesions (Ilić et al., 2004). Src is another central kinase of focal adhesion dynamics, and cells lacking Src also show a reduced ability to initiate FN fibrillogenesis (Wierzbicka-Patynowski and Schwarzbauer, 2002). Furthermore, the pharmacological inhibition of Src after FN matrix formation shows that Src is required to maintain a FN matrix (Wierzbicka-Patynowski et al., 2007).

4.3.3.2 Lateral self-association of FN molecules drives FN fibrillogenesis

Of fundamental importance to FN fibrillogenesis, and thus FN function, is the ability of FN molecules, once partially extended, to associate laterally with one another through internal FN-binding domains. Lateral self-association of FN is the driving force behind the propagation of FN fibrillogenesis and is facilitated by the clustering of FN-bound integrins, which increases the local concentration of FN (fig. 4.11 C and D).

The earliest approaches to identify the sequences within FN responsible for self-association relied on the ability of exogenous (purified and recombinant) FN to become incorporated into a cell-derived matrix, then systematically assaying the ability of a given truncated segment of recombinant FN to do the same (Hayman and Ruoslahti, 1979; McKeown-Longo and Mosher, 1983; Millis et al., 1985; Chernousov et al., 1987; Guan et al., 1990). Approaches based on affinity chromatography and solid-phase binding assays with proteolytic FN fragments, recombinant truncated FN polypeptides and blocking antibodies (i.e., monoclonal antibodies L8 or 9D2 (Chernousov et al., 1987; Chernousov et al., 1991)) that bound FN, but did not affect binding of FN by integrin α5β1, led to the identification of an essential self-association site, a 70kDa region within N-terminal FNI_{1-5} termed the assembly domain (McKeown-Longo and Mosher, 1983; McKeown-Longo and Mosher, 1985; Chernousov et al., 1985; McDonald et al., 1987; Allio and McKeown-Longo, 1988; Quade and McDonald, 1988; Barry

and Mosher, 1989). The requirement for FN-FN interactions in FN fibrillogenesis was later confirmed with experimental setups studying *de novo* assembly of recombinant FN fragments expressed and assembled by mammalian cells (Schwarzbauer, 1991).

The 70kDa N-terminal FNI_{1-5} assembly domain is recognised by a multitude of sites within the more C-terminal FNIII repeats. These FN-binding sites are cryptic in the native globular state of FN and require extension to become available to participate in intermolecular interaction. The FN assembly domain has been shown to interact with sites in $FNIII_1$ (Hocking et al., 1994), $FNIII_2$ (Aguirre et al., 1994; Sechler et al., 2001), $FNIII_{4-5}$ (HepIII) (Maqueda et al., 2007), $FNIII_{10}$ (Hocking et al., 1996) and $FNIII_{12-14}$ (HepII) (Bultmann et al., 1998). As these binding sites are hidden in the soluble globular form of native FN, they could only be identified experimentally through the partial denaturation of FN *in vitro*. *In vivo*, the availability of cryptic FN-binding domains requires conformational changes imposed by forces generated by the actin-cytoskeleton in response to integrin activation.

FN recognition sites within the FN subunit are hydrophobic stretches that lie buried in the globular native state of FN, and which, upon extension, become exposed in a thermodynamically unfavourable state. Thus, hydrophobic domains in semi-extended FN molecules would be thermodynamically driven to interact with each other. The extent of intermolecular alignment through lateral association depends on the number of FN-binding sites available as extension progresses. Thus, as FN becomes extended, it transitions from a globular form, where hydrophobic domains are sheltered from the water-based milieu, to an extended state that allows the hydrophobic domains to rapidly self-associate laterally among each other into multimeric fibrils. As to whether each individual FN-binding site is required and becomes occupied during fibrillogenesis, there appears to be substantial overlap in the interaction profile of the FN-binding domains. Not all of the above-mentioned binding sites are essential for fibrillogenesis, but their abundance would stabilise newly formed fibrils simply by lowering the rate of dissociation of FN subunits or by providing a means of controlling fibril length. Increasing the numbers of occupied FN-FN bonds along the length of the molecule would also strengthen the matrix, prevent breakage of the matrix in response to force and reduce the ease by which cells can detach from the ECM by ECM fibril breakage (Engler et al., 2009).

This combination of binding sites allows end-to-end elongation of FN as well as lateral growth of thin FN fibrils into bundles that possess extraordinary flexibility and elasticity (Klotzsch et al., 2009). As the matrix matures and fibrils grow in thickness and length, FN fibrils achieve a level of cross-linking that renders the matrix resistant to solubilisation in a detergent like sodium deoxycholate (DOC) (Choi and Hynes, 1979). Reaching the DOC-insoluble state is biochemical feature of FN that endows the ECM of a mature cell culture or tissue with physical stability. Also, DOC fractionation assays have long been the gold standard for assessing the degree of chemical cross-linking within a FN matrix (Pankov and Yamada, 2004). The insolubility of FN fibrils reflects the ability of FN to interact with itself, but the nature of these interactions has been uncertain. One possibility is that FN cross-linking bonds are covalent in nature and perhaps arise from disulfide exchange between FN molecules, which was plausible given that FN has many intra-chain disulfide bonds and putative protein disulfide

isomerase activity (Chen and Mosher, 1996; Langenbach and Sottile, 1999). However, a more recent study concluded that FN matrix DOC-insolubility is non-covalent in nature, but is strengthened by the shear number of non-covalent interactions that take place between FN molecules (Ohashi and Erickson, 2009).

4.3.3.3 The requirement for FN dimerisation in FN fibrillogenesis

More than two decades ago, Dr. Schwarzbauer published the results of experiments that were designed to identify the sites within FN involved in *de novo* FN fibrillogenesis and matrix formation (Schwarzbauer, 1991). Recombinant FN polypeptides representing defined segments of FN were expressed in mammalian cells and assayed for incorporation into a DOC-insoluble cell matrix fraction and for the formation of fibrils at the cell surface, as detected by immunofluorescence microscopy (Schwarzbauer, 1991). In one experiment, a recombinant fragment of FN lacking the C-terminal dimerisation motif was expressed in a mammalian cell culture system and thus probed for its ability to undergo *de novo* fibrillogenesis. This construct resulted in the synthesis and secretion of a form of FN that could not dimerise and which failed to assemble into a fibrillar matrix upon secretion. The conclusion was that dimerisation mediated by the C-terminal interchain disulfide bonds is essential for the conversion of FN into a fibrillar DOC-insoluble form. No earlier study had reported a requirement for the dimerisation motif for *de novo* FN fibrillogenesis, for previous experimental setups were limited to studying the ability of proteolytic fragments of FN devoid of C-terminal cysteines to become incorporated into pre-assembled matrices (Chernousov et al., 1985; McKeown-Longo and Mosher, 1985; Quade and McDonald, 1988). With both biochemical and immunocytochemical approaches, Dr. Schwarzbauer reported the minimum domain requirements for FN fibrillogenesis, which included the 70kDa N-terminal FNI_{1-5} assembly domain (described earlier) and the C-terminal region containing the dimerisation motif (Schwarzbauer, 1991). These minimum domain requirements were soon to be confirmed by other reports (Ichihara-Tanaka et al., 1992).

This finding laid the foundation for current models describing FN fibrillogenesis, and it is now widely accepted that the dimerisation motif at the C-terminus of FN is essential for the ability of FN to undergo fibrillogenesis.

4.3.4 Fibrillar FN is a master scaffolding protein of the ECM

As an extracellular ligand of a significant number of integrins, FN clearly has a prominent role as an adhesive substrate for cells. Yet the activity of FN goes beyond that of cell adhesion, owing to a variety of domains along the length of the FN molecule that endow it with the ability to interact with other ECM proteins and proteoglycans. FN is a very early fibrillar component of the ECM, and during the early steps of ECM build-up, the organisation of FN fbirls is often found to first precede and then co-localise with late ECM components. Observations like these gave the impression that FN could guide the organisation of the ECM, and indeed, it is now widely accepted that FN regulates the initial and continuous deposition and stability of several other ECM components, including ECM-associated growth factors Include Sottile and Hocking 2002 (Dallas et al., 2006).

A number of ECM proteins depend on FN, directly or indirectly, for their incorporation into the ECM. Binding domains within the N-terminal FNI_{1-5} allow FN to interact with various extracellular proteins. As examples, the ability of this region of pFN to interact with hepatocyte-derived plasma fibrinogen and fibrin clots at a site of vessel injury underlies the role of FN in hemostasis and stabilisation of a blood coagulation (Pereira et al., 2002; Ni et al., 2003). Efficient blood clots consist of polymerized fibrin that become covalently cross-linked to FN via FNI_{1-5} by factor XIII transglutaminase (Mosher, 1975; Fibronectin, 1989; Hynes, 1990). A stretch of consecutive FNI modules interrupted by two FNII modules comprise a collagen/gelatin binding domain of FN which underlies the ability of FN to organise collagen fibrils; indeed, collagen-I and -III fibril deposition has been shown to depend on the presence of fibrillar FN (McDonald et al., 1982; Sottile and Hocking, 2002; Velling et al., 2002; Li et al., 2003; Kadler et al., 2008). The same is true for thrombospondin-1; conversion of thrombospondin-1 into fibrils takes place only in the presence of FN fibrils (Sottile and Hocking, 2002). The incorporation of latent TGF-β binding protein (LTBP) into the ECM at early stages of ECM assembly is dependent on direct interactions between FN and LTBP-1 (Dallas et al., 2005; Koli et al., 2005), and at later stages of ECM assembly, fibrillin associates with and stabilises these LTBP fibrils (Massam-Wu et al., 2010). Fibrillin, too, interacts with FN, and fibrils of fibrillin co-localise with and strictly depend on FN fibrils at early stages of ECM formation (Sabatier et al., 2009). The organisation of fibulin into the ECM is also dependent on a preassembled FN matrix (Roman and McDonald, 1993; Godyna et al., 1995) and tenascin C is incorporated into a FN matrix by directly binding FN (Ingham et al., 2004a) and via perlecan binding to FN (Chung and Erickson, 1997). Even gram-positive cocci strain of bacteria, such as *Streptococcus aureus* and *Streptococcus pyogenes*, have evolved FN-binding proteins that recognize the FNI_{1-5} domain and exploit this interaction in the process of infection (Ingham et al., 2004b; Schwarz-Linek et al., 2006; Atkin et al., 2010).

4.3.5 FN regulates growth factor availability

As part of the ECM, FN has effects beyond providing structural support to cells and tissues. An important function of ECM in general, and FN specifically, is to bind, store and present growth factors. A large number of growth factors are released into the extracellular space and target a particular cell type that displays the cognate receptor. To prevent diffusion and to regulate the timing, dosage and mode of growth factor bioavailability, numerous growth factors become immobilised in the extracellular space through binding to specific components of the ECM. As such, the ECM functions as a solid-state growth factor depot for essential and potent growth factors, such as FGF, hepatocyte growth factor (HGF), TGF-β, bone morphogenic protein (BMP) and VEGF-A (Flaumenhaft and Rifkin, 1992; Taipale and Keski-Oja, 1997; Gregory et al., 2005; Rahman et al., 2005; Wijelath et al., 2006). Furthermore, the binding of growth factors to the ECM is perceived as a means to establish gradients of growth factors; such gradients are very important in patterning developmental processes, such as angiogenesis (Ruhrberg et al., 2002). In some cases, such as for FGF, the binding of a growth factor to the ECM is even a prerequisite for activating its cognate receptor (Goetz and Mohammadi, 2013). A group of growth factors (e.g. FGF and VEGF-A) bind heparin and heparan

sulphate, glycosaminoglycan moieties found on several proteoglycans of the ECM. Other growth factors bind to ECM proteins directly, and here there is growing evidence that FN plays an important part. While some growth factors are secreted in an active state and become sequestered by the ECM to prevent them from diffusing and activating their cognate receptor, other growth factors are secreted in an inactive state, and their incorporation into the ECM is a critical step of their activation mechanism. The spatial and temporal release ensures the correct order of events during tissue morphogenesis and repair.

Various modes of growth factor release have been described; they are all complex and multi-faceted, and the ECM can be either a passive or an active participant of the release mechanism, i.e. while some growth factors can be released simply by the degradation of ECM, other mechanisms employ specific properties of the ECM. Of particular interest to the topics of this thesis are growth factors whose storage and release requires FN, and so the following chapters serve to introduce these aspects of VEGF-A and TGF-β in greater detail.

4.3.5.1 VEGF

VEGF-A is a key regulator of blood vessel growth and is both absolutely critical for vascular development and a principle regulator of pathological angiogenesis. VEGF-A promotes vascular morphogenesis by activating the VEGF receptor 2 (VEGFR2) tyrosine kinase expressed by endothelial cells. The characteristic tree-like patterning of vessels is orchestrated by gradients of soluble and insoluble VEGF-A. The ECM helps to shape these gradients by providing a solid-state binding platform that regulates VEGF-A diffusion (Ruhrberg et al., 2002; Ruhrberg, 2003). While VEGF-A has long been known to bind heparan sulfates expressed on cell surfaces or on heparan sulphate proteoglycans in the ECM, it is becoming increasingly clear that FN has an important function in promoting sprouting angiogenesis by facilitating the deposition of VEGF-A into the extracellular space.

The single VEGF-A gene transcript in mammals undergoes extensive alternative splicing to generate several isoforms; what differs among the most common of these isoforms is the presence or absence of two heparin-binding domains that enable VEGF-A to interact with heparan sulfate (Park et al., 1993). In mouse, the VEGF-A_{120} isoform (VEGF-A_{121} in human) lacks both heparin-binding domains and is freely diffusible in a heparin-containing environment. VEGF-A_{164} (VEGF-A_{165} in human) retains one heparin-binding domain and has intermediate affinity for heparin-based substrates, while VEGF-A_{188} (VEGF-A_{189} in human) contains both heparin-binding sites and is fully retained on heparin-containing proteoglycans expressed on the cell surface or in the ECM. The spatial restriction in expression and differential localisation of heparin-binding forms of VEGF-A is key to establishing the VEGF-A gradients that guide blood vessel branching (Ruhrberg et al., 2002; Ruhrberg, 2003; Gerhardt et al., 2003) (fig. 4.12).

Two VEGF-A-binding domains have been described in FN. One binding site is located within N-terminal first nine FNI and the only two FNII repeats and includes a heparin-binding site I (HepI) (Wijelath et al., 2002). The second VEGF-A binding site was found within a second heparin-binding

site, HepII, in $FNIII_{13-14}$ (Barkalow and Schwarzbauer, 1991; Wijelath et al., 2002). The interaction of VEGF-A with FN influences integrin α5β1-VEGFR2 crosstalk and the endothelial cell response to VEGF-A (Wijelath et al., 2002; Wijelath et al., 2006). This crosstalk requires intact FN containing both the VEGF-binding site in $FNIII_{13-14}$ and the integrin-binding site in $FNIII_{9-10}$, which in turn reflects a need for juxtapositioning of integrin and VEGFR2 (Wijelath et al., 2006). Crosstalk between integrins and VEGFR is regarded as indispensable for the regulation of angiogenic processes (Byzova et al., 2000; Wang et al., 2001b; Podar et al., 2002; De et al., 2005) remove podar – wrong cell type. Whether the heparin-binding sites in VEGF are important for this interaction, or whether there is an independent FN-binding site in VEGF-A that can be included or excluded by alternative splicing?? awaits investigation. Not only does this interaction enhance the effect of VEGF-A on endothelial cells in culture (Wijelath et al., 2002)(Wijelath et al., 2006) merge refs, the VEGF-FN complex appears to have strong implications *in vivo*. Thrombin-activated platelets secrete VEGF-A pre-bound to FN, which could be significant with regards to neovascularisation during wound healing (Wijelath et al., 2006). In the mouse retina, FN cooperates with heparan sulphate proteoglycans in binding VEGF-A to promote directional migration of endothelial tip-cells and expansion of the retinal vasculature (Stenzel et al., 2011). The functional implications of the interaction of VEGF-A with FN will be addressed in a subsequent chapter (4.4.2.4).

4.3.5.2 TGF-β

The cytokine TGF-β has evolved a particularly interesting mode of storage because immobilisation of latent TGF-β in the ECM depends on the presence of fibrillar FN. TGF-β 1, -2 and -3 isoforms are prototypes of the large, multi-potent TGF- β family of secreted cytokines that bind and activate membrane-bound TGF-β receptor serine/threonine kinase signalling complexes I and II (TGF-βR-I and –II) to regulate cell growth, inflammation, matrix synthesis and apoptosis (Taipale et al., 1998). In this signalling complex, ligand binding to TGF-βR-II phosphorylates and thereby activates the TGF-βRI, which propagates signals from the plasma membrane to the nuclus via the SMAD (a portmanteau of the names for the homologous *Drosophila* protein, mothers against decapentaplegic (MAD) and the *Caenorhabditis elegans* protein SMA (from gene *sma* for small body size)) family of proteins. In most cell types, receptor-regulated SMADs (R-SMAD; SMAD2, SMAD3, SMAD1, SMAD5 and SMAD8) are specifically phosphorylated in response to TGF-β R-I activation. Upon phosphorylation, they associate with the common mediator SMAD4 (co-SMAD4) and translocate into the nucleus to facilitate the transcriptional activation of TGF-β target genes. Among other major morphogeneic processes, the TGF-β family proteins are involved in cardiovascular development and hematopoiesis in the embryo as well as adult tissue homeostasis (ten Dijke and Arthur, 2007).

Most cell types secrete TGF-β, which is synthesised as a homo-dimeric pro-protein (fig. 4.12). The dimeric pro-peptide, also known as latency associated peptide (LAP), undergoes cleavage by furin convertase, but remains non-covalently associated with mature TGF-β, and, as the name implies, renders the mature TGF-β latent by preventing it from binding TGF-β receptors (Lawrence et al., 1984; Dubois et al., 1995). The complex formed through association of mature TGF-β and LAP is

referred to as the small latent complex (SLC). During synthesis, the SLC becomes covalently associated with an ECM protein called latent TGF-β binding protein (LTBP) through disulfide bonds between cysteines in LAP and LTBP (Miyazono et al., 1991; Gleizes et al., 1996; Saharinen et al., 1996; Saharinen and Keski-Oja, 2000). This ternary complex is commonly referred to as the large latency complex (LLC). In essence, LTBP functions as a chaperone of TGF-β, serving three important roles by (i) facilitating the secretion of the SLC, (ii) targeting the SLC to the ECM and (iii) keeping mature TGF-β in inactive state (Miyazono et al., 1991; Taipale et al., 1994; Rifkin, 2005).

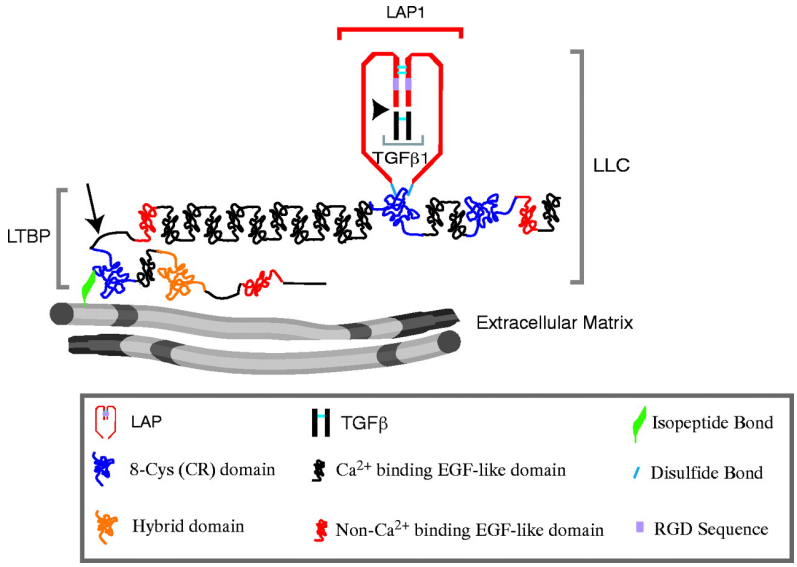

Figure 4.12. The TGF-β large latent complex, comprising TGF-β, LAP and LTBP. TGF-β and its propeptide are non-covalently associated, while LAP and covalently linked to LTBP via disulfide bonds. LAP contains two RGD motifs. LTBP is cross-linked to other ECM components, such as FN and fibrillin, through transglutaminase-generated isopeptide bonds. In FN, this involves the N-terminal 70kDa fragment. Adapted from (Annes et al., 2004).

The LTBP proteins are members of the LTBP/fibrillin family of extracellular proteins, which comprises fibrillin-1, -2 and 3, as well as LTBP-1, -2, -3 and -4 (Ramirez and Pereira, 1999). The LTBPs have distinct binding specificities for TGF-β isoform pro-peptides; LTBP-1 and -3 are the most prominent in their binding to all three TGF-β pro-peptide isoforms, whereas LTBP-4 bind only weakly to LAP1/TGF-β1 and LTBP-2 fails completely to bind any of the LAP1/TGF-β1 isoforms (Saharinen and Keski-Oja, 2000) (fig 4.13). Mice homozygous for a knock-in mutation that disrupts the association of LAP1 with LTBP show traits similar to the TGF-β1 knockout phenotype (Yoshinaga et al., 2008).

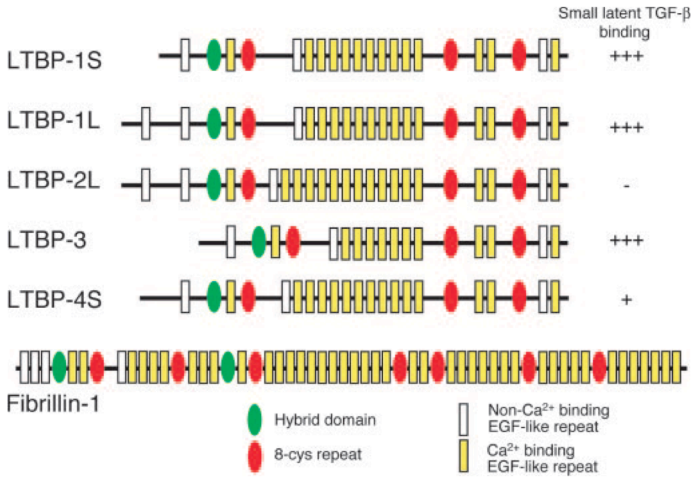

Figure 4.13. A schematic illustration of LTBP isoforms and comparison with part of the fibrillin-1 structure. On the right, the relative binding affinities of cloned LTBPs for TGF-β, where LTBP-1 and -3 are found to bind all LAP-TGF-β isoforms and LTBP-4 binds only LAP1-TGF-β1. Adapted from (Rifkin, 2005).

The interaction of LTBPs and LLC with ECM is essential in maintaining tissue homeostasis; an inability to store the LLC in the ECM may result in excess LLC, which can interact with latent TGF-β activators that are normally separated from sequestered LLC (Neptune et al., 2003). LTBPs become incorporated into the ECM through covalent bond formation involving one or several 8 cysteine repeats (8-cys repeat) (Nunes et al., 1997; Unsöld et al., 2001). This covalent association with the ECM involves a glutamine-lysine isopeptide bond in the 8-cys repeat near the N-terminus of LTBP that is catalysed by tissue transglutaminase (Nunes et al., 1997). A number of studies have investigated ECM binding partners of the LTBPs and there is a general agreement that direct binding of LTPB with fibrillin or fibronectin provides two potential modes for LTBP to interact with the ECM(Dallas et al., 2005; Taipale et al., 1996; Kantola et al., 2008) (Isogai et al., 2003; Vehviläinen et al., 2009; Massam-Wu et al., 2010). A recent systematic approach to understanding the contributions of fibrillin-1, -2 and fibronectin to LTBP deposition into the ECM *in vivo* has demonstrated that while LTBP-1 association with the ECM relies on the presence of a fibrillar FN network, LTBP-3 and -4 rely on fibrillin-1 for their incorporation into the ECM (Zilberberg et al., 2012). Interestingly, fibrillin assembly into the ECM has also been shown to depend on FN (Kinsey et al., 2008; Sabatier et al., 2009). These results collectively build a scenario in which fibrillar FN is at centre stage for the incorportation of LTBP and LLC into the ECM (Zilberberg et al., 2012). Heparin-binding domains in LTBP-1 and LTBP-4 have been shown to be critical for their deposition into the ECM (Chen et al., 2007; Kantola et al., 2008), suggesting that heparan sulfate proteoglycans may play a critical role in controlling the association of LTBP with FN and subsequent deposition of LTBP into the ECM.

The activity of latent TGF-β activity is governed by the release of TGF-β from latency. Several diverse mechanisms have been described for the process of latent TGF-β activation. Denaturing conditions, such as heat, low pH, enzymatic digestion and detergents have proven efficient for TGF-β release in *in vitro* assays (Miyazono and Heldin, 1989; Brown et al., 1990). TGF-β is also reported to undergo activation when exposed to reactive oxygen species or irradiation (Barcellos-Hoff et al., 1994; Barcellos-Hoff and Dix, 1996). The activation of TGF-β in cell culture is achieved by proteolytic

cleavage of LAP by plasmin and other proteases (Taipale et al., 1994; Yu and Stamenkovic, 2000; Ge and Greenspan, 2006). Thrombospondin-1 has been identified as a physiological regulator of latent TGF-β activation by binding LAP and inducing conformational changes that reduce its affinity for TGF-β and thereby enable TGF-β to interact with its cognate receptor (Crawford et al., 1998; Ribeiro et al., 1999). Perhaps of greatest physiological relevance is integrin-mediated activation of TGF-β (Yang et al., 2007; Wipff and Hinz, 2008). Many of the αV integrins bind RGD motifs present both in LAP-1 and -3, and integrins αVβ3, αVβ5, αVβ6 and αVβ8 have been shown to release and activate TGF-β in cell culture experiments (Munger et al., 1999; Annes et al., 2002; Mu et al., 2002; Fjellbirkeland et al., 2003; Annes et al., 2004). The physiological relevance of αVβ6 and αVβ8 integrin-mediated TGF-β activation by binding LAP *in vivo* is supported by the fact that mice lacking αV, β6 or β8 or possessing a $LAP^{RGE/RGE}$ mutation phenocopy important aspects of TGF-β1 and TGF-β3 knockout mice (Shull et al., 1992; Dickson et al., 1995; Kaartinen et al., 1995; Munger et al., 1999; Zhu et al., 2002; Yang et al., 2007; Aluwihare et al., 2009).

Integrins are proposed to facilitate latent TGF-β activation by either of two distinct mechanisms. In one model, integrin αVβ8 bound to the LLC via LAP recruits trans-membrane type 1 matrix metalloproteinase (MT1-MMP) to cleave LAP and liberate TGF-β (Araya et al., 2006; Mu et al., 2002). A second mechanism of integrin-mediated latent TGF-β release has been demonstrated for αVβ5, αVβ6 and αVβ8 and is independent of proteases in that it relies on the role of integrins as mechano-transducers to transmit traction generated by the contractile actin-myosin machinery to LAP to mechanically pry apart the LLC and release TGF-β (Munger et al., 1999; Annes et al., 2004; Wipff et al., 2007). Analysis of the level of mechanical force that is required to induce the conformational changes in the latent complex that release TGF-β1 has demonstrated that TGF-β1 activation can be achieved by application of mechanical force in the order of magnitude of what can be transmitted by single integrins (Buscemi et al., 2011).

4.3.6 FN in early vertebrate development and morphogenesis

Given the multitude of functions involving FN, it comes as no surprise that a variety of morphological events in vertebrate development rely on FN, and that ultimately, FN is an absolute requirement for vertebrate survival. This is made explicitly clear by the embryonic lethality of fish, frogs and mice carrying mutations that disrupt FN expression. While quite a few ECM molecules, such as laminins and collagens, arose early in evolution and are conserved from fly to human, FN evolved in the vertebrate phylum and thus coincided with the development of an endothelial-lined cardiovascular system (Hynes and Zhao, 2000). Indeed, the embryonic lethality of these vertebrate model organisms is to a great extent related to defects in the developing cardiovascular system. However, FN expression and function is certainly not restricted to the vascular system. In vertebrates, FN is an abundant component of ECM in a variety of embryonic tissues where it generally serves as a provisional guide to support cellular events and maintain borders in the developing vertebrate embryos, as well as in adult tissues where it serves as a provisional matrix in the healing wound.

Vertebrate embryos with disrupted FN expression die during gastrulation with a number of defects. Much of our understanding of FN functions during embryonic development comes from genetic knockout experiments in mouse, morpholino experiments in zebrafish and the use of function-blocking antibodies in frog (George et al., 1993; Georges-Labouesse et al., 1996; George et al., 1997; Marsden and DeSimone, 2001; Davidson et al., 2002; Trinh and Stainier, 2004b; Davidson et al., 2006). FN is expressed at early stages of vertebrate embryogenesis, and examination of both frog and fish embryos show that FN is assembled into an elaborate network before gastrulation movements even begin (Critchley et al., 1979; Duband and Thiery, 1982; Sanders, 1982; Boucaut and Darribere, 1983; Lee et al., 1984). Fibrillar FN is primarily depositied in the endodermal and ectodermal basal surfaces in the chick embryo, and in frog embryos fibrillar FN is found along the blastocoel roof, where it is has been shown to serve as a migration platform for the mesoderm (Boucaut et al., 1984a; Boucaut et al., 1984b; Brown and Sanders, 1991; Winklbauer and Keller, 1996).

In general, inactivation of the *Fn1* gene permits partial progression through gastrulation, and the absence of FN does not affect the gastrulation movements that give rise to the three germ layers, the endoderm, mesoderm and ectoderm. Neither does the absence of FN affect the specification of the various mesoderm regions (axial, paraxial/presomitic or lateral mesoderm). Likewise, neither the timing and location of induction of mesodermal lineages, such as the notochord, somites and heart, nor the ability of the precursor cells of these lineages to migrate, depend on the presence of FN protein (Georges-Labouesse et al., 1996; George et al., 1997; Trinh and Stainier, 2004b; Davidson et al., 2006). Later events, such as migration of neural crest cells to their final destinations is also independent of FN (Mittal et al., 2010). However, despite apparent correct cell fate specification, differentiation and migration of precursors in the absence of FN, the correct morphogenesis of the structures they will assemble ultimately relies on the presence of FN protein. For regardless of species, the consequences of disrupting the expression of FN are that somite precursors will fail to condense into somites (Georges-Labouesse et al., 1996; Jülich et al., 2005; Koshida et al., 2005), the notochord precursors will fail to form a notochord (Georges-Labouesse et al., 1996) and the cardiac precursors will fail to form a functional heart (George et al., 1997).

Elegant work in re-investigating the FN knockout mouse has revealed that FN is required as early as during morphogenesis of the node, which takes place at the tip of the primitive streak, and for the subsequent establishment of left-right asymmetry in the embryonic body plan (Pulina et al., 2011). FN protein localises to the basal surface of the ventral node, and is speculated to be important for the proper orientation and vertical intercalation of nodal cells. In the absence of FN, cells within the node fail to arrange into two well-organised layers and instead become aberrantly oriented, which gives the node a disrupted, narrow and flat appearance. Absence of FN also renders the node cells incapable of creating the leftward nodal flow (Pulina et al., 2011), which represents the very first symmetry-breaking event in the mouse embryo. Left-right asymmetry is maintained by barriers of morphogens established at the embryonic midline and by the notochord, and this recent report by Astrof and colleagues suggests that FN specifically regulates the expression of Lefty1/2 through Nodal signalling and activation of SMADs 2/3 at the floor plate (Pulina et al., 2011).

Closer examination of the morphogenesis defects in the frog model showed that FN plays subtle, but important roles in cellular activity during gastrulation. FN is required to establish cell adhesion and cell polarity, which are key processes underlying the major cell rearrangements of gastrulation (Marsden and DeSimone, 2001). Interaction between FN and integrins modulates cadherin-dependent cell-cell adhesion, which in turn influences cell intercalation (Marsden and DeSimone, 2003). Fibrillar FN is required to establish the elongate shape of migrating cells seen in wild type embryos and to polarise actin-rich protrusions of cells in the gastrulating embryo, all of which is essential to axial extension (Davidson et al., 2006). One speculation is that the density of FN fibrils maintains a level of stiffness and rigidity of the tissue, which is important for convergence and extension (Moore et al., 1995).

New light was recently shed on the role of FN in early lineage specification. It was recently shown that FN in cell culture experiments plays a role in the ability of endoderm to induce mesoderm formation through a FN/β1 integrin/Wnt/β-catenin signalling cascade (Cheng et al., 2013). FN, along with known diffusible factors, promotes the emergence of Brachyury positive mesoderm (Brachyury is a T-box-containing transcription factor expressed in the primitive streak and early mesoderm and one of the earliest lineage markers of mesodermal precursors (Wilkinson et al., 1990; Kispert and Herrmann, 1994; Inman and Downs, 2006)). In an integrin β1/Wnt/β-catenin axis, FN biases the mesoderm towards cardiac mesoderm (Cheng et al., 2013).

ECM formation and remodelling is also important as the embryo transitions into stages of organogenesis. Somite formation is a critical event during development and occurs as the paraxial mesoderm undergoes mesechymal-to-epithelial transition and condenses into epithelialised structures. As previously mentioned, the FN knockout mouse embryos lack somites (George et al., 1993). From analyses of the zebrafish FN null mutant (natter) and frog embryos injected with a dominant negative form of FAK (FAK-related nonkinase), it is known that FN plays both a structural and morphogenetic role in specifying domains of mesoderm during gastrulation. During somitogenesis in zebrafish, integrin α5 and FAK activation ($pFAK^{Y397}$) drives the accumulation of FN at the borders of newly formed somites, and this, in cooperation with other local signalling systems such as the Eph-Ephrin system, both establishes and maintains somite boundaries that stabilise the epithelialisation of the somites (Jülich et al., 2005; Koshida et al., 2005; Kragtorp and Miller, 2006).

A number of organs (lung, salivary gland, kidney) are formed during embryonic development by epithelial branching, and basement membrane remodelling is an important feature of branching morphogenesis. Branching morphogenesis entails repetitive formations of clefts and buds. Cleft formation requires remodelling of both epithelia and indentation of the basement membrane. During the development of salivary glands, transient expression and fibrillar deposition of FN in the cleft has been found to promote cleft formation; while FN promotes the interaction of the cell with the ECM, its presence in the cleft was found to alleviate cell-cell interactions by down-regulating E-cadherin in the epithelium (Sakai et al., 2003).

Gene knock-out studies in mice have shown that each FN-binding integrin has a unique function, but only integrin α5 knock-out gives rise to phenotypes reminiscent of the total FN knock-out mouse

(George et al., 1993; Georges-Labouesse et al., 1996; George et al., 1997); all embryos deficient in integrin α5 suffer defects in mesoderm-derived structures in both extra-embryonic and embryonic structures such as vasculature, heart and somites that cause lethality at E9.5-10. This strongly suggests that integrin α5β1 mediates the early functions of FN during embryogenesis. Yet, the loss of integrin α5 does not fully account for the FN knock-out phenotype and implies that other FN-binding integrins compensate, if only to some extent, for the loss of integrin α5β1. Integrin αVβ3 is another highly recognised FN-binding integrin, and genetic studies of αV integrin knock-out mice showed that 80% of all embryos deficient in αV integrins show placental defects and die around E10.5, while the remaining 20% survive until birth, but die shortly after with several defects, most notably intracerebral hemorrhage (Bader et al., 1998). The incomplete embryonic lethality most likely reflects the promiscuity of αV integrins, both for their β subunit and their extracellular ligand. Integrin αVβ3 alone, which binds FN, also interacts with fibrinogen, fibrillin, LAP-TGF–β, von Willebrand factor, vitronectin, osteopontin, tenascin, PECAM-1 and thrombospondin, while other αV integrins bind an equally wide range of ligands (Humphries, 2006). Interestingly, the compound knock-out of α5 and αV integrins showed synergies in their phenotypic defects, causing lethality at, or even slightly earlier than, the developmental stage of FN knock-out embryos, suggesting cooperative functions of these FN-binding integrins during mesoderm development (Yang et al., 1999). Other integrin knock-out mice show phenotypes at later developmental stages than the FN knock-out and α5/αV integrin double knock-out mouse, which indicates that the ability of these integrins to interact with FN and mediate functions of FN is not essential during development and/or that these integrins primarily rely on other ligands. Embryos lacking FN-binding α4 integrins are unable to undergo chorio-allantoic fusion and die between E10-12 (Yang et al., 1995) and mice that are deficient in FN-binding α8 integrins develop defects which cause lethality at or shortly after birth remove Kreidberg (alpha3 study) (Kreidberg et al., 1996; Müller et al., 1997). Integrin αIIbβ3 is a platelet-specific FN-binding integrin, and its ability to bind FN is essential in blood homeostasis and thrombus formation in adult stages of life.

4.4 Cardiovascular development in the mouse

4.4.1 Cardiogenesis

The heart is the first organ to form in vertebrate embryos, and it is vital for the distribution of blood-bourne oxygen, nutrients and waste products throughout the developing embryo. The heart's purpose as a central pump relies on the contractile nature of its principle component, the myocardium. The myocardial progenitor cells are derived from the epiblast and ingress through the primitive streak, along with head mesoderm and foregut endoderm, during gastrulation between E6.5 and E7.5. Although the morphogenetic process of gastrulation plays no role in cardiac specification, it serves to coordinate the spatial and temporal arrival of these cardiac precursor cells at the primary heart fields, which are two bilateral regions of splanchnic mesoderm on both sides of the embryonic midline that are specified shortly after gastrulation and fated to form the myocardium by the late primitive streak

stage (Tam et al., 1997). The two heart fields later converge at the embryonic midline to form the cardiac crescent just below the cranial parts of the embryo (Kaufman and Navaratnam, 1981; DeRuiter et al., 1992) (fig. 4.14 A and B).

Steps towards shaping the heart are induced by factors secreted from the surrounding endoderm (e.g. gut endoderm). In response to inductive signals, the cardiac crescent expresses several transcriptional regulatory genes of the cardiac programme, such as Mesp1, Nkx2-5, Gata4 and Mef2b/c (Lints et al., 1993; Edmondson et al., 1994; Heikinheimo et al., 1994) that induce the cardiac precursors to contribute to the three main cardiac tissues; endocardium, myocardium and pericardium. First, the formation of the intra-embryonic coelom introduces a lumen that spatially segregates the cardiac precursors into heart mesoderm on the ventral side of the lumen and pericardial mesoderm on the dorsal side. By E8.0, the heart mesoderm will undergo a lineage split to give rise to the myocardium and the endocardium which spatially orient themselves into a hollow tube structure; the endocardium will form the lining of the heart tube and the myocardium will become the muscular layer of the heart tube (fig 4.14 C and D).

By E8.5, the primitive heart has elongated in the cranio-caudal axis and is a peristaltic pump that moves blood unidirectionally as a result of a contractions along the tube, with the inflow region established caudally and the outflow region cranially (Moorman et al., 1998). The transformation of the primary heart tube into the four-chambered heart occurs as the myocardium undergoes a complex programme of local differentiation and proliferation along the length of the primary heart tube. Simultaneously, by local regions of growth and contraction within the heart tube and in effect of forces exerted on the heart by surrounding tissues, the heart tube is perturbed into a rightward torsion, a process referred to as looping morphogenesis (Harvey, 1998; Ramasubramanian et al., 2008), during which the caudal region of the heart becomes displaced to the left and the outflow region loops to the right of the embryo (fig 4.14 E and F). Hence looping morphogenesis lays out the basic plan for the future heart. The mechanical properties of the heart tube tissue and the induction of intracardiac blood flow are key factors in promoting this stage of cardiogenesis (Hove et al., 2003; Zamir et al., 2003)

Additional myocardial precursors arrive from the secondary heart field, which originates from the pharynx, to build the outflow tract (Kelly et al., 2001; Mjaatvedt et al., 2001). By E9.5, the atrioventricular canal is formed to delimit the atrial and ventricular regions. Endocardial cardiac cushion forms in both the outflow tract and the atrioventricular channel (Savolainen et al., 2009). The endocardial cushion is a subset of mesenchymal cells that arise from both the endocardium and neural crest cells migrating from the hindbrain (Jiang et al., 2000). These cells migrate into a FN-rich cardiac jelly and are known to deposit additional FN (Mjaatvedt et al., 1987; Ffrench-Constant and Hynes, 1988; Roman and McDonald, 1992; Eisenberg and Markwald, 1995). Cardiac cushions will condense to divide the outflow tract into the aorta and the pulmonary artery, and in both the outflow tract and the atrioventricular canal, cardiac cushion will contribute to the major valves of the heart (aortic, pulmonic, tricuspid and mitral valves) and closure of the heart septum (Webb et al., 1998; Savolainen et al., 2009).

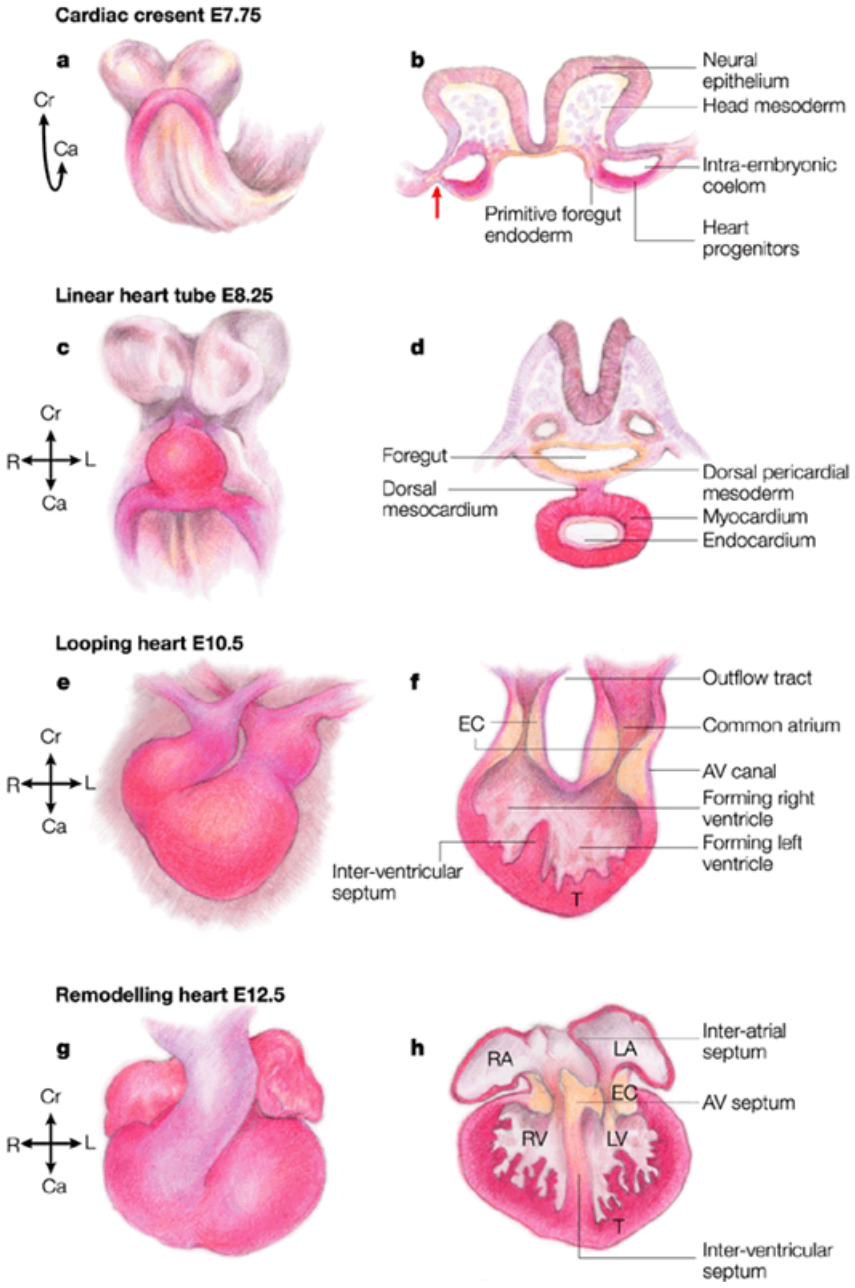

Figure 4.14. Major events in early cardiac development in the mouse embryo. Left column shows the early embryonic cardiac tissues, while the right column shows internal features in heart sections; (B) and (D) are transverse sections; (F) and (H) are longitudinal sections. Myocardium and progenitors are highlighted in red. (A-B) Cardiac progenitors assemble into the cardiac crescent extending cranio-laterally. (C-D) A linear heart tube is formed as cardiac progenitors move ventrally and fuse, differentiate and organise into an inner endocardial lining and an outer myocardial cover. Inflow occurs caudally and outflow occurs cranially. (E-F) During cardiac looping, the inflow region is placed dorsally and cradially above the developing ventricles. Endocardial cushions (EC) form in the atrioventricular (AV) canal and in the outflow tract to form the valves and split the outflow tract, respectively. Myocytes form trabeculae (T) along the inner surface of the ventricles. (G-H) By E12.5 the heart has been divided into left and right ventricles (LV, RV) and left and right atria (LA, RA) and begins to resemble the adult heart. Adapted from (Harvey, 2002).

At around E9.0, the epicardium develops and surrounds the heart to provide cellular elements of the connective tissues and coronary vasculature. Epicardial progenitor cells originate outside the developing heart and migrate onto the heart through a cyst-mediated mechanism in which the progenitors are released from the tissue of origin as cysts. These cysts float in the fluid of the pericardial cavity and attach to the myocardial surface of the heart. Once attached, the cysts

disintegrate and the cells migrate out and flatten into the epithelial sheet of the epicardium (Komiyama et al., 1987; Sengbusch et al., 2002).

Looping morphogenesis will eventually align the developing chambers according to left/right asymmetry and place the inflow portion of the heart, including the common atrium, dorsally and cranially so that it is placed above the developing ventricles by the end of E10.5 (fig 4.14 E and F). Chamber formation occurs through ballooning effect of chambers along the outer curvature of the looping heart. These chambers are characterised by trabeculated working myocardium forming a specialised inner muscle layer along the outer curvature, to which the endocardium adheres through finger-link protrusions (Christoffels et al., 2000). Trabeculated myocardium is a specialised layer of cardiac muscle that generates the contractile force of the heart and transforms the primary heart tube into a high-capacity, fast-contracting pump.

With further looping, the outflow region becomes pushed between the developing ventricles ventrally (fig. 4.14 G and H), and the inflow region spans the ventricles dorsally, now resembling the final heart structure that will persist into adulthood. The ultimate division of the heart chambers occurs by septation between the left and right ventricles and left and right atria. Finally, the cardiac conduction system is established by a specialised cardiac muscle cells that infiltrate the cardiac tissue and have distinct contractile, conductive, and pace-making properties to establish the coordinated activation of the heart (Moorman et al., 1998).

4.4.2 Requirement for FN in cardiogenesis

FN appears to be a critical regulator of cardiovascular development and vascular remodelling of the developing embryo and in the adult. Disrupting FN expression is mice causes severe defects in the the heart, vasculature and somites, causing them to die by E9.5 (George et al., 1993; George et al., 1997; Francis et al., 2002). As already mentioned, FN is dispensable for initial specification of cardiac precursors, endocardial and myocardial cells. However, the precursor cells fail to undergo the morphogenetic processes that form the functional heart and great vessels (Francis et al., 2002). Heart and vessel morphogenesis requires both the ability of the endothelium to organise into tube structures, but also requires non-endothelial cells such as mural cells to stabilise the remodelling tissue as it undergoes morphogenesis. Indeed, one speculation stemming from these studies is that FN has a role in mediating the interaction between endothelial and peri-endothelial cells (mural cells) in the heart and the dorsal aorta of the mouse.

Early studies of the WT chick embryo revealed deposits of fibrillar FN at the endoderm-mesoderm interface of the lateral heart-forming region (Linask and Lash, 1986). Precardiac (myocardial) cells encounter this fibrillar FN as they migrate along the endoderm-mesoderm interface. Levels of FN along the precardiac cell migratory route appeared to vary, with lowest amounts of fibrillar FN posterior and largest amounts anterior, where precardiac cells must stop moving. This gradient of fibrillar FN coincides with directional migration, i.e. haptotaxis, suggesting that precardiac cells find their destination by migrating along a substrate with increasing adhesiveness provided by FN.

During heart tube formation in zebrafish, FN is also critical for the timely migration of myocardial cells and their subsequent organisation at the embryonic midline to form the primitive heart tube (Trinh and Stainier, 2004a; Trinh and Stainier, 2004b). FN becomes deposited in the basal substratum around sheets of myocardial precursors and along the midline between endoderm and endocardial precursors (Trinh and Stainier, 2004b). The *nat* mutation, which stalls FN expression, allows myocardial specification, but the heart fails to form correctly and develops into cardia bifida because adherens junctions in the myocardial epithelia are not formed properly (Trinh and Stainier, 2004b). The interaction of the myocardium with a FN-based substratum stabilises the formation of adherens junctions between myocardial precursors, which in turn provides integrity to the organisation of the myocardial epithelia (Trinh and Stainier, 2004b). This integrity is critical to the coordinated movement of myocardial precursors during heart formation.

The high expression of FN in the cardiac jelly and cushion (Mjaatvedt et al., 1987; Ffrench-Constant and Hynes, 1988; Roman and McDonald, 1992; Eisenberg and Markwald, 1995) prompts the question of what function FN has in the cardiac cushion. The role of FN in cushion formation has been tested in chick embryos by microinjecting antibodies against FN into the cushion tissue. These experiments showed that FN plays a role in the migration of mesenchymal cushion cells into the cardiac jelly (Loeber and Runyan, 1990; Icardo et al., 1992), although FN is most likely not the only ECM component to modulate the activity of these mesenchymal cardiac cells (Loeber and Runyan, 1990).

4.4.3 Vasculogenesis and angiogenesis

The development of blood vessels is a key step during early vertebrate development, and the ability of blood vessels to form and remodel after birth sustains the growth and repair of tissue throughout life. Dysregulation of blood vessel formation has dire consequences at early stages of development, as the growing embryo requires greater oxygen and nutritional supply from the blood. Consequently, mutations that delay or impair blood vessel formation cause embryonic lethality.

The vascular system is a specialised network of vessels that branch in a hierarchical fashion to spatially accommodate all parts of the organism and to both deliver and collect nutrients, respiratory gases and waste products as well as transport surveying immune cells to sites of infection. The main components of the blood vessel wall are the endothelial cells, mural cells and the ECM that constitutes the vascular basement membrane. The important features of a vascular tube include apical–basal polarity of the endothelium, a continuous lumen, a glycocalyx, the distinct transmembrane proteins lining the luminal side, elaborate junction complexes at the lateral side between the lining endothelial cells and deposition of basement membrane at the basal, ablumenal side (Wacker and Gerhardt, 2011).

The vascular system arises very early during development through a series of dynamic, but highly coordinated events, generally referred to as vasculogenesis and angiogenesis. By branching, expanding and pruning of vessels, the vascular bed becomes highly optimised to meet local demands. Each step is under tight and complex molecular regulation, and a significant part of blood vessel formation depends on integrins and ECM components such as FN.

4.4.3.1 Vasculogenesis

Vasculogenesis is initiated in the developing embryo as FGFs secreted by the mesoderm induce the differentiation of hemangioblasts to give rise to the angioblast lineage (Risau and Flamme, 1995). Within the embryo, the very first embryonic blood vessels form as angioblasts acquire arterial or venous fate in the process of coalescing into the dorsal aorta and the cardinal vein, respectively. In the yolk sac, populations of haemangioblasts merge into primitive blood islands, from which both endothelial cells and cells of the hematopoietic lineages segregate. These blood islands fuse and remodel extensively in response to hemodynamic stimuli, oxygen levels and gradients of pro-angiogenic growth factors, to form a primitive plexus of arterial and venous vessels. Vasculogenesis will ultimately accomplish the complete vascularisation of the organism.

Initially, angioblasts fuse into an initial cord-like structure and maintain this structure through adhesive forces to the ECM (mediated by integrins) and neighboring cells (through adherens junctions). Within the endothelium, adherens junctions are composed of vascular endothelial cadherin (VE-cadherin), α-catenins and β-catenins and are linked to the actin cytoskeleton. The balance of cell-ECM and cell-cell junctions is important during cell polarisation and lumen formation (Zovein et al., 2010; Xu et al., 2011).

Various models and mechanisms have been described for lumen formation during vasculogenesis (Iruela-Arispe and Davis, 2009). For various vessel types, such as the mouse embryo dorsal aorta and the zebrafish embryo intersegmental vessels, lumen formation occurs by lumenisation, where the coalesced angioblasts/EC undergo dramatic shape changes to create a lumen at the cell-cell junction (Blum et al., 2008; Strilić et al., 2009).

To accommodate this lumen, the endothelial cells within the early cord must collectively determine polarity to establish apical and basolateral membranes. In the mouse aorta, adherens junctions containing VE-cadherin initially fully line the interface between what will become the apical surfaces between opposing endothelial cells (fig. 4.15). Integrins in the basolateral endothelial cell surface will mediate the interaction of the developing blood vessel with the ECM in the vascular basement membrane. Polarity is established in part by the activation of the Par3 (Partitioning defective 3) complex (consisting of Par3, Par6 and the atypical protein kinase C) (Koh et al., 2008; Zovein et al., 2010). In vitro studies have shown that PTEN (phosphatase and tensin homolog) is subsequently recruited to the apical surface, where it converts PIP_3 to PIP_2 and thereby recruits Cdc42 to promote the cytoskeletal rearrangements that assist in lumen formation (Koh et al., 2008; Kesavan et al., 2009).

VE-cadherin probably play multiple roles in defining the apical surface and driving lumen expansion. It has been shown to drive the accumulation of negatively charged CD34 sialomucin glycoproteins (CD34 and podocalyxin (PODXL). First, CD34 sialomucins were shown to participate in directing the cytoskeletal events that underly changes in cell shape with the induction of apical/basal polarity and lumenisation by integrating with the F-actin cytoskeleton through phosphorylated ERM adaptor protein moesin. Moesin requires PKC for phosphorylation, and hence both the recruitment and phosphorylation of moesin at the apical membrane could be related to the activation and localisation of the PCK-containing Par3 complex (Bretscher et al., 2002; Strilić et al., 2009; Wang et al.,

2010). A follow-up study demonstrated that in addition to participating in cytoskeletal remodelling events, the enrichment of sialomucin gives rise to an accumulation of negative charge on opposing membranes that serves to electrostatically repel apical membranes away from each other and thereby initiate the expansion of the extracellular space (Nielsen and McNagny, 2008; Strilić et al., 2010). VE-cadherin has also been shown to influence the contractility of the F-actin cytoskeleton in endothelial cells during lumen formation. Via β-catenin, plakoglobin and α-catenin, VE-cadherin becomes linked to the F-actin-cytoskeleton. Through its interaction with p120, a RhoA GDI, VE-cadherin is thought to fine-tune the regulation of the RhoA pathway. To form a tube of an appropriate diameter, endothelial cells acquire a stretched, flattened morphology. This change in shape is driven by an enrichment of MLC phosphorylation and NMII-driven actomyosin contractility at the apical membrane, which is triggered by VEGF-A-induced ROCK activation (Strilić et al., 2009).

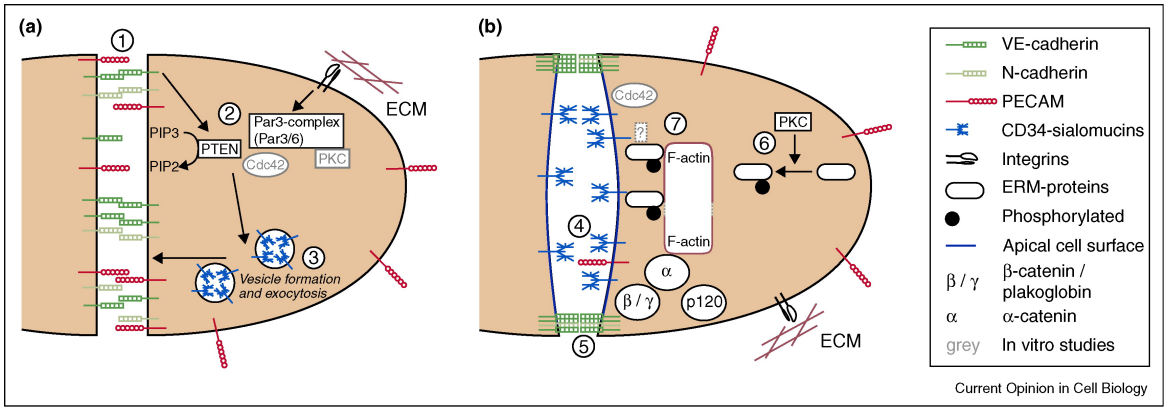

Figure 4.15. A diagrammatic representation of early endothelial cell polarisation events leading up to vascular lumen formation of an endothelial cord. Two opposing endothelial cells within a cord are shown in cross-section. (A) Junctional proteins line what is to become the apical surfaces of opposing endothelial cells. Activation of the Par3 polarity complex downstream of active β1 integrins on the basolateral surface promotes the deposition of PIP_2 in the apical plasma membrane, which in turn recruits Cdc42 to drive the exocytosis of vesicles containing negatively charged CD34 sialomucins at the apical surface that will repel the surfaces. (B) VE-cadherin translocates to the apical-basolateral borders, and both VE-cadherin and CD34 siamomucins become linked to the F-actin cytoskeleton. Adapted from (Zeeb et al., 2010).

4.4.3.2 Angiogenesis

The remodelling of the early primitive plexus of newly lumenised blood vessels into a functional hierarchy of branched vessels requires extensive morphological events, which are collectively referred to as angiogenesis (Risau, 1997). Angiogenic sprouting from the dorsal aorta, cardinal vein and vessels of the vascular plexus underlies much of this hierarchy of arteries, arterioles, capillary beds, venules and veins. VEGF-A induces many distinct aspects of endothelial cell behaviour during sprouting angiogenesis, including endothelial proliferation, migration, differentiation and survival. In the early postnatal retina, for example, VEGF-A induces angiogenic sprouting by guiding filopodial extension from specialised endothelial cells, called tip cells, situated at the tips of the vascular sprouts (Gerhardt et al., 2003). Growth of an angiogenic sprout occurs as a tip cell expresses proteases, including MMPs and MT-MMPs, to digest the surrounding basement membrane and allow outgrowth from the pre-existing vessel (Pepper, 2001; Chun et al., 2004). Tip cells are followed by proliferating stalk cells,

which form the base of the angiogenic sprout and are both far less motile and extend far fewer filopodia than tip cells (Gerhardt et al., 2003). The shape of an angiogenic sprout is determined by the weight of tip cell migration against stalk cell proliferation, which in turn is dictated by both the expression pattern of VEGFR types (VEGFR-1, -2 and -3) as well as gradients of VEGF-A (Gerhardt and Betsholtz, 2005). The molecular signature underlying the functional differences between tip and stalk cells is based on a delta-like4-(Dll4-) and Notch-mediated lateral inhibition mechanism in which VEGF-A induces Dll4 expression in the tip cell, which in turn induces Notch signal activation in the neighboring stalk cell. Notch activation in stalk cells downregulates the expression of VEGFR-2 and thereby their response of the stalk cell to the VEGF-A gradient (Hellström et al., 2007; Leslie et al., 2007; Lobov et al., 2007; Roca and Adams, 2007; Siekmann and Lawson, 2007; Suchting et al., 2007). Newly formed vessel sprouts will anastamose and form new lumens, thereby opening new sites of blood flow.

Although there is an absolute requirement for all known VEGFR types for vascular development, a differential expression pattern of VEGFR types on tip and stalk cells fine tunes the effect of VEGF-A on the angiogenic sprout. While tip cells express VEGFR-2 and VEGFR-3, which are both potent receptor tyrosine kinases and signal transducers, stalk cells express and secrete a soluble form of VEGFR-1, which serves as a decoy receptor that sequesters soluble VEGF-A (Chappell et al., 2009). Soluble VEGFR-1 secreted at the base of the angiogenic sprout modulates the local VEGF-A gradient to promote sprouting away from the stalk and prevents the new sprout from fusing with the vessel it originated from (Chappell et al., 2009).

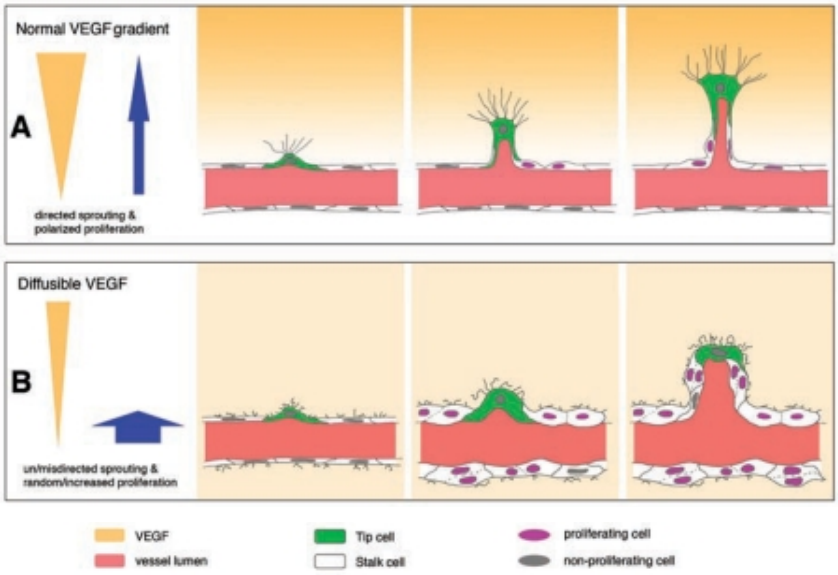

Figure 4.16. Cellular mechanisms that pattern vascular sprouting. The sequential steps from left to right illustrate the induction of a tip cell (green) and the extension of a vascular sprout towards along a gradient of VEGF-A (orange) through migration of the tip cell and polarised proliferation of the stalk cells (white). The steepness of the VEGF-A gradient determines the efficiency of the sprouting, such that a steep VEGF-A gradient promotes long and directed filopodial extension and fast migration in the tip cell (A) and a weak VEGF-A gradient results in undirected extension of short filopodia extension and slow migration of the tip cell, while stalk cells proliferate more in response to more abundant VEGF-A, but in an unpolarised manner, causing vessel dilation. Adapted from (Gerhardt, 2008).

VEGF-A gradients are established through a combination of secreted VEGF-A isoforms that differ in their ability to become immobilised by the ECM. Through alternative splicing, VEGF-A either lacks or acquires heparin-binding domains; those VEGF-A isoforms that lack heparin-binding domains are freely diffusible, while others are bound by ECM or cell surface heparan sulfates upon secretion and cannot diffuse far from the cellular source (Ruhrberg, 2003; Gerhardt, 2008). A steep VEGF-A gradient is key to polarising the endothelial tip cell and promoting long, directed filopodia extension towards higher VEGF-A concentration (fig. 4.16 A). In the mouse retina, heparan-sulfate proteoglycans cooperate with FN in binding and storing VEGF-A secreted by astrocytes to promote directional filopodial extension and migration of the endothelial tip cells and guide the radial expansion of the retinal vasculature (Stenzel et al., 2011). If a sharp gradient of VEGF-A fails to form, tip cells will extend short filopodia in all directions and migrate slower, while stalk cells will proliferate due to the abundant VEGF-A and cause vessel dilation and hypertrophy (fig. 4.16 B).

Following the establishment of the basic capillary plexus of vessels through sprouting angiogenesis, the distribution of vessels is optimised to meet the local demand of the tissue. To this end vessels undergo splitting and growth *in situ* through a process termed intussusceptive angiogenesis. This mode of angiogenesis remodels the plexus into a tree-like arrangement. Intussusceptive angiogenesis is intiated as opposing endothelial cells of the same vessel walls protrude into the lumen and establish interendothelial contact in the form of transvascular pillars. Perforation and expansion of these pillars splits a single vessel in two (Burri et al., 2004). Both the sprouting and intussusceptive modes of angiogenesis are depicted in figure 4.17.

Vessel remodelling, maturation and stabilisation are critically dependent on both the deposition of ECM into the vascular basement membrane (Iruela-Arispe et al., 1991a; Iruela-Arispe et al., 1991b) and the acquisition of mural cell coverage of the newly formed blood vessel (Darland et al., 2003; Gerhardt and Betsholtz, 2003). Depending on the type and function of the blood vessel, mural cells differ in number, type, origin and organisation. The type of mural cell that associates with newly formed vessels and microvessels in general, such as arterioles and venules, is referred to as a pericyte. Those mural cells that line larger vessels, such as arteries and veins, are called vascular smooth muscle cells (vSMCs). Mural cells are generally contractile, owing to the expression of contractile filaments such as α-smooth muscle actin (α-SMA) and desmin. They use long cytoplasmic processes to wrap themselves around the abluminal surface of an endothelial cell-lined vascular tube. Mural cells originate from various embryonic tissues (Gerhardt and Betsholtz, 2003), such as the neural crest (Bergwerff et al., 1998; Etchevers et al., 2002), the coronary vessels of the heart (Vrancken Peeters et al., 1999) or mesenchymal cells surrounding the dorsal aorta (Drake et al., 1998; Hungerford and Little, 1999). Mesenchymal cells associate with the sprouting endothelium by responding to a chemotactic gradient of PDGF-BB secreted by the sprouting endothelium (Hellström et al., 1999; Enge et al., 2002; Abramsson et al., 2003), after which they progressively differentiate into mural cells. Although still little is known about the mechanisms by which these two cell types associate with each other during developmental vascularisation, integrin α4β1 expression on the endothelium and VCAM-1 expression by proliferating mural cells is thought to mediate their close intercellular adhesion and is critical for the

survival of both endothelial cells and mural cells (Garmy-Susini et al., 2005). Pericytes help to stabilise the newly formed vasculature by contributing to the vascular basement membrane, either by secreting ECM proteins themselves and/or by stimulating the endothelium to secrete ECM proteins, such as FN, nidogen, perlecan and laminin isoforms (Mandarino et al., 1993; Stratman et al., 2009; Turlo et al., 2012). Pericytes are particular in that they embed themselves within the basement membrane of microvessels and are thought to interact with the endothelium through paracrine signalling and by direct physical contact at gap junctions and adhesion plaques shared with endothelial cells (Rucker et al., 2000). Functions of pericytes include ensuring the survival of the endothelium by secreting growth factors like VEGF-A (Shepro and Morel, 1993; Darland et al., 2003), regulating the capillary diameter of newly formed vessels by controlling endothelial proliferation (Orlidge and D'Amore, 1987; Hirschi et al., 1999; Hellström et al., 2001) and controlling lumen morphology (Hellström et al., 2001), which is how pericytes influence the flow of blood. The absence of pericytes correlates with endothelial hyperplasia, increased capillary diameter, abnormal EC shape and ultrastructure, changed cellular distribution of certain junctional proteins, and morphological signs of increased endothelial permeability (Hellström et al., 2001).

TGF-β is implicated in the maturation of new vessels by acting on both endothelium and pericytes (ten Dijke and Arthur, 2007) (fig 4.17). Both endothelial cells and pericytes produce latent TGF-β, which is stored in the vascular basement membrane. Results from *in vitro* studies implicate that the activation of the latent TGF-β may require the presence of both cells and their cell-cell adhesion via direct physical contact at gap junctions or adhesion plaques (Antonelli-Orlidge et al., 1989; Sato and Rifkin, 1989; Sato et al., 1990; Ding et al., 2004).

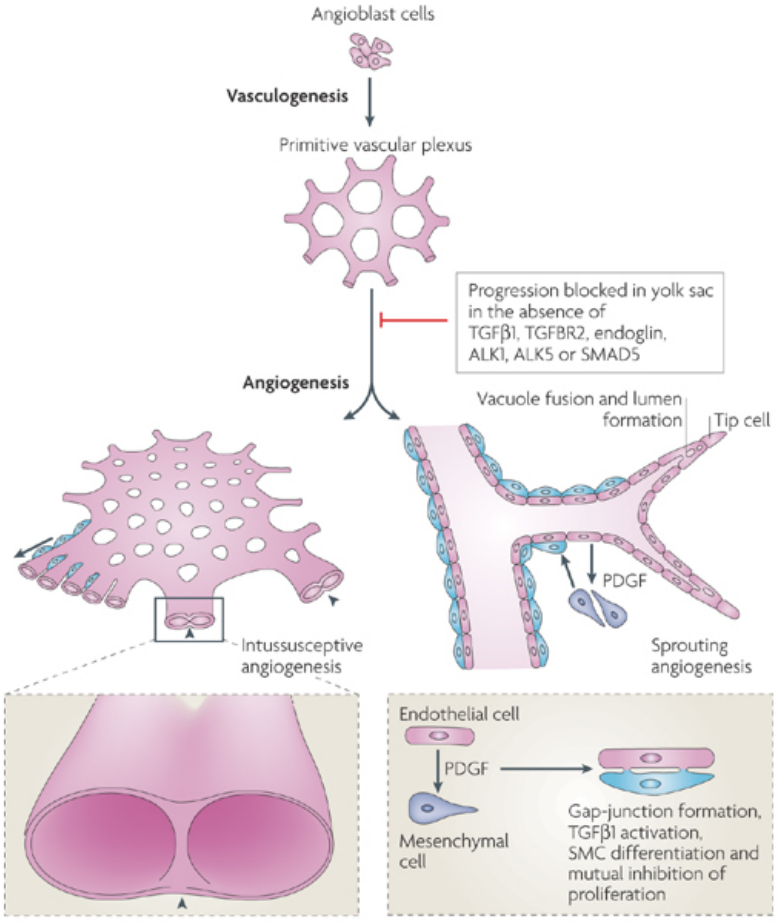

Figure 4.17. TGF-β signalling in blood vessel development. Vasculogenesis is not dependent on TGF-β. However, the progression of the primitive vascular plexus into a remodelled state by angiogenesis is blocked in the absence of TGF-β signalling components. Latent TGF-β is stored in the vascular basement membrane and requires juxtapositioning of mesenchymal cell and endothelial cell. Mesenchymal cells are recruited to the remodelling vasculature through PDGF gradients. TGF-β induces vSMC differentiation and regulates the angiogenic activity of the remodelled vasculature. Adapted from (ten Dijke and Arthur, 2007).

Endothelial cells promote paracrine TGF-β signalling to neighbouring mesenchymal cells to promote their differentiation to pericytes or vSMCs (Chen and Lechleider, 2004; Ding et al., 2004; Hirschi et al., 2003). The effects of TGF-β on the endothelium are far less clear. Both pro- and anti-angiogenic properties have been ascribed to TGF-β. Endothelial cells express high amounts of TGF-β during embryogenesis (Akhurst et al., 1990), but *in vitro* studies show that the response of endothelial cells to TGF-β is contextual, dose-dependent and biphasic (Pepper, 1997) (fig 4.18). This biphasic dose-response curve of TGF-β on endothelial cell migration may be attributable to the fact that endothelial cells express two distinct TGF-β type I receptors (ALK1 and ALK5) that respond to different concentrations of TGF-β, utilise different co-receptors (e.g. endoglin promotes TGF-β-activation of ALK1, specifically (Lebrin et al., 2004)) and phosphorylate specific sets of SMAD proteins, which in turn elict distinct genetic programmes (Goumans et al., 2002). Therefore, whether TGF-β promotes endothelial cell proliferation, migration and tube elongation, i.e. features of the active phase of angiogenesis, or whether TGF-β puts endothelial cells in a quiescent state depends on the balance in the activation of ALK1 and ALK5.

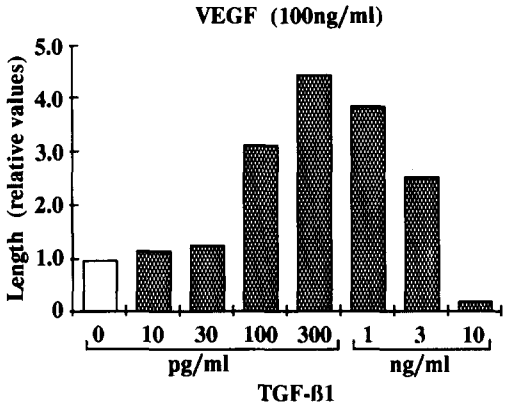

Figure 4.18. The biphasic effect of TGF-β on VEGF-induced angiogenesis *in vitro*. Total additive length of invading cell cords of bovine microvascular endothelial cells grown on the surface of three-dimensional collagen gels and treated with VEGF-A and TGF-β. TGF-β has a positive effect on VEGF-induced invasion of collagen gels, but has an inhibitory effect on VEGF-induced invasion at high concentrations. Adapted from (Pepper, 1997).

4.4.4 Role of integrins in blood vessel formation and remodelling

Endothelial cells express a range of integrin heterodimers, which in turn facilitate the interaction with a number of ECM proteins to coordinate the cytoskeletal rearrangements underlying endothelial morphogenesis, sprouting, vacuole and lumen formation during vasculogenesis and angiogenesis (Avraamides et al., 2008).

While there is substantial evidence that endothelial cell-ECM adhesions containing β1 integrins are generally required to establish a functional vascular bed (Drake et al., 1992; Carlson et al., 2008; Lei et al., 2008; Tanjore et al., 2008; Zovein et al., 2010), β1 integrins play a key mechanistic role in shaping the endothelial cytoskeleton, orchestrating vascular morphogenesis during EC polarisation, expansion of the arterial lumens as well as guiding the processes that define branching points and arterial-venous borders (Zovein et al., 2010).

In the mouse arterial endothelium, β1 integrins are predominantly found on the basal membrane and anchors the endothelium to the basement membrane and mesenchyme (Xu et al., 2011). From here, β1 integrins regulate endothelial cell polarity by inducing the activation of the Par3 complex, a well-documented determinant in cell polarity (Suzuki and Ohno, 2006; Zovein et al., 2010) that localises with β1 integrins at the endothelial basal membrane (Zovein et al., 2010). β1 integrins help to promote lumen formation by regulating the expression levels of junction proteins, such as VE-cadherin and PECAM-1 (Zovein et al., 2010), and driving these and other junction proteins (such as claudin 5 and CD99) to the lateral membranes of the lumenised vessels, where they build adherens junctions and stabilise EC-EC contacts (Zovein et al., 2010). β1 integrins are involved in promoting lumenisation by promoting the apical localisation of the CD34 sialomucin glycoprotein, PODXL (Zovein et al., 2010). The rapid expansion of an ECM-free luminal space between apical surfaces depends on the formation and coalescence of pinocytic intracellular vacuoles at the apical surface of endothelial cells. Intracellular vacuole formation and membrane targeting in endothelial cells are driven by integrin signalling and both Ccd42 and Rac1 GTPase-dependent modifications of the actin cytoskeleton (Folkman and Haudenschild, 1980; Bayless and Davis, 2002; Davis and Bayless, 2003;

Downs, 2003; Davis et al., 2007; Koh et al., 2008) (fig. 4.19). The importance of vacuole delivery to an intercellular lumen has been confirmed *in vivo* with two-photon live imaging studies in zebrafish (Kamei et al., 2006), although this mode of lumen expansion is disputed by other observations (Blum et al., 2008). However, when β1 integrins are deleted from the arterial endothelium, endothelial cells tend to accumulate vacuoles intracellularly (Zovein et al., 2010). This confirms that once intracellular vacuoles form, β1 integrins are required to promote their directional transport to, and fusion with, the apical plasma membrane to expand the lumen.

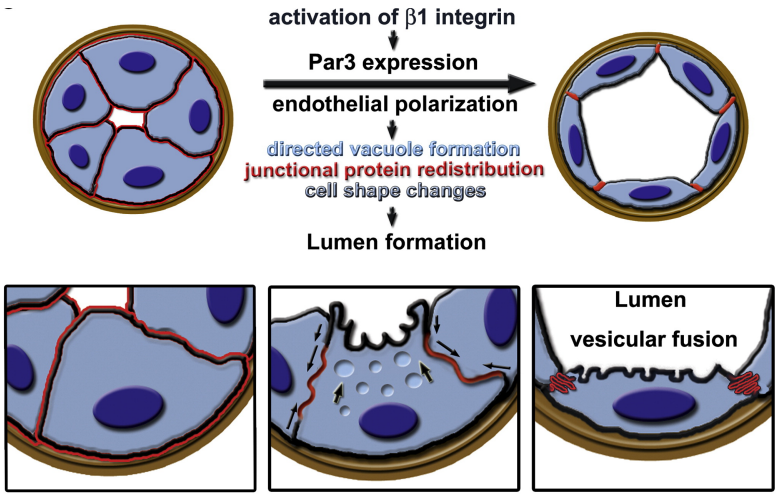

Figure 4.19. Schematic diagram illustrating the role of integrin β1 subunit in promoting lumen formation. The activation of b1 integrins on the basolateral surface of the endothelium induces the expression of Par3, which will direct the formation of vacuoles and their fusion with the apical surface. The expansion of the lumen is associated with the redistribution of junctional proteins, such as VE-cadherin, and changes in cell shape caused by remodelling of the actin cytoskeleton. Adapted from (Zovein et al., 2010).

There is also an essential requirement for β1 integrins in the assembly of vascular ECM by mural cells. An example is that of vSMCs that line the aorta during embryonic development; here, β1 integrins are not required for smooth muscle cell proliferation, migration or differentiation, but rather specifically required for aortic arch remodelling and for the assembly of ECM proteins within the vessel wall (Turlo et al., 2012).

While it is clear that β1 integrins are strong players in developmental angiogenesis, it is far less clear which α integrins are involved. The complete knockout of α4 integrins in mouse (α4β1 and α4β7, which both bind CS1 regions present in specific isoforms of FN and VCAM1) causes embryonic lethality at E10.5-11.5 due to defective chorio-allantoic fusion and defects in both epicardium and coronary vessels causing cardiac hemorrhage (Yang et al., 1995; Sengbusch et al., 2002). Integrin α4β1 is thought to promote endothelial motility and transient association of the endothelium with pericytes in a manner that underlines the survival of both cell types during angiogenesis (Garmy-Susini et al., 2005). Indeed, α4 knock-out embryos show dilated cranial vessels due to ineffective mural cell coverage (Grazioli et al., 2006). The endothelial-specific knock-out of integrin α4 integrins, however, does not cause any vascular defect, and these mice are viable (Priestley et al., 2007), suggesting that the main requirement for α4 integrins lies in non-endothelial cells. The deletion of integrin α9β1, which

binds osteopontin, tenascin C, VCAM-1, either constitutively or specifically in the endothelium, gives rise to lymphatic defects (interestingly, α9β1 also binds lymphangiogenic VEGF-C and VEGF-D (Vlahakis et al., 2005)), which ultimately causes cyclothorax and lethality at a postnatal stage (Huang et al., 2000b; Bazigou et al., 2009).

The major FN receptors in endothelial cells are the α5β1 and αVβ3 integrins, and considerable effort is still being made to elucidate the functional contributions of α5 and αV integrins in vascular formation and function. The role of αV integrins (of which αVβ3 and αVβ5 are FN receptors) in developmental and pathological angiogenesis has been addressed *in vivo* with both pharmacological and genetic tools. Early characterisations pointing to a pro-angiogenic function of αV integrins originate from reports showing that αV integrin expression in the endothelium becomes upregulated in tumour vessels or in a normal vasculature upon treatment with angiogenic growth factors (Brooks et al., 1994b) and are required to support angiogenic growth factor-induced angiogenesis, both under physiological and pathological (tumour) conditions *in vivo* (Brooks et al., 1994a; Brooks et al., 1994b; Friedlander et al., 1995; Friedlander et al., 1996; Hammes et al., 1996). Studies with agonists and antagonists specific for integrin αVβ3 indicate that integrin αVβ3 sustains neovascularisation by promoting endothelial cell survival, e.g. by activating the MAP kinase, FAK and Src signalling pathways (Eliceiri et al., 1998), inhibiting p53 activity, decreasing expression of the cell cyle inhibitor p21WAF1/CIP1 and suppressing the bax cell death pathway (Strömblad et al., 1996). Generally, results from studies of integrin antagonists indicate that αV integrins promote angiogenesis.

However, genetic experiments show that αV integrins are only remotely involved in vascular development. For example, mice that are genetically depleted of all αV integrins (i.e. αVβ1, αVβ3, αVβ5, αVβ6 and αVβ8) develop blood vessels (Bader et al., 1998); all αV knockout embryos develop normally until E9.5, and 20% of these embryos survive until birth. The remaining 80% of αV knockouts die of placental defects around E10.5-11.5. Those mice that do survive until birth ultimately die of cleft palates and brain hemorrhage, stemming from distended and leaky blood vessels (Bader et al., 1998). Thus, αV integrins seem to be involved in development of blood vessels in specific tissues such as placenta and brain. The Tie2-Cre mediated αV integrin knockout in endothelium, however, shows no detectable vascular defects, whereas αV integrin knockout in neural cells, such as glia, showed that αV integrins in cells associated with the endothelium are necessary to support cerebral vascular development (McCarty et al., 2005). This phenotype has been attributed to the loss of integrin αVβ8 since β8 integrin knockout mice most closely resemble the αV integrin knockout (Zhu et al., 2002). Interestingly, the brain hemorrhage phenotype of αV knockouts has been linked to an inability of astrocytes associated with the brain vasculature to induce αVβ8-mediated TGF-β activation (McCarty et al., 2002; Cambier et al., 2005; McCarty et al., 2005).

Hence there is a discrepancy in the reported functions of αV integrins in physiological and pathological blood vessel formation. While results from studies of integrin antagonists indicate that αVβ3 integrin promotes angiogenesis, genetic deletion studies generally suggest that αV integrins are not critical for neovessel formation and might even be negative regulators of angiogenesis given that

αV integrin knockout gives rise to such large and dilated vessels. One view on this discrepancy is that αV integrins can act both as positive and negative regulators of angiogenesis in different phases of angiogenesis and depending on environmental context (Hynes, 2002a). According to the model in which integrin αVβ3 acts as a negative regulator of angiogenesis, the engagement of the αV integrins by pharmacological agonists (e.g. monoclonal antibodies or RGD motif-containing peptides) would activate their negative regulatory functions in tissue and supress tumour angiogenesis. In turn, genetically or pharmacologically ablating integrin αV function during development would disturb an angiogenic regulatory mechanism and allow angiogenesis to occur at an accelerated rate, forming largely defective blood vessels that could support tumour growth. One mechanism for achieving anti-angiogenic activity would be for integrin αVβ3 to bind, and thereby localise, antiangiogenic thrombospondin (TSP-1 and -2) to relevant sites during vessel development (Jiménez et al., 2000; Lawler, 2000; Adams, 2001; Rodriguez-Manzaneque et al., 2001). Integrin αVβ3 has also been implicated in either generating or binding and mediating the anti-angiogenic effects of specific proteolytic ECM fragments, such as tumstatin (Brooks et al., 1998; Maeshima et al., 2000; Petitclerc et al., 2000; Rehn et al., 2001; Tarui et al., 2001). Another mode of anti-angiogenic regulation could stem from the ability of integrin αVβ3 to regulate and maintain low VEGFR2 expression in endothelium once the vasculature has formed, creating a negative feedback mechanism of angiogenesis (Reynolds et al., 2002). The role of integrins in regulating apoptosis represents yet another way of regulating angiogenesis. It is widely accepted that integrin-mediated adhesion to the ECM creates an intracellular pro-survival signal (deleted because references does not mention sigaling pathways) and forms the basis of anchorage-dependent survival (Meredith et al., 1993). A more recent model proposes that integrins in an unligated or antagonised state actively induce apoptosis by recruiting caspase-8. Such an "integrin-mediated death" model applied to integrin αVβ3 in the endothelium could account for the enhanced angiogenesis in tissue lacking integrin αVβ3 (Cheresh and Stupack, 2002).

A characteristic trait of both physiological and pathological angiogenesis is the enhanced expression of integrin α5β1 and its ligand FN (Kim et al., 2000; Muether et al., 2007), and administrating blocking antibodies or peptides that block the interaction of integrin α5β1 with FN suppresses angiogenesis (Kim et al., 2000). In full agreement with such blocking experiments, genetic ablation of integrin α5 creates a lethal phenotype dominated by vascular defects (Yang et al., 1993). The expression of integrin α5β1 also becomes induced in endothelium in response to angiogenic growth factors such as FGF-2, IL-8 and Del-1 remove kim – no mention of GF-induced integrin expression (Kim et al., 2000; Boudreau and Varner, 2004). Although these data unanimously establish integrin α5β1 as a pro-angiogenic integrin, they could not clarify how the endothelium specifically uses integrin α5β1. To this end, a recent report describes the endothelial-specific (Tie2-Cre-mediated) α5 integrin knockout mouse as viable and lacking any obvious phenotype (van der Flier et al., 2010). To address a possible functional compensation by αV integrins in the conditional integrin α5 knockout mouse, the same author group generated endothelial-specific α5/αV compound knockout mice (van der Flier et al., 2010). This model revealed that mice lacking α5 and αV integrin expression in the endothelium still show, to a large extent, vascular morphogenesis through formation of vascular plexi, large vessels and

the heart by mid-gestation. However, around mid-gestation (i.e. E11.5 onwards), the expression and cooperation of these integrins becomes crucial for the remodelling of the branchial arch arteries and vascular structures derived from these arteries. It is very interesting that a few of these compound conditional knockout mice are reported to complete development and survive to adulthood. Whatever function integrin α5β1 might have in the endothelium, it is likely that integrin α5β1 and FN also play an important part in pericytes and/or smooth muscle cells that support the growing vasculature.

4.4.5 Role of FN in blood vessel formation and remodelling

The ECM that supports the developing vasculature is dynamic, and multiple integrins participate in vascular morphogenesis, depending on the ECM context in which the vasculature is remodelling. The composition of the vascular ECM changes as the endothelium progresses through vasculogenesis and angiogenesis. During development, new vessels arise from endothelial cells proliferating, migrating and sprouting within a FN-rich matrix, while mature vessels are associated with a sheet-like basement membrane containing laminins, collagen IV and heparan sulphate proteoglycans (Risau and Lemmon, 1988). The supporting role of FN in blood vessel formation is illustrated by the phenotype of FN-null embryoid bodies; they contain PECAM-1-positive endothelial cells, but these endothelial cells do not organise into islands or form vascular structures (Francis et al., 2002). During development, the abundance of FN associated with sprouting vessels is complemented by high expression of FN-binding integrin α5β1 in the endothelium (Goh et al., 1997; Francis et al., 2002). In adult tissues, where collagen expression around blood vessels becomes more prominent, collagen receptors α1β1 and α2β1 are likely to be more important in maintaining vascular stability (Davis and Camarillo, 1996; Senger et al., 2002; Perruzzi et al., 2003). Injured adult tissue undergoing the process of wound healing shows a marked, but temporary increase in the deposition of FN while the endothelium grows and sprouts into the healing tissue (Clark et al., 1982). In this case both FN-binding integrins and collagen-binding integrins play important roles (Davis and Senger, 2005). In various pathological instances, such as in a hypoxic central nervous system, the expression of FN is induced on angiogenic vessels with concomitant expression of FN-binding integrins α5 and αV (Li et al., 2012). There is also strong evidence that FN is deposited around new blood vessels forming in tumours and enhances tumour angiogenesis, which in turn contributes to tumour growth *in vivo* (Kim et al., 2000).

There is a complex pattern of interaction among integrins, ECM and growth factor receptors throughout vasculogenesis and angiogenesis. Signals stemming from anchorage of endothelial cells to the ECM by integrins is important for both the survival and proliferation of endothelial cells, in part through activation of the mitogen-activated protein kinase (MAPK) signalling pathway, by promoting cell cycle progression and by preventing apoptosis (Eliceiri et al., 1998; Short et al., 1998; Aoudjit and Vuori, 2001). On a cellular level, FN has been shown to regulate endothelial cell migration by promoting the β1 integrin and Src-dependent phosphorylation of FGFR at tyrosines 653/654 and 766 (Zou et al., 2012). Integrins and the ECM also facilitate the chemotactic migration of sprouting endothelial cells in response to gradients of angiogenic growth factors (e.g. VEGF-A) (Dejana et al., 1985; Ruhrberg et al., 2002; Senger et al., 2002; Wijelath et al., 2006), and it is likely that sprouting

angiogenesis relies on both chemotactic gradients of angiogenic growth factors and haptotactic gradients of ECM.

The requirement for fibrillar FN in angiogenesis has been addressed with endothelial cell tubulogenesis assays in three-dimensional fibrin gels (Zhou et al., 2008). To test the consequence of preventing FN fibrillogenesis by the embedded endothelial cells, the authors of this study used a 49-mer peptide (termed the functional upstream domain, or FUD) derived from the *Streptococcus pyogenes* adhesion F1 protein, which binds directly to the N-terminal assembly domain of FN and thereby prevents self-association of FN, but does not block the binding of integrin $\alpha5\beta1$ to the cell-binding RGD motif in FN (Tomasini-Johansson et al., 2001). Without affecting apoptosis, the presence of this peptide ablated the ability of the endothelial cells to construct a pericellular fibrillar FN matrix and also blocked their migratory and proliferative preparation to transition into tubular structures (Zhou et al., 2008). While the absence of fibrillar FN did not affect phosphorylation of MAPKs (ERK1 and 2), it disrupted the organisation of the actin cytoskeleton and attenuated the ability of the endothelial cells to exert myosin-dependent traction forces on their three-dimensional environment (Zhou et al., 2008).

From work dealing with alternatively spliced variants of FN in various vertebrate model organisms, it has become clear that the extra domains EIIIA and EIIIB are instrumental in forming a fully functional cardiovascular system. The expression of alternatively spliced variants of FN containing exons EIIIA and EIIIB is a hallmark of the developing vasculature. EIIIA- and EIIIB-containing FN is amply expressed around new vessels that form both during embryonic development and wound healing as well as during pathological events that require vascular remodelling, such as tumour development and artherosclerosis. Yet these alternatively spliced isoforms are silenced in the quiescent vasculature (Ffrench-Constant and Hynes, 1989; Ffrench-Constant et al., 1989; Oyama et al., 1989; Castellani et al., 2002; Peters et al., 2002; Astrof et al., 2004; Matter et al., 2004). Deletion of both the EIIIA- and EIIIB-containing splice variants in the mouse does not affect FN expression level, but clearly affects FN function as these embryos die around E10.5 with vascular defects of the placenta, yolk sac and heart (Astrof et al., 2007).

A more recent study addresses the functions of FN in mouse retinal angiogenesis (Stenzel et al., 2011). In the retina, astrocytes enter from the optic nerve and form a network that expands radially towards the periphery of the retina. Astrocytes respond to hypoxia in this avascular tissue by expressing and establishing a gradient of VEGF-A. Endothelial tip cells expressing high levels of VEGFR2 extend filopodia and migrate towards the gradient of VEGF-A laid down by the astrocytic network (Stone et al., 1995; Ruhrberg et al., 2002; Gerhardt et al., 2003). Retinal astrocytes also secrete FN ahead of growing vessels and thereby deposit a field of FN to guide the growing vascualture (Jiang et al., 1994; Uemura et al., 2006; Stenzel et al., 2011).

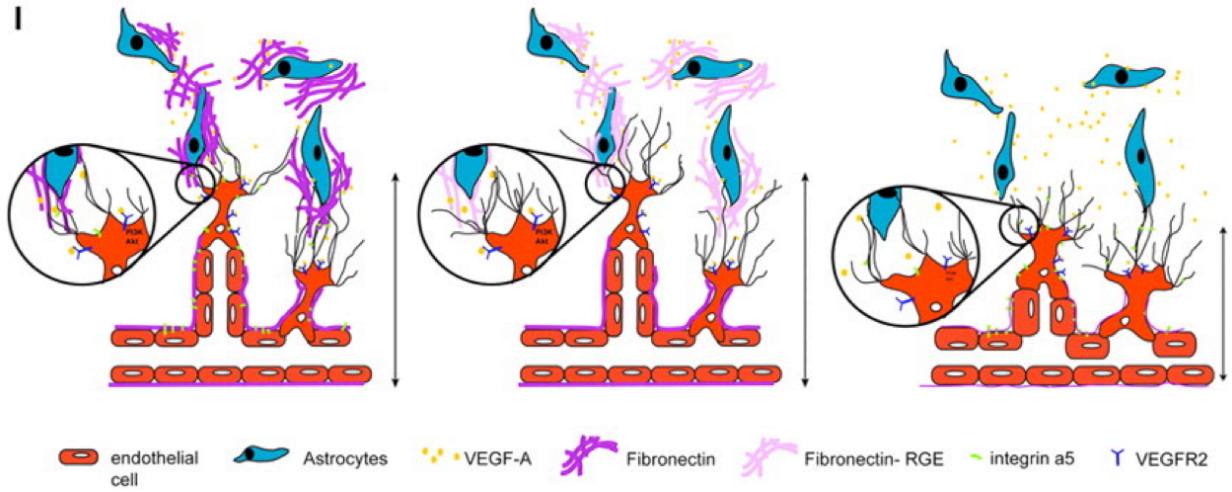

Figure 4.20. Schematic model of astrocytic VEGF-FN interaction regulating vessel migration. In the mouse retina, astrocytes migrating ahead of the growing vasculature assemble a fibrillar FN matrix. Integrins exprsesed on endothelial tip-cell filopodia mediate adhesion to the FN matrix and allow filopodial alignment along the astrocyte network. However the ability of integrins to interact with FN is not crucial to the expansion of the vascular network. Astrocytes also secrete VEGF-A, which is stored by FN. The astrocyte-derived FN establishes VEGF-A gradients that regulate filopodial extension and migration of tip cells as well as polarised proliferation of stalk cells during sprouting angiogenesis. Without astrocytic FN, the VEGF-A gradient becomes diffuse, and vascular expansion is disrupted. Adapted from (Stenzel et al., 2011).

Genetic studies showed that astrocytic FN plays a role in retinal angiogenesis by regulating vessel extension towards the retinal periphery (fig. 4.21); loss of astrocytic FN results in increased number of filopodia, increased number of vessel branch points and increased vessel diameter whereas the migration and expansion of vessels towards the periphery is diminished (Stenzel et al., 2011). These findings indicated that astrocytic FN promotes tip-cell migration and filopodial elongation. Interestingly, these functions of FN are to a large extent independent of integrin binding to FN. While the abilty of endothelial integrins to interact with FN^{RGD} does affect filopodial alignment and stabilisation, and the authors speculate that the altered fibril complexity of FN^{RGE} versus FN^{RGD} could compromise filopodial interactions with astrocytic FN, preventing integrin ligation of FN does not overwhelmingly affect radial expansion of the retinal vasculature (Stenzel et al., 2011). Rather, it is the abilty of FN to bind VEGF-A (Wijelath et al., 2002; Wijelath et al., 2006) that has the greatest implications for retinal angiogenesis, and the effects of deleting astrocytic FN can be explained by an inability to store and establish gradients of VEGF-A and a consequent reduction in VEGFR2-mediated stimulation of endothelial migration (Stenzel et al., 2011) (fig. 4.20). Hence, in the retinal vasculature, FN has both integrin-dependent and –independent functions in promoting angiogenesis.

5 AIM OF THIS STUDY

Fibronectin is deposited into the extracellular matrix and secreted into the plasma in a dimerised form. The reported requirement for FN dimerisation to promote FN fibrillogenesis, and hence FN function, is based on past studies that examined the cell-mediated deposition of truncated FN peptide fragments. The overall aim of this PhD project was to characterise the function of the FN dimerisation motif with *in vivo* and in *vitro* tools. The strategy was to address the requirement for FN dimerisation with a mouse model carrying mutant FN alleles in which the two critical cysteine residues of the dimerisation motif were mutatated to serines residues ($FN^{CC>SS/CC>SS}$).

More specifically, the first aim of this study was to address the requirement for FN dimerisation in FN fibrillogenesis, i.e. fibril matrix assembly. The second aim of this study was to understand the implications of preventing FN dimerisation in integrin function during mouse development. Finally, this study was aimed to understand the contribution of dimerised FN for the ability of the extracellular matrix to regulate growth factor bioavailabilty.

6 PREFACE

A few of the figures presented in this thesis have been adopted from the PhD thesis of Dr. M. Leiss (2009), who performed his thesis work in the laboratory of Dr. Reinhard Fässler and whose thesis work laid a foundation for this current PhD project. They are important for the understanding of the experimental design of this project and are clearly labelled in figure legends.

Dr. Julien Polleux and Dr. Kyle Legate assisted with preparation towards and performance of AFM experiments, respectively.

7 MATERIALS AND METHODS

7.1 Chemicals

The chemicals used in this work were acquired from AppliChem (Darmstadt, Germany), Carl Roth GmbH (Karlsruhe, Germany), Eurofins MWG Operon (Ebersberg, Germany), Merck (Darmstadt, Germany), Sigma Aldrich (Munich, Germany), Serva (Heidelberg, Germany) and Roche Diagnostics GmbH (Mannheim, Germany).

7.2 Mice

The mice used in this study were hosted by the animal facility of the Max Planck Institute of Biochemistry (Martinsried, Germany). The $FN^{+/CC>SS}$ knockin mouse strain was back-crossed for at least seven generations with C57BL6.

The $FN^{fl/fl}$ strain (Sakai et al., 2001) was crossed with the Mx1Cre mouse strain (Kühn et al., 1995; Schneider et al., 2003). The $FN^{fl/fl}$ Mx1Cre mouse strain was maintained on a 129Sv genetic background.

$FN^{fl/CC>SS}$Mx1Cre and control $FN^{fl/+}$Mx1Cre mice were generally made by crossing $FN^{fl/fl}$Mx1Cre mice with $FN^{+/CC>SS}$ mice. Deletion of the floxed FN allele was induced in 4–5-wk-old mice by 3 intraperitoneal injections of 250 μg polyinosinic:polycytidylic acid pI:C at 2-day intervals (Kühn et al., 1995). For experiments, mice were used at least 1 month after pI:C injection.

Mice were weaned and ear-tagged at 3-4 weeks of age. DNA for genotyping PCR was prepared from lysed tail biopsies and purified by isopropanol precipitation. Genotyping was accomplished by polymerase chain reaction (PCR) analysis of tail biopsy DNA, using oligonucleotides (Eurofins MWG Operon) listed in table 5.1. PCRs were performed in a 25μl volume according to Metabion Taq instructions. The relevant thermo-cycle conditions are listed in table 5.2.

- Tail lysis buffer: 100 mM Tris pH8.0, 5mM EDTA, 0.2% w/v SDS, 200 mM NaCl

Table 7. 1 Oligonucleotide sequences for genotyping PCR.

Application	5' - 3' sequence	Primer name	Product size
$FN^{cc>ss}$	GTG GAG ATT TGT GTC ACA GGT G	Rb2	FN+ 202 bp
	CGG GAT CCG CTC ATG AAC AAA GCA GAC AGC	Fb (HpaI BamHIF)	Deleted Neo 298 bp
FN^{fl}	GTA CTG TCC CAT ATA AGC CTC TG	mFn E1f1	FN fl 300 bp
	CTG AGC ATC TTG AGT GGA TGG GA	mFn E1r2	FN+ 250 bp
Cre	GCC TGC ATT ACC GGT CGA TGC AAC GA	Cre1	720 bp
	GTG GCA GAT GGC GCG GCA ACA CCA TT	Cre2	

Table 7. 2 Genotyping PCR programmes.

Gene	Temperature	Time	# of cycles
$FN^{cc>ss}$	95°C	3 min	1x
	95°C	30 sec	5x
	58°C	30 sec	
	72°C	30 sec	
	95°C	30 sec	28x
	62°C	30 sec	
	72°C	30 sec	
	4°C	pause	
FN^{fl}	95°C	3 min	1x
	95°C	30 sec	35x
	61°C	30 sec	
	72°C	45 sec	
	72°C	3 min	1x
	4°C	pause	
Cre	95°C	5 min	1x
	95°C	45 sec	35x
	61°C	45 sec	
	72°C	1 min	
	72°C	5min	1x
	4°C	pause	

7.2.1 Mouse breeding

Crosses were initiated between males and females once 8 weeks of age. For timed matings, a male and a female mouse were joined overnight. The presence of a female vaginal plug the next morning was taken as successful mating, and this time point was set as E0.5.

7.2.2 Dissection of mouse embryos

To analyse the features of the recessive embryonic lethal phenotype, embryos were harvested and dissected at indicated days of gestation. Dissected uteri were transferred to ice-cold PBS, and each embryo was separated from decidual tissue, yolk sac and amnion. Embryos and yolk sacs were preserved for analysis. A small piece of the yolk sac or embryo tail bud was sampled for genotyping purpose. Embryos and yolk sacs were fixed in a fixative that was compatible with the subsequent immunological staining.

- PBS: 137 mM NaCl, 2.7 mM KCl, 1.4 mM KH_2PO_4, 10mM Na_2HPO_4

7.3 Whole mount stainings of embryos and yolk sacs

7.3.1 Critical buffers

- Dent's fixative: 80% MeOH, 20% DMSO
- MEMFA: 2mM EGTA, 1mM MgSO4, 3.7% PFA in 0.1 M MOPS, pH7.4
- TBS: 0.1M Tris-HCL pH7.5, 0.15M NaCl

7.3.2 Whole mount immunofluorescence staining

Staged embryos and yolk sacs were fixed overnight at 4°C with gentle agitation in Dent's fixative or MEMFA, depending on the antibody (5.5). Tissues that had been fixed in MEMFA were subsequently dehydrated in 100% MeOH. All tissues were sequentially rehydrated in MeOH/TBS solutions with decreasing MeOH concentration (75%, 50%, 25% (v/v) MeOH/H_2O, for 20 minutes each) at room temperature. Rehydrated embryos were blocked in 5% (v/v) normal goat serum/2% (w/v) BSA/TBS for 3 hours at room temperature with agitation. Primary antibody (diluted in 5% (v/v) normal goat serum/2% (w/v) BSA/TBS) was applied for incubation for a minimum of 24 hours at 4°C with agitation. To wash away excess primary antibody, tissues were washed extensively for a minimum of 3x 1 hour in 0.05% (v/v) Tween-20/TBS. Rinsed tissues were re-blocked in 2% (w/v) BSA/TBS for 3 hours at room temperature with agitation. Fluorophore-conjugated secondary antibody (diluted 1:300 in 2% (w/v) BSA/0.05% (v/v) Tween-20/TBS) was applied for overnight incubation in the dark at 4°C with agitation. To wash away excess secondary antibody, tissues were extensively washed in 0.05% (v/v) Tween-20/TBS for a minimum of 4x 1 hour in the dark at room temperature with agitation, followed by 1 hour in 0.05% (v/v) Tween-20/TBS containing 6-Diamidino-2-phenylindole (DAPI) to stain nuclei. Tissues were mounted onto a glass microscope slide (Thermo Scientific) in Elvanol (Roth).

7.3.3 Whole mount diaminobenzidine (DAB) staining

Staged embryos and were fixed overnight at 4°C with gentle agitation in Dent's fixative. Tissues were transferred to 3% (v/v) H_2O_2/MeOH solution at room temperature for 1 hour with gentle agitation to quench endogenous peroxidase activity. Tissues were sequentially rehydrated in MeOH/PBS solutions with decreasing MeOH concentration (75%, 50%, 25% (v/v) MeOH/H_2O, for 20 minutes each) at room temperature. Rehydrated embryos were blocked in 2% (w/v) skim milk powder/0.1% (v/v) Triton-X100/PBS for 2x 1 hour at room temperature with gentle agitation. Primary antibody (diluted in 2% (w/v) skim milk powder/0.1% (v/v) Triton-X100/PBS) was applied for incubation at 4°C for minimum 24 hours. Tissues were washed extensively in 2% (w/v) skim milk powder/0.1% (v/v) Triton-X100/PBS, first 2x 1 hour at 4°C, then 3x 1 hour at room temperature. Horse radish peroxidase (HRP)-conjugated secondary antibody (1:200 diluted in 2% (w/v) skim milk powder/0.1% (v/v) Triton-X100/PBS) was applied for overnight incubation at 4°C. Tissues were washed extensively in 2% (w/v) skim milk powder/0.1% (v/v) Triton-X100/PBS, first 2x 1 hour at

4°C then 3x 1 hour at room temperature followed by washes in 0.2% (w/v) BSA/0.1% (v/v) Triton-X100/PBS for 20 minutes at room temperature. Tissues were incubated in 0.3 mg/ml DAB in 0.2% BSA (w/v)/0.1% (v/v) Triton-X100/PBS for 20-40 mininutes at room temperature. To develop the histochemical signal, H_2O_2 was added to 0.03% (v/v) for 5-15 minutes, during which time the HRP-catalysed deposition of brown precipitate would occur where antibody is bound to antigen. When sufficient signal was obtained, the reaction was stopped by rinsing tissues extensively in 0.2% (w/v) BSA/0.1% (v/v) Triton-X100/PBS. To clarify the tissues for imaging, they were sequentially dehydrated in MeOH/PBS solutions with increasing MeOH concentration (25%, 50%, 75% (v/v) MeOH/H_2O, for 20 min each) at room temperature. Then tissues were transferred to a clearing solution consisting of a benzyl alcohol and benzyl benzoate (1:2) for 20 minutes. Tissues were kept in clearing solution for imaging.

7.4 Embryo histology

7.4.1 Paraffin sectioning

In preparation for paraffin sectioning, embryos and yolk sacs were fixed in 4%PFA/PBS at 4°C with gentle agitation. For embryos at or younger than E9.5, fixation time was 1 hour. If older than E9.5, embryos were fixed for 3 hours. Tissues were sequentially dehydrated in EtOH/PBS with increasing EtOH concentrations (70%, 80%, 90%, 95% and 100% (v/v) EtOH/H_2O for 20 minutes each) at room temperature. Once fully dehydrated, the tissues were incubated in 100% EtOH for 6x 1 hour at room temperature with gentle agitation. Then tissues were transferred to 100% butanol and incubated at ascending temperature, i.e. 1 hour at 35°C, 1 hour at 40°C and 1 hour at 45°C. Finally tissue were transferred to melted paraffin at 60°C for 4 hours and transferred into fresh melted paraffin after the first and second hour. Next, tissues were embedded in a paraffin block using an embedding machine (Shandon, HistoCentre 2). Paraffin sections were cut at 8 μm thickness on a microtome (Microm, Vacutome HM5000M) and dry-mounted onto glass microscope slides. Warm water (37°C) was applied to the sections, and slides were kept on a warm surface until the sections had smoothend out before removing the water and drying the paraffin sections at 37°C overnight.

7.4.2 Cryo-sectioning

In preparation of cryo-sectioning, embryos and yolk sacs were fixed overnight in 4% (w/v) PFA/PBS at 4°C with gentle agitation. Tissues were incubated in increasing concentrations of sucrose (0.5%, 1%, 2%, 5%, 10%, 20% (v/v) sucrose/PBS, for 1 hour each, or until tissue reaches the density of the sucrose solution). Tissues were transferred to a mixture of 20% sucrose and Cryomatrix (Thermo Scientific) (1:1) for a 20-minute incubation before embedding tissue in Cryomatrix in a cryomold (Sakura, Tissue-Tek). Tissues were kept in cryomatrix for 1 hour at room temperature before freezing the tissue in the Cryomatrix on dry ice. Cryosections were cut at 10 μm thickness on a cryotome kept at -18°C. The cryosections were transferred to glass microscope slides and dried for a minimum of 20 minutes at room temperature before being stored away for later use at -80°C.

7.4.3 Haematoxylin and eosin (H&E) staining of tissue sections

H&E staining was performed to highlight morphological features of embryonic and extraembryonic tissues in effect of a blue nuclear staining by hemalum (a complex formed from aluminum ions and hematein, an oxidation product of haematoxylin) followed by a pink staining of cytoplasm and extracellular matrix by Eosin G. H&E stainings were performed on cryosections. To prepare cryosections for H&E staining, the cryomatrix was rinsed away from the tissue section through washes in destilled water 2x 3 minutes. Next, the slides were stained for 1 minute in a Hematoxylin solution (Merck, diluted 1:5 in distilled water), followed by continuous rinsing of the slides. Next the slides were stained for 1 minute in Eosin G solution (Merck). When complete, the excess eosin was washed away with distilled water. Tissue sections were mounted under dehydrated conditions, which involved sequentially dehydrating the sections in increasing concentrations of EtOH (70%, 80%, 90%, 95% and 100% (v/v) EtOH/H_2O for 1 minute each) before moutning sections in Entellan (Merck).

7.4.4 Immunofluoresence stainings of tissue sections

Both paraffin sections and cryosections of embryonic tissue were used for immunofluorescence stainings.

To prepare paraffin sections for immunofluorescence stainings, sections were deparaffinised and rehydrated. Sections were processed sequentially in xylene (3x 5 minutes), 100% EtOH (2x 10 minutes), 95% (v/v) EtOH/H_2O (2x 10 minutes) and were then sequentially rehydrated in decreasing concentrations of EtOH (90%, 80%, 70%, 60%, 50% (v/v) EtOH/H_2O for 1 minute each) at room temperature. Sections were washed in water 2x 5 minutes at room temperature. Primary antibodies used here required antigen unmasking of paraffin sections, in which case either 1mM ETDA pH8.0 or 10mM citrate buffer pH6.0 in combination with heat was applied to tissue sections. Sections were brought to 95°C in 1mM ETDA pH8.0 or 10 mM citrate buffer pH6.0, followed by 15 minutes at sub-boiling temperature. Following 10 minutes cooling time, sections were washed in distilled water for 3x 5 minutes.

To prepare embryonic cryo-sections for immunofluorescence staining, slides were air-dried for 30 minutes and washed in PBS for 3x 5 minutes.

To prepare tissue sections for stainings, tissue sections were permeablised in 0.1% (v/v) Tween-20/TBS for 5 minutes and blocked in 5% (v/v) normal goat serum/2% (w/v) BSA/0.1% (v/v) Tween-20/TBS for 1 hour at room temperature. Blocking solution was replaced with primary antibody solution (diluted in 5% (v/v) normal goat serum/2% (w/v) BSA/0.1% (v/v) Tween-20/TBS) and incubated with sections overnight at 4°C. Sections were washed in 0.1% (v/v) Tween-20/TBS 3x 5 minutes and fluorophore-conjugated secondary antibody (diluted 1:300 in 0.1% (v/v) Tween-20/TBS) was applied for 1 hour in the dark at room temperature. Excess secondary antibody was removed through washes with 0.1% (v/v) Tween-20/TBS for 2x 5 minutes, followed by a 5-minute incubation with DAPI diluted in 0.1% (v/v) Tween-20/TBS before sections were mounted in Elvanol.

7.4.5 DAB staining of tissue sections

To prepare embryonic paraffin sections for DAB stainings, sections were deparaffinised and rehydrated essentially as described in 5.3.4. Once fully rehydrated, sections were incubated in 3% (v/v) H_2O_2/water for 10 minutes at room temperature to quench endogenous peroxidase activity. Tissues were blocked in 5% (v/v) normal goat serum/0.1% (v/v) Tween-20/PBS for 1 hour at room temperature and primary antibody (diluted in 5% (v/v) normal goat serum/0.1% (v/v) Tween-20/PBS) was applied for overnight incubation at 4°C. Excess primary antibody was washed off sections with 0.1% (v/v) Tween-20/PBS for 3x 5 minutes, and HRP-conjugated secondary antibody (diluted 1:300 in 0.1% (v/v) Tween-20/PBS) was applied for 1 hour at room temperature. Thereafter, sections were washed in 0.1% (v/v) Tween-20/PBS and processed for the HRP-catalysed DAB reaction by immersing sections in a solution of 0.05% (w/v) DAB/0.015% (v/v) H_2O_2/Tris pH7.6 for 2-10 minutes, during which HRP-catalysed deposition of brown precipitate would occur where antibody is bound to antigen. The reaction was quenched in water and sections were counterstained with haematoxylin (diluted 1:5 in distilled water) for 2 minutes. After rinsing off excess haematoxylin, tissue sections sequentially dehydrating in increasing concentrations of EtOH (70%, 80%, 90%, 95% and 100% (v/v) EtOH/H_2O for 1 minute each) and mounted in Entellan.

7.5 Immunofluorescence staining of adherent cells and ECM in culture

For immunofluorescence staining of adherent cells and the ECM they deposit, cells were seeded onto glass coverslips contained in plates or onto LabTek chamber slides (Nunc). All surfaces were precoated with LM-111 at 5μg/mL in PBS prior to seeding cells at a density of 2-10 x 10^3 cells/cm^2. To prepare for immunofluorescence staining, cultures were rinsed in PBS and fixed in 4% PFA/PBS at 4°C for 10 minutes. Fixed cultures were rinsed in PBS for 3x 5 minutes and incubated in 2% (w/v) BSA/PBS for 1 hour at room temperature. The blocked cultures were incubated in primary antibody (diluted in 2% (w/v) BSA/PBS) overnight at 4°C. Excess primary antibody was washed away with PBS for 3x 5 minutes and fluorophore-conjugated secondary antibody (diluted 1:1000 in PBS) was applied for 1 hour at room temperature. Further washing in PBS for 3x 5 minutes removed secondary antibody. DAPI staining was performed for 5 minutes at room temperature. Thereafter, cultures were mouted in Elvanol.

7.6 Antibodies

Table 7. 3 Primary and secondary antibodies

Antibody	Company	Cat. #	Species	Dilutions			Requirements
				IF/IHC	WB	IP	
Endomucin	Santa Cruz	Sc-53941	rat	1:300	-	-	
PECAM-1	PharMingen	01951D	rat	1:300	-	-	IF: Fix in Dent's
pFAK^{Y397}	Biosource	44-624G	rabbit	-	1:1000	-	WB: 1% BSA
FAK	Abcam	ab71563	rabbit	-	1:1000	-	WB: 1% BSA
FN	Millipore	ab2033	rabbit	1:300	1:5000	-	WB: 1% BSA
pMLC2	Cell Signaling	3675L	mouse	-	1:1000	-	WB: 1% BSA
MLC2	Santa Cruz	sc-15370	rabbit	-	1:1000	-	WB: 1% BSA
GAPDH	Calbiochem	CB1001	mouse	-	1:1000	-	WB: 1% BSA
β-actin	Sigma	A5441-2ML	mouse	-	1:1000	-	WB: 1% BSA
α5 integrin	Cell Signaling	4705	rat	1:50		-	
4G10	Axel Ullrich		mouse	-	1:12000	-	WB: 1% BSA
LTBP-1	Heldin/ Rifkin	pAb 8579	rabbit	1:300	1:200	-	
pSMAD2	Millipore	ab3849	rabbit	-		-	WB: 1% BSA
SMAD2/3	Santa Cruz	sc-8332	rabbit	-	1:1000	-	WB: 1% BSA
pSMAD1/5/8	Cell Signaling	9511	rabbit	-	1:1000	-	IF: Fix in MEMFA WB: 1% BSA
SMAD5	Calbiochem	st1104	rabbit	-	1:1000	-	WB: 1% BSA
Phalloidin Alexa488	Molecular Probes	A12379		1:300	-	-	
α-SMA-Cy3	Sigma	C6198	mouse	1:400	-	-	
VEGFR2	Cell Signaling	2479	rabbit	1:200	-	1:100	
Anti-mouse HRP	BioRad	170-6516	goat	-	1:10000	-	
Anti-rabbit HRP	BioRad	170-6515	goat	-	1:10000	-	
Anti-rat HRP				1:300	-	-	
Anti-rabbit Alexa 488	Invitrogen	A11008	goat	1:1000	-	-	
Anti-rabbit Alexa 546	Invitrogen	A11010	goat	1:1000	-	-	
Anti-rat Alexa 488	Life Technologies	A21208	goat	1:1000	-	-	
Anti-rat Alexa 546	Invitrogen	A11081	goat	1:1000	-	-	

All primary and secondary antibodies used for western blot analysis were diluted in 1% BSA/0.5% tween-20/TBS.

6-Diamidino-2-phenylindole (DAPI) was used at 1:10000 dilution in PBS

7.7 Microscopy

7.7.1 Fluorescence microscopy

Confocal images of immunofluorescence stainings were acquired on a Leica SP5 confocal microscope using either a ×40 (oil), ×100 (oil) or ×10 (dry) objective. Fluorescence images were acquired on a Zeiss Apotome microscope with a ×20 dry objective.

7.7.2 Light microscopy

Light images of histological sections were taken using a Zeiss Axioskop light microscope equipped with a ×10 objective (Zeiss, Plan-NEOFLUAR) and a LCD camera (Leica, DCC500).

Time-lapse bright-field movies of migrating cells on decellularised ECM platforms were recorded at 5-minute intervals using an inverted Zeiss Axiovert 40 microscope equipped with a ×10 objective and a PAL cameras (Prosilica), which was triggered by custom-made software (SVS Visitek).

7.8 Cell culture methods

7.8.1 Cell lines

$FN^{CC>SS/CC>SS}$ and WT control mouse embryonic fibroblasts (MEFs) were described in the PhD thesis of Dr. Michael Leiss. Briefly, these fibroblasts were isolated from E9.5 $FN^{CC>SS/CC>SS}$ or WT embryos and immortalised through multiple rounds of retroviral transfection with the simian virus 40 large T antigen. These MEFs were either used as mixed populations (i.e. no clonal selection) or as clonal cell lines, which were isolated by limited dilution and characterised by FACS analysis of integrin expression.

$FN^{-/-}$ MEFs were described by Sakai et al. 2001. Briefly, these fibroblasts were prepared by isolating MEFs from $FN^{flox/flox}$ mouse embryos at E13.5 (Sakai et al., 2001). The floxed FN gene was deleted by transfecting MEFs with Cre-transducing adenovirus. The deletion of floxed FN alleles was confirmed by PCR.

Both the CHO cells stably transfected with the β6 integrin subunit (CHO-β6) (Annes et al., 2004) and the mink lung epithelial cells (MLEC) transfected with the reporter construct p800neoLuc (Abe et al., 1994) were kind gifts from Dr. Daniel Rifkin. Both of these cell lines were cultured in the presence of neomycin (PAA).

All cells were maintained in DMEM (Gibco) supplemented with 5% (v/v) heat-inactivated fetal bovine serum (FBS) and 1x penicillin/streptomycin supplement, unless otherwise stated. Cell passaging was done by incubating cultures in 1x Trypsin – EDTA for 2 minutes at 37°C and resuspending cells in fresh medium.

For all cell biological assays, cells were cultured in media supplemented with 0.5-2% FBS depleted of FN by affinity purification with gelatin sepharose 4b (GE Healthcare Life Sciences). To compensate for the very low serum levels, cells were cultured in a home-blended "serum replacement medium", consisting of DMEM, AIM-V (Gibco), RPMI 1640 (Gibco) and non-essential amino acids (Gibco) at 47.5: 47.5: 5: 1 ratio.

7.8.2 Plasma preparation from mouse whole blood

Plasma was prepared from whole blood of pI:C-treated $FN^{fl/CC>SS}$Mx1Cre and control $FN^{fl/+}$Mx1Cre mice for cell culture purposes. Whole blood was collected by retro-orbital bleeding into tubes containing 0.5M EDTA to prevent platelet activation. To isolate plasma, the blood samples were centrifuged at 3000 x g for 20 minutes at 4°C. The low density top layer of clear plasma was collected and centrifuged again at 3000 x g for 20 minutes at 4°C. Clarified plasma was collected and stored at -20°C.

Plasma from multiple mice of the same genotype was pooled and used to supplement normal DMEM growth media at 5% (v/v). Growth media containing mouse plasma was sterile-filtered before use.

7.8.3 Preparation of MEF-derived decellularised ECM platforms

MEF-derived ECM was decellularised in one of two different ways, depending on the application.

ECM platforms that were used for analysis of cell signalling and migration were generated by seeding $FN^{CC>SS/CC>SS}$ and WT MEFs at 31 x 10^3 cells/cm^2 onto a gelatin-coated 35-mm culture dish and incubating cells in serum replacement medium supplemented with 0.5% (v/v) FN-depleted FBS for 3 days to allow the deposition of ECM. Cultures were rinsed with PBS and cells were selectively detached from the cell culture plate with EDTA-based cell extraction buffer at 37°C for 2 hours. Subsequent rinses in PBS rendered the dishes free of rounded cells. To monitor the quality of the decellularised ECM platforms, EDTA-treated decellularised ECM was prepared on LM111-coated LabTek chamber slides to enable immunofluorescence staining of FN and detection of residual cells by nuclear staining with DAPI.

ECM platforms that were used for analysis of mechanical properties by atomic force microscopy analysis were generated by seeding $FN^{CC>SS/CC>SS}$ and WT MEFs at 10 x 10^3 cells/cm^2 onto 22-mm coverslips covalently coated with a monolayer of WT fibronectin as described elsewhere (Prewitz et al, 2013). Cultures were kept for ten days with daily changes of serum replacement medium supplemented with 2% (v/v) FN-depleted FBS. ECMs were decellularised by treatment with a detergent-based cell extraction buffer for 5 minutes at 37°C with gentle agitation, followed by treatment with DNAse (AppliChem; 0.1 mg/ml in DNase buffer containing 40 mM Tris pH7.4, 10 mM NaCl, 6 mM $MgCl_2$ and 1 mM $CaCl_2$). Decellularized matrices were rinsed and maintained in PBS at room temperature and probed immediately. The quality of the decellularised and anchored ECM platforms was monitored by fixing the decellularised ECM and carrying out an immunofluorescence staining of FN and detection of residual cells by nuclear staining with DAPI.

- EDTA-based cell extraction buffer: 20 mM EDTA in PBS
- Detergent-based cell extraction buffer: 20 mM ammonium hydroxide and 0.5% (v/v) Triton X-100 in PBS

7.8.4 Cell signalling assays on ECM platforms

To test the effect of $FN^{CC>SS}$ on selected cell signalling pathways downstream of integrin outside-in signalling, $FN^{-/-}$ fibroblasts were starved overnight and put into suspension at 37°C for 1 hour to essentially inactivate all signalling pathways related to cell adhesion. The starved, suspended $FN^{-/-}$ fibroblasts were seeded onto decellularised ECM platforms derived from either $FN^{CC>SS/CC>SS}$ or WT MEFs at equal cell densities in DMEM. $FN^{-/-}$ fibroblasts were incubated on the ECM platforms for 30 minutes, allowing cells to attach to the ECM and initiate integrins signalling. The media was aspirated, cells were gently rinsed and then lysed in cell lysis (RIPA; 7.9.1) buffer for subsequent detection of signalling activity by SDS-PAGE and western blot analysis.

7.8.5 Cell migration assays on ECM platforms

To test migration speed of $FN^{-/-}$ fibroblasts on ECM platforms containing either $FN^{CC>SS}$ or WT FN, $FN^{-/-}$ fibroblasts were starved overnight and seeded onto decellularised ECM platforms derived

from either $FN^{CC>SS/CC>SS}$ or WT MEFs (2 x 10^3 cells/cm^2). $FN^{-/-}$ fibroblasts were incubated for 1 hour before migration was stimulated by adding recombinant human PDGF-BB (Preprotech) to the culture medium at a final concentration of 50 ng/ml. Still images of fibroblasts were acquired for 12 hours at 5 minutes intervals. Single migrating fibroblasts were tracked and migration speeds were calculated using 64-bit ImageJ 1.47 with the MBF 'ImageJ for Microscopy' plugin Chemotaxis and Migration Tool installed.

7.8.6 Atomic force microscopy (AFM) of ECM platforms

The stiffness of decellularised ECM platforms derived from either $FN^{CC>SS/CC>SS}$ or WT MEFs was determined using a tipless silicon nitride cantilever with a nominal spring constant of 0.01 N/m (MLCT-O10, Veeco), functionalized by attaching a 20 μm glass bead (Kisker Biotech, Germany) using a two-component epoxy. Coverslips containing ECM were mounted onto the stage of a Zeiss Axiovert 200 M and force spectroscopy was conducted using a NanoWizard II together with a CellHesion module (JPK Instruments). Cantilevers were blocked with 100% FBS and calibrated by the thermal noise method prior to measurements. Force-distance curves were recorded in closed loop mode at an approach and retract velocity of 0.5 μm/s until a trigger force of 500pN was reached, and retracted to 3 μm.

Young's moduli were determined by fitting the approach curve using the Hertz model within the JPK analysis software.

7.8.7 TGF-β bioassays

The MLEC cell line is a sensitive tool to assay the amount of active TGF-β in a conditioned medium. The MLEC cell line is stably transfected with a luciferase gene fused to the promoter of plasminogen activator inhibitor 1 (PAI-1), which is a prominent gene target downstream of the TGF-β/SMAD signalling pathway. In this project, the MLEC cell line was used to assay the levels of latent TGF-β deposited into the ECM as well as the ability of CHO-β6 cells to activate latent TGF-β. All assays involving MLEC reporter lines were performed in 96-well plate format.

To test the deposition of latent TGF-β into ECM containing either $FN^{CC>SS}$ or WT FN, ECM was generated by seeding $FN^{CC>SS/CC>SS}$ and WT MEFs into 24-well plates, 40 x 10^3 cells/well, and culturing them in serum replacement medium supplemented with 0.5% (v/v) FN-depleted FBS. 48 hours later, the cultures were rinsed in PBS and MEFs were selectively detached from the cell culture plate with 20 mM EDTA/PBS at 37°C for 2 hours. The decellularised matrices were covered in fresh serum replacement medium, and through a heat-activating treatment at 80°C for 10 minutes the total latent TGF-β was released into the medium in an active form. This conditioned medium containing active TGF-β was cooled and incubated with a MLEC monolayer for 16 hours and luciferase activity in MLEC monocultures was assayed with Bright-Glo™ Luciferase Assay System (Promega) on a GloMax™ luminometer.

To test the ability of CHO-β6 cells to activate latent TGF-β deposited into ECM containing either $FN^{CC>SS}$ or WT FN, ECM was generated by seeding $FN^{CC>SS/CC>SS}$ and WT MEFs into 96-well plates,

10 x 10^3 cells/well, and culturing them in serum replacement medium supplemented with 0.5% (v/v) FN-depleted FBS. 48 hours later, the cultures were rinsed in PBS and MEFs were selectively detached from the cell culture plate with 20 mM EDTA/PBS at 37°C for 2 hours. The decellularised matrices were rinsed with PBS, and a co-culture of CHO-β6 cells (2 x 10^4 cells per well) and MLEC reporter cells (1.5 x 10^4 cells per well, giving a final volume of 100 µl) were plated onto the decellularised ECM in DMEM. A TGF-β neutralizing antibody (1D11; 15 µg/ml) or an αVβ6-blocking antibody (10D5; 20 µg/ml) was added to the co-culture wells as indicated. The MLEC and CHO-β6 co-cultures were incubated for 24 hours. Luciferase activity in MLEC/CHO-β6 co-cultures was assayed with Bright-Glo™ Luciferase Assay System (Promega) on a GloMax™ luminometer.

7.9 Biochemical methods

7.9.1 Preparation of total protein lysates from embryonic tissues and cell cultures

For preparation of total protein lysates from embryonic tissues, dissected embryos and yolk sacs were either snap-frozen in liquid N_2 and stored prior to lysis or processed immediately upon dissection by lysis in cell lysis buffer. Single E9.5 embryos or yolk sacs were lysed directly in 50 µl 1x Laemmli sample buffer. Complete tissue disintegration was achieved by pipetting rigorously and incubation on rotating wheel for 30 minutes at 4°C. Debris was collected by centrifugation at 15,000 x g for 5 minutes at 4°C. The concentration of soluble protein was determined with the BCA assay kit (Pierce) and spectrophotometric absorbance at 562 nanometre. Lysates were analysed by SDS-PAGE and western blotting.

For preparation of total protein lysates from cell cultures, the cultures were initially rinsed twice in ice-cold PBS. Cells were lysed in cell lysis (RIPA) buffer for 5 minutes on ice, and using a cell scraper the lysate was collected and lysis was continued by incubation on a rotating wheel for 30 minutes at 4°C. Cellular debris was collected by centrifugation at 15,000 x g for 10 minutes at 4°C. The concentration of soluble protein was determined with the BCA assay kit (Pierce) and spectrophotometric absorbance at 562 nanometre. Lysates were analysed by SDS-PAGE and western blotting.

- 4x Laemmli sample buffer: 2% (w/v) SDS, 10% (v/v) glycerol, 0.01% (w/v) bromphenol blue in 62.5 mM Tris-HCl pH 6.8 (+ 300 mM β-mercaptoethanol for a reducing Laemmli sample buffer)
- Cell lysis (RIPA) buffer: 150 mM NaCl, 1 mM EDTA, 1% (w/v) Na-deoxycholate, 0.1% (w/v) SDS, 1% (v/v) Triton X-100, 1mM PMSF, 10 mM NaF, 1 mM Na_3VO_4 in 50 mM Tris-HCl pH 7.4 and futher supplemented with protease inhibitor cocktail (Roche).

7.9.2 Na-deoxycholate (DOC) fractionation of the FN matrix

The quantification of FN matrix assembly by DOC fractionation was performed as described by Pankov and Yamada (Pankov and Yamada, 2004) and based on the work of McKeown-Longo and Mosher (McKeown-Longo and Mosher, 1983). Briefly, WT and $FN^{CC>SS/CC>SS}$ MEFs were seeded in gelatin-coated 35-mm dishes at approximately 90% confluency (i.e. 250 x 10^3 cells/well) in serum replacement medium containing 0.5% (v/v) FN-depleted FBS. After 48 hours in a tissue culture

incubator, the medium was aspirated and cells were washed three times in ice-cold PBS. Cells and ECM were lysed in 0.5 ml DOC extraction buffer for 5 minutes on ice, and the lysates were collected with a cell scraper. The lysate was passed through a 23-G needle attached to a 1-ml syringe to reduce viscosity and allow sedimentation of small, insoluble matrix aggregates during centrifugation. Lysates were centrifuged at 20,000 x g for 20 minutes at 4°C to pellet the DOC insoluble fraction.

A 100 µl aliquot of the supernatant (DOC soluble fraction) was transferred to a fresh tube, mixed with 100 µl 2 x Laemmli sample buffer and heated at 95°C for 5 minutes. The remaining supernatant was removed and the DOC insoluble pellet was washed extensively in 100 µl DOC extraction buffer before sedimentation by centrifugation at 20,000 x g for 10 minutes at 4°C. All supernatant was removed and the DOC insoluble pellet was dissolved in 50 µl 2x Laemmli sample buffer. DOC soluble and insoluble fractions were analysed by SDS-PAGE and western blotting.

- DOC extraction buffer: 1% (w/v) DOC, 20 mM Tris-HCl pH 8.5, 2 mM EDTA, 1 x protease inhibitor cocktail (Roche), 1 x phosphatase inhibitor cocktails 2 & 3 (Sigma Aldrich).

7.9.3 Immunoprecipitation of VEGFR2

Immunoprecipitation of VEGFR2 was performed in order to concentrate the protein from embryonic and yolk sac lysates and subsequently monitor the extent of VEGFR2 phosphorylation at specific tyrosine residues. E9.5 embryos and yolk sacs (7 of each) were pooled in 300 µl cell lysis buffer containing protease and phosphatase inhibitors. The lysates were passed through a 23-G needle attached to a 1-ml syringe to shear DNA, and lysis was completed under rotary agitation for an additional 30 minutes at 4°C. Insoluble protein and debris was sedimented by centrifugation at 15,000 x g for 10 minutes at 4°C. The concentration of soluble protein was determined with the BCA assay kit. The lysate volumes were adjusted to appropriate concentrations such that embryo lysates contained 250 µg and yolk sac lysates contained 150 µg. Lysates were pre-cleared with 20 µl Protein G Sepharose beads (Sigma) under rotary agitation for 30 minutes at 4°C, in order to reduce unspecific binding of proteins to the Protein G Sepharose beads in subsequent steps. To the pre-cleared lysates, VEGR2 rabbit mAb was added for overnight incubation under rotary agitation at 4°C. After the antibody incubation, 20 µl Protein G Sepharose beads were added and the lysate-antibody-bead mix was incubated under rotary agitation for 4 hours at 4°C. Next, the Protein G Sepharose beads were sedimented and the lysate was removed. After multiple rounds of washes in cell lysis buffer, VEGFR2 was eluted from the Protein G Sepharose beads with 50 µl 2x Laemmli sample buffer and heating to 95°C for 5 minutes. Lysates were analysed by SDS-PAGE and western blotting.

7.9.4 SDS-polyacrylamide gel electrophoresis (SDS-PAGE) and western blotting

Total protein lysates were adjusted in protein concentration and resolved on Tris-glycine gels (8%-12% resolving acrylamide gels, depending on application) by SDS-PAGE in SDS running buffer at constant 100 volts. Once resolved, the proteins were transferred onto PVDF membrane (Millipore) by wet transfer in Towbin buffer at constrant 50 milliampere overnight at 4°C. PVDF membranes were air dried and subsequently immersed in primary antibody (diluted in 1% bovine serum albumin/0.1%

Tween-20/TBS) for overnight incubation at 4°C. After multiple washes in 0.1% Tween-20/TBS, membranes were incubated in HRP-conjugated secondary antibody (diluted in 1% (w/v) bovine serum albumin/0.1% (v/v) Tween-20/TBS) for 1 hour at room temperature. Following multiple washes in 0.1% (v/v) Tween-20, protein bands were detected using enhanced chemiluminescence reagents (ECL, Millipore). Where necessary, PVDF membranes were stripped of antibodies using a mild stripping buffer for 2x 10 minutes at room temperature followed by extensive washing in 0.1% (v/v) Tween-20/TBS. PVDF membranes were air-dried prior to any further antibody incubation.

- SDS running buffer: 25 mM Tris, 192 mM glycine, 0.1% (w/v) SDS
- Towbin buffer: 25 mM Tris, 192 mM glycine, 10% (v/v) MeOH
- Mild stripping buffer: 1% SDS (w/v), 25 mM glycine pH 2

7.10 Real-time PCR (RT-PCR)

Total cellular RNA was isolated using RNeasy Mini kit (Qiagen). RNA concentration and purity were determined spectrophotometrically on Nanodrop equipment. 5 μg of RNA was reverse transcribed to cDNA using a blend of oligo(dT) and random hexamer primers provided as part of the iScript cDNA Synthesis Kit (BioRad).

The reaction mixes for RT-PCR were prepared with the cDNA template, oligonucleotides designed with IDT PrimerQuest (table 5.4) and the iQ™ SYBR Green supermix (BioRad). A 3-step RT-PCR protocol with a melting curve step was executed in an iCycler thermocycler (BioRad) (table 5.5).

The specificity of the amplified product was verified both by analysis of the melt curve and by agarose gel analysis of the amplified products. For the relative quantification of gene expression, the threshold cycle (C_T) values for genes of interest were internally normalised to that of GAPDH. These relative C_T values formed the basis for the quantitative comparison of WT and $FN^{CC>SS/CC>SS}$ samples.

Table 7.4 Oligonucleotide sequences for RT-PCR

Gene	5' - 3' sequence	Primer name
FN	GTG GAG ATT TGT GTC ACA GGT G	FN1 forward
	CGG GAT CCG CTC ATG AAC AAA GCA GAC AGC	FN1 reverse
Id1	AGC TGA ACT CGG AGT CTG AAG TCG	ID1 forward
	TTT CCT CTT GCC TCC TGA AGG GCT	ID1 reverse
PAI-1/Serpine1	TTC AGT GGC CAA TGG AAG ACT CCT	PAI1 forward
	GTG GCA GAT GGC GCG GCA ACA CCA TT	PAI1 reverse
GAPDH	TCC TGC ACC ACC ACC TGC TTA	GAPDH forward
	TGG ATG CAG GGA TGA TGT TCT GG	GAPDH reverse

Table 7.5 3-step RT-PCR protocol with melting curve

Cycling step	Temperature	Hold time (min:sec)	# of cycles
Initial denaturation and enzyme activation	95°C	3:00	1
Denaturing	95°C	0:15	40
Annealing	65°C	0:30	
Extension	72°C	0:30	
Melt curve	55-95°C (in 0.5°C increments)	0:10-0:30	1

8 RESULTS

8.1 Targeted disruption of the FN dimerisation motif *in vivo*

All murine and human isoforms of FN are secreted as dimers. Dimerisation of FN molecules is mediated by a dimerisation motif that consists of a pair of closely positioned cysteines at the C-terminus of each FN molecule. It has become widely accepted that FN dimerisation is one of a few criteria for FN to undergo de novo fibrillogenesis. However, the current study is the first to address the function of FN dimerisation *in vivo* with a mouse model carrying mutations in the dimerisation motif of the *Mus musculus Fn1* gene that are designed to prevent FN dimerisation. Consequently, this mouse expresses only a monomeric form of FN. The strategy behind this approach to monomerise all FN was to replace the two critical C-terminal cysteine residues of the dimerisation motif with serines by site-directed mutagenesis, i.e. $FN^{CC>SS}$ (fig. 8.1) and to introduce this mutation into the mouse germline by homologous recombination technology. The $FN^{CC>SS}$ knock-in mouse was generated by Drs. Reinhard Fässler and Takao Sakai prior to the initiation of this PhD project.

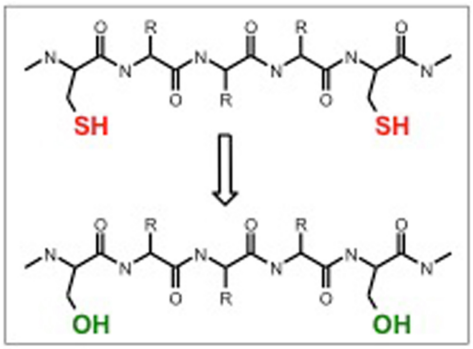

Fig 8.1. Site-directed mutagenesis of cysteine residues to serine residues in FN to create $FN^{CC>SS}$.

To generate the $FN^{CC>SS}$ knock-in targeting construct, a fragment of FN containing exon 44 and 45 was cloned into a pKS vector, and site-directed mutagenesis of Cys-encoding codons TGC to TCC was performed to achieve the substitution of C^{2458} and C^{2462} with serine residues within exon 45. In addition to the amino acid substitutions, a loxP-flanked neomycin resistance cassette (Neo^R) was inserted into intron 44 to allow for positive selection of ES clones that had genomically incorporated the targeting construct by homologous recombination (fig 8.2 A). The targeting construct $FN^{CC>SS\ NeoR}$ was introduced to 129/Sv mouse-derived embryonic stem (ES) cells through electroporation. Among the neomycin-resistant ES cells, those carrying correct gene targeting were identified byBamHI restriction enzyme digestion and subsequent Southern blotting of ES cell DNA. A 5' external probe to distinguish between fragments of a WT allele (12.9 kbp) and a targeted allele (8.8 kpb) (fig 8.2 B). To generate heterozygous mice ($FN^{CC>SS/+}$), ES cell clones carrying $FN^{CC>SS\ NeoR}$ were injected into blastocysts, and these blastocysts were transferred to C57Bl/6 recipient females. Chimeric offspring

were identified by coat colour, and chimeric males were crossed to C57Bl6 females. Germ-line transmission was confirmed if offspring were found to contain $FN^{CC>SS/+\ NeoR}$ mice, as validated by Southern blot analysis of tail biopsy DNA, following the same validation concept as described above for ES cells (fig 8.2 C). The neomycin selection cassette was removed by crossing $FN^{CC>SS/+\ NeoR}$ males with deleter-Cre C57Bl/6 females. Both the deletion of neomycin selection cassette by Cre recombinase and the presence of a WT or targeted allele in $FN^{CC>SS/+}$ mice was validated by PCR of tail tip DNA. Here, the PCR analysis was designed to detect and distinguish between $FN^{CC>SS/+\ Neo}$ (342bp), $FN^{CC>SS/+}$ (298 bp) and $FN^{+/+}$ (202 bp) (fig. 8.2 D, E).

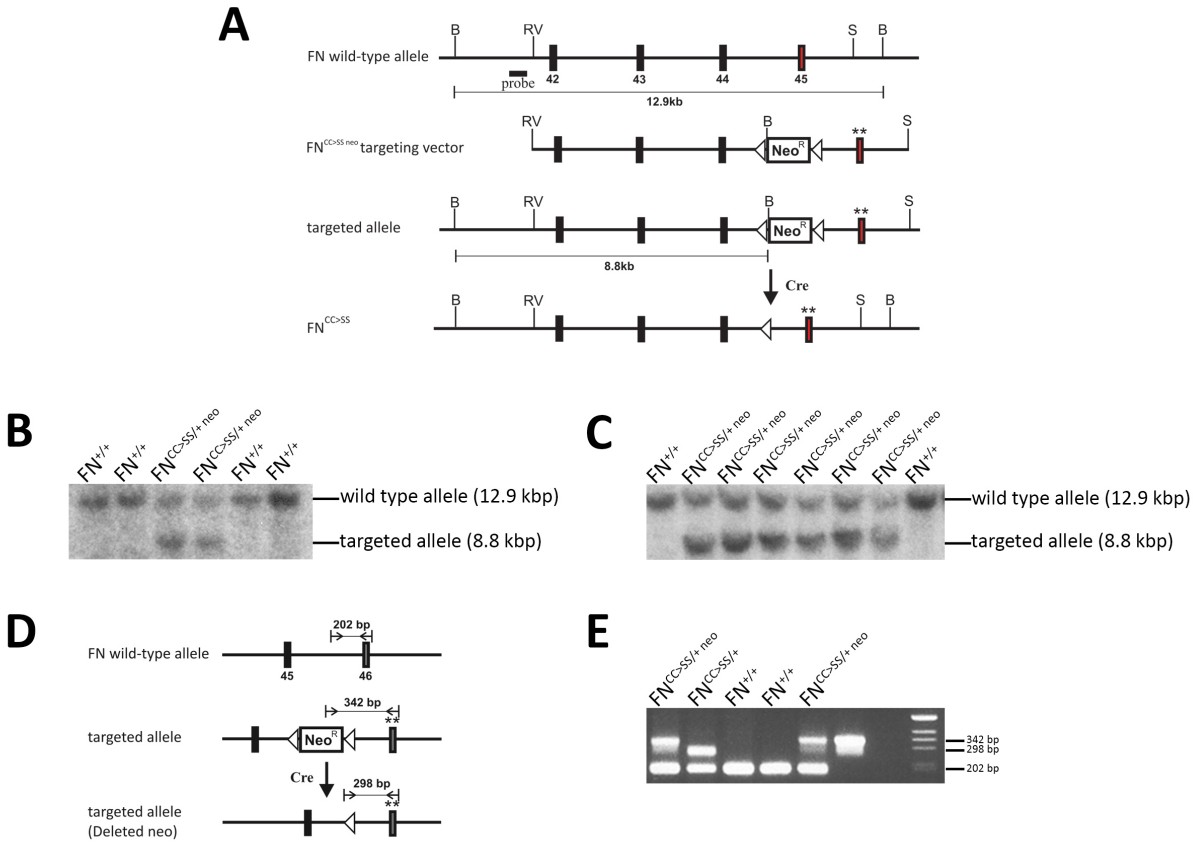

Fig 8.2. Genetic targeting of the dimerisation motif in FN. (A) Schematic representation of the FN-monomer ($FN^{CC>SS}$) knock-in strategy. The targeting vector $FN^{CC>SS\ neo}$ contains the loxP flanked neomycin cassette and the mutated exon 45 (**). Homologous recombination in ES cells results in the depicted targeted allele. The removal of the neo selection cassette from the targeted allele was performed by intercrossing $FN^{CC>SS\ neo/+}$ heterozygous mice with a deleter-Cre recombinase mouse strain. Probe indicates the binding position of the external probe used in southern blotting. Restriction sites: B, BamHI; S, SpeI; RV, EcoRV. (B-C) Confirmation of the $FN^{CC>SS}$ mutation in ES cells (B) and mice (C) by southern blot analysis of genomic DNA. DNA was hybridized with an external probe after BamHI digestion. Successful insertion of the targeting vector changes the size of WT genomic DNA fragment of 12.9 kbp to 8.8 kbp, and heterozygous $FN^{CC>SS/+}$ mice contain both the WT (12.9 kbp) and the targeted allele (8.8 kbp). (D-E) Genotyping PCR of tail DNA. Primers were designed to distinguish between a 202 bp WT allele and a 298 bp targeted allele ($FN^{CC>SS}$), from which the neo sequence had been removed by deleter-Cre (D). PCR products were resolved by electrophoresis on an agarose gel containing ethidium bromide (E). This dataset was obtained by Dr. Takao Sakai.

$FN^{CC>SS/+}$ mice were viable and fertile. To monitor weight development among heterozygotes and control littermates, all were weighed at weasning age. This analysis showed that heterozygotes are of

normal weight and thus apparently indistinguishable from WT littermates (fig. 8.3). To generate mice homozygous for the $FN^{CC>SS}$ knock-in, intercrossings of heterozygous $FN^{CC>SS/+}$ mice were performed.

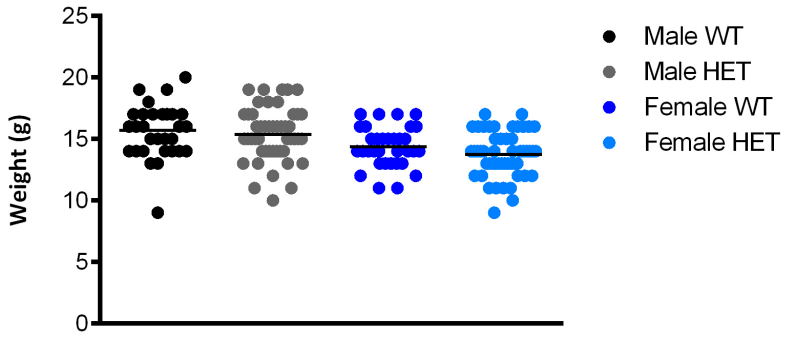

Fig 8.3. Weight distribution of WT and $FN^{CC>SS/+}$ (HET) male and female mice at weaning age (postnatal day 21).

8.2 Phenotypic analysis of the $FN^{CC>SS/CC>SS}$ mouse

$FN^{CC>SS/+}$ mice were intercrossed to generate $FN^{CC>SS/CC>SS}$ mice. As indicated in table 8.1, among the large number of progeny of $FN^{CC>SS/+}$ intercrossings that were genotyped at weaning age (21 days postnatal), none were $FN^{CC>SS/CC>SS}$ homozygous mutant.

To estimate the age at which $FN^{CC>SS/CC>SS}$ die off, timed matings were initiated between $FN^{CC>SS/+}$ mice and embryos were collected at specific developmental stages. Among embryos collected between E8.5 and E10.5, we found WT, $FN^{CC>SS/+}$ and $FN^{CC>SS/CC>SS}$ embryos at normal Mendelian ratios, i.e. 1:2:1, respectively. However, the proportion of $FN^{CC>SS/CC>SS}$ embryos was found to decline between E9.5 and E11.5, such that by E11.5, the representation of $FN^{CC>SS/CC>SS}$ embryos within a litter was drastically reduced to ca. 2.5%. Of the twenty-seven embryos recovered at E12.5, none were homozygous for the $FN^{CC>SS}$ knock in mutation. With this, we concluded that the $FN^{CC>SS}$ knock-in is a recessive embryonic lethal mutation.

		Wild-type		$FN^{CC>SS/+}$		$FN^{CC>SS/CC>SS}$	
Stage	Total	n	%	n	%	n	%
P21	448	160	35.7	288	64.3	0	0
E12.5	27	11	40.7	16	59.3	0	0
E11.5	40	12	30.0	27	67.5	1	2.5
E10.5	110	33	30.0	54	49.1	23	20.9
E9.5	307	76	24.8	148	48.2	83	27.0
E8.5	199	51	25.6	107	53.8	41	20.6

Table 8.1: Genotypes of offspring from intercrosses of $FN^{CC>SS/+}$ heterozygous mice. The normal Mendelian ratio of 1 WT: 2 $FN^{CC>SS/+}$: 1 $FN^{CC>SS/CC>SS}$ was observed for embryos collected between E8.5 to E10.5. Homozygous mutants ($FN^{CC>SS/CC>SS}$) were never identified after E11.5, indicating that lethality commences between E10.5 and E11.5. Dr. Michael Leiss contributed to this dataset.

The cause of embryonic lethality was examined in close detail. Inspection of embryos recovered between E8.5 and E10.5 revealed that all $FN^{CC>SS/CC>SS}$ embryos proceed well beyond the egg cylinder stage and the early stages of gastrulation and reach the early stages of organogenesis. At E8.5, $FN^{CC>SS/CC>SS}$ embryos were morphologically indistinguishable from WT (fig. 8.4 A and B) and heterozygous littermates (not shown). This specifically refers to finding that $FN^{CC>SS/CC>SS}$ embryos showed a proper head fold and were proceeding through somitogenesis at comparable rates, showing 6-12 somite pairs at the time of dissection. $FN^{CC>SS/CC>SS}$ embryos showed normal length and curvature along the anterior-posterior axis. Likewise, the neural tube of $FN^{CC>SS/CC>SS}$ embryos appeared normal. The heart of $FN^{CC>SS/CC>SS}$ embryos was normally enclosed by the body wall and the heart tube was producing regular contractions at the time of dissection. At the embryonic posterior, both $FN^{CC>SS/CC>SS}$ and WT embryos had developed an allantois that either had made or was in the process of making contact with the chorion at the base of the placenta, in preparation of forming the placental blood vessels and building the umbilical cord.

The mutant phenotype became apparent at E9.5, with several anomalies, albeit at various degrees of severity (fig. 8.4 C). Although most $FN^{CC>SS/CC>SS}$ embryos had successfully turned into the fetal position, they began to exhibit a general delay in growth; the head region was small and posterior region was short compared to WT littermates. Whereas WT embryos at E9.5 had developed up to 24 somite pairs, the $FN^{CC>SS/CC>SS}$ embryos were rarely found to have more than 20 somite pairs. At this embryonic stage, WT embryos had always developed the first, second and third pair of pharyngeal arches, while $FN^{CC>SS/CC>SS}$ embryos typically only develop the first pair of pharyngeal archs (occasionally a second pair). These are vascularised anlage that arise from the aortic sac, extend ventrally from the dorsal aorta to meet at the midline and will give rise to several major arteries. $FN^{CC>SS/CC>SS}$ embryos had an overall anaemic appearance with only trace amounts of blood in the dorsal aorta, heart and in the general circulation, suggesting vascular or hematopoietic malfunction. Although the heart still maintained regular contractions in E9.5 $FN^{CC>SS/CC>SS}$ embryos, the heart appeared under-developed and lacked features of a looped and segmented cardiac tube. Most striking at this stage of development was the appearance of an enlarged pericardial sac surrounding the $FN^{CC>SS/CC>SS}$ cardiac tube. The pericardial sac is a fibrous sac surrounding the heart, and under normal WT circumstances it contains only little fluid. This swelling of the pericardium seen in $FN^{CC>SS/CC>SS}$ embryos is strongly indicative of accumulating plasma, i.e. oedema, arising from leaky vessels and/or insufficient cardiac output from the under-developed heart.

Of those $FN^{CC>SS/CC>SS}$ embryos that advanced to E10.5, many showed signs of deterioration and were very fragile (fig. 8.4 D). The major phenotypic features seen in younger $FN^{CC>SS/CC>SS}$ embryos, such as anaemia and oedema, had only become more severe by E10.5. Also, the allantoic mesoderm of most $FN^{CC>SS/CC>SS}$ embryo had failed to establish the umbilical vasculature (not shown), despite the fact that at E8.5, the allantois of all $FN^{CC>SS/CC>SS}$ embryos examined had grown and appeared to have fused with the chorion. Where chorioallantoic fusion had occurred, the allantois often appeared constricted, while the base of these allantois often appeared swollen and oedemic. Brain, somite and

pharyngeal arch development had stalled, and there were no sign of forelimb development to the extent seen in WT littermates.

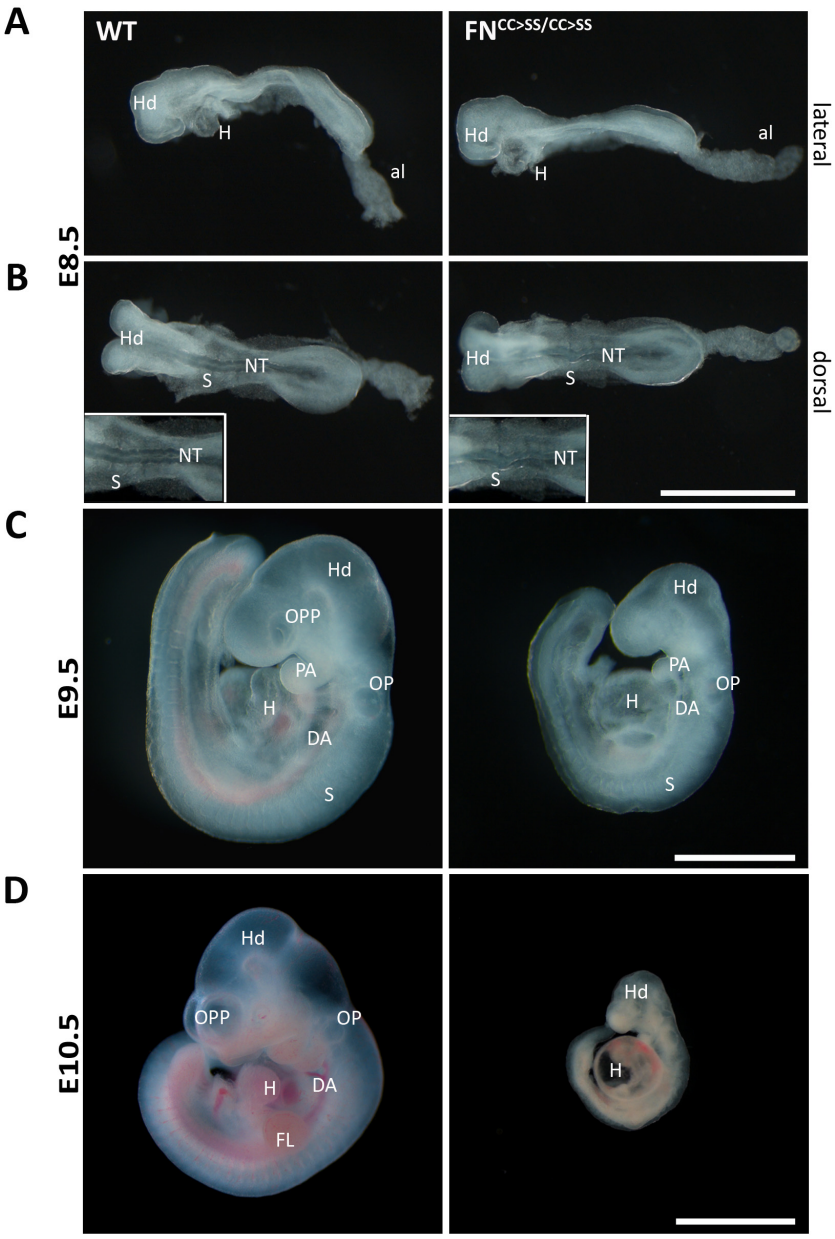

Figure 8.4. Whole mount presentation of WT and $FN^{CC>SS/CC>SS}$ embryos between E8.5 and E10.5. (A) Lateral view of E8.5 WT and $FN^{CC>SS/CC>SS}$ embryos. (B) Dorsal view of E8.5 WT and $FN^{CC>SS/CC>SS}$ embryos. Insets show magnified view of somites, 6 pairs in both embryos. (C) Lateral view of E9.5 WT and $FN^{CC>SS/CC>SS}$ embryos. (D) Lateral view of E10.5 WT and $FN^{CC>SS/CC>SS}$ embryos. al, allantois; DA, dorsal aorta; FL, forelimb, Hd, head; H, heart, NT, neural tube; OPP, optic pit; OP otic pit; PA, pharyngeal arch; S, somites. Scale bar: (A-C) 500 μm; (D) 1 mm. This dataset was obtained by Dr. Michael Leiss.

8.2.1 Extraembryonic vascular defects

Morphologically abnormal $FN^{CC>SS/CC>SS}$ embryos also exhibited defects in the development of the vasculature in extra-embryonic tissues, such as the yolk sac and the placenta. A striking, but typical, phenotypic feature of $FN^{CC>SS/CC>SS}$ yolk sacs between E9.5 and E10.5 was a blistered and anaemic appearance of the yolk sac surface revealed to stem from an unusual swelling of a highly primitive

vascular plexus (fig. 8.5). The primitive blood vessels were devoid of blood, yet small amounts of blood were often found to have accumulated within the exocoelomic cavity. Although the presence of blood indicates that hematopoiesis must have occured within the blood islands of $FN^{CC>SS/CC>SS}$ yolk sacs, the blood leakage into the exocoelomic cavity suggests that the dilated vessels of the $FN^{CC>SS/CC>SS}$ yolk are inappropriately permeable to erythrocytes and other blood components. This inevitably is associated with the deficiency of erythrocytes within the embryonic circulation and explains the anaemic appearance of the $FN^{CC>SS/CC>SS}$ embryo. Overall, these findings demonstrate that $FN^{CC>SS}$ does not support yolk sac angiogenesis and that FN dimers are required for ensuring the integrity of the yolk sac vasculature.

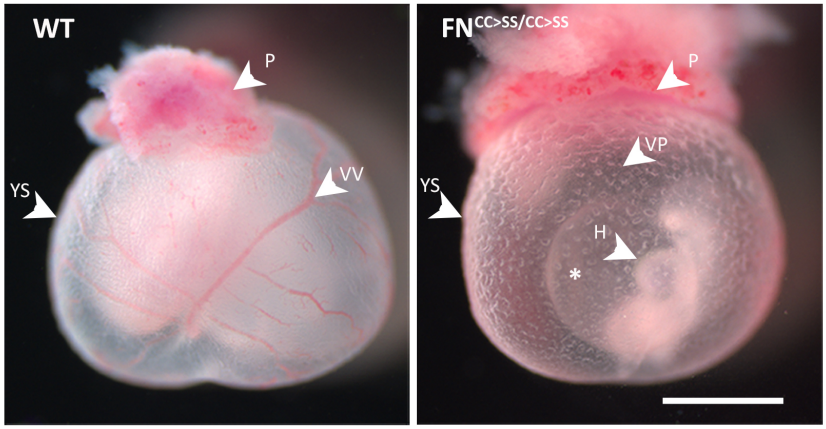

Figure 8.5. Abnormal vascular development in $FN^{CC>SS/CC>SS}$ yolk sac. Gross morphology of whole-mount yolk sacs of $FN^{CC>SS/CC>SS}$ embryos is compared to that of WT littermates at late E9.5. $FN^{CC>SS/CC>SS}$ yolk sacs exhibit severe defects in vascular development. Arrowheads show a defined and organized vessel structure in the WT yolk sac (left), whereas the $FN^{CC>SS/CC>SS}$ yolk sac contains a primitive vascular plexus of dilated blood vessels that leak into the yolk sac tissue. H, heart; P, placenta; VP, vascular plexus; VV, vitelline vessel; YS, yolk sac. * denotes oedema within the pericardium surrounding cardiac tissue in $FN^{CC>SS/CC>SS}$ embryos. Scale bar 500 μm.

Vascular development in the $FN^{CC>SS/CC>SS}$ yolk sacs was examined in closer detail by visualising vessels with an antibody specific for PECAM-1. First, I compared the vascular plexus of E8.5 yolk sacs of WT and $FN^{CC>SS/CC>SS}$ embryos and found that at this stage all yolk sacs were of comparable size and showed similar characteristics of a primitive plexus of vessels with uniform diameter and extending throughout the entire yolk sac (fig. 8.6 A). Hence vasculogenesis occurs normally in $FN^{CC>SS/CC>SS}$ yolk sacs.

Next I compared yolk sacs from E9.5 embryos. At this stage, a WT yolk sac vasculature will have undergone substantial remodelling to build a hierarchy of highly branched large and small calibre vessels. However, the vasculature of $FN^{CC>SS/CC>SS}$ yolk sacs had failed to undergo the same remodelling programme and therefore lacks any hierarchical organisation and branching of vessels (fig. 8.6 B).

Futher histological analysis of E9.5 yolk sac sections demonstrated that $FN^{CC>SS/CC>SS}$ yolk sacs have abnormally large vessel lumens (fig. 8.6 C), explaining the blistered gross-morphological appearance of $FN^{CC>SS/CC>SS}$ yolk sacs. Large vascular lumens in the yolk sac have been described

before and are often interpreted as deriving from defective cell-matrix adhesion resulting in weak attachment between the extra-embryonic endoderm and mesoderm layers of the yolk sac. Consistent with this interpretation, large lumens were described for yolk sacs of both FN knock-out (George et al., 1993; George et al., 1997) and integrin α5 knock-out mice (Yang et al., 1993), but have also been described for mutant mice lacking diverse growth factor signals such as TGF-β1 (Larsson et al., 2001) and VEGF-A (Carmeliet et al., 1996). Together these findings suggest defects in the complex interplay of growth factor- and cell adhesion-mediated vascular remodelling in the $FN^{CC>SS/CC>SS}$ mouse.

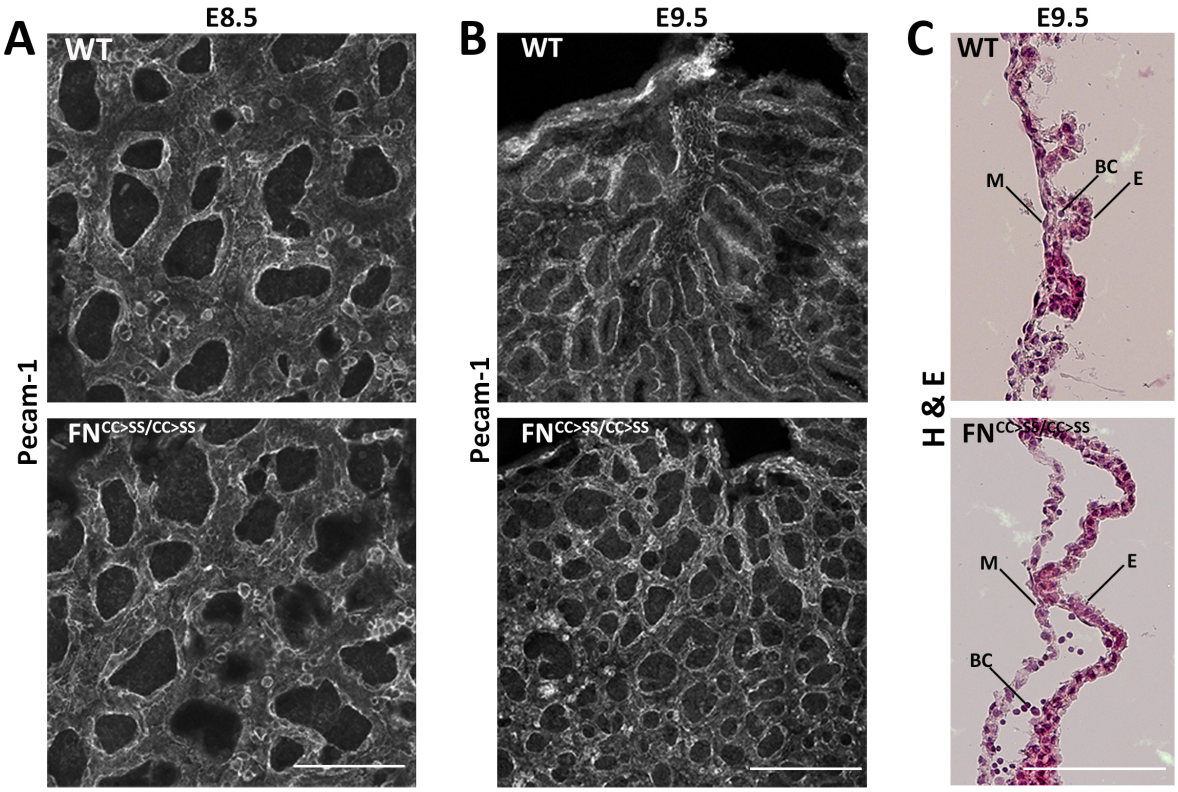

Figure 8.6. Defective remodelling of the primitive vascular plexus in $FN^{CC>SS/CC>SS}$ yolk sacs. Flat-mounted WT and $FN^{CC>SS/CC>SS}$ yolk sacs at (A) E8.5 and (B) E9.5 were immunostained with an antibody against PECAM-1. (C) Cryo-sections of WT and $FN^{CC>SS/CC>SS}$ yolk sac at E9.5 stained by H&E. BC, blood cell; E, extraembryonic endoderm; M, extraembryonic mesoderm. Scale bars: (A) 100 μm, (B) 200 μm, (C) 100 μm.

8.2.2 Distribution of mural cell within the $FN^{CC>SS/CC>SS}$ yolk sac primitive vascular plexus

Although vasculogenesis does not depend on mural cells, the subsequent survival, remodelling and stabilisation of remodelled vessels (i.e. angiogenesis) relies strongly on the short-range signalling between mural cells and endothelium (Abramsson et al., 2003) Also add Lindahl et al 1997a. $FN^{CC>SS/CC>SS}$ yolk sac vasculatures show clear signs of stalling their development at the remodelling stage, and therefore I investigated the extent of mural cell differentiation and investment of yolk sac blood vessels.

Using α-smooth muscle actin (α-SMA) as a marker for mural cells, WT yolk sacs were found to contain mural cells associating with the underlying endothelium according to vessel calibre; high-

calibre vessels were associated with a high density of mural cells whereas low-calibre capillaries showed more sparse association with mural cells (fig. 8.7 A). In $FN^{CC>SS/CC>SS}$ yolk sacs, α-SMA-positive mural cells were present in the vascular plexi, but in contrast to WT yolk sacs, these mural cells were highly abundant and distributed randomly across the entire plexus.

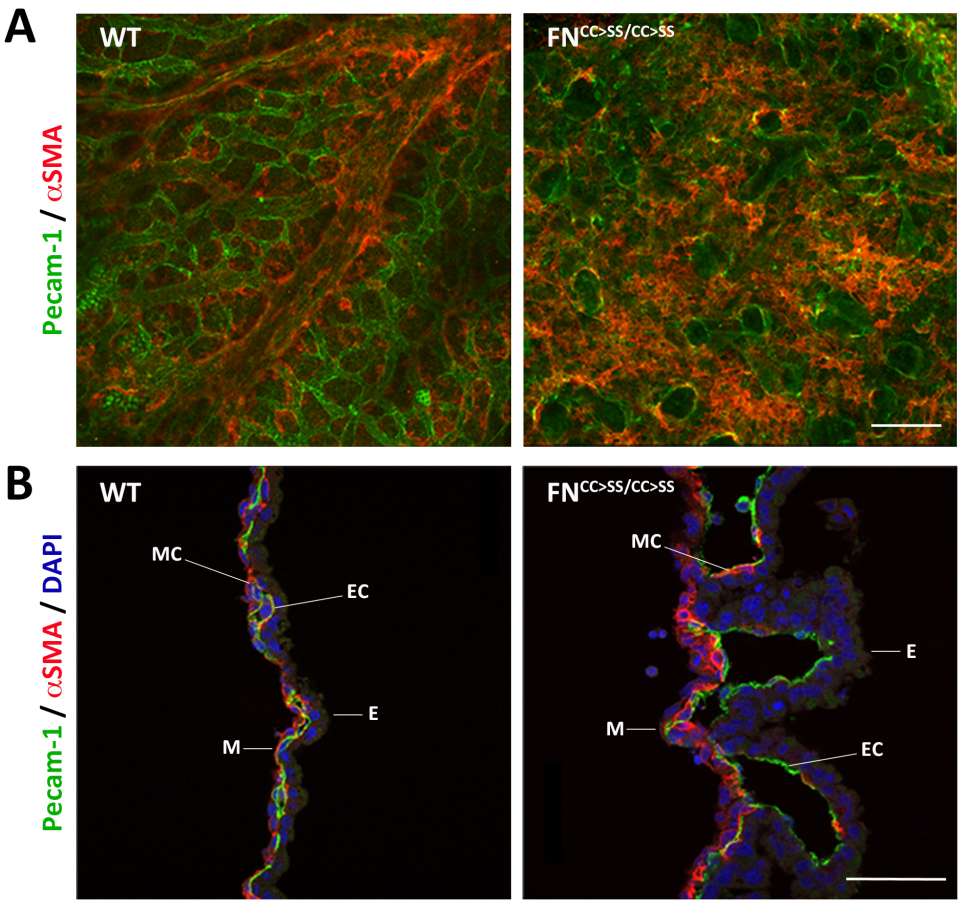

Figure 8.7. Abnormal distribution of mural cells within the vasculature of $FN^{CC>SS/CC>SS}$ yolk sac. (A) Flat-mounted WT and $FN^{CC>SS/CC>SS}$ yolk sacs at E9.5 were immunostained with antibodies against PECAM-1 (green) and α-SMA (red), and nuclei were stained with DAPI (blue). (B) Cryo-sections of WT and $FN^{CC>SS/CC>SS}$ yolk sacs at E9.5 were immunostained with antibodies against PECAM-1 (green) and α-SMA (red), and nuclei were stained with DAPI (blue). MC, mural cell; EC, endothelial cell; M, extraembryonic mesoderm; E, extraembryonic endoderm. Scale bar: 100 μm.

The association of mural cells with the endothelium was also examined in histological sections of E9.5 yolk sacs. Cross-sections of WT yolk sacs showed an intimate association between mural cells and the endothelium surrounding narrow lumens (fig. 8.7 B). Most fields of $FN^{CC>SS/CC>SS}$ yolk sac cross sections revealed abnormally large lumens that were fully lined with endothelium, but only sparsely lined by mural cells. The majority of α-SMA-positive mural cells appeared to be associated with the extraembryonic mesoderm, and those that were found lining the vessel appeared correctly associated with the endothelium. While these data unanimously indicate that the $FN^{CC>SS/CC>SS}$ endothelium supports both the recruitment of mesenchymal cells and their differentiation into α-SMA-positive mural cells, where else the functional defect lies remains unclear. The random distribution of mural cells along the $FN^{CC>SS/CC>SS}$ yolk sac endothelium appears to reflect the lack of vascular hierarchy within the underlying endothelium and suggests that the failure of the primitive plexus to remodel

primarily relates to an endothelial cell-autonomous defect. However, an inability of mural cells to migrate and align correctly with the endothelium could also abrogate the pro-angiogenic paracrine signalling events between endothelial cells and mural cells and thereby stall angiogenesis. Given that FN is a prominent component of the vascular basement membrane shared between endothelial cells and mural cells, it is possible that $FN^{CC>SS}$ impairs the alignment and paracrine signalling between endothelium and mural cells.

8.2.3 Placentation defects in $FN^{CC>SS/CC>SS}$ embryos

Placental development is accompanied by chorioallantoic fusion, vascular growth from the allantoic mesoderm and vascular infiltration of the placenta. As shown earlier, the majority of both $FN^{CC>SS/CC>SS}$ and WT embryos alike had built an allantois that appeared to have made contact to the chorion between E8.5 and E9.5. Normally, just hours after chorioallantoic fusion, embryonic vessels develop from the allantoic mesoderm and sprout into the placenta to establish the embryonic components of the placental vascular network. By E10.5, these embryonic vessels will have formed finger like projections into the placental labyrinth layer (Rossant and Cross, 2001). Indeed this was evident for WT placenta sectioned parasagitally and immunostained against endomucin (fig. 8.8). In contrast, immunohistochemical analysis of $FN^{CC>SS/CC>SS}$ placental tissue revealed a complete failure of embryonic vessels to emerge from the allantois to penetrate the chorion and sprout into the maternal labyrinthine layer of the placenta. This finding could explain the cause of the abnormal appearance of the allantoic tissue at E10.5.

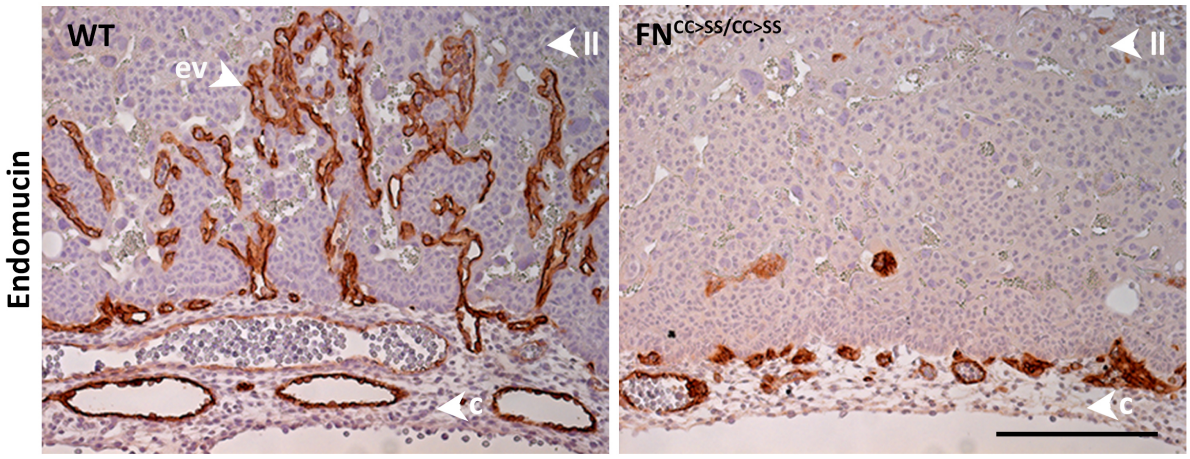

Figure 8.8. Placental vascularisation defects in $FN^{CC>SS/CC>SS}$ embryos. Histological cross-sections of E10.5 placental tissue were stained with an antibody against endomucin. c, chorion; ev, embryonic vessel; ll, labyrinthine layer. Scale bar 100 µm. This dataset was obtained by Dr. Michael Leiss.

In response to failing to establish circulation between embryonic and maternal tissue, the allantoic tissue begins to regress and degenerate, while plasma originating from the embryo accumulates at the base of the allantois and causes oedema. Without intermingling of embryonic and maternal vessels, there can be no exchange of waste products or nutrients to support the growth of the embryo. Thus

placental insufficiency caused by inefficient vascularisation is a plausible cause of lethality in $FN^{CC>SS/CC>SS}$ embryos.

8.2.4 Embryonic vascular remodelling defects

To investigate the vascular infrastructure of E9.5 $FN^{CC>SS/CC>SS}$ embryos, the embryo proper was examined by detecting vessels with an antibody against endomucin. A striking feature of the $FN^{CC>SS/CC>SS}$ embryos at E9.5 was the weak antigenicity for endomucin antibody in the cranial tissue, indicating a paucity of cranial vessels in a region where the WT littermate otherwise show dense, clearly patterned and elaborate networks of endomucin-positive blood vessels (fig. 8.9). In $FN^{CC>SS/CC>SS}$ embryos blood vessels in appear constricted and chaotically arranged, in contrast to the hierarchical arrangement of branching vessels in the head of WT embryos. Beyond the head region, the endomucin staining highlights the vascular lining of the dorsal aorta and pharyngeal arches. Again, these vascular structures were found to appear narrow in $FN^{CC>SS/CC>SS}$ embryos, which would obstruct the flow of blood to the tissues they supply.

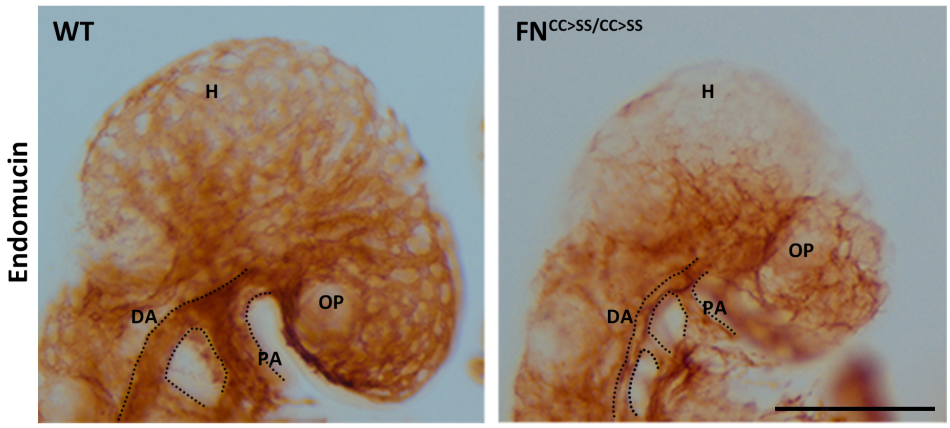

Figure 8.9. Abnormal vascular patterning in the $FN^{CC>SS/CC>SS}$ embryo proper. Whole mount E9.5 WT and $FN^{CC>SS/CC>SS}$ embryos were immunohistochemically stained with an antibody against endomucin. The dotted line outlines the dorsal aorta and pharyngeal arteries, which are well-defined in WT embryos, but appear constricted in $FN^{CC>SS/CC>SS}$ embryos. DA, dorsal aorta H, head; OP, optic pit; PA, pharyngeal artery. Scale bar: 250 μm. These data were obtained by Dr. Michael Leiss.

Similar traits of immature vascular development and defective vascular interconnections emerged from whole mount immunostainings of the vasculature in the trunk region of E9.5 $FN^{CC>SS/CC>SS}$ embryos stained with antibodies against PECAM-1 (fig. 8.10). WT embryos at E9.5 showed an extensive vascular network infiltrating the entire trunk and tail region. Vessels were found to sprout from the dorsal aorta into the intersomitic regions and emerge on the dorsal side of the somites where they anastamose. Compared to WT littermates, the blood vessels appeared scarce throughout the entire trunk and tail region of $FN^{CC>SS/CC>SS}$ embryos. Similar to the endomucin stainings above, PECAM-1 stainings outlined a very thin dorsal aorta and pharyngeal arch arteries, and particularly striking was the deficiency in sprouting of intersomitic vessels from the dorsal aorta into the intersomitic region.

I assessed the presence of myocardial tissue in E9.5 embryos by whole mount immunostaining of α–SMA, which is a prominent intracellular component of the contractile myocardium (fig. 8.10). Both WT and $FN^{CC>SS/CC>SS}$ embryonic hearts showed prominent α–SMA-positive myocardium encasing the endocardium, but highlighted striking differences in the size and shape of the $FN^{CC>SS/CC>SS}$ heart tube.

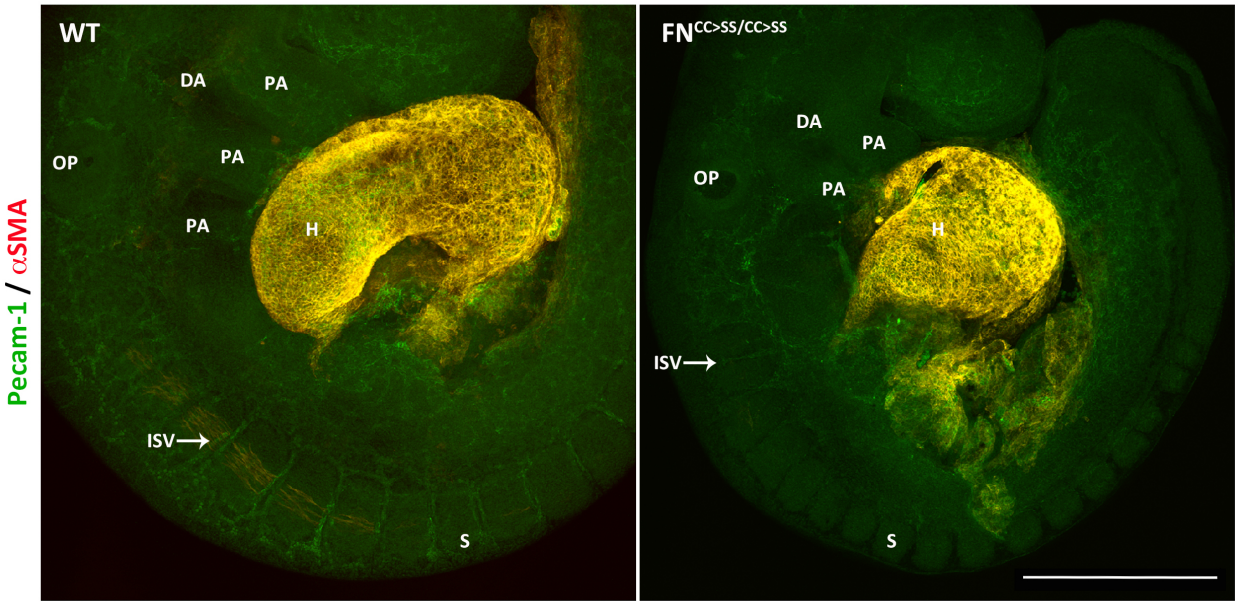

Figure 8.10. Lack of vascular expansion throughout $FN^{CC>SS/CC>SS}$ embryos. Confocal immunofluorescence images of whole mount E9.5 WT and $FN^{CC>SS/CC>SS}$ embryos stained with antibodies against PECAM-1 (green) and αSMA (red). DA, dorsal aorta; ISV, intersomitic vessel; OP, otic placode; PA, pharyngeal arch arteries; S, somite. Scale bar 500 μm.

8.2.5 $FN^{CC>SS/CC>SS}$ embryos develop cardiac defects

The enlarged pericardial sacs, heart oedema and signs of a growth defect of the myocardium shown earlier suggested a failure of the $FN^{CC>SS/CC>SS}$ primitive heart tube to elongate and undergo looping morphogenesis. This prompted me to examine how $FN^{CC>SS}$ distorts endocardial morphogenesis.

Endocardial morphology in E9.5 WT and $FN^{CC>SS/CC>SS}$ embryos was analysed by immuno-staining with an antibody against PECAM-1. At E9.5, the WT heart tube had proceeded through rightward looping morphogenesis to bring the segments of the heart tube close to their final topographical position whereas the endocardial morphology of $FN^{CC>SS/CC>SS}$ embryos was severely distorted (fig. 8.11 A). The degree of distortion varied among $FN^{CC>SS/CC>SS}$ embryos, but in all cases observed the endocardium curvature appeared irregular and the endocardial heart tube was both stunted and had failed to complete rightward looping morphogenesis. Immuno-histological analysis of E9.5 embryonic hearts sectioned in transverse and stained with antibodies against PECAM-1 demonstrated an inability of the $FN^{CC>SS/CC>SS}$ endocardium to extend and interact with the surrounding myocardium (here indicated by DAPI stain) (fig. 8.11 B).

Although these structurally deformed heart tubes in $FN^{CC>SS/CC>SS}$ embryos appeared to have adequate ample myocardial coverage (cf. fig. 8.10) and were showing regular contractions at the time of

dissection, the failure to undergo looping morphogenesis is likely to affects the ability of the mutant heart to establish and maintain a sufficient level of blood circulation as the embryos grow. Interestingly, very recent work has shown that vascular remodeling in the mouse yolk sac is secondarily affected when cardiac function and proper circulation is reduced or absent (Lucitti et al., 2007). This raises the possibility that blood vessel remodelling defects in $FN^{CC>SS/CC>SS}$ embryos is a secondary effect of the malformed cardiac tissue and a lack of hemodynamic force.

While such cardiac remodelling defects could relate to a number of faulty mechanisms, such as a general left/right asymmetry abnormality in $FN^{CC>SS/CC>SS}$ embryos, ventral closure defects or even deficiencies in the lateral plate mesoderm.

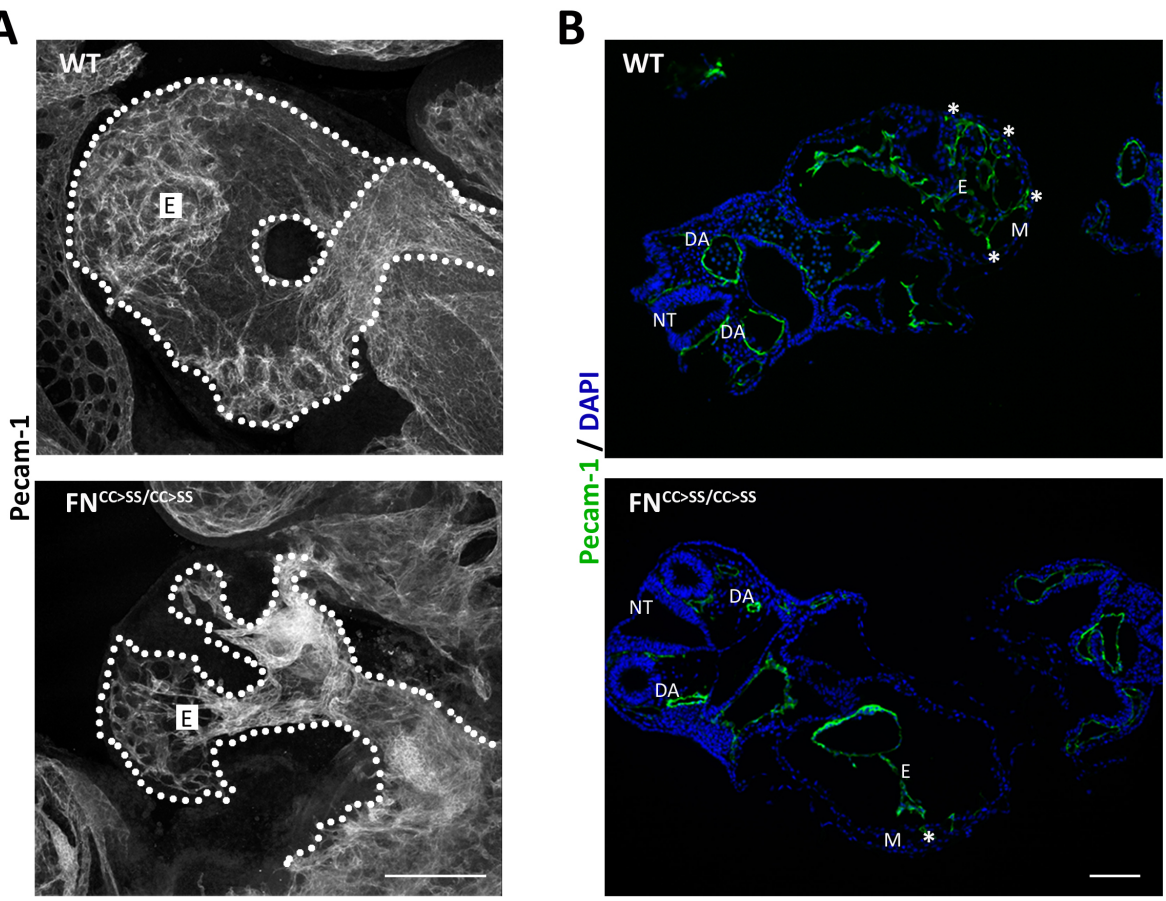

Figure 8.11. Failure in cardiac looping morphogenesis in $FN^{CC>SS/CC>SS}$ embryos. (A) Confocal images of whole mount E9.5 WT and $FN^{CC>SS/CC>SS}$ endocardiac tissue from a parasastained with an antibody against PECAM-1. The dotted line outlines the endocardium. (B) Immunofluorescence images of paraffin sectioned E9.5 WT and $FN^{CC>SS/CC>SS}$ embryos that were stained with an antibody against PECAM-1 (green) and DAPI (blue) for nuclei. * indicates point of contact between endocardium (green) and myocardium (blue), of which there are only a few in $FN^{CC>SS/CC>SS}$ cardiac tissue. DA, dorsal aorta; E, endocardium; M, myocardium; NT, neural tube. Scale bar 200μm.

8.2.6 Misoriented and deformed myotomal myocytes in $FN^{CC>SS/CC>SS}$ embryos

Although malformations in the cardiovascular system are prominent features of the $FN^{CC>SS/CC>SS}$ embryos and likely to be the cause of embryonic lethality, the developmental defects caused by the $FN^{CC>SS}$ knock-in mutation are not restricted to the cardiovascular system. For example, α-SMA-

immunostaining of whole mount E9.5 embryos revealed a striking difference in the organisation of myotomal cells within the somites. WT embryos showed clusters of fully aligned α-SMA-positive cells that were stretched and elongated through what appeared to be attachments to the intersegmental borders. In stark contrast, α-SMA-positive myotomal cells in $FN^{CC>SS/CC>SS}$ embryos were strongly reduced in numbers and found to populate only the anterior-most somites (fig. 8.12).

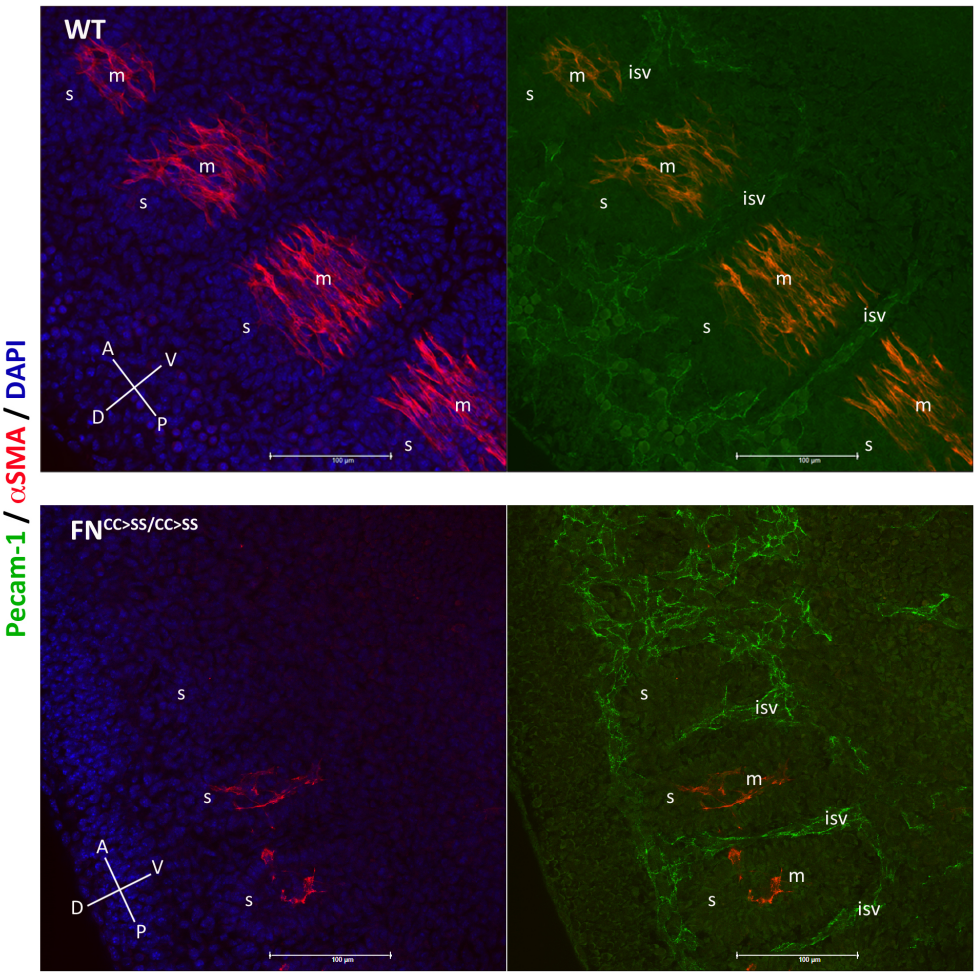

Figure 8.12. Abnormal number and orientation of α-SMA-positive myocytes residing in the somites. Confocal immunofluorescence images of a parasagittal view on whole-mount E9.5 WT and $FN^{CC>SS/CC>SS}$ embryos, stained with antibodies against PECAM-1 (green) and α-SMA (red). Nuclei are stained with DAPI (blue). Paired images compare tissue at the anterior-most somite level. A, anterior; D, dorsal; isv, intersomitic vessel; m, myotomal myocyte; P, posterior; s, somite; V, ventral. Scale bar 100 μm. Experiments of this type was performed on at least 3 indiviual embryos.

The myotome is a segmented, transitory muscle that forms within the somite and transitions into the epaxial and hypaxial muscles (deep back muscles) of the adult vertebrate organism (Deries et al., 2010). Myotomal myocytes differentiate from myoblasts and elongate to span the length of each somite in parallel to the anterior-posterior axis of the embryo by attaching to the intersegmental boundary of the somite. The unusually low number of myotomal myocytes in $FN^{CC>SS/CC>SS}$ embryos suggests an inability of dermomyotomal myoblasts to differentiate into myocytes. The misorientation and misalignment, in turn, suggest an inability of the myotomal myocytes to sense the alignment of neighboring myocytes and/or attach to the intersegmental boundary. These myotomal myocyte defects

are accompanied by their rounding up and disintegration in an anoikis-like manner. Such an attachment defect could reflect a failure of monomerised $FN^{CC>SS}$ matrix to support myocyte attachment due to mechanical flaws of the matrix, which is a theme that will be explored futher.

8.3 Characterisation of FN expression and distribution in $FN^{CC>SS/CC>SS}$ embryos

To begin understanding the cellular and molecular consequences of preventing FN dimerisation, an analysis of FN expression, distribution and assembly was performed in WT and $FN^{CC>SS/CC>SS}$ embryos. The expression level of FN in WT and $FN^{CC>SS/CC>SS}$ littermate embryos was determined by real time quantitiative PCR (RT-qPCR) analysis of cDNA isolated from single E8.5 yolk sacs. Here, WT and $FN^{CC>SS/CC>SS}$ littermates were found to have comparable levels of FN transcript (fig. 8.13 A).

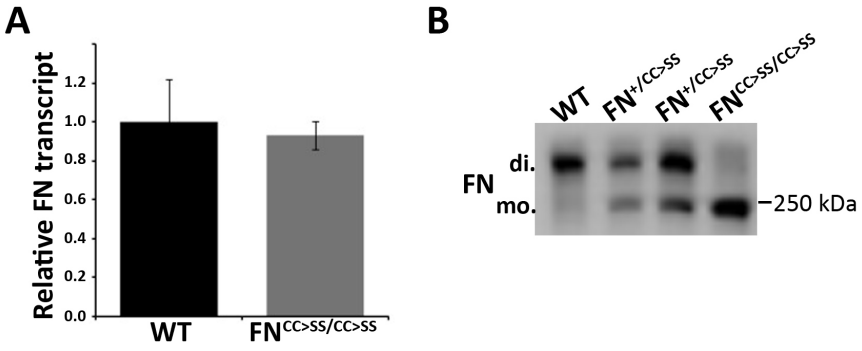

Figure 8.13. FN expression and synthesis in WT and $FN^{CC>SS/CC>SS}$ tissue. (A) RT-PCR analysis of FN gene expression based on cDNA prepared from individual E8.5 WT (n=3) and $FN^{CC>SS/CC>SS}$ (n=4) yolk sacs. Error bars represent standard deviation. (B) Non-reducing SDS-PAGE and western blot analysis of total FN in single E9.5 WT, $FN^{+/CC>SS}$ and $FN^{CC>SS/CC>SS}$ embryo lysates. di, dimeric FN; mo, monomeric FN. Data shown in (B) was obtained by Dr. Michael Leiss.

Both the total levels and molecular weight distribution of non-reduced FN protein isolated from WT and $FN^{CC>SS/CC>SS}$ embryos was analysed by western blotting. Single E8.5 embryo lysates were resolved by SDS-PAGE under non-reducing conditions to preserve disulfide-mediated dimers, when present. Western blot analysis showed that total FN protein levels were comparable between WT and $FN^{CC>SS/CC>SS}$ embryos. Furthermore, while WT embryos accumulated mainly a high molecular weight form of FN (i.e., greater than 400 kDa), representing the dimeric form of FN, the FN isolated from $FN^{CC>SS/CC>SS}$ embryos was exclusively of a low molecular weight form (i.e., ca. 250 kDa), which represents monomeric FN (fig. 8.13 B).

The distribution of FN in WT and $FN^{CC>SS/CC>SS}$ embryos was analysed by histological analysis of E9.5 embryo parasagittal sections stained with antibodies against FN. In both WT and $FN^{CC>SS/CC>SS}$ embryos, FN is abundant in the majority of tissues, including the head mesenchyme, endocardium, intersomitic regions and pre-somitic mesoderm. Hence, the monomerised form of FN is expressed and distributed normally throughout the $FN^{CC>SS/CC>SS}$ embryo (fig 8.14).

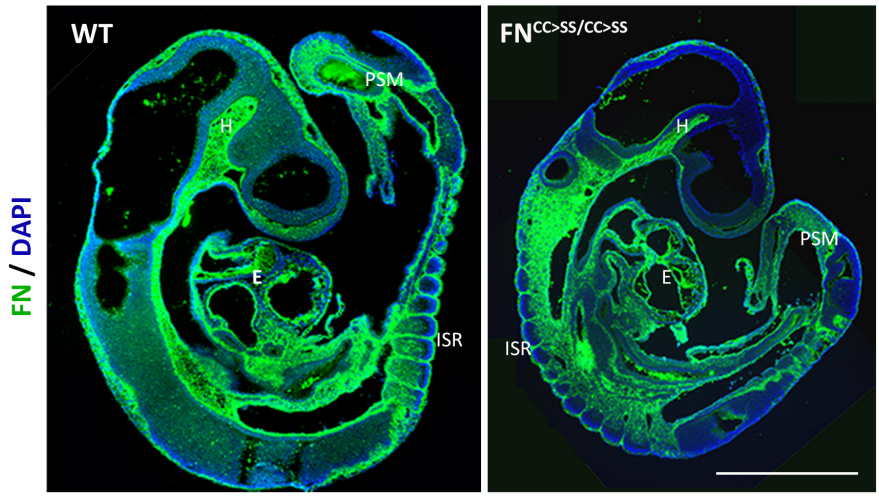

Figure 8.14. Distribution of FN in E9.5 WT and $FN^{CC>SS/CC>SS}$ embryos. Immunofluorescent images of parasagittal embryo paraffin sections stained with antibody against FN (green). Nuclei are stained by DAPI (blue). H, head mesenchyme; E, endocardium; ISR, intersomitic region; PSM, presomitic mesoderm. Scale bar 500 μm. These data were obtained by Dr. Michael Leiss.

Given the striking vascular remodelling defects of the yolk sac, I also examined the distribution of FN in histological sections of E9.5 WT and $FN^{CC>SS/CC>SS}$ yolk sacs. Cross-sections contained FN in the basement membrane between endothelium and mural cells and showed little difference in the amounts or distribution of FN between WT and $FN^{CC>SS/CC>SS}$ yolk sacs (fig. 8.15).

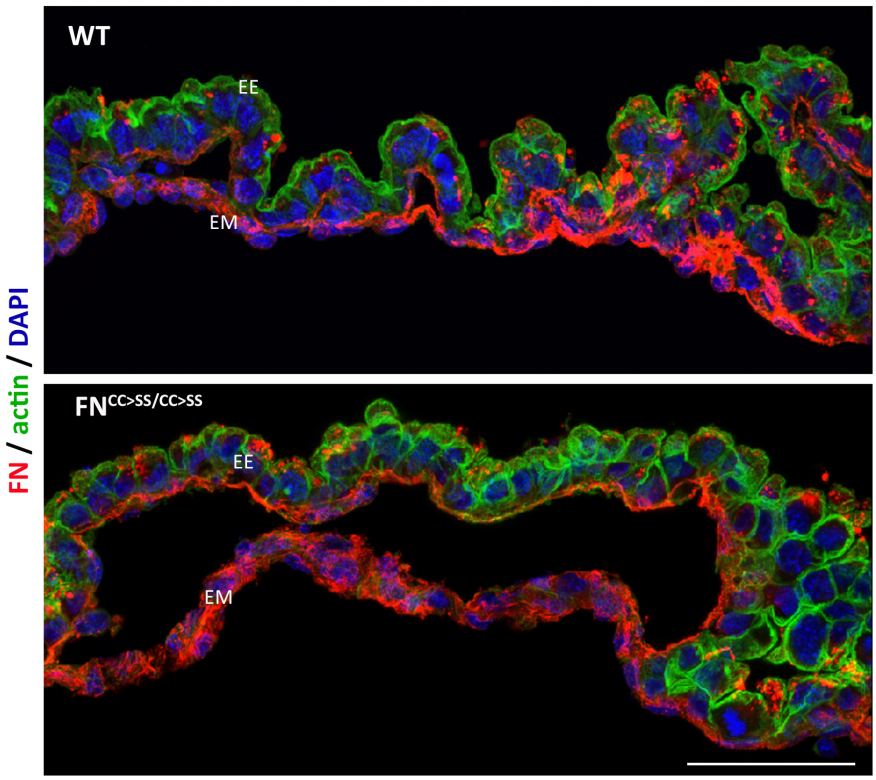

Figure 8.15. Distribution of FN in E9.5 WT and $FN^{CC>SS/CC>SS}$ yolk sacs. Immunofluorescence images of yolk sac cryosections stained with antibody against FN (green). Nuclei are stained by DAPI (blue). EE, extraembryonic endoderm; EM, extraembryonic mesoderm. Scale bar 50 μm.

Having found normal patterns of expression and distribution of FN in $FN^{CC>SS/CC>SS}$ embryos and yolk sacs, I asked whether the monomeric form of FN in $FN^{CC>SS/CC>SS}$ embryos was present in a fibrillar form. Studies from other labs have concluded that if FN is prevented from dimerising, it cannot undergo de novo fibrillogenesis and is therefore not deposited in a fibrillar form (Schwarzbauer, 1991). The fact that $FN^{CC>SS/CC>SS}$ embryos survive longer than FN knock-out mice suggests that the $FN^{CC>SS}$ deposited in embryonic tissues could retain some functions that relate to its fibrillar state. To investigate the fibrillar state of FN in WT and $FN^{CC>SS/CC>SS}$ tissue, E9.5 embryos were stained with an antibody against FN and examined as whole-mounts by confocal microscopy.

Representative images of FN in comparable regions of somite and cranial tissue demonstrate the fibrillar nature of FN in WT and $FN^{CC>SS/CC>SS}$ (fig. 8.16 A). All embryonic tissues unanimously revealed that FN in $FN^{CC>SS/CC>SS}$ embryos is present in a fibrillar form. This is the first demonstration that FN that is prevented from dimerising can undergo *de novo* fibrillogenesis and that FN fibrillogenesis does not strictly require FN dimerisation.

When compared to the FN fibrillar matrix in corresponding tissues of WT embryos, subtle morphological differences in the fibrillar character of FN in $FN^{CC>SS/CC>SS}$ embryos are noticed. In $FN^{CC>SS/CC>SS}$ embryos, FN fibrils appear both structurally less compact and mostly shorter than fibrils of WT FN. To quantify the distribution of FN fibril length, projections of high-magnification confocal z-stacks of WT and $FN^{CC>SS/CC>SS}$ embryonic tissue were analysed with a tracking function in ImageJ software. Single fibrils in z-stack projections of equal thickness were tracked manually, and the lengths of these traces were collected for statistical analysis. Care was taken to track fibrils that had clear inititation and end points within the plane of the image. To ensure an unbiased analysis, fibrils were tracked under blinded conditions, which meant that genotype of a given tissue was revealed only after the analysis.

This fibril length analysis confirmed that FN matrix in $FN^{CC>SS/CC>SS}$ tissue represents a distinct population of fibrils that are shorter than FN fibrils in WT tissue (fig. 8.16 B). FN fibrils in WT tissue tend to form fibrils greater than 6-8 μm long and have a median length of 7.46 μm, while most fibrils of monomeric FN are less than 4-6 μm long and have a median length of 4.45 μm. Statistical analysis using the Wilcoxen-Mann-Whitney test, which does not assume Gaussian distribution, showed that this difference in fibril length is highly significant ($p<0.001$) (fig. 8.16 C).

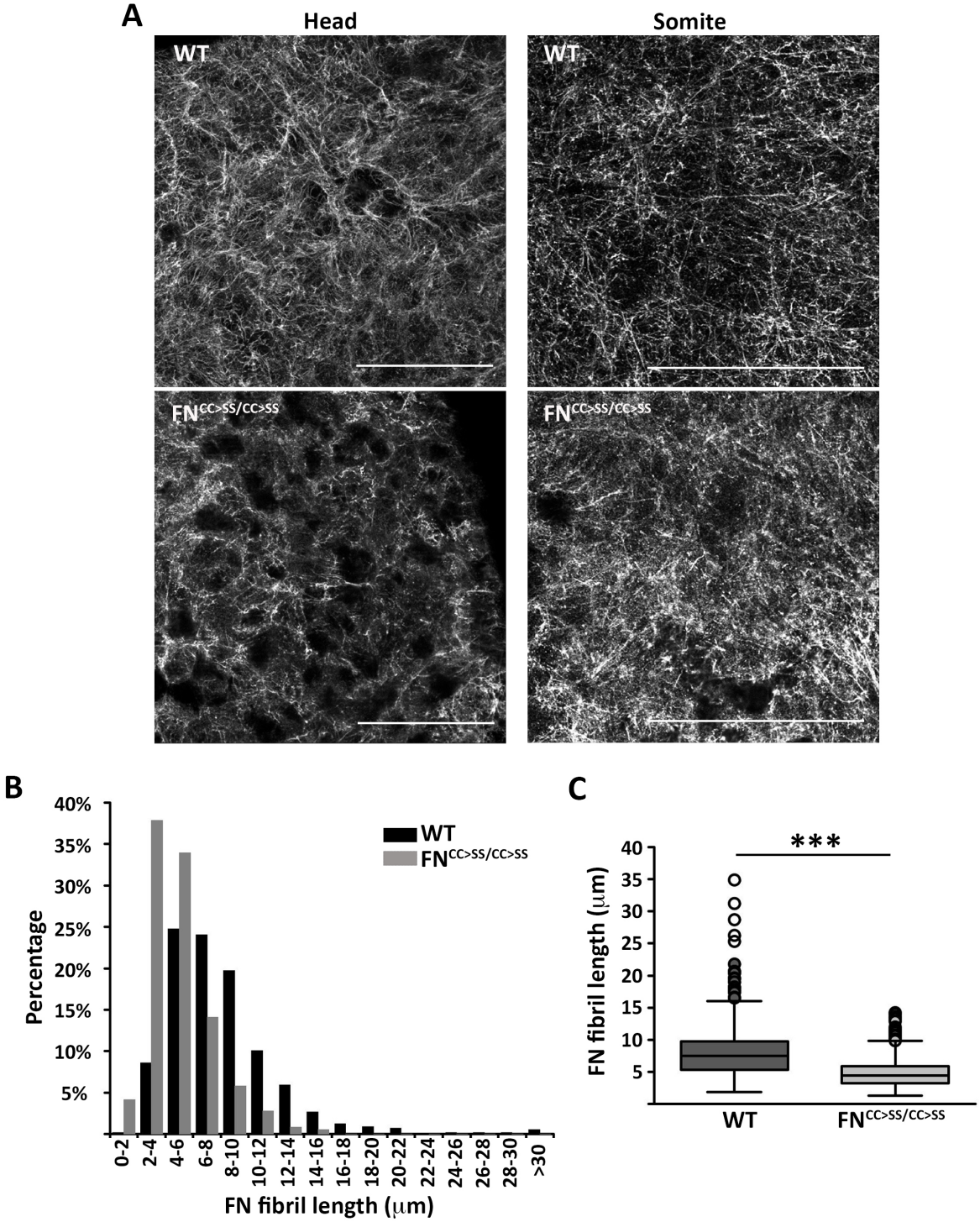

Figure 8.16. Morphology of the FN fibrillar matrix in WT and $FN^{CC>SS/CC>SS}$ embryonic tissue. (A) Confocal immunofluorescence images of head (left column) and somite tissue (right column) in whole-mount E9.5 embryos stained with antibody against FN. Scale bar 50 microns. (B) Histogram of the FN fibril length distribution in WT and $FN^{CC>SS/CC>SS}$ tissue. (C) Box and whisker plot of fibril lengths, shows that $FN^{CC>SS}$ fibrils are significantly shorter than WT FN fibrils. Grey dots indicate data points that lie outside the 75th percentile and clear dots indicate presumed otliers. Absolute median fibril length of WT FN=7.46 μm, and $FN^{CC>SS}$ =4.45 μm. Significance was determined by the Wilcoxen-Mann-Whitney test, *** $p<0.001$. Analysis was performed on at least three individual embryos of each genotype.

8.4 Biochemical and physical characterisation of the $FN^{CC>SS}$ matrix

The data presented in the previous chapter established that FN deposited by $FN^{CC>SS/CC>SS}$ embryonic tissue is fibrillar, but this fibrillar monomeric FN matrix is morphologically distinct from WT FN matrix. The following characterisation of the monomeric FN matrix is based on *in vitro*, cell culture-based experiments with cell-derived ECM. The ability to culture cells that deposit ECM allows us to investigate the kinetics of FN fibrillogenesis in a way that cannot be done *in vivo*. ECM generated in culture setups also provides a means to assay the cellular response to mutant FN, which in turn could help us understand the effect of mutant FN on embryonic development. Some of the following experiments relied on mouse embryonic fibroblasts (MEFs) that were isolated from E9.5 WT and $FN^{CC>SS/CC>SS}$ embryos by Dr. Michael Leiss and described in his thesis work. Both mixed populations and clonal cell lines of MEFs were used to address questions related to the characterisation of $FN^{CC>SS}$.

Clonal MEFs were selected on the basis of their integrin surface expression profile, which was determined by fluorescence-activated cell sorting (FACS) analysis. The selection criteria for WT and $FN^{CC>SS/CC>SS}$ clones were (a) a comparable surface expression level of FN-binding integrins, (b) low surface levels of α4 integrins, which interact with FN in an RGD motif-independent manner, and (c) low levels of α2 integrins that bind laminin, collagen and thrombospondin. As such, the clones that were chosen for subsequent analysis had equal levels of α2, α5, α6, αV, α4, β1 and β3 integrins (fig. 8.17 A).

To assess the ability of the selected clones of WT and $FN^{CC>SS/CC>SS}$ MEFs to assemble FN, the MEFs were cultured in serum replacement medium supplemented with exogenous pFN at 60 nM for 2 days. The resulting ECM was stained with antibodies against FN and integrin α5, as a molecular marker of fibrillar adhesions. The movement of α5β1 integrins along actin stress fibres to form fibrillar adhesions induces the extension of FN fibrils on the cell surface, which exposes cryptic binding sites within FN and allows it to associate with other FN molecules and form supramolecular bundles. Immunofluorescence imaging revealed the presence of long bundles of FN fibrils deposited in the ECM of both WT and $FN^{CC>SS/CC>SS}$ MEFs and that in both cultures, the FN fibrils aligned with streaks of α5 integrin-positive fibrillar adhesions. Importantly, these results indicate a comparable capacity of the FN-binding integrins expressed on the surface of WT and $FN^{CC>SS/CC>SS}$ MEF clones to assemble exogenous pFN (fig. 8.17 B). Furthermore, given that $FN^{CC>SS/CC>SS}$ clones assemble WT FN in the presence of endogenous mutant FN implies that FN derived from $FN^{CC>SS/CC>SS}$ MEFs does not have a dominant-negative effect on FN fibrillogenesis.

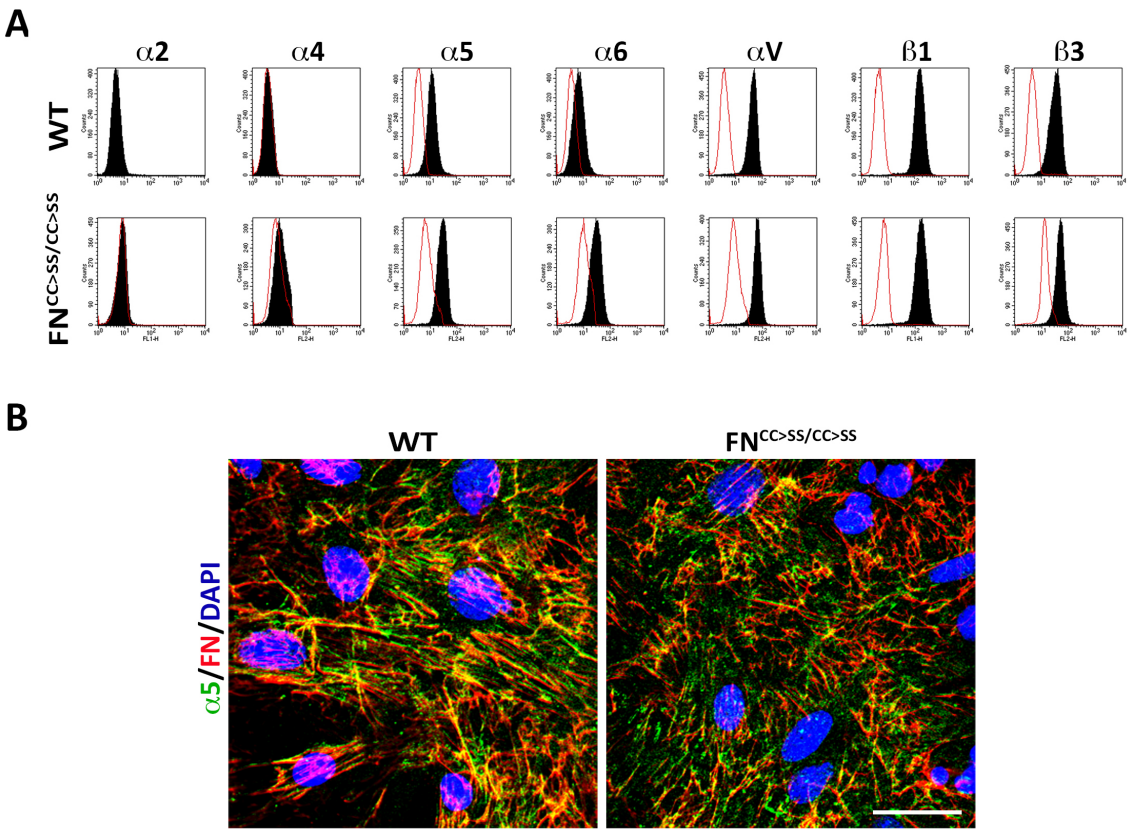

Figure 8.17. Surface integrin expression profile and FN fibrillogenesis competence of selected WT and $FN^{CC>SS/CC>SS}$ MEF clonal cell lines (A) Representative histograms of FACS analysis of integrins α2, α4, α5, α6, αV, β1 and β3 expression (red lines) compared to isotype controls (black). (B) Immunofluorescence images of WT and $FN^{CC>SS/CC>SS}$ MEF clonal cell lines, cultured in the presence of exogenous pFN (60nM), stained with antibodies against FN (red) and integrin α5 (green). Nuclei were stained by DAPI (blue). Scale bar 15 µm. These data were obtained by Dr. Michael Leiss.

8.4.1 FN fibrillogenesis by $FN^{CC>SS/CC>SS}$ mouse embryonic fibroblasts

To determine the capacity for fibrillogenesis of endogenous FN by $FN^{CC>SS/CC>SS}$ MEF and to compare the kinetics of FN fibrillogenesis by WT and $FN^{CC>SS/CC>SS}$ MEF clones, I designed time-course assays to follow the progressive deposition and assembly of FN fibrils over time. To this end, WT and $FN^{CC>SS/CC>SS}$ MEF clones were seeded on laminin111-coated glass and cultured in serum-replacement medium supplemented with 0.5% FN-depleted FBS to avoid introducing WT pFN to the cultures. At defined time points ranging from eight to ninety-six hours after cell seeding, the cultures were fixed in 4% PFA and stained with antibodies against FN.

A typical FN fibrillogenesis assay showed that after eight hours of culture time, both WT and $FN^{CC>SS/CC>SS}$ MEFs had initiated FN fibrillogenesis, generating a nearly complete carpet of short and delicate fibrils (fig. 8.18). By twenty-four hours of culture, the fibrillar morphology of FN derived from $FN^{CC>SS/CC>SS}$ MEFs remained indistinguishable from WT FN. Hence both WT and $FN^{CC>SS/CC>SS}$ MEF clones showed comparable kinetics of early fibril formation. However, after fourty-eight hours of culture time, WT FN fibrils had developed into long bundles, spanning multiple cell bodies and interconnecting with other long FN fibrils, whereas the complexity of the FN matrix derived from $FN^{CC>SS/CC>SS}$ MEFs had not changed from the previous time point such that individual FN fibrils still

appeared short and delicate. Over the course of the following fourty-eight hours, the WT FN matrix continued to evolve into a highly complex matrix of large, and heavily inter-twined bundles. In contrast, the FN matrix derived from $FN^{CC>SS/CC>SS}$ MEF cultures appeared static and failed to undergo any structural elongation or compaction. Hence, these data reiterate that FN lacking the C-terminal dimerisation motif does undergo *de novo* fibrillogenesis. However, fibrillogenesis of monomeric FN beyond the early stages appears to reach a growth plateau beyond which fibrils cannot grow in length or thickness.

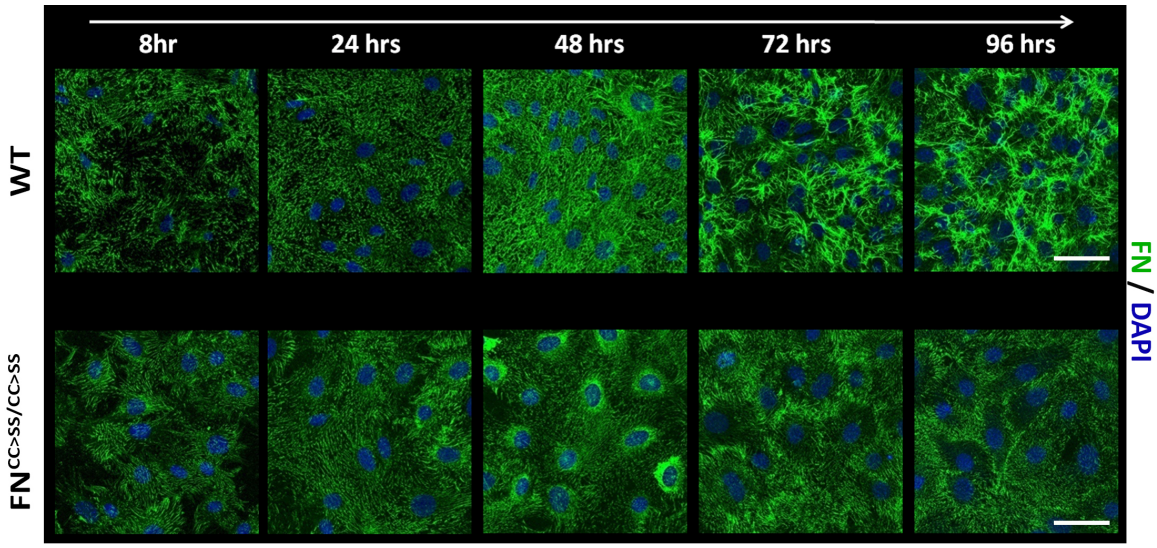

Figure 8.18. Kinetics of $FN^{CC>SS}$ fibrillogenesis. Immunofluoresence images of WT and $FN^{CC>SS/CC>SS}$ MEF clonal cell lines cultured for the indicated period of time in the presence of 0.5% FN-depleted FBS. The FN matrix is stained with antibodies against FN and nuclei are stained by DAPI. Scale bar 25 μm.

To exclude that a distinct morphology of the monomeric FN matrix arises due to differences in the total levels of FN protein deposited into the ECM, the FN content in lysatses of WT and $FN^{CC>SS/CC>SS}$ MEF cultures was analysed by western blotting. This analysis confirmed that the levels of FN synthesised and deposited into the matrix by WT and $FN^{CC>SS/CC>SS}$ MEFs was comparable (fig. 8.19). Thus the inability of monomeric FN fibrils to grow in length and thinkness was neither related to the quantity of FN nor an inability of integrins expressed on the surface of $FN^{CC>SS/CC>SS}$ MEFs to induce FN fibrillogenesis.

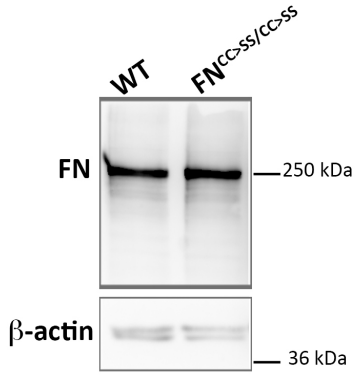

Figure 8.19. Western blot analysis of WT FN and $FN^{CC>SS}$ levels deposited into the ECM by a WT and $FN^{CC>SS/CC>SS}$ MEFs. Representative western blot comparing the FN content of lysates of

both WT and $FN^{CC>SS/CC>SS}$ MEF clonal cell line resolved by SDS-PAGE under reducing conditions.

To confirm the unique features of monomeric FN fibrillogenesis and exclude possible artefacts derived from MEF clonal cell lines, I tested the ability of $FN^{-/-}$ mouse fibroblasts (Sakai et al., 2001) to assemble either monomeric mouse pFN or WT mouse pFN. To generate monomeric mouse pFN, $FN^{+/CC>SS}$ females were crossed with males carrying the inducible Cre recombinase transgene under the control of the Mx1 promoter (Mx1Cre) (Kühn et al., 1995) and both FN alleles flanked by loxP sites ($FN^{fl/fl}$ Mx1Cre). Among the offspring of this cross, I selected $FN^{CC>SS/fl}$ Mx1Cre test mice and $FN^{+/fl}$ Mx1Cre control mice for intraperitoneal injection of poly(I:C). This double-stranded RNA induces Mx1Cre expression in the liver and thus drives the excision of the floxed FN allele in hepatocytes (Kühn et al., 1995), while the second FN allele remains intact and is continuously expressed. Succesful ablation of the floxed FN allele in liver tissue upon poly(I:C) treatment was monitored by PCR (not shown). By western blot analysis of FN content in plasma samples, I confirmed the presence of exclusively $pFN^{CC>SS}$ or WT pFN derived from the single intact FN allele in hepatocytes after poly(I:C)-induced, Cre-mediated excision of the floxed FN allele. (fig. 8.20).

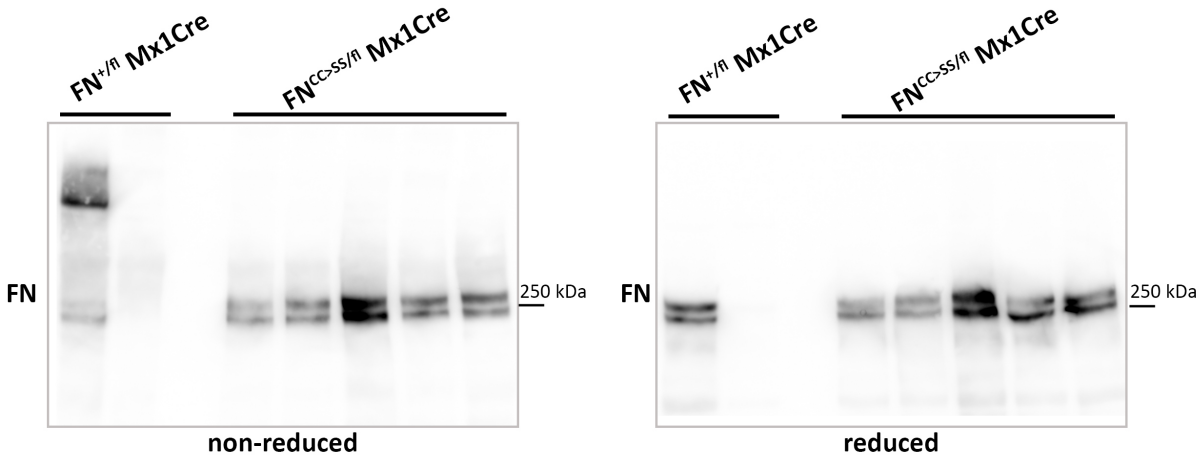

Figure 8.20. Western blot analysis of FN content in plasma from $FN^{+/fl}$ and $FN^{CC>SS/fl}$ mice after treatment with pI:C. These are representative western blots to demonstrate the analysis that was routinely performed to ensure the excision of the floxed FN allele upon pI:C treatment. These blots show that there is no floxed (WT) FN after pI:C treatment of $FN^{CC>SS/fl}$ Mx1Cre mice. Under non-reducing conditions, WT (dimeric) FN migrates as a high-molecular weight protein (>400 kDa), and monomerised $FN^{CC>SS}$ migrates at approximately 250 kDa. Under reducing conditions, both WT and monomerised FN migrate at 250 kDa. Although plasma samples from two different $FN^{+/fl}$ mice were loaded onto these gels for analysis, one sample shows no FN, indicating a technical error in the experiment.

Plasma for cell culture experiments was isolated from whole blood isolated from poly I:C-treated $FN^{CC>SS/fl}$ and $FN^{+/fl}$ Mx1Cre mice and pooled for use and storage. I specifically chose not to purify pFN from plasma to avoid artefacts that could arise from this manipulation. The pFN assembly assay was performed by seeding FN-/- mouse fibroblasts onto LM111-coated glass coverslips and culturing them in serum replacement medium supplemented with 5% (v/v) mouse plasma containing either $pFN^{CC>SS}$ or WT pFN. After two days of culture, the assembled pFN matrix was examined by immunostaining with antibodies against FN and integrin $\alpha 5$.

Immunofluorescence imaging showed a drastic difference between the fibrillar morphology of FN matrix generated with WT pFN and pFN$^{CC>SS}$ (fig. 8.21). WT pFN is assembled into a complex matrix of long and thick bundles of fibrils, whereas pFN$^{CC>SS}$ is assembled into very short fibrils that do not bundle into supramolecular structures like WT pFN fibrils do. The short fibrils within the pFN$^{CC>SS}$ matrix versus the highly complex fibrillar arrangement within a WT pFN matrix is remarkable given that the same cell type generated these two very different matrices. This finding implies that the distinct fibrillar morphology of monomeric FN is exclusively related to properties of the FN, rather than the cell line. Furthermore, these assembly assays of both pFN and cFN support the *in vivo* data showing that FN fibrils are shorter in FN$^{CC>SS/CC>SS}$ tissue ECM compared to WT ECM (fig. 8.16). These results unanimously show that preventing C-terminal disulfide bond-mediated dimerisation of FN imposes a structural limitation on the degree of fibril complexity that can be achieved once integrins have unfolded FN.

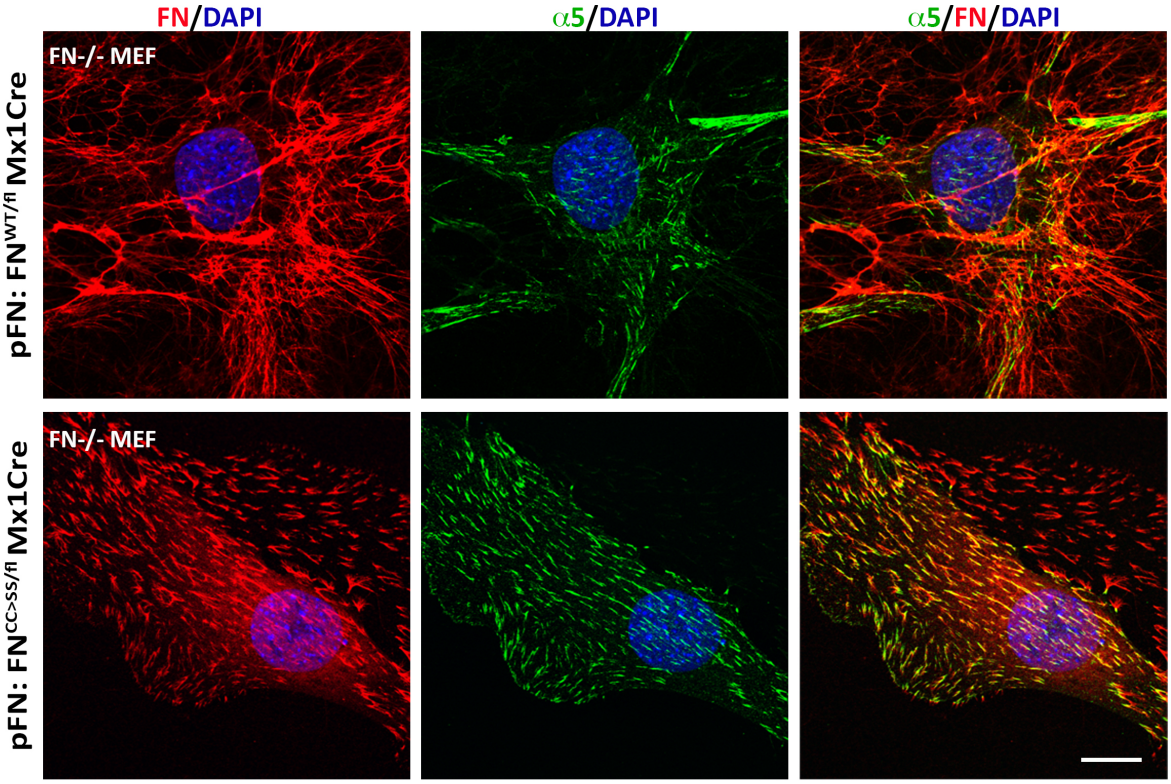

Figure 8.21. Fibrillar morphology of WT pFN and pFN$^{CC>SS}$ as assembly by FN$^{-/-}$ mouse fibroblasts. Immunofluorescence images of FN$^{-/-}$ fibroblasts cultured in the presence of mouse plasma containing either WT pFN (from FN$^{+/fl}$ Mx1Cre mouse) or pFN$^{CC>SS}$ (from FN$^{CC>SS/fl}$ Mx1Cre mouse) for 48 hours and stained with antibodies against FN (red) and integrin α5 (green). Nuclei are stained by DAPI. Scale bar: 15 μm.

The abnormal fibrillar morphology of FN observed in both the ECM of FN$^{CC>SS/CC>SS}$ MEF clones (fig. 8.18) as well as the pFN$^{CC>SS}$ matrix generated by FN$^{-/-}$ fibroblasts (fig. 8.21) raised the question whether integrin α5β1 might cluster differently within fibrillar adhesions during the assembly of FN$^{CC>SS}$. Within the same experimental framework as used to demonstrate the fibrillar nature of FN$^{CC>SS}$ matrix, I examined the morphology of fibrillar adhesions in FN$^{-/-}$ cells assembling either WT or monomeric pFN, using integrin α5 as a marker of fibrillar adhesions (fig. 8.21). Despite the

dramatic differences between pFN$^{CC>SS}$ and WT matrices in terms of supramolecular organisation of FN fibrils, the α5β1-containing fibrillar adhesions in FN$^{-/-}$ fibroblasts showed no overt difference in size or cellular distribution (fig. 8.21). Such a finding indicates that the ability of integrin α5β1 to segregate from focal adhesions and move centripetally along stress fibres does not require FN dimerisation. Furthermore, the full alignment between pFN$^{CC>SS}$ and integrin α5β1 within fibrillar adhesions shows that FN$^{CC>SS}$ incorporates into fibrillar adhesions and becomes unfolded sufficiently to allow interaction with other FN$^{CC>SS}$ molecules and thereby form small local bundles. The subsequent failure of FN$^{CC>SS}$ to transform into complex supramolecular structures indicates that failure to dimerise limits the process of lateral association and fibril elongation.

A similar approach to understanding the relationship between fibrillar adhesions and fibrillogenesis of FN$^{CC>SS}$ was taken in the clonal MEF lines depositing endogenous cFN. To this end, WT and FN$^{CC>SS/CC>SS}$ MEF clones were seeded onto LM-111-coated glass coverslips and cultured in serum replacement medium supplemented with FN-depleted FBS for eighteen hours to allow fibrillar adhesion formation and fibrillogenesis of endogenous FN. FN and integrin α5 were stained with antibodies to detect cFN fibrils and fibrillar adhesions, respectively, while cytoskeletal F-actin was stained with fluorophore-conjugated phalloidin.

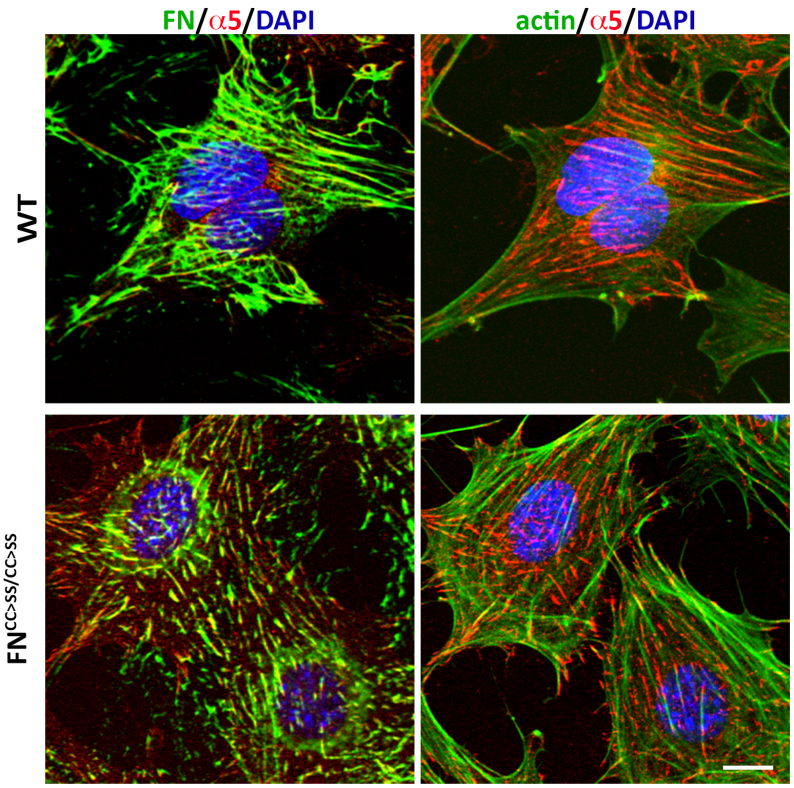

Figure 8.22. Morphology of fibrillar adhesions in WT and FN$^{CC>SS/CC>SS}$ MEFs. Immunofluorescence images of WT and FN$^{CC>SS/CC>SS}$ MEF clonal cell lines cultured in 0.5% FN-depleted serum for 18 hours and stained with antibodies against FN (green) and integrin α5 (red). Nuclei are stained by DAPI (blue). Scale bar 15 μm. These data were obtained by Dr. Michael Leiss.

Immunofluorescence imaging showed that WT MEF clones developed elongated and streak-like fibrillar adhesions in which long FN fibrils align with both integrin α5β1 and F-actin (fig. 8.22). In

contrast, fibrillar adhesions on $FN^{CC>SS/CC>SS}$ MEFs were considerably shorter, thereby closely resembling the short fibrils of $FN^{CC>SS}$ associtated with the cell surface of the $FN^{CC>SS/CC>SS}$ MEFs.

Once again, the association of integrin $\alpha5\beta1$ with $FN^{CC>SS}$ in $FN^{CC>SS/CC>SS}$ MEFs indicates that these integrins participate in the initial processing of $FN^{CC>SS}$. The stunted appearance of fibrillar adhesions could suggest that $FN^{CC>SS}$ affects the abilty of integrin $\alpha5\beta1$ to cluster and trigger the biochemical signals that activate the bundling and contractile effect of NM-II on F-actin, resulting in the failure to extend fibrillar adhesions. However, it is worth stressing that the discrepancy of these results with those of $FN^{-/-}$ cells cultured in the presence of pFN could relate to the fact that the WT and $FN^{CC>SS/CC>SS}$ MEF clones used in the latter experiment are essentially different cell lines. Despite having been selected for comparable integrin surface expression levels, we know little about how else these cells might differ. As such, the $FN^{-/-}$ cells represent a more robust system with which to evaluate the fibrillogenesis of normal and mutant FN.

8.4.2 Chemical cross-linking within a $FN^{CC>SS}$ matrix

The unique fibrillar morphology of both $pFN^{CC>SS}$ and $cFN^{CC>SS}$ prompted an investigation into the degree of intermolecular cross-linking within the $FN^{CC>SS}$ matrix. FN cross-linking is commonly addressed by assaying the fraction of total FN that remains insoluble in 1% deoxycholate (DOC), as described by Pankov and Yamada (Pankov and Yamada, 2004). Solubilising the ECMin 1% DOC fractions FN into a DOC-soluble and –insoluble fraction. While the DOC-insoluble fraction contains FN that, over time, has become cross-linked to the extent that it resists solubilisation in detergent, the DOC-soluble fraction contains only newly assembled FN that has yet to become cross-linked. Hence, the distribution of FN in DOC soluble and insoluble fractions reflects the degree of chemical cross-linking within a fibrillar FN matrix.

To perform DOC fractionation of WT FN and $FN^{CC>SS}$, mixed populations of WT and $FN^{CC>SS/CC>SS}$ MEFs were seeded onto plastic culture dishes and cultured in serum replacement medium supplemented with 0.5% (v/v) FN-depleted FBS. After fourty-eight hours in culture, at a stage of fibrillogenesis where the fibrillar morphology of $FN^{CC>SS}$ matrices begins to differ substantially from that of WT FN (cf. fig. 8.18), the cultures and ECM were lysed in an extraction buffer containing 1% DOC and essential protease inhibitors. The insoluble fractions were resolved by SDS-PAGE under reducing conditions, and the FN content was analysed by western blotting, using the DOC-insoluble intermediate filament vimentin as a loading control.

Western blot analysis of the DOC insoluble fractions showed that FN matrices derived from $FN^{CC>SS/CC>SS}$ MEFs contained only slightly less DOC-insoluble FN compared to matrices generated by WT MEFs. Hence, despite the stunted appearance, the degree of chemical cross-linking within the monomeric FN fibrils does not differ much from that of a WT FN matrix (fig. 8.23).

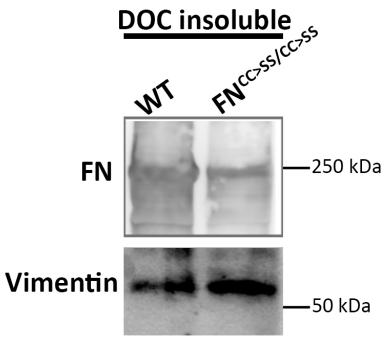

Figure 8.23. Biochemical characterisation of the WT FN and FN$^{CC>SS}$ fibrillar matrix. Western blot analysis of the DOC-insoluble fraction of FN derived from WT and FN$^{CC>SS/CC>SS}$ MEFs (mixed populations) cultured for 48 hours. This is a representative western blot out of three independent assays.

8.4.3 Mechanical properties of ECM layers containing FN$^{CC>SS}$

An increasing body of research suggests that the mechanical properties inherent to the ECM are critical regulators of cell behaviour and tissue morphogenesis. The requirement of fibrillar FN for the deposition and stabilisation of a range of structural ECM molecules puts FN at a central position to dictate the compliance of an ECM. Given the short, poorly bundled and perhaps less chemically cross-linked features of the FN$^{CC>SS}$ fibrillar matrix, I asked whether FN$^{CC>SS}$ affects the compliance of the ECM.

Measuring the compliance of embryonic tissue is technically challenging. Instead, I sought to prepare tissue-mimetic ECM platforms derived from WT and FN$^{CC>SS/CC>SS}$ MEFs. To isolate stiffness contributions of ECM only, the ECM platforms had to be decellularised. However, decellularising ECM derived from FN$^{CC>SS/CC>SS}$ MEFs has represented a recurring technical problem in that cell extraction caused partial or complete ECM delamination from the culture dish, leaving inconsistent amounts of FN$^{CC>SS}$ fibrillar matrix and ECM on the dish for subsequent stiffness assays. This inherent instability of an ECM containing FN$^{CC>SS}$ was speculated to be related to mechanical properties of the FN$^{CC>SS}$ fibrillar matrix.

A major technical advance came by adopting a novel ECM immobilisation protocol to stably anchor cell-derived ECM to a glass sufrace (Prewitz et al., 2013). This anchorage relied on immobilising a thin film of poly(octadecene-alt-maleic anhydride) (POMA) on a glass surface and subsequently depositing a monolayer of a commercially available form of pFN through covalent bond formation between reactive anhydride moieties in POMA and amino-terminated lysine residues in FN. Onto these FN-coated glass surfaces I seeded WT and FN$^{CC>SS/CC>SS}$ MEFs mixed populations and cultured them in serum replacement medium supplemented with 2% (v/v) FN-depleted FBS. Over the course of ten days, the MEFs were allowed to deposit ECM, which by virtue of the ability of FN to interact with multiple ECM components, such as collagen, fibrin and heparan sulfate proteoglycans, would become robustly anchored to the FN-coated glass and withstand decellularisation. After ten days of culture, MEFs were extracted from the ECM with an extraction buffer based on Triton X-100 and ammonium hydroxide, and the cellular content of DNA was removed by treatment with DNase.

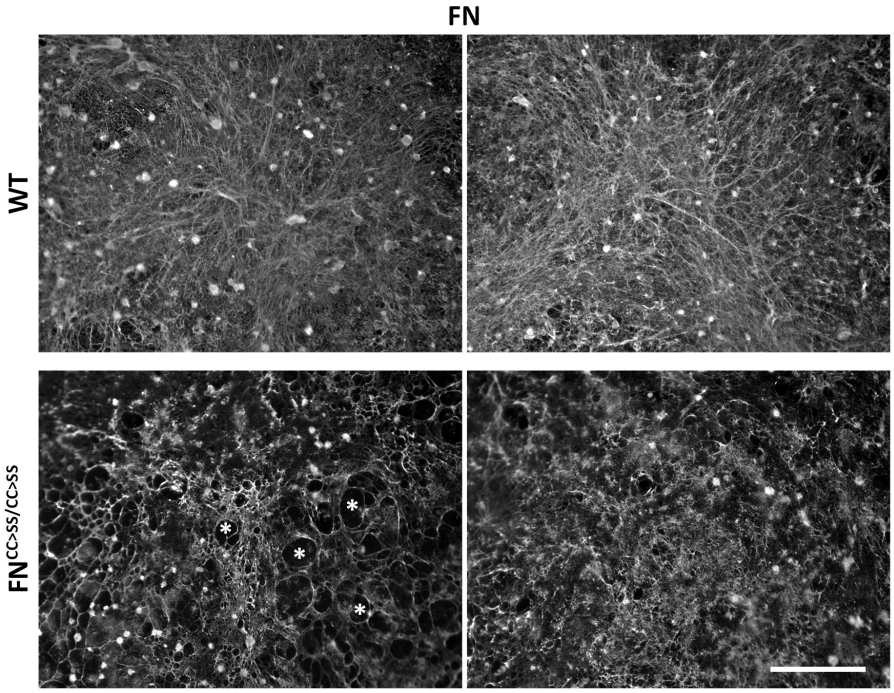

Figure 8.24. Anchored ECM platforms derived from WT and $FN^{CC>SS/CC>SS}$ MEFs. Immunofluorescence images of decellularised ECM generated by WT and $FN^{CC>SS/CC>SS}$ MEF (mixed populations) and covalently anchored to glass to provide stability during decellularisation. FN was stained with antibodies against FN. * indicate holes in the $FN^{CC>SS}$ fibrillar matrix. Scale bar 100 μm. This analysis was performed once.

To monitor the quality of the decellularised MEF-derived ECM and to ensure that the anchoring of the ECM to the glass coverslip was beneficial, the decellularised matrices were fixed and immunostained with an antibody against FN. Immunofluorescence imaging of the ECM revealed dense carpets of fibrillar FN matrices left on the coverslips after decellularisation (fig. 8.24). ECM containing $FN^{CC>SS}$ had been stabilised by the anchoring chemistry applied during preparation and had maintained a morphology distinct from WT FN fibrils characterised by a fine meshwork of short fibrils. In some regions of the ECM, however, $FN^{CC>SS}$ was found to have formed a considerably complex fibrillar network. Despite $FN^{CC>SS}$ having formed fibrils longer than seen previously, the integrity of the matrix appeared compromised, with large holes where the long fibrils of $FN^{CC>SS}$ appear to have given in to tension maintained in the ECM upon cell extraction (indicated by * in fig. 8.24).

The elasticity analysis of ECM by indentation atomic force microscopy (AFM) showed that the ECM derived from $FN^{CC>SS/CC>SS}$ MEFs is significantly more compliant (mean Young's modulus 137.249 Pa) than ECM generated by WT MEFs (mean Young's modulus 371.418 Pa) (fig. 8.25). Non-coated glass surfaces were orders of magnitude stiffer than coverslips containing ECM (not shown). Statistical analysis by the Mann-Whitney test indicated that the difference in elasticity between ECM containing $FN^{CC>SS}$ and WT FN are significantly different. Hence $FN^{CC>SS}$ truely affects the mechanical properties of an ECM.

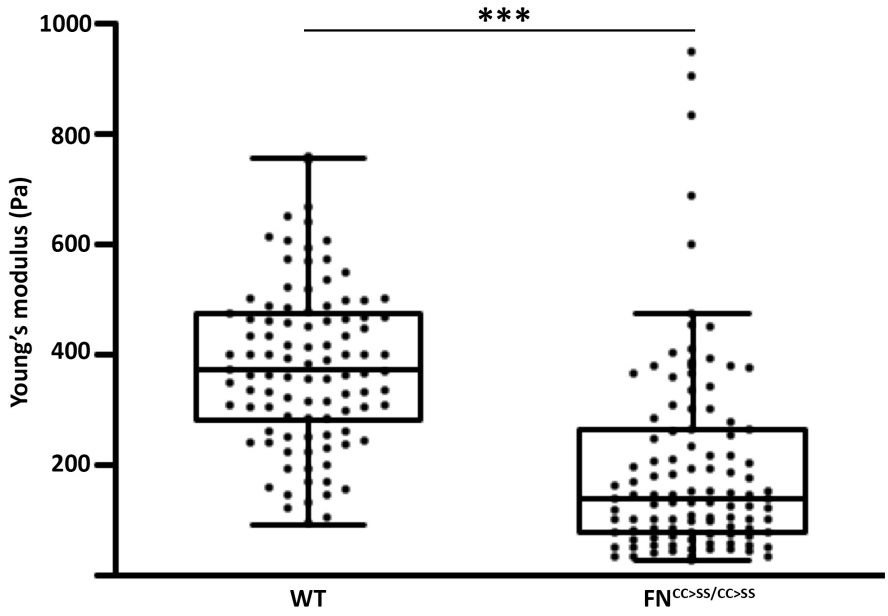

Figure 8.25. Characterisation of the mechanical properties of ECM containing WT FN and $FN^{CC>SS}$ by the indentation AFM technique. The box plot shows Young's moduli of ECM derived from WT (mean Young's modulus 371.418 Pa) and $FN^{CC>SS/CC>SS}$ (mean Young's modulus 137.249 Pa) MEF mixed populations. Each data point represents a single measurement, in total n=103 (WT ECM) and n=109 (ECM containing $FN^{CC>SS/CC>SS}$) distributed over 3 separate coverslips. ***p<0.001.

8.5 Functional characterisation of $FN^{CC>SS}$

8.5.1 Cell migration on ECM layers containing $FN^{CC>SS}$

Cells sense and respond to the mechanical properties of their microenvironment, and it has long been recognised that substrate flexibily affects focal adhesion dynamics and cell migration and that substrate rigidity regulates the formation and maintenance of tissues (Pelham and Wang, 1997; Guo et al., 2006). Most cell types respond to a gradient in matrix stiffness by moving toward areas of stiffer ECM in a process termed durotaxis (Lo et al., 2000). Durotaxis is thought to be critical for development and wound healing, and tumor cell invasion through tissue is strongly regulated by the microstructural and mechanical properties of the ECM.

In the preceding chapter, I presented indentation AFM measurements of decellularised tissue-mimetic ECM platforms and demonstrated that ECM containing $FN^{CC>SS}$ is significantly more compliant than ECM containing WT FN. This, and other features of the $FN^{CC>SS}$ matrix led to the hypothesis that ECM containing $FN^{CC>SS}$ would affect the speed of migration of cells. To test this hypothesis, I prepared decellularised, tissue-mimetic ECM platforms derived from WT and $FN^{CC>SS/CC>SS}$ MEFs seeded onto gelatin-coated plastic surfaces and cultured in serum replacement medium supplemented with 2% (v/v) FN-depleted FBS for three days. In this context, ECM platforms were decellularised by treatment with EDTA, which causes adherent cells to round up and detach from the ECM.

To characterise the morphology of the FN fibrillar matrix in these MEF-derived, decellularised ECM platforms, WT and $FN^{CC>SS/CC>SS}$ MEF clones were seeded onto LM111-coated glass coverslips,

cultured and subsequently removed from the ECM with EDTA. FN in ECM with and without cells was immunostained with antibodies against FN.

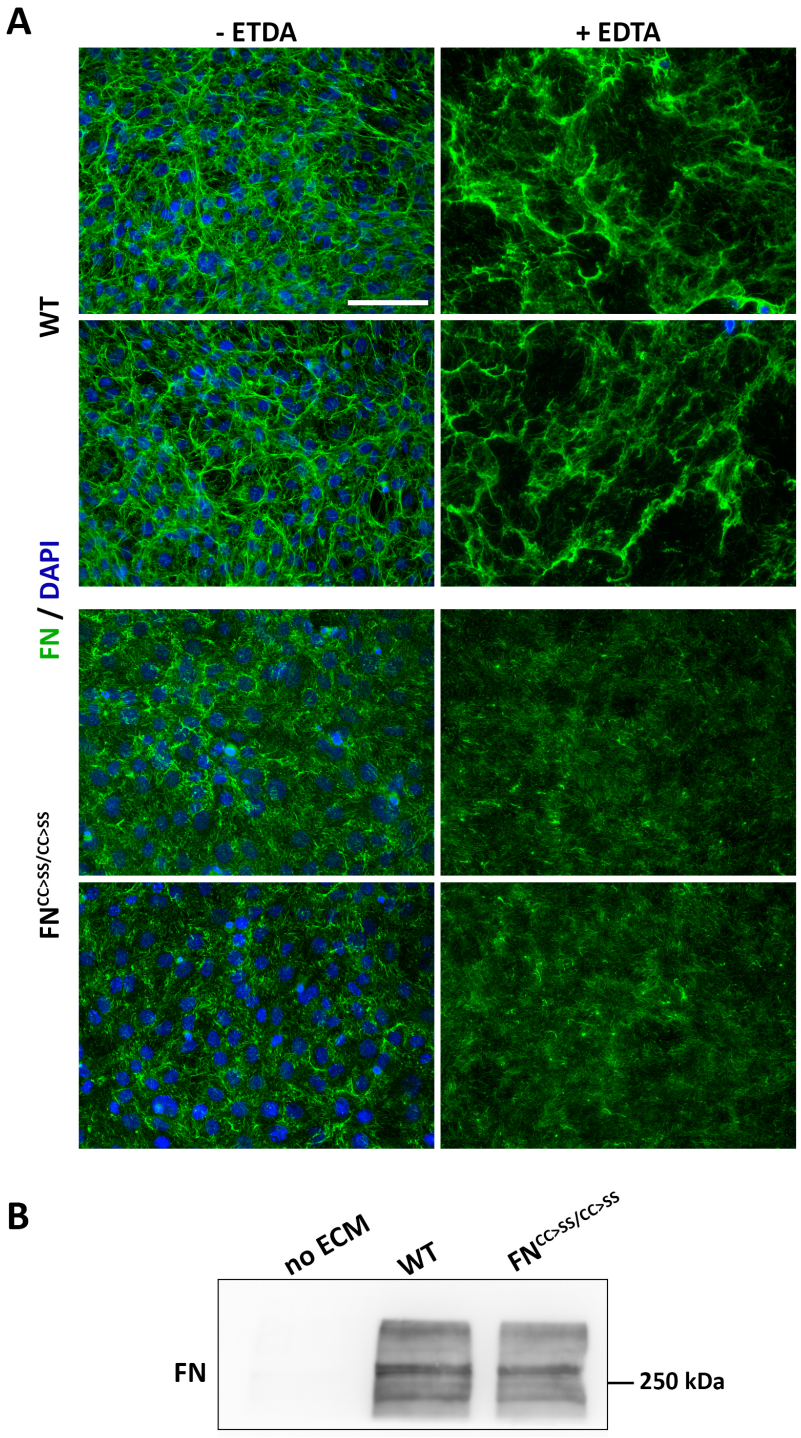

Figure 8.26. Characterisation of decellularised ECM derived from WT and $FN^{CC>SS/CC>SS}$ MEFs. (A) Immunofluorescence image of FN matrix generated by WT and $FN^{CC>SS/CC>SS}$ MEF clonal cell lines before and after cell extraction with EDTA. FN is stained with antibody against FN (green) and nuclei are stained by DAPI (blue). Scale bar: 100 μm. (B) Western blot analysis of FN content in lysates of decellularised ECM derived from WT and $FN^{CC>SS/CC>SS}$ MEF clonal cell lines (as shown in A). Decellularised ECM lysates were resolved by SDS-PAGE under reducing conditions. "no ECM" denotes a blank dish to demonstrate the abundance of FN after decellularisation. This analysis was performed twice.

Immunofluorescence images showed rather substantial changes in the fibrillar morphology upon EDTA-mediated decellularisation of MEFs cultured on plastic (fig. 8.26 A). In particular, the FN matrix derived from WT MEFs appeared to have collapsed upon cell extraction, whereas the morphology of FN fibrils derived from $FN^{CC>SS/CC>SS}$ MEFs maintained had changed very little upon cell extraction. The collapse of WT FN matrix upon cell removal could be due to the fact that cells maintain this highly complex fibrillar matrix under very high tension, and when cells are removed, this tension is lost and the matrix collapses. Finding that the matrix of $FN^{CC>SS}$ appears much less collapsed upon cell removal might reflect that less strain is exerted on the fibrils by $FN^{CC>SS/CC>SS}$ MEFs. Since the MEFs used here were clonal cell lines, it is not possible to say whether this differential strain is a response of the cell to the FN matrix or whether it is a clonal feature.

To assess the levels of FN remaining in the decellularised ECM, I prepared lysates of decellularised ECM derived from WT and $FN^{CC>SS/CC>SS}$ MEFs. Lysates were resolved by SDS-PAGE under reducing conditions, and the FN content was analysed by western blotting. Western blot analysis showed that decellularised ECM derived from WT and $FN^{CC>SS/CC>SS}$ MEFs contain comparable amounts of FN (fig. 8.26 B).

The decellularised ECM derived from WT and $FN^{CC>SS/CC>SS}$ MEFs were subsequently used as migration platforms for FN-/- fibroblasts. I chose FN-/- fibroblasts (Sakai et al., 2001) for these migration assays to eliminate the contribution of endogenous (WT) fibronectin during the analysis. FN-/- fibroblasts were seeded onto the decellularised ECM platforms at low density and left for one hour in serum replacement medium without supplemental FBS. During this hour, $FN^{-/-}$fibroblasts attached and spread equally well on ECM containing WT FN and $FN^{CC>SS}$. To induce migratory activity, $FN^{-/-}$fibroblasts were stimulated with PDGF-BB and transferred to a brightfield microscope where cellular position was recorded at five min time intervals for twelve hours. Movies of migrating cells were compiled from the still-images of $FN^{-/-}$ fibroblasts. Using the Manual Tracking plugin for ImageJ, I tracked the migration path of individual cells, and with the ImageJ Chemotaxis Tool, I calculated the average speed of migration of $FN^{-/-}$ fibroblasts migrating on ECM containing either WT FN or $FN^{CC>SS}$ (fig. 8.27)

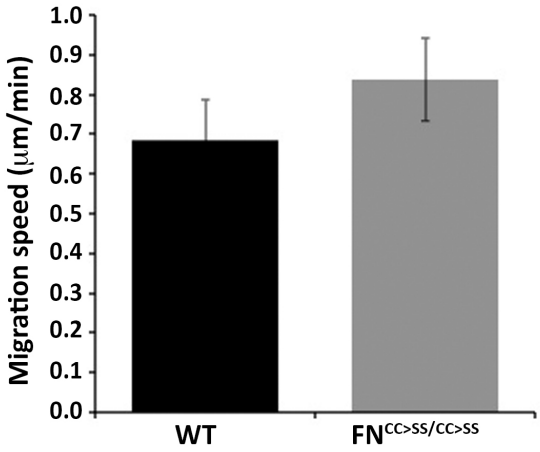

Figure 6.27. Migration analysis of FN$^{-/-}$ fibroblasts on ECM containing WT FN and FN$^{CC>SS}$. Histograms indicate mean migration speed of FN$^{-/-}$ fibroblasts on ECM derived from WT and FN$^{CC>SS/CC>SS}$ MEF clonal cell lines. PDGF-BB was added at 50 ng/ml in serum replacement medium. No directionality data is provided because not all tracks were recorded for the same period of time. This experiment was performed four times, where n>40 cells per condition.

Analysis of the cellular migration speeds suggested a tendency for FN$^{-/-}$ fibroblasts to migrate at a higher speed on ECM containing FN$^{CC>SS}$ compared to when seeded onto ECM containing WT FN (fig. 7.27). This, in turn, would point to an effect of FN$^{CC>SS}$ on adhesion stability. However, statistical analysis of the data set indicated that the difference in migration speeds were not statistically significant.

8.5.2 Effect of FN$^{CC>SS}$ on outside-in integrin signalling

Cells use their integrins and focal adhesion-associated proteins to probe and respond to the mechanical properties of their environment. Matrix rigidity regulates integrin function, as stiff matrices promote the assembly of large focal adhesions that change the cytoskeletal organisation of the cell, while compliant matrices only support the assembly of small dot-like structures containing integrins (Choquet et al., 1997; Pelham and Wang, 1997; Riveline et al., 2001; Paszek et al., 2005). As mechanotransducers, integrins convert mechanical input into intracellular biochemical signals by recruiting intracellular signalling complexes. Integrin signalling, in particular those that are triggered by active integrin $\alpha5\beta1$ are crucial to developmental vasculogenesis and angiogenesis (Francis et al., 2002). The abnormal vascular development observed in FN$^{CC>SS/CC>SS}$ embryos, combined with altered mechanical properties of ECM deposited by FN$^{CC>SS/CC>SS}$ MEF mixed populations and the stunted appearance of fibrillar adhesions in FN$^{CC>SS/CC>SS}$ MEF clones, led to the hypothesis that outside-in signalling downstream of integrin $\alpha5\beta1$ may be affected in FN$^{CC>SS/CC>SS}$ mice.

Autophosphorylation of FAK at tyrosine residue Y397 (pFAK^{Y397}) is sensitive to both number and bond-strength of the interaction between integrin $\alpha5\beta1$ and FN. Levels of pFAK^{Y397} thus reflect the mechanical tension across focal adhesions resulting from the resistance of FN to the pulling forces of the contractile actomyosin cytoskeleton (Shi and Boettiger, 2003; Friedland et al., 2009). Semi-quantitative analysis of pFAK^{Y397} levels therefore reflects not only the quantity and strength of interactions between integrin $\alpha5\beta1$ and FN, but also provides an indirect cellular read-out of ECM

stiffness. FAK is also reported to be involved in mechanosensing during fibroblast migration (Wang et al., 2001a).

First, I compared the kinetics of FAK^{Y397} phosphorylation in WT and FN$^{CC>SS/CC>SS}$ MEFs in the process of assembling a fibrillar matrix of endogenous FN. In this assay, cellular pFAK^{Y397} levels were compared as cells deposited FN into the ECM and thereby became increasingly exposed to fibrillar matrix containing either WT FN or FN$^{CC>SS}$. The assumption here was that integrin-binding sites within FN$^{CC>SS}$ are intact, and if FN$^{CC>SS}$ were to have a unique effect on integrin outside-in signalling, it would have so exclusively in a fibrillar form with true mechanical that can be probed by integrins. The time points for assaying the level of pFAK^{Y397} matched those of the FN fibrillogenesis time course presented earlier (cf. fig. 8.19). This allowed a correlation to be made between pFAK^{Y397} levels and the complexity of the FN fibrillar matrix.

WT and FN$^{CC>SS/CC>SS}$ MEF clones were seeded onto gelatin-coated culture dishes and cultured in serum-replacement medium supplemented with 0.5% (v/v) FN-depleted FBS. At defined time points after seeding, ranging from four to seventy-two hours, the cultures were lysed in the presence of protease and phosphatase inhibitors. Lysates were resolved by SDS-PAGE under reducing conditions, and both pFAK^{Y397} and total FAK protein contents were analysed by western blotting.

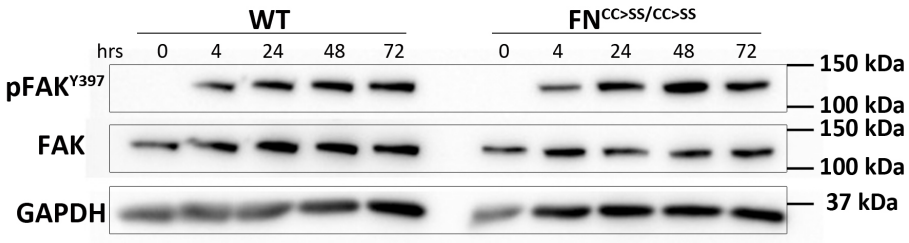

Figure 8.28. Integrin outside-in signalling through FAK^{Y397} in WT and FN$^{CC>SS/CC>SS}$ MEFs. A representative western blot of pFAK^{Y397}, total FAK and GAPDH protein levels in WT and FN$^{CC>SS/CC>SS}$ MEFs clonal cell lines cultured in serum replacement medium supplemented with 0.5% FN-depleted FBS for the indicated number of hours. This assay was performed once.

At the four hour time point, where FN fibrillogenesis has already begun and traces of small FN fibrils can be seen in a MEF culture, the ratio of pFAK^{Y397} to total FAK protein in a FN$^{CC>SS/CC>SS}$ MEF culture was indistinguishable from a WT MEF culture (fig. 8.28). Over the course of the next seventy-two hours, there continued to be no difference in the steady state levels of pFAK^{Y397}. If the levels of pFAK^{Y397} reflects the degree of integrin force coupling to the contractile actomyosin cytoskeleton, this lack of difference in pFAK^{Y397} levels between WT and FN$^{CC>SS/CC>SS}$ MEF lysates suggests that the unique structural and mechanical properties of FN$^{CC>SS}$ do not affect integrin force coupling. An alternative interpretation is that both WT and FN$^{CC>SS/CC>SS}$ MEFs reach the same steady-state ratio of pFAK^{Y397} to FAK ratio because FN$^{CC>SS/CC>SS}$ MEFs compensate for short fibrillar adhesions by generating more fibrillar adhesions, such that overall, the same number of integrins are activated and force-coupled to actomyosin to the same degree as in WT MEFs. Unfortunately, the method employed here cannot resolve such putative compensatory mechanisms.

In order to assay the level of pFAK^{Y397} in a setup that mimics the three-dimensional extracellular environment *in vivo*, I adopted a setup seeding FN$^{-/-}$ fibroblasts onto MEF-derived, tissue-mimetic ECM. FN$^{-/-}$ fibroblasts were seeded onto ECM platforms that had been decellularised with EDTA, and cultured in the presence of serum replacement medium without any supplemental FBS or growth factors. After thirty minutes, by which time the FN$^{-/-}$ fibroblasts had spread on both WT and ECM platforms containing FN$^{CC>SS}$, cells were lysed and the ratio of pFAK^{Y397} to total FAK protein in cell lysates was assessed by western blot analysis. Additionaly, lysates were probed for the levels of pMLC2^{S19} and total MLC2 protein to address whether integrin signalling via ROCK/pMLC2 is changed in the presence of FN$^{CC>SS}$. Western blot analysis showed that FN$^{-/-}$ fibroblasts responded similarly to ECM derived from WT and FN$^{CC>SS/CC>SS}$ MEF, resulting in no difference in the activation status of FAK or MLC2 (fig. 8.29 A and B, respectively).

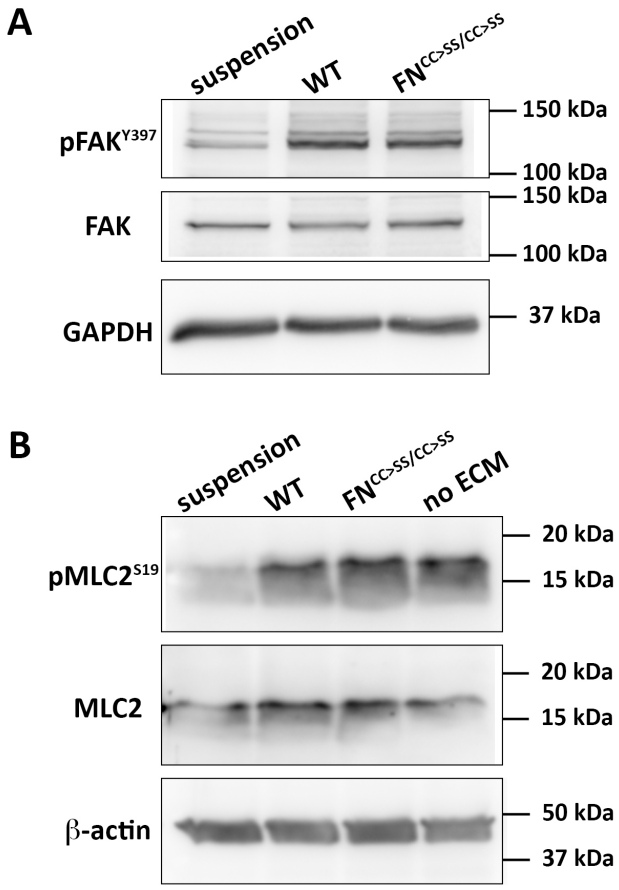

Figure 8.29. Integrin outside-in signalling in FN-/- fibroblasts on ECM platforms containing WT FN and FN$^{CC>SS/CC>SS}$. Representative western blots of (A) pFAK^{Y397}, total FAK and GAPDH and (B) pMLC2^{S19}, total MLC2 and β-actin protein levels in FN-/- fibroblasts cultured for 30 minutes on decellularised ECM generated by WT and FN$^{CC>SS/CC>SS}$ MEFs clonal cell lines. Experiments like that shown in (A) was performed three times, and the experiment shown in (B) was performed once.

A final approach to investigating the impact of FN$^{CC>SS}$ on integrin outside-in signalling focused on comparing the levels of pFAK^{Y397} in FN$^{CC>SS/CC>SS}$ embryonic and extra-embryonic tissue with that of WT embryonic tissues. Single E9.5 embryos or yolk sacs were lysed, and the ratios of pFAK^{Y397} to

total FAK protein in embryo and yolk sac lysates were assessed by western blotting (fig. 8.30 A and B, respectively).

Western blot analysis revealed a degree of natural variation in pFAK^{Y397} to FAK in lysates of tissues of the same genotype. However, band densitometry of the ratios of pFAK^{Y397} to total FAK protein showed that there was no significant difference in FAK^{Y397} activation between WT and FN$^{CC>SS/CC>SS}$ tissue (fig. 8.30 C).

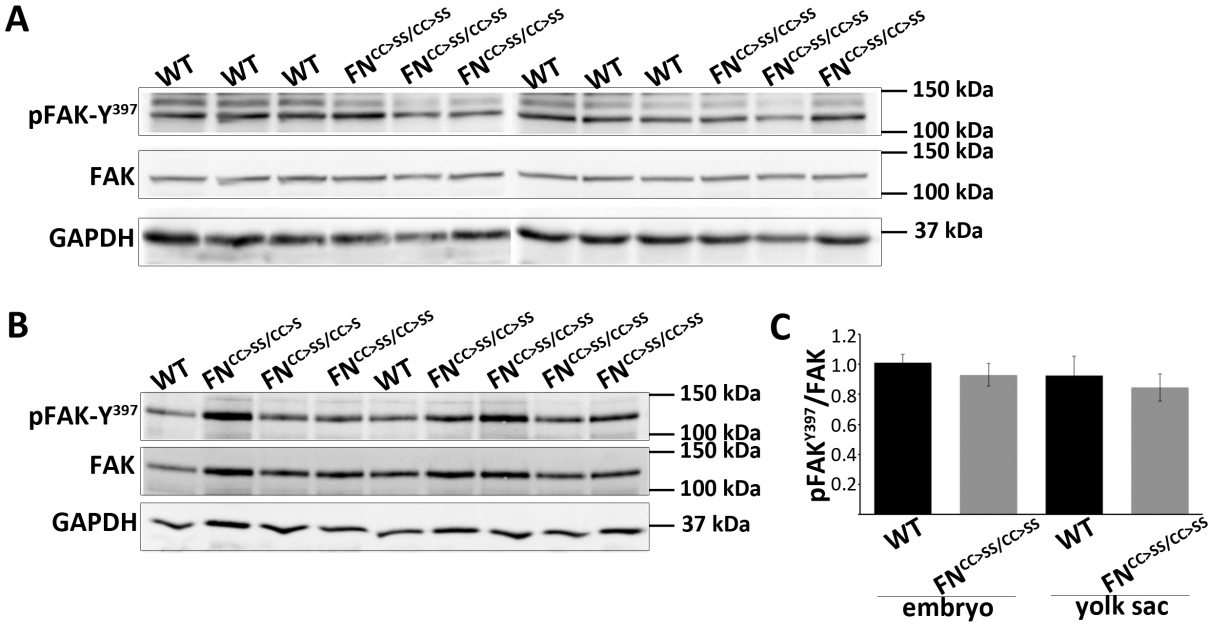

Figure 8.30. Integrin outside-in signalling in WT and FN$^{CC>SS/CC>SS}$ embryonic and extra-embryonic tissue. Levels of pFAK^{Y397}, FAK and GAPDH protein in lysates of single E9.5 embryos (A) or single E9.5 yolk sacs (B). (C) Histogram shows mean ratios of pFAK^{Y397} to total FAK, where n(WT embryo)=6, n(FN$^{CC>SS/CC>SS}$ embryo)=6; n(WT yolk sac)=2; n(FN$^{CC>SS/CC>SS}$ yolk sac)=6. Error bars represent standard deviation. This experiment was performed five times with different sets and numbers of embryos and yolk sacs, but the quantification provided in (C) accounts for the pFAK^{Y397}/FAK levels presented in (A) and (B).

8.5.3 Effect of FN$^{CC>SS}$ on latent TGF-β storage and activation

With vascular remodelling defects in both embryonic and extra-embryonic tissue as well as abnormal cardiac development resulting in embryonic lethality, the FN$^{CC>SS/CC>SS}$ mouse also shares phenotypic features with mice where TGF-β signalling has been disrupted through genetic manipulation (Dickson et al., 1995; Oshima et al., 1996; Sanford et al., 1997; Arthur et al., 2000; Oh et al., 2000; Bartram et al., 2001; Stenvers et al., 2003; Jiao et al., 2006; Seki et al., 2006; Carvalho et al., 2007; Sridurongrit et al., 2008). The phenotypic parallels between mice carrying mutations in an ECM component and mice with compromised growth factor signalling pathway reflects an important function of the ECM in regulating growth factor activity, and this relation is pivotal to tissue morphogenesis programmes such as cardiovascular patterninng.

FN is a core component of the machinery regulating the bio-availability of TGF-β by immobilising the LTBP-1 component of LLC into the ECM (Dallas et al., 2005; Koli et al., 2005). LTBP-1 plays a role in a mechanism of integrin-dependent latent TGF-β activation (Annes et al., 2004), and as LTBPs

become anchored to FN, this puts FN at centre stage in the latent TGF-β activation mechanism. This led to the hypothesis that the lethal cardiovascular defects in the $FN^{CC>SS/CC>SS}$ mouse relate to either (1) an inability of $FN^{CC>SS}$ to support the deposition of the LLC into the ECM and/or (2) a failure of $FN^{CC>SS}$ to facilitate the integrin-dependent mechanism of latent TGF-β activation.

The first hypothesis was addressed by investigating the deposition of LTBP-1 into an ECM containing $FN^{CC>SS}$. WT and $FN^{CC>SS/CC>SS}$ MEF clones were seeded onto LM-111-coated glass coverslips and cultured in serum replacement medium supplemented with 0.5% (v/v) FN-depleted FBS. After five days, the cultures were fixed and immunostained with antibodies directed against LTBP-1 and FN (fig. 8.31).

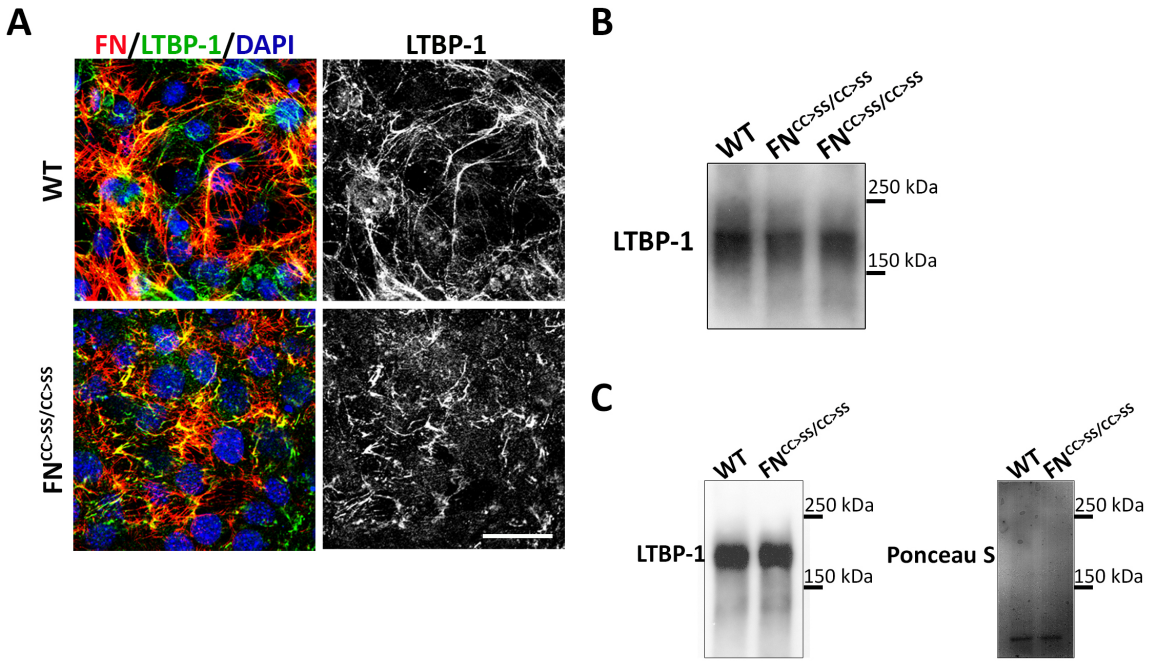

Figure 6.31. Fibrillar morphology and protein levels of LTBP-1 deposited into ECM containing WT FN and $FN^{CC>SS}$. (A) Immunofluorescence images of five-day WT and $FN^{CC>SS/CC>SS}$ MEF clonal cell lines cultured in FN-depleted FBS and stained with antibodies against FN (red) and LTBP-1 (green). Nuclei were stained by DAPI (blue). Scale bar 25 μm. (B) Representative western blot analysis of LTBP-1 protein levels in lysates of five-day cultures of WT and $FN^{CC>SS/CC>SS}$ MEF clonal cell lines. (C) LTBP-1 protein levels in WT and $FN^{CC>SS/CC>SS}$ embryos; representative western blot analysis of the total LTBP-1 protein levels in lysates of single E9.5 WT and $FN^{CC>SS/CC>SS}$ embryos. A Ponceau S staining of the PVDF membrane after protein transfer shows equal protein loading in the two lanes. These data were obtained by Dr. Michael Leiss.

Consistent with a scaffolding role for FN in directing the deposition of LTBP-1 during early ECM formation (Dallas et al., 2005; Koli et al., 2005), immunofluorescence imaging showed a high degree of colocalisation and similarity in fibril structure between LTBP-1 and FN (fig. 8.31 A). In five-day-old ECM derived from WT MEFs, LTBP-1 appeared as bundles of long fibrils. In contrast, LTBP-1 in the ECM derived from $FN^{CC>SS/CC>SS}$ MEF appeared punctate and those fibrils that had formed were severely stunted and thus reminiscent of the $FN^{CC>SS}$ fibrillar matrix. While this result shows that $FN^{CC>SS}$ does not prevent the deposition of LTBP-1, it suggests that the fibrillar growth and complexity of an LTBP-1 matrix in an early ECM is limited by the structural features of the $FN^{CC>SS}$ matrix.

To complement these data, the total amount of LTBP-1 protein deposited into the ECM was assessed by western blot analysis. WT and two different $FN^{CC>SS/CC>SS}$ MEF clones were seeded onto gelatin-coated culture dishes and cultured in the presence of serum-replacement medium supplemented with 0.5% (v/v) FN-depleted FBS. After 5 days, protein lysates of these cultures were resolved by SDS-PAGE under reducing conditions and the LTBP-1 content assessed by western blotting. This experiment showed that only very minute decreases in total LTBP-1 protein levels complemented the drastic change in LTBP-1 fibril morphology (fig. 8.31 B). This indicates that the major effect of $FN^{CC>SS}$ on LTBP-1 is on the structural arrangement of its deposition into the ECM.

The protein levels of LTBP-1 in WT and $FN^{CC>SS/CC>SS}$ embryonic tissue was also compared. For this purpose, single E9.5 embryos were lysed, and the relative content of LTBP-1 protein was assessed by western blotting analysis, which showed that the levels of LTBP-1 protein were comparable between WT and $FN^{CC>SS/CC>SS}$ embryo lysates (fig. 8.31C).

The minute changes in LTBP-1 protein levels in lysates of MEF-derived ECM (fig. 8.31 B) and E9.5 embryo (fig. 8.31C) suggest that the levels of LLC containing latent TGF-β embedded in the ECM would be comparable between WT and $FN^{CC>SS/CC>SS}$ embryos. To test this hypothesis and compare the latent TGF-β storage capacity of ECM containing WT FN or $FN^{CC>SS}$, $FN^{CC>SS/CC>SS}$ and WT MEFs were seeded to confluency onto gelatin-coated culture dishes and cultured for three days in serum replacement medium supplemented with 0.5% (v/v) FN-depleted FBS. To collect the latent TGF-β stored in the ECM only, MEFs were rinsed and selectively removed with EDTA. Decellularised ECMs in serum replacement medium were incubated at 80°C for ten minutes, causing all latent TGF-β stored in the ECM to be released into the conditioned medium in an active form (Brown et al., 1990). To assay the levels of active TGF-β present in the conditioned medium a TGF-β reporter cell line (mink lung epithelial cell line, MLEC) was cultured in the presence of the conditioned medium (Abe et al., 1994). Following incubation, the MLEC were lysed, and this lysate was assayed for total intracellular luciferase activity.

Luciferase measurements reflected comparable amounts of active TGF-β in conditioned medium derived from heat-treated ECM derived from WT and $FN^{CC>SS/CC>SS}$ MEFs (fig. 8.32 A). Hence the fibrillar complexity of LTBP-1 and FN did not affect the capacity of the ECM to store latent TGF-β.

The disrupted structural feature of LTBP-1 fibrils in an ECM derived from $FN^{CC>SS/CC>SS}$ MEFs also inspired the hypothesis that $FN^{CC>SS}$ would disrupt the ability of integrins to activate TGF-β upon traction. To examine whether the abnormal morphology of the LTBP-1 matrix formed in the presence of $FN^{CC>SS}$ could be associated with a change in integrin-mediated activation of latent TGF-β from the ECM, ECMs were generated from WT and $FN^{CC>SS/CC>SS}$ MEF clones seeded onto gelatin-coated culture dishes and cultured in serum replacement medium supplemented with 0.5% (v/v) FN-depleted FBS. Residing MEFs were removed from the ECM with ETDA, and a co-culture of TGF-β reporter MLEC and chinese hamster ovary (CHO) cells stably expressing integrin αVβ6 (CHO-β6) (Weinacker et al., 1994) was seeded onto the decellularised ECM. The co-culture was incubated on the decellularised ECM for twenty-four hours before lysing all cells and assaying intracellular luciferase activity. In this experimental setup, latent TGF-β stored in the ECM becomes activated by integrin

αVβ6, expressed by CHO-β6 cell line. Active TGF-β is released into the medium and detected by the TGF-β reporter MLEC, and luciferase activity in the lysates is proportional to the amount of active TGF-β released by integrin αVβ6. To evaluate the specific contributions to TGF-β reporter activation by integrin αVβ6-mediated TGF-β activation, co-cultures were cultured in the presence of αV integrin blocking antibody. To test the specificity of the assay, co-cultures were cultured in the presence of TGF-β pan-specific polyclonal antibody.

Analysis of luciferase activity in MLEC lysates showed no statistically significant difference in the ability of integrin αVβ6 to activate more latent TGF-β from ECM derived from $FN^{CC>SS/CC>SS}$ MEFs compared to WT MEF (fig. 8.32 B) and hence monomerised FN does not affect the ability of integrins to release TGF-β from ECM.

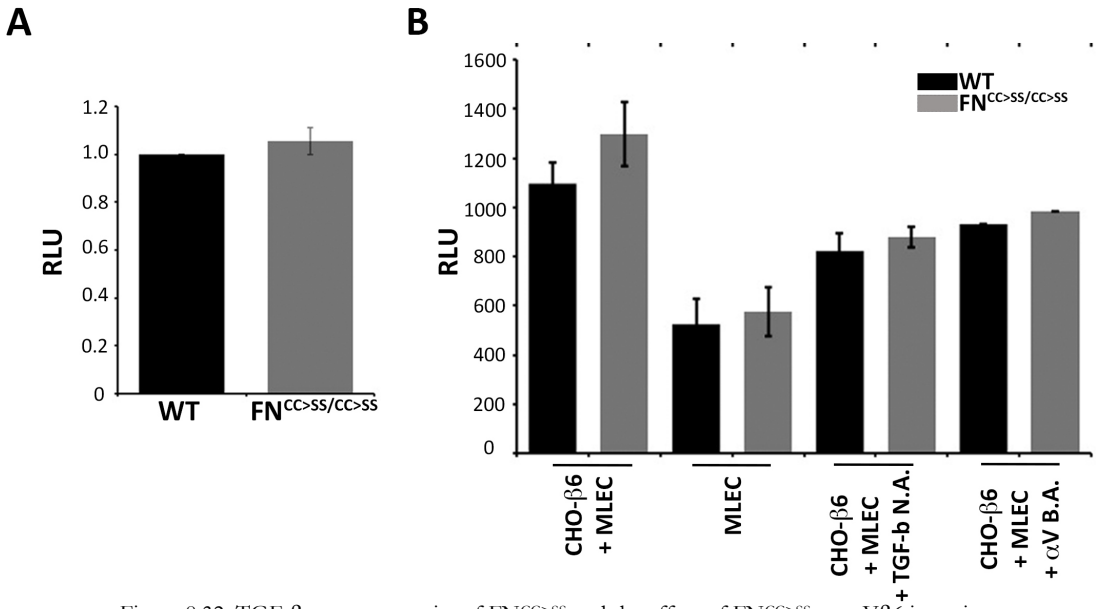

Figure 8.32. TGF-β storage capacity of $FN^{CC>SS}$ and the effect of $FN^{CC>SS}$ on αVβ6 integrin-mediated latent TGF-β activation. (A) Conditioned medium of heat-treated decellularised ECM generated by WT and $FN^{CC>SS/CC>SS}$ MEF clonal cell lines was added to TGF-β reporter MLEC and incubated for further sixteen hours prior to detection of TGF-β-induced luciferase expression. Histogram shows mean luciferase activity in TGF-β reporter MLEC and error bars represent standard deviation. (B) Co-cultures of TGF-β reporter MLEC and CHO-β6 on decellularised ECM generated by WT and $FN^{CC>SS/CC>SS}$ MEF clonal cell lines. Luciferase activity in TGF-β reporter MLEC was measured twenty-four hours after seeding. TGF-β N.A., pan-TGF-β neutralising antibody (1D11; 15 μg/ml); αV B.A., αV blocking antibody (10D5; 15 μg/ml). Histogram shows mean luciferase activity in TGF-β reporter MLEC and error bars represent standard deviation. RLU, relative light units. Experiments were performed in triplicates and performed four times.

8.5.4 TGF-β signalling in $FN^{CC>SS/CC>SS}$ embryos

TGF-β is thought to play a pivotal role in driving vascular remodelling (ten Dijke and Arthur, 2007). Although there is little mechanistic support from cell-based assays for an effect of $FN^{CC>SS}$ on either latent TGF-β storage in the ECM or on integrin-mediated latent TGF-β activation, the vascular remodelling defects in $FN^{CC>SS/CC>SS}$ embryos nevertheless called for an analysis of TGF-β receptor signalling in embryonic tissue.

SMAD phosphorylation occurs upon activation of TGF-β binding and activation of type I and type II receptors. Differences in the intracellular levels of phosphorylated SMAD complex therefore reflect the relative abundance of TGF-β ligand. In the endothelium, TGF-β activates either one of two distinct type I receptor/R-SMAD signalling pathways (Goumans et al., 2002). TGF-β activation of activin-like kinase 1 (ALK1) in the endothelium induces phosphorylation of R-SMAD1/5$^{S463/465}$ complexes, while TGF-β activation of ALK5 phosphorylates and activates R-SMAD2$^{S465/467}$ complexes. The activation of these two SMAD signalling pathways trigger different genetic responses that elicit opposing effects on endothelial biology; activation of the ALK5/SMAD1/5 pathway initiates a genetic programme that inhibits endothelial cell migration and proliferation, while activation of the the ALK1/SMAD2/3 triggers endothelial cell migration and proliferation (Goumans et al., 2002). The spatial and temporal fine-tuning of angiogenic events requires a delicate balance between these two canonical TGF- β signalling pathways.

To address and compare TGF- β signalling in embryonic tissue, single E9.5 embryos were lysed, and the ratios of pSMAD1/5/8$^{S463/S465}$ to total SMAD5 protein and pSMAD2/3$^{S465/S467}$ to total SMAD2/3 protein were assessed by western blot analysis. I found that the ratios of both pSMAD1/5/8$^{S463/S465}$ and pSMAD2/3$^{S465/S467}$ to total SMAD protein were comparable between WT and FN$^{CC>SS/CC>SS}$ embryo lysates (fig. 8.33 A and B, respectively).

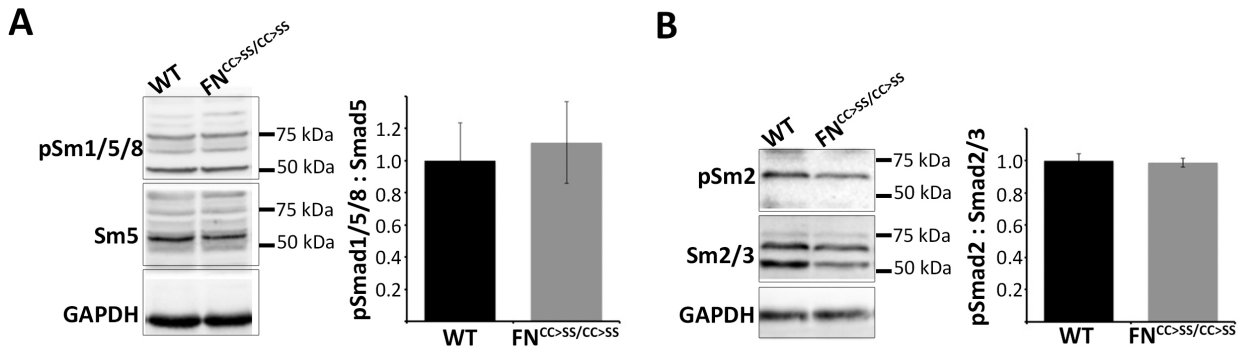

Figure 8.33. TGF-β signalling in WT and FN$^{CC>SS/CC>SS}$ embryonic tissue. Representative western blots and quantification of (A) pSMAD1/5/8$^{S463/S465}$, SMAD5 and GAPDH and (B) pSMAD2/3$^{S465/S467}$, SMAD2/3 and GAPDH protein levels in lysates of single E9.5 WT and FN$^{CC>SS/CC>SS}$ embryos. Histograms show mean ratio of pSMAD to SMAD protein levels for n=5 embryos of each genotype. Error bars represent standard deviation.

Comparable levels of phosphorylated SMAD complexes in whole embryo lysates do not exclude the possibility of there being significant differences in TGF-β signalling in a minor subset of tissues. Upon their phosphorylation, R-SMAD complexes associate with SMAD4 and translocate to the nucleus, and so to compare TGF-β signalling activity in WT and FN$^{CC>SS/CC>SS}$ tissue, I examined the distribution of pSMAD-positive nuclei in WT and FN$^{CC>SS/CC>SS}$ embryonic tissue. Given the cardiovascular defects and that the endothelium is sensitive to changes in bioavailability of TGF-β, particular focus was given to the distribution of phosphorylated SMAD-positive nuclei in highly vascularised tissues such as yolk sac and heart.

Embryos and yolk sacs were harvested at E9.5 and immunostained with antibodies against phospho-specific SMAD1/5/8$^{S463/S465}$ and PECAM-1. Whole-mount and stained embryos and yolk sacs were imaged by confocal microscopy (fig. 8.34).

A large proportion of the embryonic tissues were found to contain pSMAD1/5/8$^{S463/465}$-positive nuclei, stemming not only from TGF-β signalling, but also from BMP receptor activation in both endothelial and non-endothelial tissues (Miyazono et al., 2005). Both PECAM-1 and the characteristic flattened appearance of endothelial nuclei lining a WT vessel were used to identify the pSMAD1/5/8$^{S463/465}$-positive nuclei belonging to endothelium. In both WT and FN$^{CC>SS/CC>SS}$ yolk sacs, a fraction of the most prominent pSMAD1/5/8$^{S463/465}$-positive nuclei appeared to be associated with the PECAM-1 stain. Although the heavily distorted appearance of the endothelium in the FN$^{CC>SS/CC>SS}$ made it difficult to faithfully identify endothelial nuclei, overall there was no indication that FN$^{CC>SS/CC>SS}$ yolk sac endothelium suffered excess or moderation of TGF-β-induced pSMAD1/5/8$^{S463/465}$.

In the developing cardiac tissue of both WT and FN$^{CC>SS/CC>SS}$ embryos, the most prominent of the pSMAD1/5/8$^{S463/465}$-positive nuclei were associated with the PECAM-1-positive endocardium. Despite the compromised growth and morphology of the FN$^{CC>SS/CC>SS}$ endocardium, the endothelium appeared to contain pSMAD1/5/8$^{S463/465}$-positive nuclei. This would indicate that the endocardial remodelling defects cannot be attributed to an absence of TGF-β signalling. Overall, there is no strong indication that endothelium of FN$^{CC>SS/CC>SS}$ tissue shows any difference in TGF-β signalling activity compared to WT endothelium.

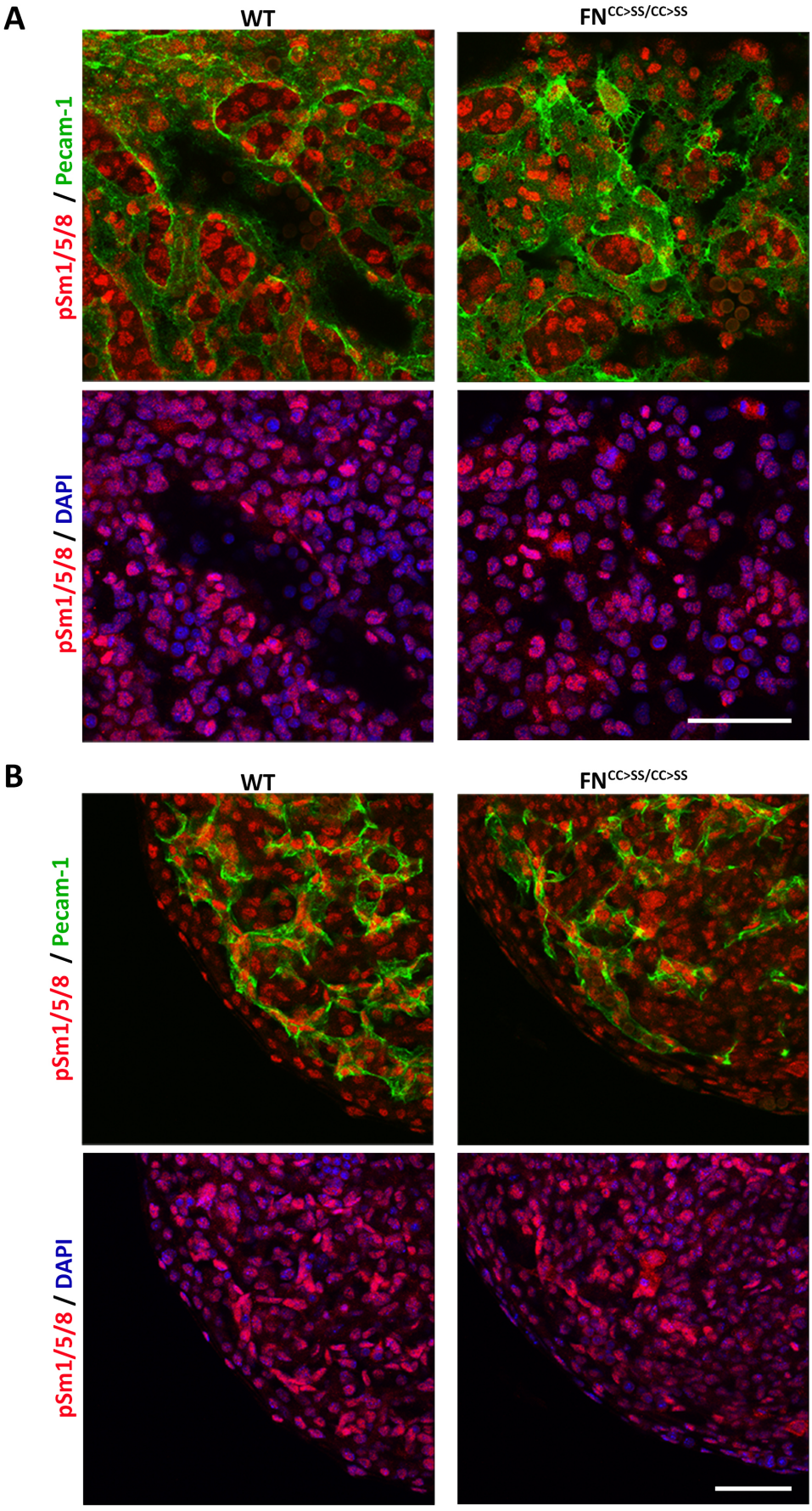

Figure 8.34. Distribution of pSMAD1/5/8$^{S463/S465}$-positive nuclei in WT and FN$^{CC>SS/CC>SS}$ embryonic tissue. Confocal immunofluorescence images of whole mount E9.5 WT and FN$^{CC>SS/CC>SS}$ embryonic tissues stained with antibodies against pSMAD1/5/8$^{S463/S465}$ (red) and PECAM-1 (green). Nuclei are stained by DAPI (blue). (A) Dorsal view of flat-mounted yolk sac and

(B) parasagittal view of embryonic heart. Scale bar 50 μm. This analysis was performed once on at least three individual embryos/yolk sacs.

A final approach to comparing the level of TGF-β signalling activity between WT and $FN^{CC>SS/CC>SS}$ embryonic tissue was undertaken through quantitative real-time PCR (RT-PCR) analysis of pSMAD target gene mRNA. Plasminogen activator inhibitor 1 (PAI-1) and Inhibitor of DNA 1 (Id1) are targets genes of activated pSMAD2/3$^{S465/467}$ and pSMAD1/5/8 $^{S463/465}$, respectively, and thus implicated in generating the endothelial response to TGF-β (Goumans et al., 2002). cDNA was prepared from mRNA isolated from single E8.5 yolk sacs, and the transcript levels of both PAI-1 and Id1 were normalised to GAPDH transcript levels (fig. 8.35). Both Id1 and PAI-1 transcript levels were lower in $FN^{CC>SS/CC>SS}$ yolk sac compared to WT, and the 1.6 fold decrease in Id1 transcript level was statistically significant. Id1 is a target of pSMAD1/5/8$^{S463/465}$, and so this suggests that TGF-β signalling is very mildly compromised in $FN^{CC>SS/CC>SS}$ yolk sac tissue.

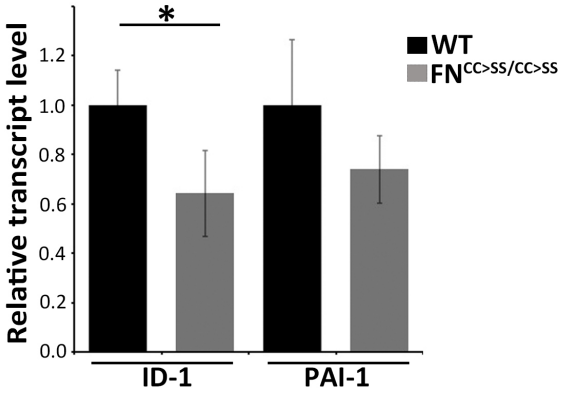

Figure 8.35. Expression of TGF-β/SMAD target genes in WT and $FN^{CC>SS/CC>SS}$ yolk sac. RT-PCR of cDNA that was isolated from single E8.5 WT and $FN^{CC>SS/CC>SS}$ yolk sacs. For each sample, the transcript level of the gene of interest was normalised to the transcript level of GAPDH. Histogram shows relative mean transcript levels of Id1 and PAI-1 for n(WT)=3 and n($FN^{CC>SS/CC>SS}$)=4, and the mean WT relative transcript levels are set to 1. *p=0.025, statistically analysed by Student's T-test.

8.5.5 Effect of $FN^{CC>SS}$ on VEGF signalling

The phenotype of the $FN^{CC>SS/CC>SS}$ mouse cannot be explained by an ECM-related defect in latent TGF-β storage and activation. Focusing on the vascular defect and staying with the hypothesis that monomeric $FN^{CC>SS}$ could disturb FN-mediated growth factor deposition into the ECM, I asked whether $FN^{CC>SS}$ could alter the availability of VEGF-A in $FN^{CC>SS/CC>SS}$ embryos. VEGF-A is a growth factor that becomes immobilised in the ECM, and the interaction between VEGF-A and FN is important for establishing the VEGF-A gradients that promote angiogenesis, for example in retinal angiogenesis (Stenzel et al., 2011). These observations led to the hypthesis that $FN^{CC>SS}$ affects vascular remodelling by disturbing the ability of ECM to regulate the availability of VEGF-A.

To begin exploring the effect of $FN^{CC>SS}$ on the availability of VEGF-A, I compared the levels of VEGFR2 phosphorylation between WT and $FN^{CC>SS/CC>SS}$ embryonic and extraembryonic tissue. One approach was based on immunohistochemical analysis of phosphorylated VEGFR2 in embryonic and extraembryonic tissue sections. However, for technical reasons, multiple attempts to detect various

forms of phosphorylated VEGFR2 (pVEGFR2^{Y951} and pVEGFR2^{Y1175}) failed to provide specific immunohistochemical signals (not shown).

VEGFR activation was then investigated by western blot analysis. An intial attempt to detect the pVEGFR2^{Y951} in lysates of embryos or yolk sacs, either single or pooled, failed to provide single specific bands to allow a fair comparison of VEGFR2 activation between WT and FN$^{CC>SS/CC>SS}$ lysates (not shown). To circumvent this technical problem, I decided to compare the level of phosphorylated tyrosine residues (pY) in VEGFR2 immunoprecipitated from either embryo or yolk sac lysates.

From lysates of either pooled embryos or yolk sacs, VEGFR2 was immunoprecipitated using a monoclonal VEGFR2 antibody. The VEGFR2 immunoprecipitate was resolved by SDS-PAGE, and the content of phospholated tyrosine residues was analysed by western blotting using the 4G10 monoclonal antibody (fig. 8.36).

Western blot analysis of phosphorylated tyrosine content in the immunoprecipitated VEGFR2 showed that WT and FN$^{CC>SS/CC>SS}$ embryonic and yolk sac lysates contain comparable levels of tyrosine-phosphorylated VEGFR2 (fig. 8.36). Thus, on a global, whole tissue level, the activation status of VEGFR2 is the same between WT and FN$^{CC>SS/CC>SS}$ embryonic tissue, which suggests that the VEGF-A ligand availability is not affected by FN$^{CC>SS}$. However, these data do not reflect whether the gradients of VEGF-A are intact or achieve the appropriate strength within FN$^{CC>SS/CC>SS}$ tissue, which is crucial for the correct extent of endothelial activation and vascular growth.

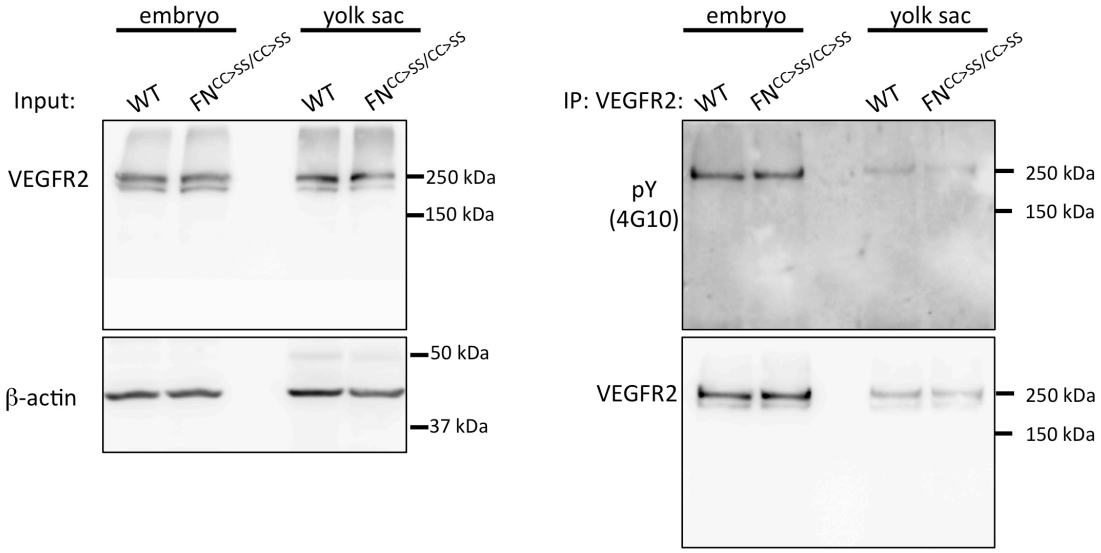

Figure 8.36. VEGFR2 activation status in WT and FN$^{CC>SS/CC>SS}$ embryonic tissue. VEGFR2 was immunoprecipitated from lysates of pooled E9.5 embryos and yolk sacs (n=7 of each) and the phospho-tyrosine content of immunoprecipitated VEGFR2 was analysed by western blot, using the 4G10 monoclonal antibody to detect phosphorylated tyrosine residues in VEGFR2. Input: the embryo and yolk sac lysates before VEGFR2 immunoprecipitation. IP: immunoprecipitated VEGFR2.

9 DISCUSSION

In this study, I have addressed the requirement for the dimerisation motif for FN fibrillogenesis and its role in FN function *in vivo*. With the analysis of a genetically modified mouse strain that exclusively expresses a form of FN that cannot dimerise, this study provides a more complete understanding of the requirement for FN dimers in FN fibrillogenesis. Here I provide evidence that dimerisation of FN is important for maintaining structural and mechanical properties of the FN matrix and the ECM that assembles around FN, and I demonstrate the consequences of preventing FN dimerisation to mouse development.

Disruption of the FN dimerisation motif was achieved by replacing the two critical cysteines within the dimerisation motif with serines ($FN^{CC>SS/CC>SS}$) and thereby ablating the formation of the two critical disulfide bonds responsible for dimersing FN (fig. 8.1 and 8.2). This mutation in FN disrupts embryonic development at mid-gestation and is recessive lethal around E10.5, such that the majority of $FN^{CC>SS/CC>SS}$ mice are lost by E11.5 (table 8.1). This demonstrates vital functions of FN that rely on properties unique to the dimerised form of FN. Preventing FN dimerisation causes defects in mesoderm-derived structures of both the embryo proper and extraembryonic tissue. This mutant phenotype is consistent with, albeit milder than, mice lacking expression of FN (George et al., 1993; George et al., 1997; Georges-Labouesse et al., 1996) or FN-binding integrin $\alpha5\beta1$ (Goh et al., 1997; Yang et al., 1993; Yang et al., 1999). Hence, while the lethality of $FN^{CC>SS/CC>SS}$ embryos clearly demonstrates that $FN^{CC>SS}$ fails to support normal development, the survival beyond that of FN knockout or integrin $\alpha5$ knock-out implies that $FN^{CC>SS}$ is not a null-mutation. For this thesis, I have explored the functional implications of monomerising FN and conclusively show that the $FN^{CC>SS}$ fibrillar matrix is both structurally and mechanically compromised.

9.1 Monomerised FN undergoes *de novo* fibrillogenesis

Reports published more than two decades ago proposed that the minimal requirements for *de novo* fibrillogenesis are (1) the assembly domain within the N-terminal FNI_{1-5} and (2) the C-terminal disulfide bonds bridging two monomers of FN into a dimer (Schwarzbauer, 1991; Ichihara-Tanaka et al., 1992). In the FN field, two main criteria are applied to determine the competence of FN (or a recombinant, truncated version thereof) in matrix assembly: (1) incorporation of the FN into a DOC-insoluble fraction and (2) formation of fibrils associated with cells that are detectable by immunofluorescence microscopy. In the studies reported by Dr. Schwarzbauer, cultured cells were engineered to express and secrete fragments of FN lacking the C-terminal dimerisation motif. The result was a complete failure of such FN fragments to become assembled into a fibrillar matrix (Schwarzbauer, 1991). From these *in vitro* studies a dogma emerged stating that FN dimerisation is essential for FN fibrillogenesis. Projecting this conclusion to predict the consequences of genetically disrupting FN dimerisation in the mouse, the hypothesis would be that cells fail to deposit

monomerised FN into the ECM, and the mouse would succumb with lethal defects reminiscent of the FN knock-out mouse (George et al., 1993).

Two decades later, with the analysis of the $FN^{CC>SS/CC>SS}$ mouse and work based on MEFs isolated from the $FN^{CC>SS/CC>SS}$ mouse, the requirement for C-terminal disulfide bond-mediated FN dimerisation in *de novo* FN fibrillogenesis has been thoroughly revisited. In both embryonic tissue and MEF systems, $FN^{CC>SS}$ protein was confirmed to be exclusively monomeric (fig. 8.13), deposited into the ECM at normal levels (fig. 8.14) and, importantly, exhibits a fibrillar nature (fig. 8.15). First and foremost, this demonstrates that dimerisation of FN is not strictly essential for FN fibrillogenesis, as was once proposed. Yet close examination of the fibrillar monomerised $FN^{CC>SS}$ matrix revealed morphological features that suggested a structural compromise in the ability of monomerised $FN^{CC>SS}$ to undergo supramolecular remodelling into a complex network of fibrils. In $FN^{CC>SS/CC>SS}$ embryos, $FN^{CC>SS}$ fibrils distribute within a distinct regime of short fibril lengths compared to FN fibrils in WT embryos. On average, $FN^{CC>SS}$ forms significantly shorter fibrils than WT FN (fig. 8.15). The morphological difference was more pronounced between $FN^{CC>SS}$ and WT FN matrices derived from cultured MEFs. Within just two days of culture, WT MEFs build an elaborate, highly branched and interconnected network of long fibrils of FN, while the matrix of $FN^{CC>SS}$ derived from $FN^{CC>SS/CC>SS}$ MEFs consists of only short and thin fibrils, with fewer branch points and a low degree of interconnectivity (fig. 8.18). The same was true for pFN matrices deposited by FN-/- fibroblasts cultured in the presence of plasma containing either $pFN^{CC>SS}$ or WT pFN (fig. 8.21). It is remarkable that this drastic compromise in fibril complexity was not reflected in biochemical DOC fractionation assays of chemical cross-linking within the $FN^{CC>SS}$ matrix (fig. 8.23).

Following the generation of FN matrices in cultures of $FN^{CC>SS/CC>SS}$ MEF and WT MEFs over time was particularly informative about the kinetics of $FN^{CC>SS}$ fibrillogenesis (fig. 8.18). Fibrillogenesis of both WT FN and $FN^{CC>SS}$ was well underway by eight hours of incubation, and matrices were morphologically indistinguishable from one another up until fourty-eight hours of incubation. Beyond this time point, the morphological features of $FN^{CC>SS}$ began to deviate substantially from a WT FN matrix. As these WT FN fibrils continued to grow longitudinally and associate laterally among each other into complex supramolecular structures, the $FN^{CC>SS}$ fibrillar matrix fails to remodel beyond a state of short and delicate structures.

These findings give reason to reconsider the details of the model describing integrin-dependent FN fibrillogenesis (Singh et al., 2010). The current model of FN fibrillogenesis predicts that the initial unfolding and stretching of FN molecules in nascent adhesions requires that each of the two RGD motifs within the dimeric FN molecule become engaged by integrin $\alpha5\beta1$, such that each FN molecule is ligated by two $\alpha5\beta1$ integrins. The mechanical coupling of FN-bound $\alpha5\beta1$ integrins to the F-actin cytoskeleton allows contractile acto-myosin-generated forces to translocate integrin $\alpha5\beta1$ centripetally from the cell-peripheral focal adhesions towards the cell body, pulling bound FN along and thereby giving rise to fibrillar adhesions. During translocation, the two $\alpha5\beta1$ integrins that are bound to the same molecule of FN segregate, and this segregation exerts the force required to pry open the globular FN dimer. The exposure of FN-binding sites within FN upon unfolding of the globular state allows

lateral self-association among multiple FN molecules and thereby drives the transformation of FN into a fibrillar form (Ohashi et al., 2002). Subsequently, FN fibrils undergo extensive branching, cross-linking and bundling as cells continue to remodel the ECM, creating a complex three-dimensional matrix with mechanical properties that dictacte cell behaviour.

Monomerised $FN^{CC>SS}$ presents only a single RGD motif to integrins, yet in a cell-dependent manner, $FN^{CC>SS}$ does become deposited into the ECM in a fibrillar state (fig. 8.18). Hence despite the presence of only a single intact RGD motif, the integrin-dependent phase of $FN^{CC>SS}$ fibrillogenesis was intact,. It became clear that integrin $\alpha5\beta1$ could associate with $FN^{CC>SS}$, both in focal adhesions and fibrillar adhesions (figs. 8.21 and 8.22) and that during early time points of $FN^{CC>SS}$ fibrillogenesis, this association of integrin $\alpha5\beta1$ with $FN^{CC>SS}$ was accompanied by the formation of $FN^{CC>SS}$ fibrillar structures. These observations revealed a sufficient degree of integrin-mediated unfolding and lateral self-association in $FN^{CC>SS}$. Whether the binding of one integrin $\alpha5\beta1$ to the single RGD motif in $FN^{CC>SS}$ is sufficient to promote fibrillogenesis, or whether compensatory mechanisms are needed to assist in promoting fibrillogenesis of monomerised $FN^{CC>SS,}$ are issues I will speculate on in the following paragraphs.

In order to achieve the conformational changes in $FN^{CC>SS}$ molecule and expose its FN-binding sites for lateral association, tension must build up within $FN^{CC>SS}$ that overcomes the intramolecular interactions that maintain $FN^{CC>SS}$ in a globular state. A single integrin $\alpha5\beta1$ bound to the one RGD motif in $FN^{CC>SS}$ will transduce the contractile force emanating from the actomyosin machinery, but in order to establish tension across $FN^{CC>SS}$, a level of resistance to the contractile force must be met by $FN^{CC>SS}$. In the absence of a second $\alpha5\beta1$ integrin bound to $FN^{CC>SS}$ to create this resistance, there must be alternative means of inducing the conformational changes. Perhaps the $FN^{CC>SS}$ molecule that is bound by integrin and still in its globular state interacts with the microenvironment to an extent that integrin $\alpha5\beta1$ meets resistance when tugging on $FN^{CC>SS}$. In cell culture experiments, the $FN^{CC>SS}$ that is secreted by $FN^{CC>SS/CC>SS}$ MEFs is likely to become partially absorbed by the uncoated or gelatin-coated culture surface. In embryonic tissue, $FN^{CC>SS}$ is secreted into a confined three-dimensional extracellular environment that offers ample opportunity for $FN^{CC>SS}$ to immobilise through non-covalent interactions with other glycoproteins, and this might be sufficient to assist integrin $\alpha5\beta1$ in building the tension required for stretching $FN^{CC>SS}$ molecules.

Another possibility is that the monomerised state of $FN^{CC>SS}$ is less globular than WT FN and that fibrillogenesis of $FN^{CC>SS}$ does not require the same level of integrin-mediated tension to open $FN^{CC>SS}$. The compact, globular conformation of WT pFN is reported to rely on intramolecular ionic interactions between $FNIII_{12-14}$ of one subunit and $FNIII_{2-3}$ of the other subunit of the FN dimer (Johnson et al., 1999). These interactions between subunits are far less likely to exist between monomerised $FN^{CC>SS}$ molecules, but given that plasma $FN^{CC>SS}$ is expressed in a solube state there must be other intramolecular interactions that maintain a globular conformation. The strength of these interactions would determine the degree of integrin-mediated build-up of tension required to induce conformational changes in $FN^{CC>SS}$ molecules that expose FN-binding sites. If these intramolecular

forces are weak, then one can imagine that contractile forces transmitted to globular $FN^{CC>SS}$ through a single integrin would be sufficient to achieve this unfolding.

Finally, there is the possibility that integrin α5β1 might not be the only integrin involved in the extension of $FN^{CC>SS}$. Hypothetically, extension is achieved through engagement of multiple integrin-binding sites along the length of the $FN^{CC>SS}$ molecule. Previous studies have demonstrated that the RGD motif in FN is dispensable for FN fibrillogenesis, albeit strictly required for mouse development, because αV integrins can engage a GNGRG peptide sequence motif within the FNI_{1-5} domains and promote fibrillogenesis (Takahashi et al., 2007). One way of explaining the fibrillogenesis of $FN^{CC>SS}$ is that integrin α5β1 and αV integrins cooperate to promote $FN^{CC>SS}$ fibril formation by engaging the RGD motif in $FNIII_{10}$ and the GNGRG motif within FNI_{1-5} domains, respectively. In such a scenario, one would expect the fibrillar adhesions to be stunted because of an inability of αV integrins to translocate into fibrillar adhesions like integrin α5β1.

In a $FN^{CC>SS/CC>SS}$ MEF clonal cell line, the short $FN^{CC>SS}$ fibrils were accompanied by similarly stunted fibrillar adhesions (fig. 8.22). Although short fibrillar adhesions were not apparent in $FN^{-/-}$ fibroblasts assembling $pFN^{CC>SS}$ (fig. 8.21), it suggests that $FN^{CC>SS}$ either delays the formation or affects the stability of fibrillar adhesions. In speculating how FN dimerisation could affect the formation and stabilisation of fibrillar adhesions, it is clear that dimerisation of WT FN not only duplicates both the number of integrin-binding sites and the number of FN-binding sites within one molecule, but also brings these binding potentials into closer proximity of each other. For each FN dimer, two integrins can be brought into close proximity of each other and essentially seed an integrin cluster. Similarly, for each integrin-bound stretched FN dimer, additional FN dimers can be brought to the adhesion complex, which in turn, will favour additional integrin clustering. By reducing the degree of freedom between essential components of the fibrillogenesis reaction (i.e. integrin-binding sites and FN-binding sites), dimerisation facilitates integrin clustering and FN–FN interactions such that fibrillogenesis can occur at a higher rate. In contrast, monomerised FN molecules possess half the potential for interacting with integrins and other FN molecules. Here, an increase in the degree of freedom between the reaction components of $FN^{CC>SS}$ fibrillogenesis causes the reaction to rely to a greater extent on diffusion of each molecule $FN^{CC>SS}$ molecules to integrins compared to dimeric FN. The diffusion-limited arrival of globular $FN^{CC>SS}$ molecules will delay their incorporation into fibrillar adhesions, and hence at any given point, fibrillar adhesions will appear shorter than normal.

Once assembled into short fibrillar structures in fibrillar adhesions, $FN^{CC>SS}$ fibrils do not continue to mature into as complex a fibrillar matrix as seen with WT FN. The question is, why does the disruption of a single pair of interchain disulfide bonds have such a major effect on fibril growth at a stage of fibrillogenesis that is driven by lateral association? The limitation in fibrillar remodelling of $FN^{CC>SS}$ is most probably related to the fact that fibrils start out so small. Although $FN^{CC>SS}$ protein levels are normal and despite that FN-binding sites in $FN^{CC>SS}$ are intact and fully competent to associate laterally with each other, the delay in fibril growth at the fibrillar adhesion renders the average $FN^{CC>SS}$ fibril shorter and lacking the capacity to build the same complex supramolecular network as WT FN. The difference in fibrillar complexity is more obvious in MEF-derived matrices than in tissue,

and this might reflect that three-dimensional confinement of tissues creates a favourable environment to promote the fibrillar remodelling process.

The $FN^{CC>SS/CC>SS}$ mouse offers a model for examining the specific requirement for the pair of disulfide bonds, constituting the dimerisation motif, for FN fibrillogenesis. This model provides a pure system to evaluate the monomerisation of an otherwise full-length $FN^{CC>SS}$ molecule. In contrast, the study published by Dr. Schwarzbauer, which established the current dogma on the requirement for the dimerisation motif, were based on mammalian cells expressing a fusion construct of FNI_{1-9} and the most extreme 100 kDa of the C-terminus (recFNI$_{1-9}$/C110) that lacked a twenty-amino acid segment containing the C-terminal dimerisation motif (recFNI$_{1-9}$/C110$_M$). The cells expressing this recombinant fragment failed completely to deposit this form of FN into fibrillar matrix, and all the protein was released into the medium (Schwarzbauer, 1991).

Based on the observation that monomerised $FN^{CC>SS}$ is assembled into a matrix of shortened fibrils, there appears to be no absolute requirement for FN dimerisation, if simply for the purpose of duplicating the number of RGD motifs that can employ integrin $\alpha5\beta1$. Nevertheless, the fibrillar morphology of monomerised FN is strongly compromised, and I conclude that dimerisation is crucial to achieving the appropriate rate of FN fibrillogenesis because it serves to limit the degrees of freedom and increases the local concentration of the reaction components. The delay in fibril elongation will render fibrils of monomerised $FN^{CC>SS}$ shorter, and these short fibrils will never have the capacity to achieve the same matrix complexity as WT FN.

The discrepancy between the results presented herein and those presented by Dr. Schwarzbauer must relate to the design of the recombinant fragment (recFNI$_{1-9}$/C110$_M$). First of all, deleting a twenty-amino acid segment of the C-terminus, including the dimerisation motif, might cause more of a change to FN than controlled for. Secondly, and possibly most importantly, although the recFNI$_{1-9}$/C110$_M$ contains both the N-terminal assembly domain and the cell-binding domain RGD motif, it has a large internal deletion of repeats $FNIII_{1-7}$ such that the collagen-binding domain becomes connected to the cell-binding domain. Although the $FNIII_{1-7}$ segment might not be critical for fibrillogenesis of FNI$_{1-9}$/C110 when both the assembly domain and dimerisation motif are available, the $FNIII_{1-7}$ might very well become essential in the absence of a dimerisation motif because the $FNIII_{1-7}$ repeats offer abundant potential to interact with the N-terminal assembly domain and promote the lateral association among extended FN molecules. For example, the 70kDa N-terminal assembly domain in FN has been shown to interact with sites in $FNIII_1$ (Hocking et al., 1994), $FNIII_2$ (Aguirre et al., 1994; Sechler et al., 2001) and $FNIII_{4-5}$ (HepIII) (Maqueda et al., 2007) in addition to sites within $FNIII_{10}$ and $FNIII_{12-14}$ (Hocking et al., 1996; Bultmann et al., 1998). Therefore, it is conceivable that the failure of recFNI$_{1-9}$/C110$_M$ to undergo conversion into a fibrillar and DOC-insoluble matrix (Schwarzbauer, 1991) relates to more than just the inability of this form of FN to dimerise and highlights the important contributions of the cryptic FN-binding sites to fibrillogenesis. With the $FN^{CC>SS/CC>SS}$ mouse, monomerised $FN^{CC>SS}$ is full-length and all FN-binding sites are intact as well as in their correct positions relative to each other.

9.2 Unique properties of the $FN^{CC>SS}$ fibrillar matrix

The structural characterisation of the $FN^{CC>SS}$ fibrillar matrix was complemented with an analysis of the mechanical properties of cell-derived ECM containing $FN^{CC>SS}$ fibrils (fig. 8.24). Applying the state-of-the-art AFM indentation technique to MEF-derived ECM platforms, I found that the unique structural features of $FN^{CC>SS}$ fibrillar matrix were associated with a change in the elasticity of ECM that forms around $FN^{CC>SS}$, despite the fact that FN is far beyond the only matrix component of a cell-derived ECM. In comparing the elasticity of WT ECM with an ECM containing $FN^{CC>SS}$, I concluded that FN dimerisation contributed to make the ECM nearly three times stiffer than an ECM containing $FN^{CC>SS}$. It is quite possible that this difference in elasticity reflects the fibrillar complexity of the FN matrix and that of other fibrillar ECM components, whose deposition relies on FN (e.g. LTBP-1).

The ECM is being recognised for its influential role in controlling cell behaviour, particularly with regards to the functional importance of physical/mechanical properties of the ECM. Cells are very sensitive to tissue-level elasticity; diverse cell types such as fibroblasts, tumour cells and stem cells have the ability to detect and respond to local matrix stiffness and deformability. A collection of seminal papers demonstrates the importance of matrix stiffness in development, differentiation, tissue morphogenesis, regeneration and disease (Discher et al., 2005; Engler et al., 2006; Guo et al., 2006; Levental et al., 2009; Mammoto et al., 2009). In the absence of AFM indentation analysis of $FN^{CC>SS/CC>SS}$ embryonic tissue, I can only speculate that the differences in ECM stiffness that were shown between MEF-derived ECM are representative of the relative differences in the tissue mechanical properties between $FN^{CC>SS/CC>SS}$ and WT embryos. The measured elasticities in MEF-derived ECM fell in the range of elasticity found in bone marrow ECM (~0.1–0.3 kPa) (Prewitz et al., 2013). Interesting questions are those that ask what the implication of such stiffness differences is on tissue function and cell behaviour, and could an increase in embryonic tissue pliability of ECM containing $FN^{CC>SS}$ compared to WT ECM explain the cardiovascular phenotype of the $FN^{CC>SS/CC>SS}$ embryo?

At the cellular level, ECM rigidity is reported to influence morphology, adhesion, contractility (Yeung et al., 2005), differentiation (Engler et al., 2004) and motility (Lo et al., 2000). These cellular responses to ECM stiffness are largely mediated by active integrins in focal adhesions. Matrix stiffness modulates integrin adhesions by strengthening the mechanical link between integrin and the actin cytoskeleton and altering the clustering of integrins (Paszek et al., 2005; Levental et al., 2009). A number of intracellular signalling kinases associated with the focal adhesion are tension-sensitive, and in this way, ECM stiffness can affect the volume of biochemical signals emanating from the adhesion. Integrins relay biochemical signals on ECM compliance through major signalling pathways involving ROCK, FAK, ERK and Akt (Wozniak et al., 2003; Paszek et al., 2005). For example, FAK activation at tyrosine residue 397 is regulated by acto-myosin contractility, integrin-mediated adhesion and matrix stiffness in a tension-responsive manner (Tilghman and Parsons, 2008). It is noteworthy that only on stiff subtrates are cells found to assemble stress fibres and phosphorylate FAK^{Y397} within focal adhesions (Paszek et al., 2005).

Integrin α5β1 and F-actin in $FN^{CC>SS/CC>SS}$ MEF clonal cell lines displayed markedly altered fibrillar adhesion structures (fig. 8.22). In addition to previously mentioned speculations the stunted appeareance of fibrillar adhesions could relate to the compliant $FN^{CC>SS}$ matrix unable to resist the contractile force transmitted by integrins to the same degree as a WT FN matrix, and this would cause a weakening of the integrin adhesion complex. In an approach to evaluating cell-matrix adhesion stability, I compared motility of $FN^{-/-}$ fibroblasts seeded onto tissue-mimetic ECM platforms derived from either WT or $FN^{CC>SS/CC>SS}$ MEFs. This analysis showed no difference in migration speed between cells migrating in response to PDGF-BB on an ECM platform containing WT FN and $FN^{CC>SS}$ (fig. 8.27). In addition, I addressed integrin outside-in signalling through $pFAK^{Y397}$ in (1) WT and $FN^{CC>SS/CC>SS}$ MEFs generating their own fibrillar matrix (fig. 8.28), (2) FN-/- fibroblasts seeded onto tissue-mimetic ECM derived from WT and $FN^{CC>SS/CC>SS}$ MEFs (fig. 8.29) as well as (3) WT and $FN^{CC>SS/CC>SS}$ embryonic tissue (fig. 8.30). In none of these systems did I identify an abnormality in the levels of $pFAK^{Y397}$ in response to $FN^{CC>SS}$ matrices. Similiary, I saw no change in the levels of $pMLC2^{S19}$ between $FN^{-/-}$ fibroblasts seeded onto ECM derived from WT and $FN^{CC>SS/CC>SS}$ MEFs, indicating that integrin outside-in signalling through the RhoA/ROCK axis is also unaffected by the structural and mechanical properties of $FN^{CC>SS}$ matrices.

Unfortunately, I do not have measurements of Young's moduli of the ECM preparations that were used to perform cell migration assays and integrin outside-in signalling assays. These matrices were prepared through decellularisation with EDTA of three-day cultures (fig. 8.26). When prepared in this fashion, the resulting ECM platforms are too thin for AFM indentation measurements. Yet, these matrices were morphologically similar to the thicker matrices used for AFM indentation analysis. Therefore the relative difference in compliance of these matrices is assumed to compare to those of thicker matrices prepared through anchorage (cf. fig. 8.24), such that ECM containing FN dimers is still about three-fold stiffer than ECM containing $FN^{CC>SS}$. Despite this assumption, it is not clear why the cellular response to the structural and mechanical features of the $FN^{CC>SS}$ matrix is undetectable. It could be that even though I find a three-fold difference in stiffness between ECM containing WT FN and $FN^{CC>SS}$, the absolute Young's moduli for these matrices are very low and hence too soft for changes of hundreds of Pascals to trigger differences that are significant enough to detect by the biochemical or cell biological techniques employed here. Indeed, when naïve mesenchymal stem cells have been shown to commit to a lineage and phenotype with extreme sensitivity to tissue-level elasticity, this was on matrices that range between 100 Pa ("soft") and 40 kPa ("stiff") (Engler et al., 2006). When matrix stiffness has been found to regulate focal assembly, modify growth factor signalling and cell phenotype through ERK and Rho activity, it was based on culturing cells on soft and stiff matrices that range for 400 Pa ("soft") to 5000 Pa ("stiff") (Paszek et al., 2005). Also, comparison of smooth muscle cell migration speeds have been based on substrates designed with Young's moduli values ranging from 1000 Pa ("soft") to 308 kPa ("stiff"). Hence, while the Young's moduli of both the WT ECM and ECM containing $FN^{CC>SS}$ must be relevant to cells in the developing embryo because they were generated by MEFs from E9.5 embryos, it appears that conventional

methods to detect cellular output (e.g. integrin outside-in signalling and migration assays) are insufficient to distinguish between differences within such a low stiffness regime.

9.3 The $FN^{CC>SS}$ knock-in mutation causes cardiovascular remodelling defects

Even though I could identify no accute change in the cellular response to the unique structural and mechanical properties of $FN^{CC>SS}$ matrix, the complete halt in development is evidence that the qualities of the $FN^{CC>SS}$ matrix severely disturb cellular function. Most prominent were the defects arising within the cardiovascular system. The cardiovascular system is the first functional organ to develop in vertebrates, and failure of the cardiac or vascular tissue to perform is lethal.

9.3.1 Cardiac defects

The effused pericardial sac and the malformed ventricular structures in the heart of E9.5 $FN^{CC>SS/CC>SS}$ embryos (fig. 8.4) suggested severe defects of the developing heart. Immunological whole mount stainings of the endocardium in $FN^{CC>SS/CC>SS}$ embryos revealed an irregular curvature of the endocardium, an inability of the endocardium to interact extensively with the myocardium, the stunted growth of the heart tube and a failure of the heart tube to undergo rightward looping morphogenesis (figs. 8.10 and 8.11). These heart looping morphogenesis defects could possibly reflect a general left/right asymmetry defect in $FN^{CC>SS/CC>SS}$ embryos. FN is known to have an important effect on establishing left-right asymmetry along the embryonic body anterior-posterior axis by regulating morphogenesis of the node at very early stages of development (Pulina et al., 2011). Preventing FN dimeristaion could change structural features of the FN matrix to a degree that prevents it from shaping the node and promoting the establishment of asymmetric gene expression patterns. Such questions would require electron microscopical analysis of embryonic structures, such as the node, and *in situ* hybridisation to visualise the spatial expression patterns of *Nodal* and other genes, such as *Lefty1*, *Lefty2* and *Pitx2c*, which are known to be asymmetrically expressed on the left side of the lateral plate mesoderm (Pulina et al., 2011).

At this critical stage of cardiac development, FN is an abundant component of the cardiac jelly, into which mesenchymal cells migrate to establish the cardiac cushion that must form in both the outflow tract and the atrioventricular channel, a process that involves additional deposition of FN (Mjaatvedt et al., 1987; Ffrench-Constant and Hynes, 1988; Roman and McDonald, 1992; Eisenberg and Markwald, 1995). Cardiac cushion is essential to heart development because it will condense to divide the outflow tract into the aorta and the pulmonary artery and contribute both to forming the major valves of the heart and closure of the heart septum (Webb et al., 1998; Savolainen et al., 2009). Given the morphology of the $FN^{CC>SS/CC>SS}$ cardiac tissue, it is apparent that dimerisation of FN confers specific properties that support the formation of these cardiac structures.

The physical mechanisms that drive and regulate cardiac looping morphogenesis are currently incompletely understood (Taber et al., 2010). Elegant work on chick embryos, which, with caution, can be extrapolated to that of other vertebrate organisms such as the mouse embryos, has demonstrated that the first phase of cardiac looping occurs as specific regions of the heart tube grow and contract.

Looping is driven further by forces exerted on the heart tube by surrounding tissues as they press against the ventral surface of the heart. One interesting study sheds light on the role of regional stiffness along the heart tube in promoting the bending and rightward looping (Zamir et al., 2003). Based on microindentation measurements along intact embryonic heart tubes, the tissue lining what would become the inner curvature of the embryonic cardiac tube was significantly stiffer than the tissues that would line the outer curvature or dorsal and ventral sides of the heart tube. In the process of cardiac looping, the tissue lining the outer curvature of the cardiac tube has to stretch and extend further than tissue lining the inner curvature and therefore it appears that that modulating the local stiffness along the cardiac tube dictates which of the faces of the tube forms the outer and inner curvatures in response to the external pushing at the ventral side. The authors of this study suggest that this regional variation in stiffness is due to the mechanical properties of the myocardium. FN is important for establishing the integrity of myocardial tissue during cardiogenesis (Trinh and Stainier, 2004b), and perhaps fibrillar FN plays a role in shaping the mechanical properties of the myocardium, either by the complexity of the FN fibrillar matrix itself or that of the ECM components that rely of the presence of a fibrillar FN matrix. The inability of $FN^{CC>SS/CC>SS}$ cardiac tubes to undergo looping morphogenesis could be associated with a decrease in the tissue stiffness caused by the presence of $FN^{CC>SS}$ in the myocardial basement membrane, and this alteration in the elasticity of the myocardium would cause the failure to establish the regional stiffness that dictates the correct bending of the cardiac tube.

The cardiac malformation in $FN^{CC>SS/CC>SS}$ embryos could also reflect an inadequate level of intracardiac shear forces as blood flows through the heart tube. Hemodynamics is considered a key epigenetic factor in cardiogenesis, as impaired blood flow disrupts looping morphogenesis and impairs the formation of heart valves (Hove et al., 2003). Cardiac endothelial cells have been shown to respond to shear forces by reorganising their cytoskeleton and changing their genetic expression profiles (Davies, 1995; Topper and Gimbrone, 1999). FN is a core basement membrane component of the developing vessel wall (Risau and Lemmon, 1988), which provides mechanical resistance to the increasing flow of blood of the growing embryo. Having learned that $FN^{CC>SS}$ causes a softening of the ECM, it is plausible that the vascular basement membrane containing $FN^{CC>SS}$ does not provide adequate mechanical support to the endothelium. As a result, blood flow would not expose the endocardium to normal hemodynamic forces to promote its development.

9.3.2 Vascular defects

Another hallmark of the $FN^{CC>SS/CC>SS}$ phenotype are the vascular remodelling defects, both in the embryo proper (fig. 8.9) and extraembryonic tissues (figs 8.5, 8.6 and 8.8). Very prominent are both the anemic appearance and the failure to form a hierarchical network of branched high-calibre and low-calibre vessels in the yolk sac (fig. 8.5). The yolk sac is a large, but thin extra-embryonic tissue that envelops the embryo proper at E7.0. This tissue is of major importance to the development of the embryo because it is a source of the first primitive erythrocytes cells and progenitors of the hematopoitic system, which are required until the aorta/gonad/mesonephros-derived hematopoetic

stem cells seed into the fetal liver, where they can differentiate into erythrocytes (Palis and Yoder, 2001; McGrath and Palis, 2005). The delivery of these first primitive erythrocytes to the embryo proper relies on the development of a yolk sac vasculature and its connection to the embryonic vasculature. The immunological and histochemical analyses of the $FN^{CC>SS/CC>SS}$ yolk sac revealed that vasculogenesis had succeeded to build a primitive vascular plexus, but that the endothelial branching, remodelling and pruning events of angiogenesis that must follow the establishment of a primitive plexus (Risau, 1997) had failed in $FN^{CC>SS/CC>SS}$ yolk sac. A strong indication of integrity failure of the primitive vascular plexus in $FN^{CC>SS/CC>SS}$ yolk sacs was the accumulation of erythrocytes in the yolk sac, strongly suggestive of leaky vessels. Immunohistochemical analysis of the E9.5 $FN^{CC>SS/CC>SS}$ embryo proper revealed a chaotic vascular infrastructure in the head as well as an abnormal vessel length and diameter of the dorsal aorta, pharyngeal arteries and intersomitic vessels. The allantoic mesoderm in $FN^{CC>SS/CC>SS}$ had also failed to grow to allow the embryonic vasculature to intermingle with the maternal vasculature in the placenta for the effective blood-based exchange of gases and nutrients between embryo and mother. These defects in vascular development in both embryonic and extra-embryonic tissues appear at the stage of development where the normal mouse embryo can no longer survive by direct diffusion-based exchange of gases, nutrients and toxic metabolites with the surrounding amniotic fluid (Rossant and Cross, 2001). Hence I conclude that the vascular defects in $FN^{CC>SS/CC>SS}$ embryos are the cause of embryonic growth arrest prior to the 20 somite stage of development and ultimately result in lethality.

The expansion and remodelling of the blood vasculature is closely coordinated with the development of the embryonic heart. The yolk sac vasculature is particularly sensitive to increasing heart fuction, and so it is relevant to explore the possible relationship between the defective cardiac tissue in $FN^{CC>SS/CC>SS}$ embryos and the concurrent failure in vascular remodelling. By E8.0 (4-6 somite stage), the heart has become physically connected to the yolk sac via an extensive network of blood vessels such that as the heart begins to beat, primitive erythroblasts originating in blood islands of the yolk sac can flow into the blood circulation of the embryo proper (Ji et al., 2003; McGrath, 2003). The major remodelling events of the yolk sac vasculature take place immediately following the established circulation.

The development of the cardiovascular system has been shown to rely on interplay between a great number of genes (e.g. *Hedgehog*, *TGF-β* and *VEGF-A*) (Solloway and Harvey, 2003; Trinh and Stainier, 2004a; Argraves and Drake, 2005). However, not all genes that are required for vascular remodelling are actually expressed by the endothelium; in some cases, genes (e.g. *Nkx2.5*, *Ncx1*, *MLC2a* and *Titin* genes) that are critical for vascular remodelling are primarily expressed by cardiac cell types (Tanaka et al., 1999; Koushik et al., 2001; Huang et al., 2003; May et al., 2004). A clear example of the key function of the heart in promoting vascular remodelling is given by the rescue of the vascular defects in the complete N-cadherin knockout mouse by re-introducing expression of either N- or E-cadherin only in heart tissue (Luo et al., 2001). One conclusion from these mouse knockout studies is that vascular remodelling defects arise as secondary effects of impaired cardiac contractility and circulation. Circulation is essential to the embryo because it delivers both oxygen and nutrients to all tissues of the

organism (Conway et al., 2003), but in recent years it has become clear that circulation also positively influences developmental angiogenesis by exerting hemodynamic force on the endothelium (Lucitti et al., 2007). Endothelial cells respond to the hemodynamic force exerted by blood flow (i.e. shear stress and circumferential strain) with changes in cell morphology, activation of intracellular signalling pathways and induction of specific genetic expression patterns (Li et al., 2005b). A disturbance or reduction in fluid dynamics caused by cardiac defects has been proposed to lead to the disruption of the mechanical signals necessary for proper vascular development (Jones et al., 2004). An elegant study by Lucitti and colleagues has demonstrated that vascular remodelling in the yolk sac is driven by those very first events occurring at E8.0, where the heartbeat-driven entrance of erythrocytes from blood islands into circulation (Ji et al., 2003; McGrath, 2003) causes a change in the effective viscosity of the blood flow that mechanically stimulates the endothelium and initiates proper remodelling (Lucitti et al., 2007).

This intimate coupling between cardiac function and vascular development offers a possibility that the vascular remodelling defects of the $FN^{CC>SS/CC>SS}$ embryos are secondary effects of cardiac malfunction. Although the cardiac tissue of $FN^{CC>SS/CC>SS}$ embryos show spontaneous contractions, the failure of the cardiac tube to remodel and the accumulation of plasma in the pericardial sac suggest that its pumping function is compromised and fails to establish the embryonic circulation. Furthermore, the anemic appearance of the $FN^{CC>SS/CC>SS}$ yolk sacs, accompanied by an accumulation of small amounts of blood in the yolk sac cavity, indicate that the vessels of the primitive vascular plexus are leaking erythrocytes into extravascular space. The combination of cardiac failure with the loss of erythrocytes from the yolk sac would prevent the heartbeat-driven entrance of erythrocytes into the embryonic circulation to elevate the hemodynamic force exerted on the endothelium and drive the remodelling of the $FN^{CC>SS/CC>SS}$ yolk sac vasculature. The phenotypic parallels between mice deficient in atrial MLC2a (Huang et al., 2003) and $FN^{CC>SS/CC>SS}$ embryos lend support to the possibility that cardiac dysfunction in $FN^{CC>SS/CC>SS}$ embryos relates to the inability of $FN^{CC>SS}$ in adhesions to stabilise the atrial myofibrillar apparatus and sustain atrial contraction.

The cardiac and vascular remodelling the $FN^{CC>SS/CC>SS}$ embryos could also be uncoupled events in that the vascular defect does not derive from the heart defect. In this case, developmental angiogenesis fails to occur because of a negative response of endothelial and/or mural cells to $FN^{CC>SS}$ present within the vascular basement membrane. In the $FN^{CC>SS/CC>SS}$ yolk sac, the endothelial cells were found to have coalesced into a primitive plexus of lumenised vessels, characterised by several abnormalities; but lumens were abnormally wide, mural cell recruitment and investment of the vessel wall appeared chaotic, and sprout formation, fusion, pruning and remodelling of these vessels had failed. Several studies have shown that endothelial-specific knockout of β1 integrins results in severe vascular defects and lethality at E10 (Carlson et al., 2008; Lei et al., 2008; Tanjore et al., 2008; Zovein et al., 2010). This prompted the hypothesis that $FN^{CC>SS}$ disrupts developmental angiogenesis by interfering with β1 integrin activation in the endothelium. However, my investigation of integrin signal activation by western blot analysis of FAK^{Y397} phosphorylation and $MLC2^{S19}$ in $FN^{CC>SS/CC>SS}$ embryonic tissue or highly vascularised tissue such as the yolk sac showed no obvious change in

integrin outside-in signalling via FAK or RhoA/ROCK. If $FN^{CC>SS}$ was influencing the activation of integrins, the change in $pFAK^{Y397}$ was either below detection level or simply not reflected in the levels of $pFAK^{Y397}$ or $pMLC2^{S19}$ (figs. 8.28, 8.29, 8.30). Interestingly, Richard Hynes and colleagues have very recently demonstrated that the endothelial-specific knockout of the FN receptor integrin α5β1 has no obvious effect on developmental angiogenesis; in fact neither FN receptors α5β1 or αVβ3 are required by the endothelium for vasculogenesis or angiogenesis at early stages of development. Instead, they are necessary for the subsequent remodelling of the great vessels and heart occurring from E11.5 onwards (van der Flier et al., 2010). This stands in contrast to the early cardiovascular defects of Tie2-Cre-mediated endothelial-specific knockout of all β1 integrins (Carlson et al., 2008; Lei et al., 2008; Tanjore et al., 2008; Zovein et al., 2010) or the endothelial-specific knockout of integrin adhesion scaffolding or signalling molecules, such as ILK (Friedrich et al., 2004) and FAK (Braren et al., 2006), all of which succumb to early angiogenesis defects in embryo, placenta and yolk sac and die before E11.5. This contrast suggests that at early stages of angiogenesis, (1) the endothelium operates with β1 integrins other than FN-binding integrin α5β1 (e.g. receptors for laminin, collagen, thrombospondin), and (2) these β1 integrin-mediated signals drive the cellular processes of early developmental angiogenesis. Which β1 integrins are responsible for these early angiogenic processes awaits further investigation. In light of these studies, the developmental angiogenesis defects found in $FN^{CC>SS/CC>SS}$ embryos cannot be interpreted to reflect aberrant activation of endothelial α5β1 integrin by $FN^{CC>SS}$.

The discrepancy between the vital requirement for FN and integrin α5β1 in vascular development on the one hand (Yang et al., 1993; George et al., 1997), and the ability of endothelial cells to manage without FN-binding integrins on the other also highlights the likelihood that FN-binding integrin function is required in non-endothelial cell types, such as mural cells (pericytes and vSMCs). These cells associate with the endothelium, either directly or through a shared basement membrane containing FN (Courtoy and Boyles, 1983), among other ECM proteins, and promote vascular development and function in part because this association stimulates VEGF-A production by mural cells (Darland et al., 2003). A transient, but direct interaction of mural cells with endothelial cells is mediated though integrin α4β1 expressed by endothelial cells and VCAM-1 expressed by mural cells (Garmy-Susini et al., 2005) and therefore this mode of integrin-dependent interaction between endothelial cells and mural cells to interact is probably not influenced by the presence of $FN^{CC>SS}$ in the vascular basement membrane. Yet within $FN^{CC>SS/CC>SS}$ yolk sacs, α-SMA-positive mural cells are chaotically distributed and aberrantly associated with the endothelium, giving the impression that despite the correct differentiation from precursor cells (an observation I will return to shortly), these mural cells might not associate properly with the endothelium to support their development. Interestingly, there is a reported case showing that FAK plays a role in promoting the motility of vSMCs, and this is particularly important for their recruitment to the outflow tract of the heart, which they divide into the aorta and pulmonary artery (Cheng et al., 2011). As a signalling molecule that is activated within focal adhesions, FAK could propagate motility signals downstream of FN-binding integrins expressed on mural cells. Here it is tempting to speculate that $FN^{CC>SS}$ deposited by the

developing endothelial cells and mesoderm affects the ability of mural cells to mobilise and invest the endothelium. Without the appropriate balance in mural cell investment, the $FN^{CC>SS/CC>SS}$ endothelium might not be receiving the necessary levels of VEGF to promote its remodelling (Darland et al., 2003). The ability of mural cells to support blood vessels integrity relies on β1 integrin-mediated cell adhesion (Abraham et al., 2008), although the requirement of FN-binding integrins remains to be formally proven. However this β1 integrin-mediated effect of mural cells on the endothelium is apparently not essential at early stages of developmental angiogenesis because mice lacking β1 integrins in mural cell die at perinatal stages (Abraham et al., 2008). Clearly there is a very complex interplay between endothelial and mural cells, and with both cell types in such close proximity and dependent on each other, it is difficult to draw conclusions on which cell type is affected by $FN^{CC>SS}$ and disrupts developmental angiogenesis. The proximity of both endothelium and mural cell to $FN^{CC>SS}$ makes it very likely that both cell types are challenged by $FN^{CC>SS}$.

There is substantial evidence in the scientific literature that both endothelium and mural cells are sensitive to the mechanical properties of their microenvironment. The processes of vascular differentiation and remodelling are sensitive to tensional homeostasis, of which ECM stiffness is a key parameter. Therefore ECM stiffness must be considered as a possible contribution to the vascular defects in the $FN^{CC>SS/CC>SS}$ embryos and yolk sacs. *In vitro* studies have demonstrated that endothelial behaviour is regulated by ECM stiffness. For example, increases in collagen gel stiffness increases endothelial cell spreading as well as the number and length of angiogenic sprouts extended by endothelial spheroids (Mason et al., 2013). Another study addressed the positive effect of hydrogel stiffness on endothelial proliferation (Yeh et al., 2012). Furthermore, both the stiffness and shape of endothelial cells changes according to the stiffness of a substrate (Byfield et al., 2009; Califano and Reinhart-King, 2010). A groundbreaking paper on this topic describes how angiogenesis is directed by endothelial cell integration of both chemical cues, such as VEGF gradients, and mechanical cues from the substrate. Here, the degree of elasticity of the endothelial substrate governs a complex transcriptional programme that regulates the expression of VEGFR2 by the endothelial cell and thereby regulates the sensitivity of the endothelium to soluble VEGF gradients (Mammoto et al., 2009).

vSMCs are known to show a response to changes in substrate stiffness in terms of cell motility, and through intracellular mechanisms that involve Rho-mediated cytoskeletal rearrangements and cell contractility, the vSMC reaches an optimum migration speed on a substrate that is "neither too soft nor too stiff" (Peyton and Putnam, 2005). Furthermore, the activation and differentiation of α-SMA-positive myofibroblasts from progenitors cells depends on both TGF-β (Desmoulière et al., 1993; Hirschi et al., 2003; Chen and Lechleider, 2004; Ding et al., 2004) and ECM stiffness (Hinz et al., 2001; Goffin et al., 2006; Hinz, 2010). The spontaneous contractile activity of myofibroblasts is also governed by the mechanical environment, as demonstrated by a very recent study in which the mechanical conditions of the extracellular environment controlled the contractile activity of myofibroblasts by modulating the oscillation frequency of intracellular calcium ions (Godbout et al., 2013). It is not only the absolute values of matrix stiffness that determine the cellular response, but

also the steepness in the gradient of matrix stiffness sensed by cells. For example, durotaxis of vSMCs depends on substrate stiffness gradient strength (Isenberg et al., 2009).

When it comes to building a functional vasculature, there is still far to go before understanding how endothelium and mural cells respond to abnormal mechanical properties of the ECM *in vivo*, if at all. This is because we are still far from defining the stiffness requirements of the embryos and recognising defects that relate to tissue stiffness. Perhaps the change in the mechanical properties of the ECM lower the proliferation and sprouting activities in the $FN^{CC>SS/CC>SS}$ endothelium. Perhaps it affects the expression of VEGFR2 by the endothelium and renders the endothelium insensitive to VEGF gradients. Alternatively, the change in the ECM stiffness regime caused by $FN^{CC>SS}$ could affect the steepness of the gradient in ECM stiffness, which could be hypothesised to affect the ability of the vSMCs to reach their correct destination at the right time.

9.4 Exploring growth factor signalling defects in the $FN^{CC>SS/CC>SS}$ mouse

Growth factors and their cognate receptors are in large part responsible for the morphogenetic induction and shaping of tissues within the cardiovascular system. Given the defects in cardiac development in the $FN^{CC>SS/CC>SS}$ mouse, it was of great importance to investigate the impact of monomerised FN on growth factor signalling. A significant part of this project was dedicated to investigating the phenotypic parallels between the $FN^{CC>SS/CC>SS}$ mouse and mice in which TGF-β signalling is compromised, while a minor part went to exploring the effect of monomerised $FN^{CC>SS}$ on VEGF receptor signalling.

Just like the $FN^{CC>SS/CC>SS}$ mouse, cardiac remodelling defects causing embryonic lethality are a common theme of TGF-β (Dickson et al., 1995; Sanford et al., 1997; Bartram et al., 2001), TGF-β receptor (Oshima et al., 1996; Oh et al., 2000; Jiao et al., 2006; Seki et al., 2006; Carvalho et al., 2007; Sridurongrit et al., 2008) and TGF-β co-receptor knock-out mice (Arthur et al., 2000; Stenvers et al., 2003). The prominent roles of TGF-β signalling during heart development appears to be in promoting endothelial-mesenchymal transition in the endocardium leading up to the formation of the cardiac cushions as well as regulating cell-cell contacts to shape the modelling of chambers.

TGF-β is also a potent regulator of angiogenesis, acting both on the endothelial and the mural cell compartments of the developing vasculature. However, TGF-β has context-dependent effects on endothelial cells, and different endothelial responses are mediated by signalling through ALK1/SMAD1/5 (triggering proliferation) and ALK5/SMAD2/3 (triggering quiescence) (Goumans et al., 2002). The expression of endoglin by endothelial cells promotes ALK1 signalling, thereby shifting the TGF-β response toward proliferation. *In vivo*, an important role of TGF-β is to stabilise the vasculature post-angiogenesis by inducing a stabilising microenvironment. One way by which TGF-β stabilises the vasculature is by promoting the buildup of the vascular basement membrane. TGF-β1 is a potent inducer of numerous ECM protein-coing genes, both of provisional matrix proteins, such as FN, but also of proteins of the mature ECM, such as collagen (Roberts et al., 1986; Ignotz et al., 1987; Keski-Oja et al., 1988). Consistent with this role of TGF-β, the TGF-βRI knockout mice show a lack of FN synthesis by extraembryonic mesoderm in the yolk sac vasculature and the

vasculature fails to remodel correctly (Larsson et al., 2001). In fibroblast- or endothelial cell-based studies, TGF-β was also found to modulate the activity of ECM-degrading enzymes by increasing the expression of PAI-1, an inhibitor of the plasminogen activator (Laiho et al., 1986; Pepper et al., 1990), tissue inhibitor of metalloprotease (TIMP) as well as inhibiting the expression of collagenase (Edwards et al., 1987) so as to minimise the proteolytic degradation of the ECM. Furthermore, TGF-β modulates integrin expression, both positively (Heino et al., 1989; Riikonen et al., 1995; Nejjari et al., 1999; Thibault et al., 2001; Giannelli et al., 2002) and negatively (Heino and Massagué, 1989; Kumar et al., 1995; Lim et al., 1998), in a contextual manner.

Another way by which TGF-β stabilises the endothelium is achieved through the recruitment of mural cells. Indeed, as mesenchymal cells are recruited to the endothelium through PDGF-BB gradients, they become exposed to TGF-β and differentiate into mural cells which will invest and stabilise the vasculature (Hirschi et al., 1998; Sinha, 2004; Wurdak et al., 2005). TGF-β is involved in crosstalk between endothelial cells and mural cells, for diisrupted TGF-β signalling in endothelial cells impairs the TGF-β/ALK5 signalling in adjacent mesenchymal cells, inhibiting their differentiation into mural cells and association with the endothelial tubes (Carvalho et al., 2004).

In addition to exogenous agents, such as heat, pH and proteolysis, studies have highlighted the importance of juxtaposition of endothelial and mural cell types for the activation of latent TGF-β and its availability to either cell type (Antonelli-Orlidge et al., 1989; Sato and Rifkin, 1989; Sato et al., 1990). Within this system, latent TGF-β is deposited into the vascular basement membrane via LTBP (Flaumenhaft et al., 1993), and release mechanisms are in place, possibly involving gap junctions (Hirschi et al., 2003), to activate latent TGF-β stored in the ECM in an integrin-dependent manner. Analogous to mural cells, astrocytes associate closely with the brain endothelium to help provide vascular integrity. This role of astrocytes relies in part on their ability to activate latent TGF-β from the vascular basement membrane through integrin αVβ8–dependent metalloproteolytic mechanism of latent TGF-β activation (Cambier et al., 2005).

In the context of exploring the cardiovascular remodelling defects in the $FN^{CC>SS/CC>SS}$ embryo and yolk sac, I examined the circumstantial evidence for abnormal TGF-β signalling in the $FN^{CC>SS/CC>SS}$ embryo (figs 8.33 and 8.34). With the current understanding of TGF-β-mediated effects on the vasculature, one would hypothesise that a distortion in TGF-β signalling would be associated with a change in the levels of FN protein in the ECM. However, by RT-PCR analysis of FN mRNA (fig. 8.13), western blot analysis of FN protein levels (fig. 8.14) and immunofluorescence imaging of FN in tissue sections (fig. 8.15), I found comparable levels of FN and $FN^{CC>SS}$.

Abnormalities in TGF-β availability would also be expected to disturb the differentiation of mesenchymal cells into α-SMA-positive mural cells as they are recruited to the developing endothelium. With immunofluorescence stainings of α-SMA in yolk sac, I found an abundance of α-SMA-positive cells associated with the primitive vascular plexus of $FN^{CC>SS/CC>SS}$ yolk sacs. Although the distribution of these mural cells along the endothelium appeared chaotic and abnormal, their expression of α-SMA was indicative of successful TGF-β-mediated induction of the mural cell phenotype in the presence of $FN^{CC>SS}$ (fig. 8.7).

For a direct evaluation of TGF-β receptor activation by TGF-β, I assayed the levels of phosphorylated SMAD proteins as well as the transcript level of TGF-β/SMAD target genes that are of key relevance to vascular development. By western blot analysis of single E9.5 embryos, I found no significant difference in the total levels of pSMAD1/5/8 or pSMAD2/3 (fig. 8.33), and with immunofluorescence microscopy of whole mount E9.5 embryos I did not identify any striking change in the distribution of pSMAD1/5/8-positive nuclei within heart tissue or yolk sac vasculature in response to $FN^{CC>SS}$ (fig. 8.34).

Despite not identifying changes in SMAD protein phosphorylation by western blot analysis or changes in the distribution of phosphorylated SMADs by IF imaging analysis, a final dataset highlighted that there are differences in the extent of TGF-βR activation between $FN^{CC>SS/CC>SS}$ and WT tissue. By analysis of specific TGF-β/SMAD target gene transcript levels in E8.5 yolk sacs, I could show a mild, but significant decrease in the transcript level of *Id1* (inhibitor of differentiation or DNA binding) in $FN^{CC>SS/CC>SS}$ yolk sacs relative to WT yolk sacs (fig. 8.35). *Id1* is a specific downstream target gene of TGF-β/ALK1/SMAD1/5/8 in the endothelium (Goumans et al., 2002). Id proteins (Id1, -2 and -3) belong to the helix-loop-helix (HLH) family of transcription factors that regulate gene expression and thereby orchestrate cell cycle control, cell lineage commitment and cell differentiation (Norton, 2000). The Id proteins represent a distinct subtype of the HLH protein family in that they lack a DNA-binding region and function solely by dimerising with other transcriptional regulators, primarily those of the bHLH type (Norton, 2000). This interaction with Id blocks the ability of bHLH proteins to bind DNA, and hence the Id proteins are generally considered negative regulators of bHLH proteins and their ability to positively regulate sets of genes that promote cell fate determination and cell differentiation (Benezra et al., 1990). Id proteins are expressed by endothelial cells in a SMAD-dependent manner (Korchynskyi and ten Dijke, 2002) and promote proliferative, migratory and invasive behaviour of endothelial cells in a pro-angiogenic manner (Lyden et al., 1999; Goumans et al., 2002). I have demonstrated that the angiogenic remodelling defect of the $FN^{CC>SS/CC>SS}$ yolk sac vasculature is accompanied by a significant decrease in the expression of *Id1* target gene. A dimished *Id1* expression in $FN^{CC>SS/CC>SS}$ endothelium could explain the inability of the endothelium to expand and remodel the primitive vascular plexus, but also suggests that $FN^{CC>SS/CC>SS}$ endothelium does not receive adequate TGF-β-induced ALK1 signal.

A similar trend, albeit statistically insignificant, was found for transcript levels of PAI-1 (fig. 8.35). PAI-1 is an inhibitor of the urokinase-type plasminogen activator (uPA). When uPa binds its receptor, uPA-R, it converts plasminogen into plasmin, a broad-spectrum serine protease, which in turn degrades many components of the ECM. The proteolytic activity of uPA is inhibited by PAI-1, and hence PAI-1 serves to promote the accumulation of ECM. Endothelial cells express PAI-1 in response to TGF-β/ALK5 activation (Sawdey et al., 1989; Goumans et al., 2002), and by contributing to the formation of the vascular basement membrane, TGF-β signalling can promote the quiescence of the endothelium and the maturation of the blood vessel wall following angiogenesis. The trend for $FN^{CC>SS/CC>SS}$ yolk sacs to contain lower levels of PAI-1 transcript than WT yolk sacs reflects a lower extent of activation of the TGF-β/ALK5 pathway, but also shows that the signalling events that would

usually put the vasculature in a quiescent phase are mild and therefore cannot explain the lack of remodelling of the primitive vascular plexus.

Collectively, these analyses on TGF-βR activation and downstream signalling provide only weak evidence that the $FN^{CC>SS/CC>SS}$ phenotype is related to deficits in classical TGF-β-mediated effects.

In addition to the phenotypic similarities, the rationale behind exploring the possible involvement of TGF-β in the context of the $FN^{CC>SS/CC>SS}$ cardiovascular phenotype was driven by the hypothesis that changes in the structural and mechanical properties of ECM or tissue associated with $FN^{CC>SS}$ would affect the ability of the ECM to store latent TGF-β or the ability of integrins to activate latent TGF-β. The deposition of LTBP-1, a extracellular carrier for latent TGF-β, into ECM containing $FN^{CC>SS}$ showed a distinct deviation from normal fibrillar morphology, forming punctate structures and short fibrils that very closely resembled that of $FN^{CC>SS}$ (fig. 8.31). Although consistent with a role of FN to provide a template for the deposition of LTBP into the ECM (Dallas et al., 2005; Chen et al., 2007; Kantola et al., 2008), $FN^{CC>SS}$ affected the deposition of LTBP-1 to an extent that was expected to diminish the storage capacity of the ECM for latent TGF-β. However, it became apparently from MEF-derived matrices that the aberrant morphology of LTBP-1 deposited by $FN^{CC>SS/CC>SS}$ MEFs did not influence the amount of latent TGF-β stored in the ECM (fig. 8.32 A). Given the structural morphology of LTBP-1 fibrils and the more elastic properties of ECM containing $FN^{CC>SS}$, I hypothesised that the resistance of the LTBP-1 fibrillar matrix would fail to allow integrin-mediated activation of latent TGF-β. Yet, the ability of integrin αVβ6 to activate latent TGF-β from MEF-deposited ECM was unaffected by the presence of $FN^{CC>SS}$ (fig. 8.32 B).

While I have shown that the ability of integrin αVβ6 to activate latent TGF-β does not appear to be affected by the presence of $FN^{CC>SS}$, I have not tested the effect of $FN^{CC>SS}$ on αVβ8-dependent activation of latent TGF-β. This is the predominant mechanism by which astrocytes in the brain vasculature activate latent TGF-β (Cambier et al., 2005) and could also be a way by which mural cells of the yolk sac vasculature regulate TGF-β availability. This mechanism relies on integrin αVβ8 binding to LAP and recruiting MT1-MMP to cleave LAP and release TGF-β from latency (Mu et al., 2002).

Although the available antibody against LTBP-1 has been used successfully by others, I was not able to apply it to to embryonic tissue and detect fibrillar LTBP-1. Therefore I could not discern the effect of $FN^{CC>SS}$ on the fibrillar morphology of LTBP-1 in embryonic tissue. Given that the $FN^{CC>SS}$ fibrillar matrix in embryonic tissue is characterised by short fibrils (fig. 8.16) it is plausible that LTBP-1 fibrils are equally distorted in length and complexity *in vivo*. An inabilty to store latent TGF-β deposition is accompanied by abberant levels of active TGF-β, and in various cases, the failure to deposit latent TGF-β in tissue results in elevated levels of TGF-β signalling (Neptune et al., 2003; Kantola et al., 2008). However, as already discussed, I found no evidence for elevated TGF-β signalling associated with the $FN^{CC>SS/CC>SS}$ phenotype.

TGF-β is not alone in regulating blood vessel development and is also not unique in its requirement for ECM to regulate its bioavailability. VEGF is a potent pro-angiogenic factor, and the affinity of secreted VEGF for both heparan sulfates and FN is fundamental to the ability of the ECM

to establish gradients of VEGF in the extracellular environment. Having found that monomerised $FN^{CC>SS}$ distorts the fibrillar morphology of the resulting matrix and that the $FN^{CC>SS/CC>SS}$ phenotype is dominated by vascular remodelling defects, I proposed the possibility that preventing FN dimerisation could distort the binding of VEGF to FN and that the $FN^{CC>SS/CC>SS}$ phenotype could reflect a VEGF hypomorphism.

To test this hypothesis, I sought to compare the level of VEGF receptor signalling in WT and $FN^{CC>SS/CC>SS}$ embryonic and extraembryonic tissue. VEGFR2 phosphorylation is an immediate effect of VEGF binding to the extracellular domain and thus reflects the bioavailability of VEGF and the represents the initiation of biochemical signalling events downstream of VEGFR2 receptor. Through immunoprecipitation of VEGFR2 from either embryo or yolk sac lysates, I was able to biochemically analyse the extent of VEGFR2 phosphorylation using a monoclonal antibody against phospho-tyrosines (4G10) (fig. 8.36). This analysis revealed no difference in the degree of VEGFR2 phosphorylation between WT and $FN^{CC>SS/CC>SS}$ embryonic or yolk sac tissue. Therefore, the $FN^{CC>SS/CC>SS}$ phenotype cannot be explained by reduced levels of VEGF and hence the morphological abnormalities of a $FN^{CC>SS}$ fibrillar matrix are not sufficient to ablate or distort the ability of the ECM to regulate the bioavailability of VEGF in the developing embryo.

9.5 Non-cardiovascular defects in $FN^{CC>SS/CC>SS}$ embryos

$FN^{CC>SS/CC>SS}$ embryos die at mid-gestation because this is a stage of development where cardiovascular function is crucial to the survival of the embryo. Midgestation represents a stage of development organogenesis, and by E9.5 a multitude of developmental processes are underway to shape the organs of the developing embryo. Because $FN^{CC>SS/CC>SS}$ embryos die at mid-gestation, we can barely discover the impact of monomerising FN on the formation of other organs. Serendipitously, the immunofluorescence imaging of α-SMA in whole mount embryos gave a glimpse of the developing myotome in $FN^{CC>SS/CC>SS}$ embryos, and thus an opportunity to examine the requirement for FN dimerisation in very early stages of myogenesis.

Soon after the somites form through segmentation, they undergo a compartmentalisation that gives rise to the sclerotome (origin of vertebrae, ribs, and tendons of back muscles) and the epithelial dermomyotome (origin of skeletal muscle, dermal, some endothelium, smooth muscle, and brown fat precursors). Muscle progenitors that differentiate within the myotomal compartment of the somites enter the myogenic program *in situ* and form the segmented muscle masses, called the myotomes. In amniotes the myotome does not become innervated (Deries et al., 2008) and is only a transient structure that is transformed into the deep back muscles epaxially and into the intercostal and body wall muscles hypaxially (Deries et al., 2010).

In the mouse, the formation of the myotome starts in the anterior somites at E8.5 (Venters et al., 1999). At E9.5, myoblasts will have differentiated from myoblasts into myosin-positive myocytes, which elongate in the anterior-posterior axis of the embryonic body. By E10.5, myotomal myocytes are more numerous and span the entire width of the somite. After multiple stages of expansion in the dorso-medial to ventro-lateral direction, the myotome undergoes a developmentally regulated

translocation and splitting (Deries et al., 2010), which culminates in a new organisation into muscle masses by E12.5.

The ECM plays an important role in several steps of myogenesis. FN is an abundant component of the ECM around the dermomyotome and myotome as well as within the intersegmental (intersomitic) boundaries at all stages of myotome development (Deries et al., 2012). Lack of FN in mouse embryos leads to defects in somitogenesis and neural tube morphogenesis (George et al., 1993; Georges-Labouesse et al., 1996), and studies in the chick embryo have shown that FN is not only needed for somitogenesis, but also, once formed, the maintenance of the epithelial and segmented organisation of somites (Martins et al., 2009). In zebrafish, the development of the myotome from within the somites is also dependent on FN (Snow et al., 2008). Tenascin, another ECM protein found associated with somites, is deposited into a matrix within the intersegmental boundary and is thus much more restricted in its distribution than FN (Crossin et al., 1986; Deries et al., 2012). In a recent study that applied confocal imaging of whole-mount immunofluorescence-stained embryos followed by three dimensional image reconstruction, myotomal myocytes elongating across the full length of the segment were found to insert their tips into the FN- and tenascin-rich matrices at the intersegmental boundaries. With this FN and tenascin were proposed to serve a tendon-like function for myotomal myocytes (Deries et al., 2012). Elongated myocytes have also been found to express integrins on their tips, providing a plausible mechanism of achieving attachment to the intersegmental boundary; while the expression of integrins $\alpha4\beta1$, $\alpha V\beta3$ and $\alpha5\beta1$ is thought to enable the attachment of myotomal myocytes to FN matrix at the intersegmental border, the expression of $\alpha V\beta3$ would allow myocytes to also attach to tenascin (Bajanca et al., 2004; Deries et al., 2012). In addition to lining the intersegmental boundary, bundles of FN and tenascin fibrils have been described to run along the elongated myocytes, which puts FN and tenascin in a good position to promote the alignment of myocytes among each other (Deries et al., 2012). Despite this apparent central role of tenascin in muscle attachment, mice develop normally without tenascin (Saga et al., 1992), and hence FN must have the predominant role in providing a tendon-like substrate for myocyte attachment to intersegmental boundaries at this stage of myogenesis.

Although myosin heavy chain is the traditional cell marker of myotomal myocytes (Bajanca et al., 2004; Deries et al., 2012), I have identified this population of differentiated cells within E9.5 embryos by IF staining of α-SMA (fig. 8.12). In WT embryos, myotomal myocytes were readily identified as clusters of numerous, elongated and fully aligned α-SMA-positive cells that were seemingly attached to the intersegmental borders. In contrast, only very few α-SMA-positive cells were identified in the anterior-most somites of $FN^{CC>SS/CC>SS}$ embryos, and these were misaligned and misoriented. Hence despite somitogenesis proceeding to form around 20-somite pair stage, the subsequent compartmentalisation within the somite, which occurs as soon as a somite has formed, is severely distorted in the presence of monomerised $FN^{CC>SS}$. At present, this myotomal myocytes defect is perhaps the clearest example of how cells fail to attach to and manoeuver along a substrate of monomerised $FN^{CC>SS}$. However, it is not possible to conclude whether the requirement for dimeric FN lies in promoting myocyte differentiation from dermomyotomal myoblasts or whether FN

dimerisation ensures that the resulting FN matrix lining the intersegmental boundaries possesses the appropriate mechanical properties such that upon attachment, elongating myotomal myocytes will remain firmly attached. In a manner analogous to *Drosophila* muscle attachment defects (Dr. Frank Schnorrer, unpublished), myotomal myocytes that fail to attach to a substrate would round up and deteriorate.

9.6 Conclusion and outlook

In conclusion, the dimerisation motif of FN facilitates its assembly into a structurally complex and mechanically robust fibrillar matrix. However, monomerised $FN^{CC>SS}$ can be assembled into a matrix network *in vivo* and *in vitro*, in contrast to expectations from widely accepted models of FN fibrillogenesis. Hence, FN dimerisation is not required to assist integrin-mediated extension of the FN molecule to expose the cryptic FN-binding sites. Rather, FN dimerisation is required to promote the self-assembly of unfolded FN molecules into long and stable fibrils. $FN^{CC>SS}$ matrices generated *in vitro* show a drastic shortening of fibril length, and although less obvious, this shortening is also a feature of $FN^{CC>SS}$ matrices *in vivo* within the ECM of $FN^{CC>SS/CC>SS}$ embryonic tissue. The structural abnormality of the $FN^{CC>SS}$ matrix is associated with a significant reduction in the elastic modulus of the ECM that forms around $FN^{CC>SS}$.

To the developing $FN^{CC>SS/CC>SS}$ embryo, the consequences of preventing FN dimerisation are severe, and hence the requirement for the FN dimerisation motif is important. $FN^{CC>SS/CC>SS}$ embryos fail to develop beyond E10.5-11.5 for reasons that are most likely related to an inadequacy of the cardiovascular system to support the growing embryo at a stage where it becomes dependent on blood-based exchange of nutrients and gases with the mother, which it requires a circulatory system. Not only does the development of the heart tube in $FN^{CC>SS/CC>SS}$ embryos stall at the looping morphogenesis stage. Also the embryonic and extraembryonic blood vascular systems of $FN^{CC>SS/CC>SS}$ embryos show a lack of vascular vessel wall integrity as well as clear signs of endothelial remodelling and sprouting defects. A strong co-dependence between the cardiac and vascular system during development makes it difficult to discern which tissue is mostly affected by monomerised $FN^{CC>SS}$, and why. An interesting speculation is that the cardiovascular system is the first tissue to develop that demands robust physical support from the ECM components of the basemene membrane. That is, the cardiovascular system is the first to fail in the absence of FN dimers because it is the first to challenge the compromised mechanical properties of the ECM containing monomerised $FN^{CC>SS}$.

While defects in the cardiovascular systems are responsible for embryonic lethality, the cardiovascular system is not the only tissue that is affected by the monomerisation of $FN^{CC>SS}$. Such additional defects are far less obvious because they either (1) are not severe enough to cause embryonic lethality or (2) occur in tissues that have not fully developed by the time the embryo becomes dependent on the cardiovascular system. In the latter case, $FN^{CC>SS}$ could cause problems later during embryonic or postnatal development. One example of the latter situation was identified in the abberant numbers and orientation of the myotomal myocyte developing within the somites of $FN^{CC>SS/CC>SS}$ embryos. These myocytes use FN deposited along the borders of the somite for

attachment substrate, and it is particularly interesting that this failure to attach, align and elongate in the anterior-posterior axis of the embryonic body could reflect an inability of the monomerised $FN^{CC>SS}$ matrix to support myotomal myocyte attachment.

Despite the multiple indications that ECM containing $FN^{CC>SS}$ matrix fails to meet the mechanical requirements of the developing tissues, integrin outside-in signalling assays and migration assays led to the conclusion that the small, but significant changes in the physical properties of the ECM caused by monomerisation of FN do not affect integrin function. In agreement with the role of FN in providing a template for the assembly of other ECM components, the assembly of LTBP-1 into a fibrillar matrix is indeed affected by the structural features of FN and is heavily distorted in the presence of the monomerised $FN^{CC>SS}$ matrix. Suprisingly, the effect of $FN^{CC>SS}$ on the morphology of the LTBP-1 fibrillar matrix does not affect the abilty of the ECM to store latent TGF-β. Neither do the mechanical properties of the ECM containing $FN^{CC>SS}$ affect the abilty of αVβ6 integrins to mechanically release TGF-β from latency. Despite the phenotypic similarity between $FN^{CC>SS/CC>SS}$ embryos and mice with defects in the TGF-β signalling pathway, $FN^{CC>SS/CC>SS}$ embryos do not contain overtly abnormal levels or nuclear distribution of phosphorylated SMAD. Although a reduction in the transcript level of the specific phosphorylated SMAD1/5/8 gene target, Id1, was reduced in $FN^{CC>SS/CC>SS}$ embryos, this reduction was very mild and probably does not explain the severe phenotype. Similarly, assays of VEGFR2 signalling in embryonic tissue led to the conclusion that the dimerisation of FN does not affect the abilty of the ECM to regulate VEGF-A bioavailability.

The $FN^{CC>SS/CC>SS}$ mouse is a model that reveals the role of FN dimerisation in building a robust ECM that can support tissue homeostasis and development. To come closer to understanding the requirement for FN dimerisation in vascular development would require futher studies in a well-defined angiogenesis model system. For example, the mouse retina, where astrocyte-derived FN induces both integrin-dependent and –independent functions in endothelial cells and pericytes as they build the retinal vasculature, could offer a system for studying the requirement for FN dimerisation in angiogenesis. In an experiment similar to that described by Stenzel et al. (2011) the $FN^{CC>SS/fl}$ heterozygouse mice would be crossed with a mouse strain expressing Cre under the control of a astrocyte-specific promoter, such as GFAP-Cre, to generate a mouse model in which all GFAP-expressing astrocytes no longer express WT FN, but express monomerised $FN^{CC>SS}$. Analysis of the retinal vasculature, e.g. the vessel migratory length and branching as well as alignment and stability of tip cells along the $FN^{CC>SS}$ network, would provide an alternative approach to understanding the role of FN fibrillar structure imposed by the FN dimerisation motif in angiogenesis.

Although pFN is dispensable for hemostasis, FN, along with fibrin, is an integral part of a thrombus to stop the bleeding from a damaged blood vessel. An alternative approach to examining the physical stability of the $FN^{CC>SS}$ matrix and its effect on thrombus stability could involve experiments testing bleeding times of $FN^{CC>SS/fl}$ Mx1Cre induced by pI:C. A compromise in thrombus stability caused by $FN^{CC>SS}$ matrix would cause longer bleeding times.

The requirement for FN dimerisation in the regulation of VEGF-A was only addressed briefly in this project. Although the accumulated VEGFR2 signalling appeared unaffected by the monomerised

$FN^{CC>SS}$, the effect on VEGF-A gradients was not addressed. The embryonic hindbrain is a tissue in which developing blood vessels migrate, expand and anastamose at the midline in effect of a VEGF-A gradient that reaches its peak at the midline. Histological analysis of VEGF gradients in the hindbrain of $FN^{CC>SS/CC>SS}$ embryos would show if monomerisation of $FN^{CC>SS}$ alters any aspect of the VEGF-A gradient, such as its steepness.

10 REFERENCES

Abe, M., Harpel, J. G., Metz, C. N., Nunes, I., Loskutoff, D. J. and Rifkin, D. B. (1994). An assay for transforming growth factor-beta using cells transfected with a plasminogen activator inhibitor-1 promoter-luciferase construct. *Anal. Biochem.* **216**, 276–284.

Abraham, S., Kogata, N., Fassler, R. and Adams, R. H. (2008). Integrin 1 Subunit Controls Mural Cell Adhesion, Spreading, and Blood Vessel Wall Stability. *Circ. Res.* **102**, 562–570.

Abramsson, A., Lindblom, P. and Betsholtz, C. (2003). Endothelial and nonendothelial sources of PDGF-B regulate pericyte recruitment and influence vascular pattern formation in tumors. *J. Clin. Invest.* **112**, 1142–1151.

Adams, J. C. (2001). Thrombospondins: multifunctional regulators of cell interactions. *Annu. Rev. Cell Dev. Biol.* **17**, 25–51.

Aguirre, K. M., McCormick, R. J. and Schwarzbauer, J. E. (1994). Fibronectin self-association is mediated by complementary sites within the amino-terminal one-third of the molecule. *J. Biol. Chem.* **269**, 27863–27868.

Akhurst, R. J., Lehnert, S. A., Faissner, A. and Duffie, E. (1990). TGF beta in murine morphogenetic processes: the early embryo and cardiogenesis. *Dev. Camb. Engl.* **108**, 645–656.

Akiyama, S. K., Yamada, S. S., Chen, W. T. and Yamada, K. M. (1989). Analysis of fibronectin receptor function with monoclonal antibodies: roles in cell adhesion, migration, matrix assembly, and cytoskeletal organization. *J. Cell Biol.* **109**, 863–875.

Alexandrova, A. Y., Arnold, K., Schaub, S., Vasiliev, J. M., Meister, J.-J., Bershadsky, A. D. and Verkhovsky, A. B. (2008). Comparative dynamics of retrograde actin flow and focal adhesions: formation of nascent adhesions triggers transition from fast to slow flow. *PloS One* **3**, e3234.

Ali, I. U. and Hynes, R. O. (1977). Effects of cytochalasin B and colchicine on attachment of a major surface protein of fibroblasts. *Biochim. Biophys. Acta* **471**, 16–24.

Allio, A. E. and McKeown-Longo, P. J. (1988). Extracellular matrix assembly of cell-derived and plasma-derived fibronectins by substrate-attached fibroblasts. *J. Cell. Physiol.* **135**, 459–466.

Altroff, H. (2004). Interdomain Tilt Angle Determines Integrin-dependent Function of the Ninth and Tenth FIII Domains of Human Fibronectin. *J. Biol. Chem.* **279**, 55995–56003.

Aluwihare, P., Mu, Z., Zhao, Z., Yu, D., Weinreb, P. H., Horan, G. S., Violette, S. M. and Munger, J. S. (2009). Mice that lack activity of alphavbeta6- and alphavbeta8-integrins reproduce the abnormalities of Tgfb1- and Tgfb3-null mice. *J. Cell Sci.* **122**, 227–232.

Amano, M., Ito, M., Kimura, K., Fukata, Y., Chihara, K., Nakano, T., Matsuura, Y. and Kaibuchi, K. (1996). Phosphorylation and activation of myosin by Rho-associated kinase (Rho-kinase). *J. Biol. Chem.* **271**, 20246–20249.

Annes, J. P., Rifkin, D. B. and Munger, J. S. (2002). The integrin alphaVbeta6 binds and activates latent TGFbeta3. *FEBS Lett.* **511**, 65–68.

Annes, J. P., Chen, Y., Munger, J. S. and Rifkin, D. B. (2004). Integrin αVβ6-mediated activation of latent TGF-β requires the latent TGF-β binding protein-1. *J. Cell Biol.* **165**, 723–734.

Antonelli-Orlidge, A., Saunders, K. B., Smith, S. R. and D'Amore, P. A. (1989). An activated form of transforming growth factor beta is produced by cocultures of endothelial cells and pericytes. *Proc. Natl. Acad. Sci. U. S. A.* **86**, 4544–4548.

Aota, S., Nomizu, M. and Yamada, K. M. (1994). The short amino acid sequence Pro-His-Ser-Arg-Asn in human fibronectin enhances cell-adhesive function. *J. Biol. Chem.* **269**, 24756–24761.

Aoudjit, F. and Vuori, K. (2001). Matrix attachment regulates Fas-induced apoptosis in endothelial cells: a role for c-flip and implications for anoikis. *J. Cell Biol.* **152**, 633–643.

Araya, J., Cambier, S., Morris, A., Finkbeiner, W. and Nishimura, S. L. (2006). Integrin-mediated transforming growth factor-beta activation regulates homeostasis of the pulmonary epithelial-mesenchymal trophic unit. *Am. J. Pathol.* **169**, 405–415.

Argraves, W. S. and Drake, C. J. (2005). Genes critical to vasculogenesis as defined by systematic analysis of vascular defects in knockout mice. *Anat. Rec. A. Discov. Mol. Cell. Evol. Biol.* **286**, 875–884.

Arroyo, A. G., Yang, J. T., Rayburn, H. and Hynes, R. O. (1999). Alpha4 integrins regulate the proliferation/differentiation balance of multilineage hematopoietic progenitors in vivo. *Immunity* **11**, 555–566.

Arthur, H. M., Ure, J., Smith, A. J., Renforth, G., Wilson, D. I., Torsney, E., Charlton, R., Parums, D. V., Jowett, T., Marchuk, D. A., et al. (2000). Endoglin, an ancillary TGFbeta receptor, is required for extraembryonic angiogenesis and plays a key role in heart development. *Dev. Biol.* **217**, 42–53.

Astrof, S., Crowley, D., George, E. L., Fukuda, T., Sekiguchi, K., Hanahan, D. and Hynes, R. O. (2004). Direct test of potential roles of EIIIA and EIIIB alternatively spliced segments of fibronectin in physiological and tumor angiogenesis. *Mol. Cell. Biol.* **24**, 8662–8670.

Astrof, S., Crowley, D. and Hynes, R. O. (2007). Multiple cardiovascular defects caused by the absence of alternatively spliced segments of fibronectin. *Dev. Biol.* **311**, 11–24.

Aszódi, A., Legate, K. R., Nakchbandi, I. and Fässler, R. (2006). What mouse mutants teach us about extracellular matrix function. *Annu. Rev. Cell Dev. Biol.* **22**, 591–621.

Atkin, K. E., Brentnall, A. S., Harris, G., Bingham, R. J., Erat, M. C., Millard, C. J., Schwarz-Linek, U., Staunton, D., Vakonakis, I., Campbell, I. D., et al. (2010). The streptococcal binding site in the gelatin-binding domain of fibronectin is consistent with a non-linear arrangement of modules. *J. Biol. Chem.* **285**, 36977–36983.

Avraamides, C. J., Garmy-Susini, B. and Varner, J. A. (2008). Integrins in angiogenesis and lymphangiogenesis. *Nat. Rev. Cancer* **8**, 604–617.

Babaev, V. R., Porro, F., Linton, M. F., Fazio, S., Baralle, F. E. and Muro, A. F. (2008). Absence of regulated splicing of fibronectin EDA exon reduces atherosclerosis in mice. *Atherosclerosis* **197**, 534–540.

Bader, B. L., Rayburn, H., Crowley, D. and Hynes, R. O. (1998). Extensive vasculogenesis, angiogenesis, and organogenesis precede lethality in mice lacking all alpha v integrins. *Cell* **95**, 507–519.

Bajanca, F., Luz, M., Duxson, M. J. and Thorsteinsdóttir, S. (2004). Integrins in the mouse myotome: developmental changes and differences between the epaxial and hypaxial lineage. *Dev. Dyn. Off. Publ. Am. Assoc. Anat.* **231**, 402–415.

Baneyx, G., Baugh, L. and Vogel, V. (2002). Fibronectin extension and unfolding within cell matrix fibrils controlled by cytoskeletal tension. *Proc. Natl. Acad. Sci. U. S. A.* **99**, 5139–5143.

Barcellos-Hoff, M. H. and Dix, T. A. (1996). Redox-mediated activation of latent transforming growth factor-beta 1. *Mol. Endocrinol. Baltim. Md* **10**, 1077–1083.

Barcellos-Hoff, M. H., Derynck, R., Tsang, M. L. and Weatherbee, J. A. (1994). Transforming growth factor-beta activation in irradiated murine mammary gland. *J. Clin. Invest.* **93**, 892–899.

Barczyk, M., Carracedo, S. and Gullberg, D. (2009). Integrins. *Cell Tissue Res.* **339**, 269–280.

Barkalow, F. J. and Schwarzbauer, J. E. (1991). Localization of the major heparin-binding site in fibronectin. *J. Biol. Chem.* **266**, 7812–7818.

Barkalow, F. J. and Schwarzbauer, J. E. (1994). Interactions between fibronectin and chondroitin sulfate are modulated by molecular context. *J. Biol. Chem.* **269**, 3957–3962.

Baron, M., Main, A. L., Driscoll, P. C., Mardon, H. J., Boyd, J. and Campbell, I. D. (1992). 1H NMR assignment and secondary structure of the cell adhesion type III module of fibronectin. *Biochemistry (Mosc.)* **31**, 2068–2073.

Barry, E. L. and Mosher, D. F. (1989). Factor XIIIa-mediated cross-linking of fibronectin in fibroblast cell layers. Cross-linking of cellular and plasma fibronectin and of amino-terminal fibronectin fragments. *J. Biol. Chem.* **264**, 4179–4185.

Bartram, U., Molin, D. G., Wisse, L. J., Mohamad, A., Sanford, L. P., Doetschman, T., Speer, C. P., Poelmann, R. E. and Gittenberger-de Groot, A. C. (2001). Double-outlet right ventricle and overriding tricuspid valve reflect

disturbances of looping, myocardialization, endocardial cushion differentiation, and apoptosis in TGF-beta(2)-knockout mice. *Circulation* **103**, 2745–2752.

Bayless, K. J. and Davis, G. E. (2002). The Cdc42 and Rac1 GTPases are required for capillary lumen formation in three-dimensional extracellular matrices. *J. Cell Sci.* **115**, 1123–1136.

Bazigou, E., Xie, S., Chen, C., Weston, A., Miura, N., Sorokin, L., Adams, R., Muro, A. F., Sheppard, D. and Makinen, T. (2009). Integrin-alpha9 is required for fibronectin matrix assembly during lymphatic valve morphogenesis. *Dev. Cell* **17**, 175–186.

Benezra, R., Davis, R. L., Lockshon, D., Turner, D. L. and Weintraub, H. (1990). The protein Id: a negative regulator of helix-loop-helix DNA binding proteins. *Cell* **61**, 49–59.

Bengtsson, T., Aszodi, A., Nicolae, C., Hunziker, E. B., Lundgren-Akerlund, E. and Fässler, R. (2005). Loss of alpha10beta1 integrin expression leads to moderate dysfunction of growth plate chondrocytes. *J. Cell Sci.* **118**, 929–936.

Bergwerff, M., Verberne, M. E., DeRuiter, M. C., Poelmann, R. E. and Gittenberger-de Groot, A. C. (1998). Neural crest cell contribution to the developing circulatory system: implications for vascular morphology? *Circ. Res.* **82**, 221–231.

Bledzka, K., Liu, J., Xu, Z., Perera, H. D., Yadav, S. P., Bialkowska, K., Qin, J., Ma, Y.-Q. and Plow, E. F. (2012). Spatial coordination of kindlin-2 with talin head domain in interaction with integrin β cytoplasmic tails. *J. Biol. Chem.* **287**, 24585–24594.

Blum, Y., Belting, H.-G., Ellertsdottir, E., Herwig, L., Lüders, F. and Affolter, M. (2008). Complex cell rearrangements during intersegmental vessel sprouting and vessel fusion in the zebrafish embryo. *Dev. Biol.* **316**, 312–322.

Bork, P. and Doolittle, R. F. (1992). Proposed acquisition of an animal protein domain by bacteria. *Proc. Natl. Acad. Sci. U. S. A.* **89**, 8990–8994.

Boucaut, J. C. and Darribere, T. (1983). Presence of fibronectin during early embryogenesis in amphibian Pleurodeles waltlii. *Cell Differ.* **12**, 77–83.

Boucaut, J. C., Darribère, T., Boulekbache, H. and Thiery, J. P. (1984a). Prevention of gastrulation but not neurulation by antibodies to fibronectin in amphibian embryos. *Nature* **307**, 364–367.

Boucaut, J. C., Darribère, T., Poole, T. J., Aoyama, H., Yamada, K. M. and Thiery, J. P. (1984b). Biologically active synthetic peptides as probes of embryonic development: a competitive peptide inhibitor of fibronectin function inhibits gastrulation in amphibian embryos and neural crest cell migration in avian embryos. *J. Cell Biol.* **99**, 1822–1830.

Boudreau, N. J. and Varner, J. A. (2004). The homeobox transcription factor Hox D3 promotes integrin alpha5beta1 expression and function during angiogenesis. *J. Biol. Chem.* **279**, 4862–4868.

Bouvard, D., Vignoud, L., Dupé-Manet, S., Abed, N., Fournier, H.-N., Vincent-Monegat, C., Retta, S. F., Fassler, R. and Block, M. R. (2003). Disruption of focal adhesions by integrin cytoplasmic domain-associated protein-1 alpha. *J. Biol. Chem.* **278**, 6567–6574.

Bouvard, D., Pouwels, J., De Franceschi, N. and Ivaska, J. (2013). Integrin inactivators: balancing cellular functions in vitro and in vivo. *Nat. Rev. Mol. Cell Biol.* **14**, 432–444.

Bowditch, R. D., Hariharan, M., Tominna, E. F., Smith, J. W., Yamada, K. M., Getzoff, E. D. and Ginsberg, M. H. (1994). Identification of a novel integrin binding site in fibronectin. Differential utilization by beta 3 integrins. *J. Biol. Chem.* **269**, 10856–10863.

Braren, R., Hu, H., Kim, Y. H., Beggs, H. E., Reichardt, L. F. and Wang, R. (2006). Endothelial FAK is essential for vascular network stability, cell survival, and lamellipodial formation. *J. Cell Biol.* **172**, 151–162.

Bretscher, A., Edwards, K. and Fehon, R. G. (2002). ERM proteins and merlin: integrators at the cell cortex. *Nat. Rev. Mol. Cell Biol.* **3**, 586–599.

Brooks, P. C., Clark, R. A. and Cheresh, D. A. (1994a). Requirement of vascular integrin alpha v beta 3 for angiogenesis. *Science* **264**, 569–571.

Brooks, P. C., Montgomery, A. M., Rosenfeld, M., Reisfeld, R. A., Hu, T., Klier, G. and Cheresh, D. A. (1994b). Integrin alpha v beta 3 antagonists promote tumor regression by inducing apoptosis of angiogenic blood vessels. *Cell* **79**, 1157–1164.

Brooks, P. C., Silletti, S., von Schalscha, T. L., Friedlander, M. and Cheresh, D. A. (1998). Disruption of angiogenesis by PEX, a noncatalytic metalloproteinase fragment with integrin binding activity. *Cell* **92**, 391–400.

Brown, A. J. and Sanders, E. J. (1991). Interactions between mesoderm cells and the extracellular matrix following gastrulation in the chick embryo. *J. Cell Sci.* **99 (Pt 2)**, 431–441.

Brown, P. D., Wakefield, L. M., Levinson, A. D. and Sporn, M. B. (1990). Physicochemical activation of recombinant latent transforming growth factor-beta's 1, 2, and 3. *Growth Factors Chur Switz.* **3**, 35–43.

Brown, C. M., Hebert, B., Kolin, D. L., Zareno, J., Whitmore, L., Horwitz, A. R. and Wiseman, P. W. (2006). Probing the integrin-actin linkage using high-resolution protein velocity mapping. *J. Cell Sci.* **119**, 5204–5214.

Brunet, A., Bonni, A., Zigmond, M. J., Lin, M. Z., Juo, P., Hu, L. S., Anderson, M. J., Arden, K. C., Blenis, J. and Greenberg, M. E. (1999). Akt promotes cell survival by phosphorylating and inhibiting a Forkhead transcription factor. *Cell* **96**, 857–868.

Bultmann, H., Santas, A. J. and Peters, D. M. (1998). Fibronectin fibrillogenesis involves the heparin II binding domain of fibronectin. *J. Biol. Chem.* **273**, 2601–2609.

Burri, P. H., Hlushchuk, R. and Djonov, V. (2004). Intussusceptive angiogenesis: Its emergence, its characteristics, and its significance. *Dev. Dyn.* **231**, 474–488.

Burton-Wurster, N., Gendelman, R., Chen, H., Gu, D. N., Tetreault, J. W., Lust, G., Schwarzbauer, J. E. and MacLeod, J. N. (1999). The cartilage-specific (V+C)- fibronectin isoform exists primarily in homodimeric and monomeric configurations. *Biochem. J.* **341 (Pt 3)**, 555–561.

Buscemi, L., Ramonet, D., Klingberg, F., Formey, A., Smith-Clerc, J., Meister, J.-J. and Hinz, B. (2011). The single-molecule mechanics of the latent TGF-β1 complex. *Curr. Biol. CB* **21**, 2046–2054.

Byfield, F. J., Reen, R. K., Shentu, T.-P., Levitan, I. and Gooch, K. J. (2009). Endothelial actin and cell stiffness is modulated by substrate stiffness in 2D and 3D. *J. Biomech.* **42**, 1114–1119.

Byzova, T. V., Goldman, C. K., Pampori, N., Thomas, K. A., Bett, A., Shattil, S. J. and Plow, E. F. (2000). A mechanism for modulation of cellular responses to VEGF: activation of the integrins. *Mol. Cell* **6**, 851–860.

Calalb, M. B., Polte, T. R. and Hanks, S. K. (1995). Tyrosine phosphorylation of focal adhesion kinase at sites in the catalytic domain regulates kinase activity: a role for Src family kinases. *Mol. Cell. Biol.* **15**, 954–963.

Calalb, M. B., Zhang, X., Polte, T. R. and Hanks, S. K. (1996). Focal adhesion kinase tyrosine-861 is a major site of phosphorylation by Src. *Biochem. Biophys. Res. Commun.* **228**, 662–668.

Calderwood, D. A., Yan, B., de Pereda, J. M., Alvarez, B. G., Fujioka, Y., Liddington, R. C. and Ginsberg, M. H. (2002). The phosphotyrosine binding-like domain of talin activates integrins. *J. Biol. Chem.* **277**, 21749–21758.

Calderwood, D. A., Fujioka, Y., de Pereda, J. M., García-Alvarez, B., Nakamoto, T., Margolis, B., McGlade, C. J., Liddington, R. C. and Ginsberg, M. H. (2003). Integrin beta cytoplasmic domain interactions with phosphotyrosine-binding domains: a structural prototype for diversity in integrin signaling. *Proc. Natl. Acad. Sci. U. S. A.* **100**, 2272–2277.

Califano, J. P. and Reinhart-King, C. A. (2010). Substrate Stiffness and Cell Area Predict Cellular Traction Stresses in Single Cells and Cells in Contact. *Cell. Mol. Bioeng.* **3**, 68–75.

Cambier, S., Gline, S., Mu, D., Collins, R., Araya, J., Dolganov, G., Einheber, S., Boudreau, N. and Nishimura, S. L. (2005). Integrin alpha(v)beta8-mediated activation of transforming growth factor-beta by perivascular astrocytes: an angiogenic control switch. *Am. J. Pathol.* **166**, 1883–1894.

Carlson, T. R., Hu, H., Braren, R., Kim, Y. H. and Wang, R. A. (2008). Cell-autonomous requirement for beta1 integrin in endothelial cell adhesion, migration and survival during angiogenesis in mice. *Dev. Camb. Engl.* **135**, 2193–2202.

Carman, C. V. and Springer, T. A. (2003). Integrin avidity regulation: are changes in affinity and conformation underemphasized? *Curr. Opin. Cell Biol.* **15**, 547–556.

Carmeliet, P., Ferreira, V., Breier, G., Pollefeyt, S., Kieckens, L., Gertsenstein, M., Fahrig, M., Vandenhoeck, A., Harpal, K., Eberhardt, C., et al. (1996). Abnormal blood vessel development and lethality in embryos lacking a single VEGF allele. *Nature* **380**, 435–439.

Carvalho, R. L. C., Jonker, L., Goumans, M.-J., Larsson, J., Bouwman, P., Karlsson, S., Dijke, P. T., Arthur, H. M. and Mummery, C. L. (2004). Defective paracrine signalling by TGFbeta in yolk sac vasculature of endoglin mutant mice: a paradigm for hereditary haemorrhagic telangiectasia. *Dev. Camb. Engl.* **131**, 6237–6247.

Carvalho, R. L. C., Itoh, F., Goumans, M.-J., Lebrin, F., Kato, M., Takahashi, S., Ema, M., Itoh, S., Rooijen, M. van, Bertolino, P., et al. (2007). Compensatory signalling induced in the yolk sac vasculature by deletion of TGFβ receptors in mice. *J. Cell Sci.* **120**, 4269–4277.

Cary, L. A., Han, D. C., Polte, T. R., Hanks, S. K. and Guan, J. L. (1998). Identification of p130Cas as a mediator of focal adhesion kinase-promoted cell migration. *J. Cell Biol.* **140**, 211–221.

Castellani, P., Borsi, L., Carnemolla, B., Birò, A., Dorcaratto, A., Viale, G. L., Neri, D. and Zardi, L. (2002). Differentiation between high- and low-grade astrocytoma using a human recombinant antibody to the extra domain-B of fibronectin. *Am. J. Pathol.* **161**, 1695–1700.

Chada, D., Mather, T. and Nollert, M. U. (2006). The synergy site of fibronectin is required for strong interaction with the platelet integrin alphaIIbbeta3. *Ann. Biomed. Eng.* **34**, 1542–1552.

Chappell, J. C., Taylor, S. M., Ferrara, N. and Bautch, V. L. (2009). Local guidance of emerging vessel sprouts requires soluble Flt-1. *Dev. Cell* **17**, 377–386.

Chauhan, A. K., Iaconcig, A., Baralle, F. E. and Muro, A. F. (2004). Alternative splicing of fibronectin: a mouse model demonstrates the identity of in vitro and in vivo systems and the processing autonomy of regulated exons in adult mice. *Gene* **324**, 55–63.

Chauhan, A. K., Kisucka, J., Cozzi, M. R., Walsh, M. T., Moretti, F. A., Battiston, M., Mazzucato, M., De Marco, L., Baralle, F. E., Wagner, D. D., et al. (2008). Prothrombotic effects of fibronectin isoforms containing the EDA domain. *Arterioscler. Thromb. Vasc. Biol.* **28**, 296–301.

Chen, S. and Lechleider, R. J. (2004). Transforming growth factor-beta-induced differentiation of smooth muscle from a neural crest stem cell line. *Circ. Res.* **94**, 1195–1202.

Chen, H. and Mosher, D. F. (1996). Formation of sodium dodecyl sulfate-stable fibronectin multimers. Failure to detect products of thiol-disulfide exchange in cyanogen bromide or limited acid digests of stabilized matrix fibronectin. *J. Biol. Chem.* **271**, 9084–9089.

Chen, H. C., Appeddu, P. A., Isoda, H. and Guan, J. L. (1996). Phosphorylation of tyrosine 397 in focal adhesion kinase is required for binding phosphatidylinositol 3-kinase. *J. Biol. Chem.* **271**, 26329–26334.

Chen, J., Diacovo, T. G., Grenache, D. G., Santoro, S. A. and Zutter, M. M. (2002). The alpha(2) integrin subunit-deficient mouse: a multifaceted phenotype including defects of branching morphogenesis and hemostasis. *Am. J. Pathol.* **161**, 337–344.

Chen, Q., Sivakumar, P., Barley, C., Peters, D. M., Gomes, R. R., Farach-Carson, M. C. and Dallas, S. L. (2007). Potential role for heparan sulfate proteoglycans in regulation of transforming growth factor-beta (TGF-beta) by modulating assembly of latent TGF-beta-binding protein-1. *J. Biol. Chem.* **282**, 26418–26430.

Cheng, Z., Sundberg-Smith, L. J., Mangiante, L. E., Sayers, R. L., Hakim, Z. S., Musunuri, S., Maguire, C. T., Majesky, M. W., Zhou, Z., Mack, C. P., et al. (2011). Focal adhesion kinase regulates smooth muscle cell recruitment to the developing vasculature. *Arterioscler. Thromb. Vasc. Biol.* **31**, 2193–2202.

Cheng, P., Andersen, P., Hassel, D., Kaynak, B. L., Limphong, P., Juergensen, L., Kwon, C. and Srivastava, D. (2013). Fibronectin mediates mesendodermal cell fate decisions. *Development* **140**, 2587–2596.

Cheresh, D. A. and Stupack, D. G. (2002). Integrin-mediated death: An explanation of the integrin-knockout phenotype? *Nat. Med.* **8**, 193–194.

Chernousov, M. A., Metsis, M. L. and Koteliansky, V. E. (1985). Studies of extracellular fibronectin matrix formation with fluoresceinated fibronectin and fibronectin fragments. *FEBS Lett.* **183**, 365–369.

Chernousov, M. A., Faerman, A. I., Frid, M. G., Printseva OYu and Koteliansky, V. E. (1987). Monoclonal antibody to fibronectin which inhibits extracellular matrix assembly. *FEBS Lett.* **217**, 124–128.

Chernousov, M. A., Fogerty, F. J., Koteliansky, V. E. and Mosher, D. F. (1991). Role of the I-9 and III-1 modules of fibronectin in formation of an extracellular fibronectin matrix. *J. Biol. Chem.* **266**, 10851–10858.

Cho, J. and Mosher, D. F. (2006). Role of fibronectin assembly in platelet thrombus formation. *J. Thromb. Haemost. JTH* **4**, 1461–1469.

Choi, M. G. and Hynes, R. O. (1979). Biosynthesis and processing of fibronectin in NIL.8 hamster cells. *J. Biol. Chem.* **254**, 12050–12055.

Choi, C. K., Vicente-Manzanares, M., Zareno, J., Whitmore, L. A., Mogilner, A. and Horwitz, A. R. (2008). Actin and alpha-actinin orchestrate the assembly and maturation of nascent adhesions in a myosin II motor-independent manner. *Nat. Cell Biol.* **10**, 1039–1050.

Choquet, D., Felsenfeld, D. P. and Sheetz, M. P. (1997). Extracellular matrix rigidity causes strengthening of integrin-cytoskeleton linkages. *Cell* **88**, 39–48.

Christoffels, V. M., Habets, P. E., Franco, D., Campione, M., de Jong, F., Lamers, W. H., Bao, Z. Z., Palmer, S., Biben, C., Harvey, R. P., et al. (2000). Chamber formation and morphogenesis in the developing mammalian heart. *Dev. Biol.* **223**, 266–278.

Christopher, R. A., Kowalczyk, A. P. and McKeown-Longo, P. J. (1997). Localization of fibronectin matrix assembly sites on fibroblasts and endothelial cells. *J. Cell Sci.* **110 (Pt 5)**, 569–581.

Chrzanowska-Wodnicka, M. and Burridge, K. (1996). Rho-stimulated contractility drives the formation of stress fibers and focal adhesions. *J. Cell Biol.* **133**, 1403–1415.

Chun, T.-H., Sabeh, F., Ota, I., Murphy, H., McDonagh, K. T., Holmbeck, K., Birkedal-Hansen, H., Allen, E. D. and Weiss, S. J. (2004). MT1-MMP-dependent neovessel formation within the confines of the three-dimensional extracellular matrix. *J. Cell Biol.* **167**, 757–767.

Chung, C. Y. and Erickson, H. P. (1997). Glycosaminoglycans modulate fibronectin matrix assembly and are essential for matrix incorporation of tenascin-C. *J. Cell Sci.* **110 (Pt 12)**, 1413–1419.

Clark, R. A., DellaPelle, P., Manseau, E., Lanigan, J. M., Dvorak, H. F. and Colvin, R. B. (1982). Blood vessel fibronectin increases in conjunction with endothelial cell proliferation and capillary ingrowth during wound healing. *J. Invest. Dermatol.* **79**, 269–276.

Conway, S. J., Kruzynska-Frejtag, A., Kneer, P. L., Machnicki, M. and Koushik, S. V. (2003). What cardiovascular defect does my prenatal mouse mutant have, and why? *Genes. N. Y. N 2000* **35**, 1–21.

Couchman, J. R. (2010). Transmembrane signaling proteoglycans. *Annu. Rev. Cell Dev. Biol.* **26**, 89–114.

Courtoy, P. J. and Boyles, J. (1983). Fibronectin in the microvasculature: localization in the pericyte-endothelial interstitium. *J. Ultrastruct. Res.* **83**, 258–273.

Coxon, A., Rieu, P., Barkalow, F. J., Askari, S., Sharpe, A. H., von Andrian, U. H., Arnaout, M. A. and Mayadas, T. N. (1996). A novel role for the beta 2 integrin CD11b/CD18 in neutrophil apoptosis: a homeostatic mechanism in inflammation. *Immunity* **5**, 653–666.

Crawford, S. E., Stellmach, V., Murphy-Ullrich, J. E., Ribeiro, S. M., Lawler, J., Hynes, R. O., Boivin, G. P. and Bouck, N. (1998). Thrombospondin-1 is a major activator of TGF-beta1 in vivo. *Cell* **93**, 1159–1170.

Critchley, D. R., England, M. A., Wakely, J. and Hynes, R. O. (1979). Distribution of fibronectin in the ectoderm of gastrulating chick embryos. *Nature* **280**, 498–500.

Crossin, K. L., Hoffman, S., Grumet, M., Thiery, J. P. and Edelman, G. M. (1986). Site-restricted expression of cytotactin during development of the chicken embryo. *J. Cell Biol.* **102**, 1917–1930.

Curnis, F., Longhi, R., Crippa, L., Cattaneo, A., Dondossola, E., Bachi, A. and Corti, A. (2006). Spontaneous formation of L-isoaspartate and gain of function in fibronectin. *J. Biol. Chem.* **281**, 36466–36476.

Dallas, S. L., Sivakumar, P., Jones, C. J. P., Chen, Q., Peters, D. M., Mosher, D. F., Humphries, M. J. and Kielty, C. M. (2005). Fibronectin Regulates Latent Transforming Growth Factor-β (TGFβ) by Controlling Matrix Assembly of Latent TGFβ-binding Protein-1. *J. Biol. Chem.* **280**, 18871–18880.

Dallas, S. L., Chen, Q. and Sivakumar, P. (2006). Dynamics of assembly and reorganization of extracellular matrix proteins. *Curr. Top. Dev. Biol.* **75**, 1–24.

Danen, E. H., Aota, S., van Kraats, A. A., Yamada, K. M., Ruiter, D. J. and van Muijen, G. N. (1995). Requirement for the synergy site for cell adhesion to fibronectin depends on the activation state of integrin alpha 5 beta 1. *J. Biol. Chem.* **270**, 21612–21618.

Danen, E. H. J., Sonneveld, P., Brakebusch, C., Fassler, R. and Sonnenberg, A. (2002). The fibronectin-binding integrins alpha5beta1 and alphavbeta3 differentially modulate RhoA-GTP loading, organization of cell matrix adhesions, and fibronectin fibrillogenesis. *J. Cell Biol.* **159**, 1071–1086.

Danussi, C., Del Bel Belluz, L., Pivetta, E., Modica, T. M. E., Muro, A., Wassermann, B., Doliana, R., Sabatelli, P., Colombatti, A. and Spessotto, P. (2013). EMILIN1/ 9 1 Integrin Interaction Is Crucial in Lymphatic Valve Formation and Maintenance. *Mol. Cell. Biol.* **33**, 4381–4394.

Darland, D. C., Massingham, L. J., Smith, S. R., Piek, E., Saint-Geniez, M. and D'Amore, P. A. (2003). Pericyte production of cell-associated VEGF is differentiation-dependent and is associated with endothelial survival. *Dev. Biol.* **264**, 275–288.

Davidson, L. A., Hoffstrom, B. G., Keller, R. and DeSimone, D. W. (2002). Mesendoderm extension and mantle closure in Xenopus laevis gastrulation: combined roles for integrin alpha(5)beta(1), fibronectin, and tissue geometry. *Dev. Biol.* **242**, 109–129.

Davidson, L. A., Marsden, M., Keller, R. and Desimone, D. W. (2006). Integrin alpha5beta1 and fibronectin regulate polarized cell protrusions required for Xenopus convergence and extension. *Curr. Biol. CB* **16**, 833–844.

Davies, P. F. (1995). Flow-mediated endothelial mechanotransduction. *Physiol. Rev.* **75**, 519–560.

Davis, G. E. and Bayless, K. J. (2003). An Integrin and Rho GTPase-Dependent Pinocytic Vacuole Mechanism Controls Capillary Lumen Formation in Collagen and Fibrin Matrices. *Microcirculation* **10**, 27–44.

Davis, G. E. and Camarillo, C. W. (1996). An alpha 2 beta 1 integrin-dependent pinocytic mechanism involving intracellular vacuole formation and coalescence regulates capillary lumen and tube formation in three-dimensional collagen matrix. *Exp. Cell Res.* **224**, 39–51.

Davis, G. E. and Senger, D. R. (2005). Endothelial extracellular matrix: biosynthesis, remodeling, and functions during vascular morphogenesis and neovessel stabilization. *Circ. Res.* **97**, 1093–1107.

Davis, G. E., Koh, W. and Stratman, A. N. (2007). Mechanisms controlling human endothelial lumen formation and tube assembly in three-dimensional extracellular matrices. *Birth Defects Res. Part C Embryo Today Rev.* **81**, 270–285.

De, S., Razorenova, O., McCabe, N. P., O'Toole, T., Qin, J. and Byzova, T. V. (2005). VEGF-integrin interplay controls tumor growth and vascularization. *Proc. Natl. Acad. Sci. U. S. A.* **102**, 7589–7594.

Dejana, E., Languino, L. R., Polentarutti, N., Balconi, G., Ryckewaert, J. J., Larrieu, M. J., Donati, M. B., Mantovani, A. and Marguerie, G. (1985). Interaction between fibrinogen and cultured endothelial cells. Induction of migration and specific binding. *J. Clin. Invest.* **75**, 11–18.

Deries, M., Collins, J. J. P. and Duxson, M. J. (2008). The mammalian myotome: a muscle with no innervation. *Evol. Dev.* **10**, 746–755.

Deries, M., Schweitzer, R. and Duxson, M. J. (2010). Developmental fate of the mammalian myotome. *Dev. Dyn.* **239**, 2898–2910.

Deries, M., Gonçalves, A. B., Vaz, R., Martins, G. G., Rodrigues, G. and Thorsteinsdóttir, S. (2012). Extracellular matrix remodeling accompanies axial muscle development and morphogenesis in the mouse. *Dev. Dyn. Off. Publ. Am. Assoc. Anat.* **241**, 350–364.

DeRuiter, M. C., Poelmann, R. E., VanderPlas-de Vries, I., Mentink, M. M. and Gittenberger-de Groot, A. C. (1992). The development of the myocardium and endocardium in mouse embryos. Fusion of two heart tubes? *Anat. Embryol. (Berl.)* **185**, 461–473.

Desmoulière, A., Geinoz, A., Gabbiani, F. and Gabbiani, G. (1993). Transforming growth factor-beta 1 induces alpha-smooth muscle actin expression in granulation tissue myofibroblasts and in quiescent and growing cultured fibroblasts. *J. Cell Biol.* **122**, 103–111.

Dickson, M. C., Martin, J. S., Cousins, F. M., Kulkarni, A. B., Karlsson, S. and Akhurst, R. J. (1995). Defective haematopoiesis and vasculogenesis in transforming growth factor-beta 1 knock out mice. *Dev. Camb. Engl.* **121**, 1845–1854.

Digman, M. A., Brown, C. M., Horwitz, A. R., Mantulin, W. W. and Gratton, E. (2008). Paxillin dynamics measured during adhesion assembly and disassembly by correlation spectroscopy. *Biophys. J.* **94**, 2819–2831.

Ding, R., Darland, D. C., Parmacek, M. S. and D'Amore, P. A. (2004). Endothelial-mesenchymal interactions in vitro reveal molecular mechanisms of smooth muscle/pericyte differentiation. *Stem Cells Dev.* **13**, 509–520.

DiPersio, C. M., Hodivala-Dilke, K. M., Jaenisch, R., Kreidberg, J. A. and Hynes, R. O. (1997). alpha3beta1 Integrin is required for normal development of the epidermal basement membrane. *J. Cell Biol.* **137**, 729–742.

Discher, D. E., Janmey, P. and Wang, Y.-L. (2005). Tissue cells feel and respond to the stiffness of their substrate. *Science* **310**, 1139–1143.

Dowling, J., Yu, Q. C. and Fuchs, E. (1996). Beta4 integrin is required for hemidesmosome formation, cell adhesion and cell survival. *J. Cell Biol.* **134**, 559–572.

Downs, K. M. (2003). Florence Sabin and the mechanism of blood vessel lumenization during vasculogenesis. *Microcirc. N. Y. N 1994* **10**, 5–25.

Downward, J. (1998). Mechanisms and consequences of activation of protein kinase B/Akt. *Curr. Opin. Cell Biol.* **10**, 262–267.

Drake, C. J., Davis, L. A. and Little, C. D. (1992). Antibodies to beta 1-integrins cause alterations of aortic vasculogenesis, in vivo. *Dev. Dyn. Off. Publ. Am. Assoc. Anat.* **193**, 83–91.

Drake, C. J., Hungerford, J. E. and Little, C. D. (1998). Morphogenesis of the first blood vessels. *Ann. N. Y. Acad. Sci.* **857**, 155–179.

Duband, J. L. and Thiery, J. P. (1982). Distribution of fibronectin in the early phase of avian cephalic neural crest cell migration. *Dev. Biol.* **93**, 308–323.

Dubois, C. M., Laprise, M. H., Blanchette, F., Gentry, L. E. and Leduc, R. (1995). Processing of transforming growth factor beta 1 precursor by human furin convertase. *J. Biol. Chem.* **270**, 10618–10624.

Edin, M. L. and Juliano, R. L. (2005). Raf-1 serine 338 phosphorylation plays a key role in adhesion-dependent activation of extracellular signal-regulated kinase by epidermal growth factor. *Mol. Cell. Biol.* **25**, 4466–4475.

Edmondson, D. G., Lyons, G. E., Martin, J. F. and Olson, E. N. (1994). Mef2 gene expression marks the cardiac and skeletal muscle lineages during mouse embryogenesis. *Dev. Camb. Engl.* **120**, 1251–1263.

Edwards, D. R., Murphy, G., Reynolds, J. J., Whitham, S. E., Docherty, A. J., Angel, P. and Heath, J. K. (1987). Transforming growth factor beta modulates the expression of collagenase and metalloproteinase inhibitor. *EMBO J.* **6**, 1899–1904.

Eisenberg, L. M. and Markwald, R. R. (1995). Molecular regulation of atrioventricular valvuloseptal morphogenesis. *Circ. Res.* **77**, 1–6.

Eliceiri, B. P., Klemke, R., Strömblad, S. and Cheresh, D. A. (1998). Integrin alphavbeta3 requirement for sustained mitogen-activated protein kinase activity during angiogenesis. *J. Cell Biol.* **140**, 1255–1263.

Enge, M., Bjarnegård, M., Gerhardt, H., Gustafsson, E., Kalén, M., Asker, N., Hammes, H.-P., Shani, M., Fässler, R. and Betsholtz, C. (2002). Endothelium-specific platelet-derived growth factor-B ablation mimics diabetic retinopathy. *EMBO J.* **21**, 4307–4316.

Engler, A. J., Griffin, M. A., Sen, S., Bönnemann, C. G., Sweeney, H. L. and Discher, D. E. (2004). Myotubes differentiate optimally on substrates with tissue-like stiffness: pathological implications for soft or stiff microenvironments. *J. Cell Biol.* **166**, 877–887.

Engler, A. J., Sen, S., Sweeney, H. L. and Discher, D. E. (2006). Matrix elasticity directs stem cell lineage specification. *Cell* **126**, 677–689.

Engler, A. J., Chan, M., Boettiger, D. and Schwarzbauer, J. E. (2009). A novel mode of cell detachment from fibrillar fibronectin matrix under shear. *J. Cell Sci.* **122**, 1647–1653.

Etchevers, H. C., Couly, G. and Le Douarin, N. M. (2002). Morphogenesis of the branchial vascular sector. *Trends Cardiovasc. Med.* **12**, 299–304.

Even-Ram, S., Doyle, A. D., Conti, M. A., Matsumoto, K., Adelstein, R. S. and Yamada, K. M. (2007). Myosin IIA regulates cell motility and actomyosin–microtubule crosstalk. *Nat. Cell Biol.* **9**, 299–309.

Fässler, R. and Meyer, M. (1995). Consequences of lack of beta 1 integrin gene expression in mice. *Genes Dev.* **9**, 1896–1908.

Ffrench-Constant, C. and Hynes, R. O. (1988). Patterns of fibronectin gene expression and splicing during cell migration in chicken embryos. *Dev. Camb. Engl.* **104**, 369–382.

Ffrench-Constant, C. and Hynes, R. O. (1989). Alternative splicing of fibronectin is temporally and spatially regulated in the chicken embryo. *Dev. Camb. Engl.* **106**, 375–388.

Ffrench-Constant, C., Van de Water, L., Dvorak, H. F. and Hynes, R. O. (1989). Reappearance of an embryonic pattern of fibronectin splicing during wound healing in the adult rat. *J. Cell Biol.* **109**, 903–914.

Fibronectin (1989). San Diego: Academic Press.

Fjellbirkeland, L., Cambier, S., Broaddus, V. C., Hill, A., Brunetta, P., Dolganov, G., Jablons, D. and Nishimura, S. L. (2003). Integrin alphavbeta8-mediated activation of transforming growth factor-beta inhibits human airway epithelial proliferation in intact bronchial tissue. *Am. J. Pathol.* **163**, 533–542.

Flaumenhaft, R. and Rifkin, D. B. (1992). Cell density dependent effects of TGF-beta demonstrated by a plasminogen activator-based assay for TGF-beta. *J. Cell. Physiol.* **152**, 48–55.

Flaumenhaft, Abe and Rifkin, D. B. (1993). Role of the latent TGF-beta binding protein in the activation of latent TGF-beta by co-cultures of endothelial and smooth muscle cells. *J. Cell Biol.* **120**, 995–1002.

Flintoff-Dye, N. L., Welser, J., Rooney, J., Scowen, P., Tamowski, S., Hatton, W. and Burkin, D. J. (2005). Role for the alpha7beta1 integrin in vascular development and integrity. *Dev. Dyn. Off. Publ. Am. Assoc. Anat.* **234**, 11–21.

Fogerty, F. J., Akiyama, S. K., Yamada, K. M. and Mosher, D. F. (1990). Inhibition of binding of fibronectin to matrix assembly sites by anti-integrin (alpha 5 beta 1) antibodies. *J. Cell Biol.* **111**, 699–708.

Folkman, J. and Haudenschild, C. (1980). Angiogenesis in vitro. *Nature* **288**, 551–556.

Francis, S. E., Goh, K. L., Hodivala-Dilke, K., Bader, B. L., Stark, M., Davidson, D. and Hynes, R. O. (2002). Central roles of alpha5beta1 integrin and fibronectin in vascular development in mouse embryos and embryoid bodies. *Arterioscler. Thromb. Vasc. Biol.* **22**, 927–933.

Friedland, J. C., Lee, M. H. and Boettiger, D. (2009). Mechanically activated integrin switch controls alpha5beta1 function. *Science* **323**, 642–644.

Friedlander, M., Brooks, P. C., Shaffer, R. W., Kincaid, C. M., Varner, J. A. and Cheresh, D. A. (1995). Definition of two angiogenic pathways by distinct alpha v integrins. *Science* **270**, 1500–1502.

Friedlander, M., Theesfeld, C. L., Sugita, M., Fruttiger, M., Thomas, M. A., Chang, S. and Cheresh, D. A. (1996). Involvement of integrins alpha v beta 3 and alpha v beta 5 in ocular neovascular diseases. *Proc. Natl. Acad. Sci. U. S. A.* **93**, 9764–9769.

Friedrich, E. B., Liu, E., Sinha, S., Cook, S., Milstone, D. S., MacRae, C. A., Mariotti, M., Kuhlencordt, P. J., Force, T., Rosenzweig, A., et al. (2004). Integrin-Linked Kinase Regulates Endothelial Cell Survival and Vascular Development. *Mol. Cell. Biol.* **24**, 8134–8144.

Frisch, S. M. and Francis, H. (1994). Disruption of epithelial cell-matrix interactions induces apoptosis. *J. Cell Biol.* **124**, 619–626.

Fukuda, T., Yoshida, N., Kataoka, Y., Manabe, R.-I., Mizuno-Horikawa, Y., Sato, M., Kuriyama, K., Yasui, N. and Sekiguchi, K. (2002). Mice lacking the EDB segment of fibronectin develop normally but exhibit reduced cell growth and fibronectin matrix assembly in vitro. *Cancer Res.* **62**, 5603–5610.

Gallant, N. D. (2005). Cell Adhesion Strengthening: Contributions of Adhesive Area, Integrin Binding, and Focal Adhesion Assembly. *Mol. Biol. Cell* **16**, 4329–4340.

Gardner, H., Broberg, A., Pozzi, A., Laato, M. and Heino, J. (1999). Absence of integrin alpha1beta1 in the mouse causes loss of feedback regulation of collagen synthesis in normal and wounded dermis. *J. Cell Sci.* **112 (Pt 3)**, 263–272.

Garmy-Susini, B., Jin, H., Zhu, Y., Sung, R.-J., Hwang, R. and Varner, J. (2005). Integrin alpha4beta1-VCAM-1-mediated adhesion between endothelial and mural cells is required for blood vessel maturation. *J. Clin. Invest.* **115**, 1542–1551.

Ge, G. and Greenspan, D. S. (2006). BMP1 controls TGFβ1 activation via cleavage of latent TGFβ-binding protein. *J. Cell Biol.* **175**, 111–120.

Geiger, B., Spatz, J. P. and Bershadsky, A. D. (2009). Environmental sensing through focal adhesions. *Nat. Rev. Mol. Cell Biol.* **10**, 21–33.

George, E. L., Georges-Labouesse, E. N., Patel-King, R. S., Rayburn, H. and Hynes, R. O. (1993). Defects in mesoderm, neural tube and vascular development in mouse embryos lacking fibronectin. *Dev. Camb. Engl.* **119**, 1079–1091.

George, E. L., Baldwin, H. S. and Hynes, R. O. (1997). Fibronectins are essential for heart and blood vessel morphogenesis but are dispensable for initial specification of precursor cells. *Blood* **90**, 3073–3081.

Georges-Labouesse, E., Messaddeq, N., Yehia, G., Cadalbert, L., Dierich, A. and Le Meur, M. (1996). Absence of integrin α6 leads to epidermolysis bullosa and neonatal death in mice. *Nat. Genet.* **13**, 370–373.

Georges-Labouesse, E. N., George, E. L., Rayburn, H. and Hynes, R. O. (1996). Mesodermal development in mouse embryos mutant for fibronectin. *Dev. Dyn.* **207**, 145–156.

Gerhardt, H. (2008). VEGF and endothelial guidance in angiogenic sprouting. *Organogenesis* **4**, 241–246.

Gerhardt, H. and Betsholtz, C. (2003). Endothelial-pericyte interactions in angiogenesis. *Cell Tissue Res.* **314**, 15–23.

Gerhardt, H. and Betsholtz, C. (2005). How do endothelial cells orientate? *EXS* 3–15.

Gerhardt, H., Golding, M., Fruttiger, M., Ruhrberg, C., Lundkvist, A., Abramsson, A., Jeltsch, M., Mitchell, C., Alitalo, K., Shima, D., et al. (2003). VEGF guides angiogenic sprouting utilizing endothelial tip cell filopodia. *J. Cell Biol.* **161**, 1163–1177.

Giancotti, F. G. and Ruoslahti, E. (1990). Elevated levels of the alpha 5 beta 1 fibronectin receptor suppress the transformed phenotype of Chinese hamster ovary cells. *Cell* **60**, 849–859.

Giannelli, G., Fransvea, E., Marinosci, F., Bergamini, C., Colucci, S., Schiraldi, O. and Antonaci, S. (2002). Transforming growth factor-beta1 triggers hepatocellular carcinoma invasiveness via alpha3beta1 integrin. *Am. J. Pathol.* **161**, 183–193.

Ginsberg, M., Pierschbacher, M. D., Ruoslahti, E., Marguerie, G. and Plow, E. (1985). Inhibition of fibronectin binding to platelets by proteolytic fragments and synthetic peptides which support fibroblast adhesion. *J. Biol. Chem.* **260**, 3931–3936.

Gleizes, P. E., Beavis, R. C., Mazzieri, R., Shen, B. and Rifkin, D. B. (1996). Identification and characterization of an eight-cysteine repeat of the latent transforming growth factor-beta binding protein-1 that mediates bonding to the latent transforming growth factor-beta1. *J. Biol. Chem.* **271**, 29891–29896.

Godbout, C., Follonier Castella, L., Smith, E. A., Talele, N., Chow, M. L., Garonna, A. and Hinz, B. (2013). The mechanical environment modulates intracellular calcium oscillation activities of myofibroblasts. *PloS One* **8**, e64560.

Godyna, S., Mann, D. M. and Argraves, W. S. (1995). A quantitative analysis of the incorporation of fibulin-1 into extracellular matrix indicates that fibronectin assembly is required. *Matrix Biol. J. Int. Soc. Matrix Biol.* **14**, 467–477.

Goetz, R. and Mohammadi, M. (2013). Exploring mechanisms of FGF signalling through the lens of structural biology. *Nat. Rev. Mol. Cell Biol.* **14**, 166–180.

Goffin, J. M., Pittet, P., Csucs, G., Lussi, J. W., Meister, J.-J. and Hinz, B. (2006). Focal adhesion size controls tension-dependent recruitment of -smooth muscle actin to stress fibers. *J. Cell Biol.* **172**, 259–268.

Goh, K. L., Yang, J. T. and Hynes, R. O. (1997). Mesodermal defects and cranial neural crest apoptosis in alpha5 integrin-null embryos. *Dev. Camb. Engl.* **124**, 4309–4319.

Goksoy, E., Ma, Y.-Q., Wang, X., Kong, X., Perera, D., Plow, E. F. and Qin, J. (2008). Structural basis for the autoinhibition of talin in regulating integrin activation. *Mol. Cell* **31**, 124–133.

Gottschalk, K.-E. (2005). A coiled-coil structure of the alphaIIbbeta3 integrin transmembrane and cytoplasmic domains in its resting state. *Struct. Lond. Engl. 1993* **13**, 703–712.

Goumans, M.-J., Valdimarsdottir, G., Itoh, S., Rosendahl, A., Sideras, P. and Dijke, P. ten (2002). Balancing the activation state of the endothelium via two distinct TGF-β type I receptors. *EMBO J.* **21**, 1743–1753.

Grazioli, A., Alves, C. S., Konstantopoulos, K. and Yang, J. T. (2006). Defective blood vessel development and pericyte/pvSMC distribution in alpha 4 integrin-deficient mouse embryos. *Dev. Biol.* **293**, 165–177.

Green, J. A., Berrier, A. L., Pankov, R. and Yamada, K. M. (2009). beta1 integrin cytoplasmic domain residues selectively modulate fibronectin matrix assembly and cell spreading through talin and Akt-1. *J. Biol. Chem.* **284**, 8148–8159.

Gregory, K. E., Ono, R. N., Charbonneau, N. L., Kuo, C.-L., Keene, D. R., Bächinger, H. P. and Sakai, L. Y. (2005). The prodomain of BMP-7 targets the BMP-7 complex to the extracellular matrix. *J. Biol. Chem.* **280**, 27970–27980.

Guan, J. L. and Hynes, R. O. (1990). Lymphoid cells recognize an alternatively spliced segment of fibronectin via the integrin receptor alpha 4 beta 1. *Cell* **60**, 53–61.

Guan, J. L., Trevithick, J. E. and Hynes, R. O. (1990). Retroviral expression of alternatively spliced forms of rat fibronectin. *J. Cell Biol.* **110**, 833–847.

Guertin, D. A., Stevens, D. M., Thoreen, C. C., Burds, A. A., Kalaany, N. Y., Moffat, J., Brown, M., Fitzgerald, K. J. and Sabatini, D. M. (2006). Ablation in mice of the mTORC components raptor, rictor, or mLST8 reveals that mTORC2 is required for signaling to Akt-FOXO and PKCalpha, but not S6K1. *Dev. Cell* **11**, 859–871.

Guo, W., Frey, M. T., Burnham, N. A. and Wang, Y. (2006). Substrate rigidity regulates the formation and maintenance of tissues. *Biophys. J.* **90**, 2213–2220.

Hammes, H. P., Brownlee, M., Jonczyk, A., Sutter, A. and Preissner, K. T. (1996). Subcutaneous injection of a cyclic peptide antagonist of vitronectin receptor-type integrins inhibits retinal neovascularization. *Nat. Med.* **2**, 529–533.

Harvey, R. P. (1998). Cardiac looping--an uneasy deal with laterality. *Semin. Cell Dev. Biol.* **9**, 101–108.

Harvey, R. P. (2002). Organogenesis: Patterning the vertebrate heart. *Nat. Rev. Genet.* **3**, 544–556.

Hayman, E. G. and Ruoslahti, E. (1979). Distribution of fetal bovine serum fibronectin and endogenous rat cell fibronectin in extracellular matrix. *J. Cell Biol.* **83**, 255–259.

Heikinheimo, M., Scandrett, J. M. and Wilson, D. B. (1994). Localization of transcription factor GATA-4 to regions of the mouse embryo involved in cardiac development. *Dev. Biol.* **164**, 361–373.

Heino, J. and Massagué, J. (1989). Transforming growth factor-beta switches the pattern of integrins expressed in MG-63 human osteosarcoma cells and causes a selective loss of cell adhesion to laminin. *J. Biol. Chem.* **264**, 21806–21811.

Heino, J., Ignotz, R. A., Hemler, M. E., Crouse, C. and Massagué, J. (1989). Regulation of cell adhesion receptors by transforming growth factor-beta. Concomitant regulation of integrins that share a common beta 1 subunit. *J. Biol. Chem.* **264**, 380–388.

Hellström, M., Kalén, M., Lindahl, P., Abramsson, A. and Betsholtz, C. (1999). Role of PDGF-B and PDGFR-beta in recruitment of vascular smooth muscle cells and pericytes during embryonic blood vessel formation in the mouse. *Dev. Camb. Engl.* **126**, 3047–3055.

Hellström, M., Gerhardt, H., Kalén, M., Li, X., Eriksson, U., Wolburg, H. and Betsholtz, C. (2001). Lack of pericytes leads to endothelial hyperplasia and abnormal vascular morphogenesis. *J. Cell Biol.* **153**, 543–553.

Hellström, M., Phng, L.-K., Hofmann, J. J., Wallgard, E., Coultas, L., Lindblom, P., Alva, J., Nilsson, A.-K., Karlsson, L., Gaiano, N., et al. (2007). Dll4 signalling through Notch1 regulates formation of tip cells during angiogenesis. *Nature* **445**, 776–780.

Hinz, B. (2010). The myofibroblast: paradigm for a mechanically active cell. *J. Biomech.* **43**, 146–155.

Hinz, B., Mastrangelo, D., Iselin, C. E., Chaponnier, C. and Gabbiani, G. (2001). Mechanical Tension Controls Granulation Tissue Contractile Activity and Myofibroblast Differentiation. *Am. J. Pathol.* **159**, 1009–1020.

Hirschi, K. K., Rohovsky, S. A. and D'Amore, P. A. (1998). PDGF, TGF-beta, and heterotypic cell-cell interactions mediate endothelial cell-induced recruitment of 10T1/2 cells and their differentiation to a smooth muscle fate. *J. Cell Biol.* **141**, 805–814.

Hirschi, K. K., Rohovsky, S. A., Beck, L. H., Smith, S. R. and D'Amore, P. A. (1999). Endothelial cells modulate the proliferation of mural cell precursors via platelet-derived growth factor-BB and heterotypic cell contact. *Circ. Res.* **84**, 298–305.

Hirschi, K. K., Burt, J. M., Hirschi, K. D. and Dai, C. (2003). Gap junction communication mediates transforming growth factor-beta activation and endothelial-induced mural cell differentiation. *Circ. Res.* **93**, 429–437.

Hocking, D. C., Sottile, J. and McKeown-Longo, P. J. (1994). Fibronectin's III-1 module contains a conformation-dependent binding site for the amino-terminal region of fibronectin. *J. Biol. Chem.* **269**, 19183–19187.

Hocking, D. C., Smith, R. K. and McKeown-Longo, P. J. (1996). A novel role for the integrin-binding III-10 module in fibronectin matrix assembly. *J. Cell Biol.* **133**, 431–444.

Hodivala-Dilke, K. M., McHugh, K. P., Tsakiris, D. A., Rayburn, H., Crowley, D., Ullman-Culleré, M., Ross, F. P., Coller, B. S., Teitelbaum, S. and Hynes, R. O. (1999). Beta3-integrin-deficient mice are a model for Glanzmann thrombasthenia showing placental defects and reduced survival. *J. Clin. Invest.* **103**, 229–238.

Holtkötter, O., Nieswandt, B., Smyth, N., Müller, W., Hafner, M., Schulte, V., Krieg, T. and Eckes, B. (2002). Integrin alpha 2-deficient mice develop normally, are fertile, but display partially defective platelet interaction with collagen. *J. Biol. Chem.* **277**, 10789–10794.

Hove, J. R., Köster, R. W., Forouhar, A. S., Acevedo-Bolton, G., Fraser, S. E. and Gharib, M. (2003). Intracardiac fluid forces are an essential epigenetic factor for embryonic cardiogenesis. *Nature* **421**, 172–177.

Huang, X. Z., Wu, J. F., Cass, D., Erle, D. J., Corry, D., Young, S. G., Farese, R. V., Jr and Sheppard, D. (1996). Inactivation of the integrin beta 6 subunit gene reveals a role of epithelial integrins in regulating inflammation in the lung and skin. *J. Cell Biol.* **133**, 921–928.

Huang, X., Griffiths, M., Wu, J., Farese, R. V., Jr and Sheppard, D. (2000a). Normal development, wound healing, and adenovirus susceptibility in beta5-deficient mice. *Mol. Cell. Biol.* **20**, 755–759.

Huang, X. Z., Wu, J. F., Ferrando, R., Lee, J. H., Wang, Y. L., Farese, R. V., Jr and Sheppard, D. (2000b). Fatal bilateral chylothorax in mice lacking the integrin alpha9beta1. *Mol. Cell. Biol.* **20**, 5208–5215.

Huang, C., Sheikh, F., Hollander, M., Cai, C., Becker, D., Chu, P.-H., Evans, S. and Chen, J. (2003). Embryonic atrial function is essential for mouse embryogenesis, cardiac morphogenesis and angiogenesis. *Dev. Camb. Engl.* **130**, 6111–6119.

Humphries, J. D. (2006). Integrin ligands at a glance. *J. Cell Sci.* **119**, 3901–3903.

Humphries, J. D., Wang, P., Streuli, C., Geiger, B., Humphries, M. J. and Ballestrem, C. (2007). Vinculin controls focal adhesion formation by direct interactions with talin and actin. *J. Cell Biol.* **179**, 1043–1057.

Hungerford, J. E. and Little, C. D. (1999). Developmental biology of the vascular smooth muscle cell: building a multilayered vessel wall. *J. Vasc. Res.* **36**, 2–27.

Huveneers, S., Truong, H., Fässler, R., Sonnenberg, A. and Danen, E. H. J. (2008). Binding of soluble fibronectin to integrin alpha5 beta1 - link to focal adhesion redistribution and contractile shape. *J. Cell Sci.* **121**, 2452–2462.

Hynes, R. O. (1990). *Fibronectins*. New York: Springer-Verlag.

Hynes, R. O. (2002a). A reevaluation of integrins as regulators of angiogenesis. *Nat. Med.* **8**, 918–921.

Hynes, R. O. (2002b). Integrins: bidirectional, allosteric signaling machines. *Cell* **110**, 673–687.

Hynes, R. O. and Zhao, Q. (2000). The evolution of cell adhesion. *J. Cell Biol.* **150**, F89–96.

Icardo, J. M., Nakamura, A., Fernandez-Teran, M. A. and Manasek, F. J. (1992). Effects of injecting fibronectin and antifibronectin antibodies on cushion mesenchyme formation in the chick. An in vivo study. *Anat. Embryol. (Berl.)* **185**, 239–247.

Ichihara-Tanaka, K., Maeda, T., Titani, K. and Sekiguchi, K. (1992). Matrix assembly of recombinant fibronectin polypeptide consisting of amino-terminal 70 kDa and carboxyl-terminal 37 kDa regions. *FEBS Lett.* **299**, 155–158.

Ignotz, R. A., Endo, T. and Massagué, J. (1987). Regulation of fibronectin and type I collagen mRNA levels by transforming growth factor-beta. *J. Biol. Chem.* **262**, 6443–6446.

Ikenoue, T., Inoki, K., Yang, Q., Zhou, X. and Guan, K.-L. (2008). Essential function of TORC2 in PKC and Akt turn motif phosphorylation, maturation and signalling. *EMBO J.* **27**, 1919–1931.

Ilić, D., Kovacic, B., Johkura, K., Schlaepfer, D. D., Tomasević, N., Han, Q., Kim, J.-B., Howerton, K., Baumbusch, C., Ogiwara, N., et al. (2004). FAK promotes organization of fibronectin matrix and fibrillar adhesions. *J. Cell Sci.* **117**, 177–187.

Ingham, K. C., Brew, S. A. and Erickson, H. P. (2004a). Localization of a cryptic binding site for tenascin on fibronectin. *J. Biol. Chem.* **279**, 28132–28135.

Ingham, K. C., Brew, S., Vaz, D., Sauder, D. N. and McGavin, M. J. (2004b). Interaction of Staphylococcus aureus fibronectin-binding protein with fibronectin: affinity, stoichiometry, and modular requirements. *J. Biol. Chem.* **279**, 42945–42953.

Iruela-Arispe, M. L. and Davis, G. E. (2009). Cellular and molecular mechanisms of vascular lumen formation. *Dev. Cell* **16**, 222–231.

Iruela-Arispe, M. L., Hasselaar, P. and Sage, H. (1991a). Differential expression of extracellular proteins is correlated with angiogenesis in vitro. *Lab. Investig. J. Tech. Methods Pathol.* **64**, 174–186.

Iruela-Arispe, M. L., Diglio, C. A. and Sage, E. H. (1991b). Modulation of extracellular matrix proteins by endothelial cells undergoing angiogenesis in vitro. *Arterioscler. Thromb. J. Vasc. Biol. Am. Heart Assoc.* **11**, 805–815.

Isenberg, B. C., Dimilla, P. A., Walker, M., Kim, S. and Wong, J. Y. (2009). Vascular smooth muscle cell durotaxis depends on substrate stiffness gradient strength. *Biophys. J.* **97**, 1313–1322.

Isogai, Z., Ono, R. N., Ushiro, S., Keene, D. R., Chen, Y., Mazzieri, R., Charbonneau, N. L., Reinhardt, D. P., Rifkin, D. B. and Sakai, L. Y. (2003). Latent Transforming Growth Factor β-binding Protein 1 Interacts with Fibrillin and Is a Microfibril-associated Protein. *J. Biol. Chem.* **278**, 2750–2757.

Jaffe, A. B. and Hall, A. (2005). Rho GTPases: biochemistry and biology. *Annu. Rev. Cell Dev. Biol.* **21**, 247–269.

Ji, R. P., Phoon, C. K. L., Aristizábal, O., McGrath, K. E., Palis, J. and Turnbull, D. H. (2003). Onset of cardiac function during early mouse embryogenesis coincides with entry of primitive erythroblasts into the embryo proper. *Circ. Res.* **92**, 133–135.

Jiang, B., Liou, G. I., Behzadian, M. A. and Caldwell, R. B. (1994). Astrocytes modulate retinal vasculogenesis: effects on fibronectin expression. *J. Cell Sci.* **107 (Pt 9)**, 2499–2508.

Jiang, X., Rowitch, D. H., Soriano, P., McMahon, A. P. and Sucov, H. M. (2000). Fate of the mammalian cardiac neural crest. *Dev. Camb. Engl.* **127**, 1607–1616.

Jiang, G., Giannone, G., Critchley, D. R., Fukumoto, E. and Sheetz, M. P. (2003). Two-piconewton slip bond between fibronectin and the cytoskeleton depends on talin. *Nature* **424**, 334–337.

Jiao, K., Langworthy, M., Batts, L., Brown, C. B., Moses, H. L. and Baldwin, H. S. (2006). Tgfbeta signaling is required for atrioventricular cushion mesenchyme remodeling during in vivo cardiac development. *Dev. Camb. Engl.* **133**, 4585–4593.

Jiménez, B., Volpert, O. V., Crawford, S. E., Febbraio, M., Silverstein, R. L. and Bouck, N. (2000). Signals leading to apoptosis-dependent inhibition of neovascularization by thrombospondin-1. *Nat. Med.* **6**, 41–48.

Johnson, K. J., Sage, H., Briscoe, G. and Erickson, H. P. (1999). The compact conformation of fibronectin is determined by intramolecular ionic interactions. *J. Biol. Chem.* **274**, 15473–15479.

Jones, E. A. V., Baron, M. H., Fraser, S. E. and Dickinson, M. E. (2004). Measuring hemodynamic changes during mammalian development. *Am. J. Physiol. Heart Circ. Physiol.* **287**, H1561–1569.

Jülich, D., Geisler, R. and Holley, S. A. (2005). Integrinalpha5 and delta/notch signaling have complementary spatiotemporal requirements during zebrafish somitogenesis. *Dev. Cell* **8**, 575–586.

Kaartinen, V., Voncken, J. W., Shuler, C., Warburton, D., Bu, D., Heisterkamp, N. and Groffen, J. (1995). Abnormal lung development and cleft palate in mice lacking TGF-beta 3 indicates defects of epithelial-mesenchymal interaction. *Nat. Genet.* **11**, 415–421.

Kadler, K. E., Hill, A. and Canty-Laird, E. G. (2008). Collagen fibrillogenesis: fibronectin, integrins, and minor collagens as organizers and nucleators. *Curr. Opin. Cell Biol.* **20**, 495–501.

Kahner, B. N., Kato, H., Banno, A., Ginsberg, M. H., Shattil, S. J. and Ye, F. (2012). Kindlins, integrin activation and the regulation of talin recruitment to αIIbβ3. *PloS One* **7**, e34056.

Kamei, M., Saunders, W. B., Bayless, K. J., Dye, L., Davis, G. E. and Weinstein, B. M. (2006). Endothelial tubes assemble from intracellular vacuoles in vivo. *Nature* **442**, 453–456.

Kanchanawong, P., Shtengel, G., Pasapera, A. M., Ramko, E. B., Davidson, M. W., Hess, H. F. and Waterman, C. M. (2010). Nanoscale architecture of integrin-based cell adhesions. *Nature* **468**, 580–584.

Kantola, A. K., Keski-Oja, J. and Koli, K. (2008). Fibronectin and heparin binding domains of latent TGF-β binding protein (LTBP)-4 mediate matrix targeting and cell adhesion. *Exp. Cell Res.* **314**, 2488–2500.

Katz, B.-Z., Zamir, E., Bershadsky, A., Kam, Z., Yamada, K. M. and Geiger, B. (2000). Physical State of the Extracellular Matrix Regulates the Structure and Molecular Composition of Cell-Matrix Adhesions. *Mol. Biol. Cell* **11**, 1047–1060.

Kaufman, M. H. and Navaratnam, V. (1981). Early differentiation of the heart in mouse embryos. *J. Anat.* **133**, 235–246.

Kelly, R. G., Brown, N. A. and Buckingham, M. E. (2001). The arterial pole of the mouse heart forms from Fgf10-expressing cells in pharyngeal mesoderm. *Dev. Cell* **1**, 435–440.

Kennedy, S. G., Wagner, A. J., Conzen, S. D., Jordán, J., Bellacosa, A., Tsichlis, P. N. and Hay, N. (1997). The PI 3-kinase/Akt signaling pathway delivers an anti-apoptotic signal. *Genes Dev.* **11**, 701–713.

Kesavan, G., Sand, F. W., Greiner, T. U., Johansson, J. K., Kobberup, S., Wu, X., Brakebusch, C. and Semb, H. (2009). Cdc42-mediated tubulogenesis controls cell specification. *Cell* **139**, 791–801.

Keski-Oja, J., Raghow, R., Sawdey, M., Loskutoff, D. J., Postlethwaite, A. E., Kang, A. H. and Moses, H. L. (1988). Regulation of mRNAs for type-1 plasminogen activator inhibitor, fibronectin, and type I procollagen by transforming growth factor-beta. Divergent responses in lung fibroblasts and carcinoma cells. *J. Biol. Chem.* **263**, 3111–3115.

Kilian, O., Dahse, R., Alt, V., Zardi, L., Hentschel, J., Schnettler, R. and Kosmehl, H. (2008). mRNA expression and protein distribution of fibronectin splice variants and high-molecular weight tenascin-C in different phases of human fracture healing. *Calcif. Tissue Int.* **83**, 101–111.

Kim, S.-H. and Kim, S. H. (2008). Antagonistic effect of EGF on FAK phosphorylation/dephosphorylation in a cell. *Cell Biochem. Funct.* **26**, 539–547.

Kim, S., Bell, K., Mousa, S. A. and Varner, J. A. (2000). Regulation of angiogenesis in vivo by ligation of integrin alpha5beta1 with the central cell-binding domain of fibronectin. *Am. J. Pathol.* **156**, 1345–1362.

Kim, M., Carman, C. V. and Springer, T. A. (2003). Bidirectional transmembrane signaling by cytoplasmic domain separation in integrins. *Science* **301**, 1720–1725.

Kimura, K., Ito, M., Amano, M., Chihara, K., Fukata, Y., Nakafuku, M., Yamamori, B., Feng, J., Nakano, T., Okawa, K., et al. (1996). Regulation of myosin phosphatase by Rho and Rho-associated kinase (Rho-kinase). *Science* **273**, 245–248.

King, W. G., Mattaliano, M. D., Chan, T. O., Tsichlis, P. N. and Brugge, J. S. (1997). Phosphatidylinositol 3-kinase is required for integrin-stimulated AKT and Raf-1/mitogen-activated protein kinase pathway activation. *Mol. Cell. Biol.* **17**, 4406–4418.

Kinsey, R., Williamson, M. R., Chaudhry, S., Mellody, K. T., McGovern, A., Takahashi, S., Shuttleworth, C. A. and Kielty, C. M. (2008). Fibrillin-1 microfibril deposition is dependent on fibronectin assembly. *J. Cell Sci.* **121**, 2696–2704.

Kiyokawa, E., Hashimoto, Y., Kobayashi, S., Sugimura, H., Kurata, T. and Matsuda, M. (1998). Activation of Rac1 by a Crk SH3-binding protein, DOCK180. *Genes Dev.* **12**, 3331–3336.

Klass, C. M., Couchman, J. R. and Woods, A. (2000). Control of extracellular matrix assembly by syndecan-2 proteoglycan. *J. Cell Sci.* **113 (Pt 3)**, 493–506.

Klotzsch, E., Smith, M. L., Kubow, K. E., Muntwyler, S., Little, W. C., Beyeler, F., Gourdon, D., Nelson, B. J. and Vogel, V. (2009). Fibronectin forms the most extensible biological fibers displaying switchable force-exposed cryptic binding sites. *Proc. Natl. Acad. Sci. U. S. A.* **106**, 18267–18272.

Koh, W., Mahan, R. D. and Davis, G. E. (2008). Cdc42- and Rac1-mediated endothelial lumen formation requires Pak2, Pak4 and Par3, and PKC-dependent signaling. *J. Cell Sci.* **121**, 989–1001.

Koli, K., Hyytiäinen, M., Ryynänen, M. J. and Keski-Oja, J. (2005). Sequential deposition of latent TGF-β binding proteins (LTBPs) during formation of the extracellular matrix in human lung fibroblasts. *Exp. Cell Res.* **310**, 370–382.

Komiyama, M., Ito, K. and Shimada, Y. (1987). Origin and development of the epicardium in the mouse embryo. *Anat. Embryol. (Berl.)* **176**, 183–189.

Kong, F., García, A. J., Mould, A. P., Humphries, M. J. and Zhu, C. (2009). Demonstration of catch bonds between an integrin and its ligand. *J. Cell Biol.* **185**, 1275–1284.

Korchynskyi, O. and ten Dijke, P. (2002). Identification and functional characterization of distinct critically important bone morphogenetic protein-specific response elements in the Id1 promoter. *J. Biol. Chem.* **277**, 4883–4891.

Kornblihtt, A. R., Vibe-Pedersen, K. and Baralle, F. E. (1984). Human fibronectin: cell specific alternative mRNA splicing generates polypeptide chains differing in the number of internal repeats. *Nucleic Acids Res.* **12**, 5853–5868.

Kornblihtt, A. R., Umezawa, K., Vibe-Pedersen, K. and Baralle, F. E. (1985). Primary structure of human fibronectin: differential splicing may generate at least 10 polypeptides from a single gene. *EMBO J.* **4**, 1755–1759.

Koshida, S., Kishimoto, Y., Ustumi, H., Shimizu, T., Furutani-Seiki, M., Kondoh, H. and Takada, S. (2005). Integrinα5-Dependent Fibronectin Accumulation for Maintenance of Somite Boundaries in Zebrafish Embryos. *Dev. Cell* **8**, 587–598.

Koukoulis, G. K., Howeedy, A. A., Korhonen, M., Virtanen, I. and Gould, V. E. (1993). Distribution of tenascin, cellular fibronectins and integrins in the normal, hyperplastic and neoplastic breast. *J. Submicrosc. Cytol. Pathol.* **25**, 285–295.

Koushik, S. V., Wang, J., Rogers, R., Moskophidis, D., Lambert, N. A., Creazzo, T. L. and Conway, S. J. (2001). Targeted inactivation of the sodium-calcium exchanger (Ncx1) results in the lack of a heartbeat and abnormal myofibrillar organization. *FASEB J. Off. Publ. Fed. Am. Soc. Exp. Biol.* **15**, 1209–1211.

Kragtorp, K. A. and Miller, J. R. (2006). Regulation of somitogenesis by Ena/VASP proteins and FAK during Xenopus development. *Dev. Camb. Engl.* **133**, 685–695.

Kreidberg, J. A., Donovan, M. J., Goldstein, S. L., Rennke, H., Shepherd, K., Jones, R. C. and Jaenisch, R. (1996). Alpha 3 beta 1 integrin has a crucial role in kidney and lung organogenesis. *Dev. Camb. Engl.* **122**, 3537–3547.

Kühn, R., Schwenk, F., Aguet, M. and Rajewsky, K. (1995). Inducible gene targeting in mice. *Science* **269**, 1427–1429.

Kumar, N. M., Sigurdson, S. L., Sheppard, D. and Lwebuga-Mukasa, J. S. (1995). Differential modulation of integrin receptors and extracellular matrix laminin by transforming growth factor-beta 1 in rat alveolar epithelial cells. *Exp. Cell Res.* **221**, 385–394.

Kuo, J.-C., Han, X., Hsiao, C.-T., Yates, J. R., 3rd and Waterman, C. M. (2011). Analysis of the myosin-II-responsive focal adhesion proteome reveals a role for β-Pix in negative regulation of focal adhesion maturation. *Nat. Cell Biol.* **13**, 383–393.

LaFlamme, S. E. (1994). Single subunit chimeric integrins as mimics and inhibitors of endogenous integrin functions in receptor localization, cell spreading and migration, and matrix assembly. *J. Cell Biol.* **126**, 1287–1298.

Laiho, M., Saksela, O., Andreasen, P. A. and Keski-Oja, J. (1986). Enhanced production and extracellular deposition of the endothelial-type plasminogen activator inhibitor in cultured human lung fibroblasts by transforming growth factor-beta. *J. Cell Biol.* **103**, 2403–2410.

Langenbach, K. J. and Sottile, J. (1999). Identification of protein-disulfide isomerase activity in fibronectin. *J. Biol. Chem.* **274**, 7032–7038.

Larsson, J., Goumans, M. J., Sjöstrand, L. J., van Rooijen, M. A., Ward, D., Levéen, P., Xu, X., ten Dijke, P., Mummery, C. L. and Karlsson, S. (2001). Abnormal angiogenesis but intact hematopoietic potential in TGF-beta type I receptor-deficient mice. *EMBO J.* **20**, 1663–1673.

Laukaitis, C. M., Webb, D. J., Donais, K. and Horwitz, A. F. (2001). Differential dynamics of alpha 5 integrin, paxillin, and alpha-actinin during formation and disassembly of adhesions in migrating cells. *J. Cell Biol.* **153**, 1427–1440.

Lawler, J. (2000). The functions of thrombospondin-1 and-2. *Curr. Opin. Cell Biol.* **12**, 634–640.

Lawrence, D. A., Pircher, R., Krycève-Martinerie, C. and Jullien, P. (1984). Normal embryo fibroblasts release transforming growth factors in a latent form. *J. Cell. Physiol.* **121**, 184–188.

Leahy, D. J., Hendrickson, W. A., Aukhil, I. and Erickson, H. P. (1992). Structure of a fibronectin type III domain from tenascin phased by MAD analysis of the selenomethionyl protein. *Science* **258**, 987–991.

Lebrin, F., Goumans, M.-J., Jonker, L., Carvalho, R. L. C., Valdimarsdottir, G., Thorikay, M., Mummery, C., Arthur, H. M. and ten Dijke, P. (2004). Endoglin promotes endothelial cell proliferation and TGF-beta/ALK1 signal transduction. *EMBO J.* **23**, 4018–4028.

Lee, G., Hynes, R. and Kirschner, M. (1984). Temporal and spatial regulation of fibronectin in early Xenopus development. *Cell* **36**, 729–740.

Legate, K. R. and Fässler, R. (2009). Mechanisms that regulate adaptor binding to beta-integrin cytoplasmic tails. *J. Cell Sci.* **122**, 187–198.

Legate, K. R., Montañez, E., Kudlacek, O. and Fässler, R. (2006). ILK, PINCH and parvin: the tIPP of integrin signalling. *Nat. Rev. Mol. Cell Biol.* **7**, 20–31.

Legate, K. R., Wickstrom, S. A. and Fassler, R. (2009). Genetic and cell biological analysis of integrin outside-in signaling. *Genes Dev.* **23**, 397–418.

Legate, K. R., Takahashi, S., Bonakdar, N., Fabry, B., Boettiger, D., Zent, R. and Fässler, R. (2011). Integrin adhesion and force coupling are independently regulated by localized PtdIns(4,5)2 synthesis. *EMBO J.* **30**, 4539–4553.

Lei, L., Liu, D., Huang, Y., Jovin, I., Shai, S.-Y., Kyriakides, T., Ross, R. S. and Giordano, F. J. (2008). Endothelial expression of beta1 integrin is required for embryonic vascular patterning and postnatal vascular remodeling. *Mol. Cell. Biol.* **28**, 794–802.

Leiss, M., Beckmann, K., Girós, A., Costell, M. and Fässler, R. (2008). The role of integrin binding sites in fibronectin matrix assembly in vivo. *Curr. Opin. Cell Biol.* **20**, 502–507.

Leslie, J. D., Ariza-McNaughton, L., Bermange, A. L., McAdow, R., Johnson, S. L. and Lewis, J. (2007). Endothelial signalling by the Notch ligand Delta-like 4 restricts angiogenesis. *Dev. Camb. Engl.* **134**, 839–844.

Lessey, E. C., Guilluy, C. and Burridge, K. (2012). From mechanical force to RhoA activation. *Biochemistry (Mosc.)* **51**, 7420–7432.

Levental, K. R., Yu, H., Kass, L., Lakins, J. N., Egeblad, M., Erler, J. T., Fong, S. F. T., Csiszar, K., Giaccia, A., Weninger, W., et al. (2009). Matrix crosslinking forces tumor progression by enhancing integrin signaling. *Cell* **139**, 891–906.

Li, F. and Higgs, H. N. (2003). The mouse Formin mDia1 is a potent actin nucleation factor regulated by autoinhibition. *Curr. Biol. CB* **13**, 1335–1340.

Li, S., Van Den Diepstraten, C., D'Souza, S. J., Chan, B. M. C. and Pickering, J. G. (2003). Vascular smooth muscle cells orchestrate the assembly of type I collagen via alpha2beta1 integrin, RhoA, and fibronectin polymerization. *Am. J. Pathol.* **163**, 1045–1056.

Li, S., Guan, J.-L. and Chien, S. (2005a). Biochemistry and biomechanics of cell motility. *Annu. Rev. Biomed. Eng.* **7**, 105–150.

Li, Y.-S. J., Haga, J. H. and Chien, S. (2005b). Molecular basis of the effects of shear stress on vascular endothelial cells. *J. Biomech.* **38**, 1949–1971.

Li, L., Welser-Alves, J., van der Flier, A., Boroujerdi, A., Hynes, R. O. and Milner, R. (2012). An angiogenic role for the α5β1 integrin in promoting endothelial cell proliferation during cerebral hypoxia. *Exp. Neurol.* **237**, 46–54.

Liao, Y.-F., Gotwals, P. J., Koteliansky, V. E., Sheppard, D. and Van De Water, L. (2002). The EIIIA segment of fibronectin is a ligand for integrins alpha 9beta 1 and alpha 4beta 1 providing a novel mechanism for regulating cell adhesion by alternative splicing. *J. Biol. Chem.* **277**, 14467–14474.

Lim, S. P., Leung, E. and Krissansen, G. W. (1998). The beta7 integrin gene (Itgb-7) promoter is responsive to TGF-beta1: defining control regions. *Immunogenetics* **48**, 184–195.

Linask, K. K. and Lash, J. W. (1986). Precardiac cell migration: Fibronectin localization at mesoderm-endoderm interface during directional movement. *Dev. Biol.* **114**, 87–101.

Lints, T. J., Parsons, L. M., Hartley, L., Lyons, I. and Harvey, R. P. (1993). Nkx-2.5: a novel murine homeobox gene expressed in early heart progenitor cells and their myogenic descendants. *Dev. Camb. Engl.* **119**, 969.

Liu, J., Fukuda, K., Xu, Z., Ma, Y.-Q., Hirbawi, J., Mao, X., Wu, C., Plow, E. F. and Qin, J. (2011). Structural basis of phosphoinositide binding to kindlin-2 protein pleckstrin homology domain in regulating integrin activation. *J. Biol. Chem.* **286**, 43334–43342.

Lo, S. H., Janmey, P. A., Hartwig, J. H. and Chen, L. B. (1994). Interactions of tensin with actin and identification of its three distinct actin-binding domains. *J. Cell Biol.* **125**, 1067–1075.

Lo, C. M., Wang, H. B., Dembo, M. and Wang, Y. L. (2000). Cell movement is guided by the rigidity of the substrate. *Biophys. J.* **79**, 144–152.

Lobov, I. B., Renard, R. A., Papadopoulos, N., Gale, N. W., Thurston, G., Yancopoulos, G. D. and Wiegand, S. J. (2007). Delta-like ligand 4 (Dll4) is induced by VEGF as a negative regulator of angiogenic sprouting. *Proc. Natl. Acad. Sci. U. S. A.* **104**, 3219–3224.

Loeber, C. P. and Runyan, R. B. (1990). A comparison of fibronectin, laminin, and galactosyltransferase adhesion mechanisms during embryonic cardiac mesenchymal cell migration in vitro. *Dev. Biol.* **140**, 401–412.

Lucitti, J. L., Jones, E. A. V., Huang, C., Chen, J., Fraser, S. E. and Dickinson, M. E. (2007). Vascular remodeling of the mouse yolk sac requires hemodynamic force. *Dev. Camb. Engl.* **134**, 3317–3326.

Luo, Y., Ferreira-Cornwell, M., Baldwin, H., Kostetskii, I., Lenox, J., Lieberman, M. and Radice, G. (2001). Rescuing the N-cadherin knockout by cardiac-specific expression of N- or E-cadherin. *Dev. Camb. Engl.* **128**, 459–469.

Luo, B.-H., Carman, C. V. and Springer, T. A. (2007). Structural basis of integrin regulation and signaling. *Annu. Rev. Immunol.* **25**, 619–647.

Lyden, D., Young, A. Z., Zagzag, D., Yan, W., Gerald, W., O'Reilly, R., Bader, B. L., Hynes, R. O., Zhuang, Y., Manova, K., et al. (1999). Id1 and Id3 are required for neurogenesis, angiogenesis and vascularization of tumour xenografts. *Nature* **401**, 670–677.

Ma, Y.-Q., Qin, J., Wu, C. and Plow, E. F. (2008). Kindlin-2 (Mig-2): a co-activator of beta3 integrins. *J. Cell Biol.* **181**, 439–446.

MacLeod, J. N., Burton-Wurster, N., Gu, D. N. and Lust, G. (1996). Fibronectin mRNA splice variant in articular cartilage lacks bases encoding the V, III-15, and I-10 protein segments. *J. Biol. Chem.* **271**, 18954–18960.

Maekawa, M. (1999). Signaling from Rho to the Actin Cytoskeleton Through Protein Kinases ROCK and LIM-kinase. *Science* **285**, 895–898.

Maeshima, Y., Colorado, P. C. and Kalluri, R. (2000). Two RGD-independent alpha vbeta 3 integrin binding sites on tumstatin regulate distinct anti-tumor properties. *J. Biol. Chem.* **275**, 23745–23750.

Main, A. L., Harvey, T. S., Baron, M., Boyd, J. and Campbell, I. D. (1992). The three-dimensional structure of the tenth type III module of fibronectin: an insight into RGD-mediated interactions. *Cell* **71**, 671–678.

Mammoto, A., Connor, K. M., Mammoto, T., Yung, C. W., Huh, D., Aderman, C. M., Mostoslavsky, G., Smith, L. E. H. and Ingber, D. E. (2009). A mechanosensitive transcriptional mechanism that controls angiogenesis. *Nature* **457**, 1103–1108.

Manabe, R., Ohe, N., Maeda, T., Fukuda, T. and Sekiguchi, K. (1997). Modulation of cell-adhesive activity of fibronectin by the alternatively spliced EDA segment. *J. Cell Biol.* **139**, 295–307.

Mandarino, L. J., Sundarraj, N., Finlayson, J. and Hassell, H. R. (1993). Regulation of fibronectin and laminin synthesis by retinal capillary endothelial cells and pericytes in vitro. *Exp. Eye Res.* **57**, 609–621.

Maqueda, A., Moyano, J. V., Hernández Del Cerro, M., Peters, D. M. and Garcia-Pardo, A. (2007). The heparin III-binding domain of fibronectin (III4-5 repeats) binds to fibronectin and inhibits fibronectin matrix assembly. *Matrix Biol. J. Int. Soc. Matrix Biol.* **26**, 642–651.

Marcoux, N. and Vuori, K. (2003). EGF receptor mediates adhesion-dependent activation of the Rac GTPase: a role for phosphatidylinositol 3-kinase and Vav2. *Oncogene* **22**, 6100–6106.

Marsden, M. and DeSimone, D. W. (2001). Regulation of cell polarity, radial intercalation and epiboly in Xenopus: novel roles for integrin and fibronectin. *Dev. Camb. Engl.* **128**, 3635–3647.

Marsden, M. and DeSimone, D. W. (2003). Integrin-ECM interactions regulate cadherin-dependent cell adhesion and are required for convergent extension in Xenopus. *Curr. Biol. CB* **13**, 1182–1191.

Martins, G. G., Rifes, P., Amândio, R., Rodrigues, G., Palmeirim, I. and Thorsteinsdóttir, S. (2009). Dynamic 3D cell rearrangements guided by a fibronectin matrix underlie somitogenesis. *PloS One* **4**, e7429.

Mason, B. N., Starchenko, A., Williams, R. M., Bonassar, L. J. and Reinhart-King, C. A. (2013). Tuning three-dimensional collagen matrix stiffness independently of collagen concentration modulates endothelial cell behavior. *Acta Biomater.* **9**, 4635–4644.

Massam-Wu, T., Chiu, M., Choudhury, R., Chaudhry, S. S., Baldwin, A. K., McGovern, A., Baldock, C., Shuttleworth, C. A. and Kielty, C. M. (2010). Assembly of fibrillin microfibrils governs extracellular deposition of latent TGFβ. *J. Cell Sci.* **123**, 3006 –3018.

Matter, C. M., Schuler, P. K., Alessi, P., Meier, P., Ricci, R., Zhang, D., Halin, C., Castellani, P., Zardi, L., Hofer, C. K., et al. (2004). Molecular imaging of atherosclerotic plaques using a human antibody against the extra-domain B of fibronectin. *Circ. Res.* **95**, 1225–1233.

May, S. R., Stewart, N. J., Chang, W. and Peterson, A. S. (2004). A Titin mutation defines roles for circulation in endothelial morphogenesis. *Dev. Biol.* **270**, 31–46.

Mayer, U., Saher, G., Fässler, R., Bornemann, A., Echtermeyer, F., von der Mark, H., Miosge, N., Pöschl, E. and von der Mark, K. (1997). Absence of integrin alpha 7 causes a novel form of muscular dystrophy. *Nat. Genet.* **17**, 318–323.

McCarty, J. H., Monahan-Earley, R. A., Brown, L. F., Keller, M., Gerhardt, H., Rubin, K., Shani, M., Dvorak, H. F., Wolburg, H., Bader, B. L., et al. (2002). Defective associations between blood vessels and brain parenchyma lead to cerebral hemorrhage in mice lacking alphav integrins. *Mol. Cell. Biol.* **22**, 7667–7677.

McCarty, J. H., Lacy-Hulbert, A., Charest, A., Bronson, R. T., Crowley, D., Housman, D., Savill, J., Roes, J. and Hynes, R. O. (2005). Selective ablation of alphav integrins in the central nervous system leads to cerebral hemorrhage, seizures, axonal degeneration and premature death. *Dev. Camb. Engl.* **132**, 165–176.

McDonald, J. A., Kelley, D. G. and Broekelmann, T. J. (1982). Role of fibronectin in collagen deposition: Fab' to the gelatin-binding domain of fibronectin inhibits both fibronectin and collagen organization in fibroblast extracellular matrix. *J. Cell Biol.* **92**, 485–492.

McDonald, J. A., Quade, B. J., Broekelmann, T. J., LaChance, R., Forsman, K., Hasegawa, E. and Akiyama, S. (1987). Fibronectin's cell-adhesive domain and an amino-terminal matrix assembly domain participate in its assembly into fibroblast pericellular matrix. *J. Biol. Chem.* **262**, 2957–2967.

McDonald, P. C., Oloumi, A., Mills, J., Dobreva, I., Maidan, M., Gray, V., Wederell, E. D., Bally, M. B., Foster, L. J. and Dedhar, S. (2008). Rictor and integrin-linked kinase interact and regulate Akt phosphorylation and cancer cell survival. *Cancer Res.* **68**, 1618–1624.

McGrath, K. E. (2003). Circulation is established in a stepwise pattern in the mammalian embryo. *Blood* **101**, 1669–1675.

McGrath, K. E. and Palis, J. (2005). Hematopoiesis in the yolk sac: more than meets the eye. *Exp. Hematol.* **33**, 1021–1028.

McHugh, K. P., Hodivala-Dilke, K., Zheng, M. H., Namba, N., Lam, J., Novack, D., Feng, X., Ross, F. P., Hynes, R. O. and Teitelbaum, S. L. (2000). Mice lacking beta3 integrins are osteosclerotic because of dysfunctional osteoclasts. *J. Clin. Invest.* **105**, 433–440.

McKeown-Longo, P. J. and Mosher, D. F. (1983). Binding of plasma fibronectin to cell layers of human skin fibroblasts. *J. Cell Biol.* **97**, 466–472.

McKeown-Longo, P. J. and Mosher, D. F. (1985). Interaction of the 70,000-mol-wt amino-terminal fragment of fibronectin with the matrix-assembly receptor of fibroblasts. *J. Cell Biol.* **100**, 364–374.

Meredith, J. E., Jr, Fazeli, B. and Schwartz, M. A. (1993). The extracellular matrix as a cell survival factor. *Mol. Biol. Cell* **4**, 953–961.

Millis, A. J., Hoyle, M., Mann, D. M. and Brennan, M. J. (1985). Incorporation of cellular and plasma fibronectins into smooth muscle cell extracellular matrix in vitro. *Proc. Natl. Acad. Sci. U. S. A.* **82**, 2746–2750.

Mittal, A., Pulina, M., Hou, S.-Y. and Astrof, S. (2010). Fibronectin and integrin alpha 5 play essential roles in the development of the cardiac neural crest. *Mech. Dev.* **127**, 472–484.

Miyamoto, S., Akiyama, S. K. and Yamada, K. M. (1995). Synergistic roles for receptor occupancy and aggregation in integrin transmembrane function. *Science* **267**, 883–885.

Miyamoto, S., Teramoto, H., Gutkind, J. S. and Yamada, K. M. (1996). Integrins can collaborate with growth factors for phosphorylation of receptor tyrosine kinases and MAP kinase activation: roles of integrin aggregation and occupancy of receptors. *J. Cell Biol.* **135**, 1633–1642.

Miyazono, K. and Heldin, C. H. (1989). Role for carbohydrate structures in TGF-beta 1 latency. *Nature* **338**, 158–160.

Miyazono, K., Olofsson, A., Colosetti, P. and Heldin, C. H. (1991). A role of the latent TGF-beta 1-binding protein in the assembly and secretion of TGF-beta 1. *EMBO J.* **10**, 1091–1101.

Miyazono, K., Maeda, S. and Imamura, T. (2005). BMP receptor signaling: transcriptional targets, regulation of signals, and signaling cross-talk. *Cytokine Growth Factor Rev.* **16**, 251–263.

Mjaatvedt, C. H., Lepera, R. C. and Markwald, R. R. (1987). Myocardial specificity for initiating endothelial-mesenchymal cell transition in embryonic chick heart correlates with a particulate distribution of fibronectin. *Dev. Biol.* **119**, 59–67.

Mjaatvedt, C. H., Nakaoka, T., Moreno-Rodriguez, R., Norris, R. A., Kern, M. J., Eisenberg, C. A., Turner, D. and Markwald, R. R. (2001). The outflow tract of the heart is recruited from a novel heart-forming field. *Dev. Biol.* **238**, 97–109.

Montanez, E., Ussar, S., Schifferer, M., Bösl, M., Zent, R., Moser, M. and Fässler, R. (2008). Kindlin-2 controls bidirectional signaling of integrins. *Genes Dev.* **22**, 1325–1330.

Moore, S. W., Keller, R. E. and Koehl, M. A. (1995). The dorsal involuting marginal zone stiffens anisotropically during its convergent extension in the gastrula of Xenopus laevis. *Dev. Camb. Engl.* **121**, 3131–3140.

Moorman, A. F. M., de Jong, F., Denyn, M. M. F. J. and Lamers, W. H. (1998). Development of the Cardiac Conduction System. *Circ. Res.* **82**, 629–644.

Moretti, F. A., Chauhan, A. K., Iaconcig, A., Porro, F., Baralle, F. E. and Muro, A. F. (2007). A major fraction of fibronectin present in the extracellular matrix of tissues is plasma-derived. *J. Biol. Chem.* **282**, 28057–28062.

Morgan, M. R., Humphries, M. J. and Bass, M. D. (2007). Synergistic control of cell adhesion by integrins and syndecans. *Nat. Rev. Mol. Cell Biol.* **8**, 957–969.

Moro, L., Venturino, M., Bozzo, C., Silengo, L., Altruda, F., Beguinot, L., Tarone, G. and Defilippi, P. (1998). Integrins induce activation of EGF receptor: role in MAP kinase induction and adhesion-dependent cell survival. *EMBO J.* **17**, 6622–6632.

Moro, L., Dolce, L., Cabodi, S., Bergatto, E., Boeri Erba, E., Smeriglio, M., Turco, E., Retta, S. F., Giuffrida, M. G., Venturino, M., et al. (2002). Integrin-induced epidermal growth factor (EGF) receptor activation requires c-Src and p130Cas and leads to phosphorylation of specific EGF receptor tyrosines. *J. Biol. Chem.* **277**, 9405–9414.

Moser, M., Nieswandt, B., Ussar, S., Pozgajova, M. and Fässler, R. (2008). Kindlin-3 is essential for integrin activation and platelet aggregation. *Nat. Med.* **14**, 325–330.

Moser, M., Bauer, M., Schmid, S., Ruppert, R., Schmidt, S., Sixt, M., Wang, H.-V., Sperandio, M. and Fässler, R. (2009a). Kindlin-3 is required for beta2 integrin-mediated leukocyte adhesion to endothelial cells. *Nat. Med.* **15**, 300–305.

Moser, M., Legate, K. R., Zent, R. and Fässler, R. (2009b). The tail of integrins, talin, and kindlins. *Science* **324**, 895–899.

Mosher, D. F. (1975). Cross-linking of cold-insoluble globulin by fibrin-stabilizing factor. *J. Biol. Chem.* **250**, 6614–6621.

Mould, A. P., Komoriya, A., Yamada, K. M. and Humphries, M. J. (1991). The CS5 peptide is a second site in the IIICS region of fibronectin recognized by the integrin alpha 4 beta 1. Inhibition of alpha 4 beta 1 function by RGD peptide homologues. *J. Biol. Chem.* **266**, 3579–3585.

Mu, D., Cambier, S., Fjellbirkeland, L., Baron, J. L., Munger, J. S., Kawakatsu, H., Sheppard, D., Broaddus, V. C. and Nishimura, S. L. (2002). The integrin αvβ8 mediates epithelial homeostasis through MT1-MMP–dependent activation of TGF-β1. *J. Cell Biol.* **157**, 493–507.

Muether, P. S., Dell, S., Kociok, N., Zahn, G., Stragies, R., Vossmeyer, D. and Joussen, A. M. (2007). The role of integrin alpha5beta1 in the regulation of corneal neovascularization. *Exp. Eye Res.* **85**, 356–365.

Müller, U., Wang, D., Denda, S., Meneses, J. J., Pedersen, R. A. and Reichardt, L. F. (1997). Integrin alpha8beta1 is critically important for epithelial-mesenchymal interactions during kidney morphogenesis. *Cell* **88**, 603–613.

Munger, J. S., Huang, X., Kawakatsu, H., Griffiths, M. J., Dalton, S. L., Wu, J., Pittet, J. F., Kaminski, N., Garat, C., Matthay, M. A., et al. (1999). The integrin alpha v beta 6 binds and activates latent TGF beta 1: a mechanism for regulating pulmonary inflammation and fibrosis. *Cell* **96**, 319–328.

Muro, A. F., Chauhan, A. K., Gajovic, S., Iaconcig, A., Porro, F., Stanta, G. and Baralle, F. E. (2003). Regulated splicing of the fibronectin EDA exon is essential for proper skin wound healing and normal lifespan. *J. Cell Biol.* **162**, 149–160.

Muro, A. F., Moretti, F. A., Moore, B. B., Yan, M., Atrasz, R. G., Wilke, C. A., Flaherty, K. R., Martinez, F. J., Tsui, J. L., Sheppard, D., et al. (2008). An essential role for fibronectin extra type III domain A in pulmonary fibrosis. *Am. J. Respir. Crit. Care Med.* **177**, 638–645.

Nagai, T., Yamakawa, N., Aota, S., Yamada, S. S., Akiyama, S. K., Olden, K. and Yamada, K. M. (1991). Monoclonal antibody characterization of two distant sites required for function of the central cell-binding domain of fibronectin in cell adhesion, cell migration, and matrix assembly. *J. Cell Biol.* **114**, 1295–1305.

Nejjari, M., Hafdi, Z., Dumortier, J., Bringuier, A. F., Feldmann, G. and Scoazec, J. Y. (1999). alpha6beta1 integrin expression in hepatocarcinoma cells: regulation and role in cell adhesion and migration. *Int. J. Cancer J. Int. Cancer* **83**, 518–525.

Neptune, E. R., Frischmeyer, P. A., Arking, D. E., Myers, L., Bunton, T. E., Gayraud, B., Ramirez, F., Sakai, L. Y. and Dietz, H. C. (2003). Dysregulation of TGF-beta activation contributes to pathogenesis in Marfan syndrome. *Nat. Genet.* **33**, 407–411.

Ni, H., Yuen, P. S. T., Papalia, J. M., Trevithick, J. E., Sakai, T., Fässler, R., Hynes, R. O. and Wagner, D. D. (2003). Plasma fibronectin promotes thrombus growth and stability in injured arterioles. *Proc. Natl. Acad. Sci. U. S. A.* **100**, 2415–2419.

Nielsen, J. S. and McNagny, K. M. (2008). Novel functions of the CD34 family. *J. Cell Sci.* **121**, 3683–3692.

Nojima, Y., Humphries, M. J., Mould, A. P., Komoriya, A., Yamada, K. M., Schlossman, S. F. and Morimoto, C. (1990). VLA-4 mediates CD3-dependent CD4+ T cell activation via the CS1 alternatively spliced domain of fibronectin. *J. Exp. Med.* **172**, 1185–1192.

Norton, J. D. (2000). ID helix-loop-helix proteins in cell growth, differentiation and tumorigenesis. *J. Cell Sci.* **113 (Pt 22)**, 3897–3905.

Nunes, I., Gleizes, P. E., Metz, C. N. and Rifkin, D. B. (1997). Latent transforming growth factor-beta binding protein domains involved in activation and transglutaminase-dependent cross-linking of latent transforming growth factor-beta. *J. Cell Biol.* **136**, 1151–1163.

Oh, S. P., Seki, T., Goss, K. A., Imamura, T., Yi, Y., Donahoe, P. K., Li, L., Miyazono, K., ten Dijke, P., Kim, S., et al. (2000). Activin receptor-like kinase 1 modulates transforming growth factor-beta 1 signaling in the regulation of angiogenesis. *Proc. Natl. Acad. Sci. U. S. A.* **97**, 2626–2631.

Ohashi, K. (2000). Rho-associated Kinase ROCK Activates LIM-kinase 1 by Phosphorylation at Threonine 508 within the Activation Loop. *J. Biol. Chem.* **275**, 3577–3582.

Ohashi, T. and Erickson, H. P. (2009). Revisiting the mystery of fibronectin multimers: the fibronectin matrix is composed of fibronectin dimers cross-linked by non-covalent bonds. *Matrix Biol. J. Int. Soc. Matrix Biol.* **28**, 170–175.

Ohashi, T., Kiehart, D. P. and Erickson, H. P. (2002). Dual labeling of the fibronectin matrix and actin cytoskeleton with green fluorescent protein variants. *J. Cell Sci.* **115**, 1221–1229.

Olorundare, O. E., Peyruchaud, O., Albrecht, R. M. and Mosher, D. F. (2001). Assembly of a fibronectin matrix by adherent platelets stimulated by lysophosphatidic acid and other agonists. *Blood* **98**, 117–124.

Orlidge, A. and D'Amore, P. A. (1987). Inhibition of capillary endothelial cell growth by pericytes and smooth muscle cells. *J. Cell Biol.* **105**, 1455 –1462.

Oshima, M., Oshima, H. and Taketo, M. M. (1996). TGF-beta receptor type II deficiency results in defects of yolk sac hematopoiesis and vasculogenesis. *Dev. Biol.* **179**, 297–302.

Oyama, F., Murata, Y., Suganuma, N., Kimura, T., Titani, K. and Sekiguchi, K. (1989). Patterns of alternative splicing of fibronectin pre-mRNA in human adult and fetal tissues. *Biochemistry (Mosc.)* **28**, 1428–1434.

Pagani, F., Zagato, L., Vergani, C., Casari, G., Sidoli, A. and Baralle, F. E. (1991). Tissue-specific splicing pattern of fibronectin messenger RNA precursor during development and aging in rat. *J. Cell Biol.* **113**, 1223–1229.

Palis, J. and Yoder, M. C. (2001). Yolk-sac hematopoiesis: the first blood cells of mouse and man. *Exp. Hematol.* **29**, 927–936.

Pankov, R. and Yamada, K. M. (2004). Non-radioactive quantification of fibronectin matrix assembly. *Curr. Protoc. Cell Biol. Editor. Board Juan Bonifacino Al* **Chapter 10**, Unit 10.13.

Pankov, R., Cukierman, E., Katz, B. Z., Matsumoto, K., Lin, D. C., Lin, S., Hahn, C. and Yamada, K. M. (2000). Integrin dynamics and matrix assembly: tensin-dependent translocation of alpha(5)beta(1) integrins promotes early fibronectin fibrillogenesis. *J. Cell Biol.* **148**, 1075–1090.

Park, J. E., Keller, G. A. and Ferrara, N. (1993). The vascular endothelial growth factor (VEGF) isoforms: differential deposition into the subepithelial extracellular matrix and bioactivity of extracellular matrix-bound VEGF. *Mol. Biol. Cell* **4**, 1317–1326.

Parsons, J. T., Horwitz, A. R. and Schwartz, M. A. (2010). Cell adhesion: integrating cytoskeletal dynamics and cellular tension. *Nat. Rev. Mol. Cell Biol.* **11**, 633–643.

Paszek, M. J., Zahir, N., Johnson, K. R., Lakins, J. N., Rozenberg, G. I., Gefen, A., Reinhart-King, C. A., Margulies, S. S., Dembo, M., Boettiger, D., et al. (2005). Tensional homeostasis and the malignant phenotype. *Cancer Cell* **8**, 241–254.

Pelham, R. J., Jr and Wang, Y. l (1997). Cell locomotion and focal adhesions are regulated by substrate flexibility. *Proc. Natl. Acad. Sci. U. S. A.* **94**, 13661–13665.

Pepper, M. S. (1997). Transforming growth factor-beta: vasculogenesis, angiogenesis, and vessel wall integrity. *Cytokine Growth Factor Rev.* **8**, 21–43.

Pepper, M. S. (2001). Role of the matrix metalloproteinase and plasminogen activator-plasmin systems in angiogenesis. *Arterioscler. Thromb. Vasc. Biol.* **21**, 1104–1117.

Pepper, M. S., Belin, D., Montesano, R., Orci, L. and Vassalli, J. D. (1990). Transforming growth factor-beta 1 modulates basic fibroblast growth factor-induced proteolytic and angiogenic properties of endothelial cells in vitro. *J. Cell Biol.* **111**, 743–755.

Pereira, M., Rybarczyk, B. J., Odrljin, T. M., Hocking, D. C., Sottile, J. and Simpson-Haidaris, P. J. (2002). The incorporation of fibrinogen into extracellular matrix is dependent on active assembly of a fibronectin matrix. *J. Cell Sci.* **115**, 609–617.

Perruzzi, C. A., de Fougerolles, A. R., Koteliansky, V. E., Whelan, M. C., Westlin, W. F. and Senger, D. R. (2003). Functional overlap and cooperativity among alphav and beta1 integrin subfamilies during skin angiogenesis. *J. Invest. Dermatol.* **120**, 1100–1109.

Peters, J., Sechrist, J., Luetolf, S., Loredo, G. and Bronner-Fraser, M. (2002). Spatial expression of the alternatively spliced EIIIB and EIIIA segments of fibronectin in the early chicken embryo. *Cell Commun. Adhes.* **9**, 221–238.

Petersen, T. E., Thøgersen, H. C., Skorstengaard, K., Vibe-Pedersen, K., Sahl, P., Sottrup-Jensen, L. and Magnusson, S. (1983). Partial primary structure of bovine plasma fibronectin: three types of internal homology. *Proc. Natl. Acad. Sci. U. S. A.* **80**, 137–141.

Petitclerc, E., Boutaud, A., Prestayko, A., Xu, J., Sado, Y., Ninomiya, Y., Sarras, M. P., Jr, Hudson, B. G. and Brooks, P. C. (2000). New functions for non-collagenous domains of human collagen type IV. Novel integrin ligands inhibiting angiogenesis and tumor growth in vivo. *J. Biol. Chem.* **275**, 8051–8061.

Peyton, S. R. and Putnam, A. J. (2005). Extracellular matrix rigidity governs smooth muscle cell motility in a biphasic fashion. *J. Cell. Physiol.* **204**, 198–209.

Pierschbacher, M. D. and Ruoslahti, E. (1984a). Cell attachment activity of fibronectin can be duplicated by small synthetic fragments of the molecule. *Nature* **309**, 30–33.

Pierschbacher, M. D. and Ruoslahti, E. (1984b). Variants of the cell recognition site of fibronectin that retain attachment-promoting activity. *Proc. Natl. Acad. Sci. U. S. A.* **81**, 5985–5988.

Pierschbacher, M., Hayman, E. G. and Ruoslahti, E. (1983). Synthetic peptide with cell attachment activity of fibronectin. *Proc. Natl. Acad. Sci. U. S. A.* **80**, 1224–1227.

Plow, E. F., Pierschbacher, M. D., Ruoslahti, E., Marguerie, G. A. and Ginsberg, M. H. (1985). The effect of Arg-Gly-Asp-containing peptides on fibrinogen and von Willebrand factor binding to platelets. *Proc. Natl. Acad. Sci. U. S. A.* **82**, 8057–8061.

Podar, K., Tai, Y.-T., Lin, B. K., Narsimhan, R. P., Sattler, M., Kijima, T., Salgia, R., Gupta, D., Chauhan, D. and Anderson, K. C. (2002). Vascular endothelial growth factor-induced migration of multiple myeloma cells is associated with beta 1 integrin- and phosphatidylinositol 3-kinase-dependent PKC alpha activation. *J. Biol. Chem.* **277**, 7875–7881.

Popova, S. N., Barczyk, M., Tiger, C.-F., Beertsen, W., Zigrino, P., Aszodi, A., Miosge, N., Forsberg, E. and Gullberg, D. (2007). Alpha11 beta1 integrin-dependent regulation of periodontal ligament function in the erupting mouse incisor. *Mol. Cell. Biol.* **27**, 4306–4316.

Pozzi, A., Moberg, P. E., Miles, L. A., Wagner, S., Soloway, P. and Gardner, H. A. (2000). Elevated matrix metalloprotease and angiostatin levels in integrin alpha 1 knockout mice cause reduced tumor vascularization. *Proc. Natl. Acad. Sci. U. S. A.* **97**, 2202–2207.

Prewitz, M. C., Seib, F. P., von Bonin, M., Friedrichs, J., Stißel, A., Niehage, C., Müller, K., Anastassiadis, K., Waskow, C., Hoflack, B., et al. (2013). Tightly anchored tissue-mimetic matrices as instructive stem cell microenvironments. *Nat. Methods* **10**, 788–794.

Priestley, G. V., Ulyanova, T. and Papayannopoulou, T. (2007). Sustained alterations in biodistribution of stem/progenitor cells in Tie2Cre+ alpha4(f/f) mice are hematopoietic cell autonomous. *Blood* **109**, 109–111.

Pulina, M. V., Hou, S.-Y., Mittal, A., Julich, D., Whittaker, C. A., Holley, S. A., Hynes, R. O. and Astrof, S. (2011). Essential roles of fibronectin in the development of the left–right embryonic body plan. *Dev. Biol.* **354**, 208–220.

Qu, H., Tu, Y., Shi, X., Larjava, H., Saleem, M. A., Shattil, S. J., Fukuda, K., Qin, J., Kretzler, M. and Wu, C. (2011). Kindlin-2 regulates podocyte adhesion and fibronectin matrix deposition through interactions with phosphoinositides and integrins. *J. Cell Sci.* **124**, 879–891.

Quade, B. J. and McDonald, J. A. (1988). Fibronectin's amino-terminal matrix assembly site is located within the 29-kDa amino-terminal domain containing five type I repeats. *J. Biol. Chem.* **263**, 19602–19609.

Rahman, S., Patel, Y., Murray, J., Patel, K. V., Sumathipala, R., Sobel, M. and Wijelath, E. S. (2005). Novel hepatocyte growth factor (HGF) binding domains on fibronectin and vitronectin coordinate a distinct and amplified Met-integrin induced signalling pathway in endothelial cells. *BMC Cell Biol.* **6**, 8.

Ramasubramanian, A., Nerurkar, N. L., Achtien, K. H., Filas, B. A., Voronov, D. A. and Taber, L. A. (2008). On modeling morphogenesis of the looping heart following mechanical perturbations. *J. Biomech. Eng.* **130**, 061018.

Ramirez, F. and Pereira, L. (1999). The fibrillins. *Int. J. Biochem. Cell Biol.* **31**, 255–259.

Rantala, J. K., Pouwels, J., Pellinen, T., Veltel, S., Laasola, P., Mattila, E., Potter, C. S., Duffy, T., Sundberg, J. P., Kallioniemi, O., et al. (2011). SHARPIN is an endogenous inhibitor of β1-integrin activation. *Nat. Cell Biol.* **13**, 1315–1324.

Redick, S. D., Settles, D. L., Briscoe, G. and Erickson, H. P. (2000). Defining fibronectin's cell adhesion synergy site by site-directed mutagenesis. *J. Cell Biol.* **149**, 521–527.

Rehn, M., Veikkola, T., Kukk-Valdre, E., Nakamura, H., Ilmonen, M., Lombardo, C., Pihlajaniemi, T., Alitalo, K. and Vuori, K. (2001). Interaction of endostatin with integrins implicated in angiogenesis. *Proc. Natl. Acad. Sci. U. S. A.* **98**, 1024–1029.

Reynolds, L. E., Wyder, L., Lively, J. C., Taverna, D., Robinson, S. D., Huang, X., Sheppard, D., Hynes, R. O. and Hodivala-Dilke, K. M. (2002). Enhanced pathological angiogenesis in mice lacking beta3 integrin or beta3 and beta5 integrins. *Nat. Med.* **8**, 27–34.

Ribeiro, S. M., Poczatek, M., Schultz-Cherry, S., Villain, M. and Murphy-Ullrich, J. E. (1999). The activation sequence of thrombospondin-1 interacts with the latency-associated peptide to regulate activation of latent transforming growth factor-beta. *J. Biol. Chem.* **274**, 13586–13593.

Rifkin, D. B. (2005). Latent Transforming Growth Factor-β (TGF-β) Binding Proteins: Orchestrators of TGF-β Availability. *J. Biol. Chem.* **280**, 7409–7412.

Riikonen, T., Koivisto, L., Vihinen, P. and Heino, J. (1995). Transforming growth factor-beta regulates collagen gel contraction by increasing alpha 2 beta 1 integrin expression in osteogenic cells. *J. Biol. Chem.* **270**, 376–382.

Risau, W. (1997). Mechanisms of angiogenesis. *Nature* **386**, 671–674.

Risau, W. and Flamme, I. (1995). Vasculogenesis. *Annu. Rev. Cell Dev. Biol.* **11**, 73–91.

Risau, W. and Lemmon, V. (1988). Changes in the vascular extracellular matrix during embryonic vasculogenesis and angiogenesis. *Dev. Biol.* **125**, 441–450.

Riveline, D., Zamir, E., Balaban, N. Q., Schwarz, U. S., Ishizaki, T., Narumiya, S., Kam, Z., Geiger, B. and Bershadsky, A. D. (2001). Focal contacts as mechanosensors: externally applied local mechanical force induces growth of focal contacts by an mDia1-dependent and ROCK-independent mechanism. *J. Cell Biol.* **153**, 1175–1186.

Roberts, A. B., Sporn, M. B., Assoian, R. K., Smith, J. M., Roche, N. S., Wakefield, L. M., Heine, U. I., Liotta, L. A., Falanga, V. and Kehrl, J. H. (1986). Transforming growth factor type beta: rapid induction of fibrosis and angiogenesis in vivo and stimulation of collagen formation in vitro. *Proc. Natl. Acad. Sci. U. S. A.* **83**, 4167–4171.

Roca, C. and Adams, R. H. (2007). Regulation of vascular morphogenesis by Notch signaling. *Genes Dev.* **21**, 2511–2524.

Rodriguez-Manzaneque, J. C., Lane, T. F., Ortega, M. A., Hynes, R. O., Lawler, J. and Iruela-Arispe, M. L. (2001). Thrombospondin-1 suppresses spontaneous tumor growth and inhibits activation of matrix metalloproteinase-9 and mobilization of vascular endothelial growth factor. *Proc. Natl. Acad. Sci. U. S. A.* **98**, 12485–12490.

Roman, J. and McDonald, J. A. (1992). Expression of fibronectin, the integrin alpha 5, and alpha-smooth muscle actin in heart and lung development. *Am. J. Respir. Cell Mol. Biol.* **6**, 472–480.

Roman, J. and McDonald, J. A. (1993). Fibulin's organization into the extracellular matrix of fetal lung fibroblasts is dependent on fibronectin matrix assembly. *Am. J. Respir. Cell Mol. Biol.* **8**, 538–545.

Roovers, K., Davey, G., Zhu, X., Bottazzi, M. E. and Assoian, R. K. (1999). Alpha5beta1 integrin controls cyclin D1 expression by sustaining mitogen-activated protein kinase activity in growth factor-treated cells. *Mol. Biol. Cell* **10**, 3197–3204.

Rossant, J. and Cross, J. C. (2001). Placental development: lessons from mouse mutants. *Nat. Rev. Genet.* **2**, 538–548.

Rucker, H. K., Wynder, H. J. and Thomas, W. E. (2000). Cellular mechanisms of CNS pericytes. *Brain Res. Bull.* **51**, 363–369.

Ruhrberg, C. (2003). Growing and shaping the vascular tree: multiple roles for VEGF. *BioEssays News Rev. Mol. Cell. Dev. Biol.* **25**, 1052–1060.

Ruhrberg, C., Gerhardt, H., Golding, M., Watson, R., Ioannidou, S., Fujisawa, H., Betsholtz, C. and Shima, D. T. (2002). Spatially restricted patterning cues provided by heparin-binding VEGF-A control blood vessel branching morphogenesis. *Genes Dev.* **16**, 2684–2698.

Sabatier, L., Chen, D., Fagotto-Kaufmann, C., Hubmacher, D., McKee, M. D., Annis, D. S., Mosher, D. F. and Reinhardt, D. P. (2009). Fibrillin Assembly Requires Fibronectin. *Mol. Biol. Cell* **20**, 846–858.

Saga, Y., Yagi, T., Ikawa, Y., Sakakura, T. and Aizawa, S. (1992). Mice develop normally without tenascin. *Genes Dev.* **6**, 1821–1831.

Saharinen, J. and Keski-Oja, J. (2000). Specific sequence motif of 8-Cys repeats of TGF-beta binding proteins, LTBPs, creates a hydrophobic interaction surface for binding of small latent TGF-beta. *Mol. Biol. Cell* **11**, 2691–2704.

Saharinen, J., Taipale, J. and Keski-Oja, J. (1996). Association of the small latent transforming growth factor-beta with an eight cysteine repeat of its binding protein LTBP-1. *EMBO J.* **15**, 245–253.

Sakai, T., Johnson, K. J., Murozono, M., Sakai, K., Magnuson, M. A., Wieloch, T., Cronberg, T., Isshiki, A., Erickson, H. P. and Fässler, R. (2001). Plasma fibronectin supports neuronal survival and reduces brain injury following transient focal cerebral ischemia but is not essential for skin-wound healing and hemostasis. *Nat. Med.* **7**, 324–330.

Sakai, T., Larsen, M. and Yamada, K. M. (2003). Fibronectin requirement in branching morphogenesis. *Nature* **423**, 876–881.

Saltel, F., Mortier, E., Hytönen, V. P., Jacquier, M.-C., Zimmermann, P., Vogel, V., Liu, W. and Wehrle-Haller, B. (2009). New PI(4,5)P2- and membrane proximal integrin-binding motifs in the talin head control beta3-integrin clustering. *J. Cell Biol.* **187**, 715–731.

Sanders, E. J. (1982). Ultrastructural immunocytochemical localization of fibronectin in the early chick embryo. *J. Embryol. Exp. Morphol.* **71**, 155–170.

Sanford, L. P., Ormsby, I., Gittenberger-de Groot, A. C., Sariola, H., Friedman, R., Boivin, G. P., Cardell, E. L. and Doetschman, T. (1997). TGFbeta2 knockout mice have multiple developmental defects that are non-overlapping with other TGFbeta knockout phenotypes. *Dev. Camb. Engl.* **124**, 2659–2670.

Sato and Rifkin, D. B. (1989). Inhibition of endothelial cell movement by pericytes and smooth muscle cells: activation of a latent transforming growth factor-beta 1-like molecule by plasmin during co-culture. *J. Cell Biol.* **109**, 309–315.

Sato, Y., Tsuboi, R., Lyons, R., Moses, H. and Rifkin, D. B. (1990). Characterization of the activation of latent TGF-beta by co-cultures of endothelial cells and pericytes or smooth muscle cells: a self-regulating system. *J. Cell Biol.* **111**, 757–763.

Saunders, S. and Bernfield, M. (1988). Cell surface proteoglycan binds mouse mammary epithelial cells to fibronectin and behaves as a receptor for interstitial matrix. *J. Cell Biol.* **106**, 423–430.

Savolainen, S. M., Foley, J. F. and Elmore, S. A. (2009). Histology atlas of the developing mouse heart with emphasis on E11.5 to E18.5. *Toxicol. Pathol.* **37**, 395–414.

Sawdey, M., Podor, T. J. and Loskutoff, D. J. (1989). Regulation of type 1 plasminogen activator inhibitor gene expression in cultured bovine aortic endothelial cells. Induction by transforming growth factor-beta, lipopolysaccharide, and tumor necrosis factor-alpha. *J. Biol. Chem.* **264**, 10396–10401.

Schaller, M. D., Hildebrand, J. D., Shannon, J. D., Fox, J. W., Vines, R. R. and Parsons, J. T. (1994). Autophosphorylation of the focal adhesion kinase, pp125FAK, directs SH2-dependent binding of pp60src. *Mol. Cell. Biol.* **14**, 1680–1688.

Scharffetter-Kochanek, K., Lu, H., Norman, K., van Nood, N., Munoz, F., Grabbe, S., McArthur, M., Lorenzo, I., Kaplan, S., Ley, K., et al. (1998). Spontaneous skin ulceration and defective T cell function in CD18 null mice. *J. Exp. Med.* **188**, 119–131.

Schiefner, A., Gebauer, M. and Skerra, A. (2012). Extra-domain B in oncofetal fibronectin structurally promotes fibrillar head-to-tail dimerization of extracellular matrix protein. *J. Biol. Chem.* **287**, 17578–17588.

Schiller, H. B. and Fässler, R. (2013). Mechanosensitivity and compositional dynamics of cell-matrix adhesions. *EMBO Rep.* **14**, 509–519.

Schlaepfer, D. D., Hanks, S. K., Hunter, T. and van der Geer, P. (1994). Integrin-mediated signal transduction linked to Ras pathway by GRB2 binding to focal adhesion kinase. *Nature* **372**, 786–791.

Schmits, R., Kündig, T. M., Baker, D. M., Shumaker, G., Simard, J. J., Duncan, G., Wakeham, A., Shahinian, A., van der Heiden, A., Bachmann, M. F., et al. (1996). LFA-1-deficient mice show normal CTL responses to virus but fail to reject immunogenic tumor. *J. Exp. Med.* **183**, 1415–1426.

Schneider, A., Zhang, Y., Guan, Y., Davis, L. S. and Breyer, M. D. (2003). Differential, inducible gene targeting in renal epithelia, vascular endothelium, and viscera of Mx1Cre mice. *Am. J. Physiol. Renal Physiol.* **284**, F411–417.

Schön, M. P., Arya, A., Murphy, E. A., Adams, C. M., Strauch, U. G., Agace, W. W., Marsal, J., Donohue, J. P., Her, H., Beier, D. R., et al. (1999). Mucosal T lymphocyte numbers are selectively reduced in integrin alpha E (CD103)-deficient mice. *J. Immunol. Baltim. Md 1950* **162**, 6641–6649.

Schwarz-Linek, U., Höök, M. and Potts, J. R. (2006). Fibronectin-binding proteins of gram-positive cocci. *Microbes Infect. Inst. Pasteur* **8**, 2291–2298.

Schwarzbauer, J. E. (1991). Identification of the fibronectin sequences required for assembly of a fibrillar matrix. *J. Cell Biol.* **113**, 1463–1473.

Schwarzbauer, J. E. and DeSimone, D. W. (2011). Fibronectins, their fibrillogenesis, and in vivo functions. *Cold Spring Harb. Perspect. Biol.* **3**,.

Schwarzbauer, J. E., Tamkun, J. W., Lemischka, I. R. and Hynes, R. O. (1983). Three different fibronectin mRNAs arise by alternative splicing within the coding region. *Cell* **35**, 421–431.

Schwarzbauer, J. E., Patel, R. S., Fonda, D. and Hynes, R. O. (1987). Multiple sites of alternative splicing of the rat fibronectin gene transcript. *EMBO J.* **6**, 2573–2580.

Sechler, J. L., Corbett, S. A. and Schwarzbauer, J. E. (1997). Modulatory roles for integrin activation and the synergy site of fibronectin during matrix assembly. *Mol. Biol. Cell* **8**, 2563–2573.

Sechler, J. L., Cumiskey, A. M., Gazzola, D. M. and Schwarzbauer, J. E. (2000). A novel RGD-independent fibronectin assembly pathway initiated by alpha4beta1 integrin binding to the alternatively spliced V region. *J. Cell Sci.* **113 (Pt 8)**, 1491–1498.

Sechler, J. L., Rao, H., Cumiskey, A. M., Vega-Colón, I., Smith, M. S., Murata, T. and Schwarzbauer, J. E. (2001). A novel fibronectin binding site required for fibronectin fibril growth during matrix assembly. *J. Cell Biol.* **154**, 1081–1088.

Seki, T., Hong, K.-H. and Oh, S. P. (2006). Nonoverlapping expression patterns of ALK1 and ALK5 reveal distinct roles of each receptor in vascular development. *Lab. Investig. J. Tech. Methods Pathol.* **86**, 116–129.

Sengbusch, J. K., He, W., Pinco, K. A. and Yang, J. T. (2002). Dual functions of [alpha]4[beta]1 integrin in epicardial development: initial migration and long-term attachment. *J. Cell Biol.* **157**, 873–882.

Senger, D. R., Perruzzi, C. A., Streit, M., Koteliansky, V. E., de Fougerolles, A. R. and Detmar, M. (2002). The alpha(1)beta(1) and alpha(2)beta(1) integrins provide critical support for vascular endothelial growth factor signaling, endothelial cell migration, and tumor angiogenesis. *Am. J. Pathol.* **160**, 195–204.

Shattil, S. J., Kim, C. and Ginsberg, M. H. (2010). The final steps of integrin activation: the end game. *Nat. Rev. Mol. Cell Biol.* **11**, 288–300.

Shepro, D. and Morel, N. M. (1993). Pericyte physiology. *FASEB J. Off. Publ. Fed. Am. Soc. Exp. Biol.* **7**, 1031–1038.

Shi, Q. and Boettiger, D. (2003). A novel mode for integrin-mediated signaling: tethering is required for phosphorylation of FAK Y397. *Mol. Biol. Cell* **14**, 4306–4315.

Shi, X., Ma, Y.-Q., Tu, Y., Chen, K., Wu, S., Fukuda, K., Qin, J., Plow, E. F. and Wu, C. (2007). The MIG-2/integrin interaction strengthens cell-matrix adhesion and modulates cell motility. *J. Biol. Chem.* **282**, 20455–20466.

Shier, P., Otulakowski, G., Ngo, K., Panakos, J., Chourmouzis, E., Christjansen, L., Lau, C. Y. and Fung-Leung, W. P. (1996). Impaired immune responses toward alloantigens and tumor cells but normal thymic selection in mice deficient in the beta2 integrin leukocyte function-associated antigen-1. *J. Immunol. Baltim. Md 1950* **157**, 5375–5386.

Shinde, A. V., Bystroff, C., Wang, C., Vogelezang, M. G., Vincent, P. A., Hynes, R. O. and Van De Water, L. (2008). Identification of the peptide sequences within the EIIIA (EDA) segment of fibronectin that mediate integrin alpha9beta1-dependent cellular activities. *J. Biol. Chem.* **283**, 2858–2870.

Short, S. M., Talbott, G. A. and Juliano, R. L. (1998). Integrin-mediated signaling events in human endothelial cells. *Mol. Biol. Cell* **9**, 1969–1980.

Shull, M. M., Ormsby, I., Kier, A. B., Pawlowski, S., Diebold, R. J., Yin, M., Allen, R., Sidman, C., Proetzel, G. and Calvin, D. (1992). Targeted disruption of the mouse transforming growth factor-beta 1 gene results in multifocal inflammatory disease. *Nature* **359**, 693–699.

Siekmann, A. F. and Lawson, N. D. (2007). Notch signalling limits angiogenic cell behaviour in developing zebrafish arteries. *Nature* **445**, 781–784.

Singh, P., Carraher, C. and Schwarzbauer, J. E. (2010). Assembly of fibronectin extracellular matrix. *Annu. Rev. Cell Dev. Biol.* **26**, 397–419.

Sinha, S. (2004). Transforming growth factor- 1 signaling contributes to development of smooth muscle cells from embryonic stem cells. *AJP Cell Physiol.* **287**, C1560–C1568.

Slack-Davis, J. K., Eblen, S. T., Zecevic, M., Boerner, S. A., Tarcsafalvi, A., Diaz, H. B., Marshall, M. S., Weber, M. J., Parsons, J. T. and Catling, A. D. (2003). PAK1 phosphorylation of MEK1 regulates fibronectin-stimulated MAPK activation. *J. Cell Biol.* **162**, 281–291.

Smith, M. L., Gourdon, D., Little, W. C., Kubow, K. E., Eguiluz, R. A., Luna-Morris, S. and Vogel, V. (2007). Force-induced unfolding of fibronectin in the extracellular matrix of living cells. *PLoS Biol.* **5**, e268.

Snow, C. J., Peterson, M. T., Khalil, A. and Henry, C. A. (2008). Muscle development is disrupted in zebrafish embryos deficient for fibronectin. *Dev. Dyn. Off. Publ. Am. Assoc. Anat.* **237**, 2542–2553.

Soldi, R., Mitola, S., Strasly, M., Defilippi, P., Tarone, G. and Bussolino, F. (1999). Role of alphavbeta3 integrin in the activation of vascular endothelial growth factor receptor-2. *EMBO J.* **18**, 882–892.

Solloway, M. J. and Harvey, R. P. (2003). Molecular pathways in myocardial development: a stem cell perspective. *Cardiovasc. Res.* **58**, 264–277.

Sottile, J. and Hocking, D. C. (2002). Fibronectin polymerization regulates the composition and stability of extracellular matrix fibrils and cell-matrix adhesions. *Mol. Biol. Cell* **13**, 3546–3559.

Sridurongrit, S., Larsson, J., Schwartz, R., Ruiz-Lozano, P. and Kaartinen, V. (2008). Signaling via the Tgf-beta type I receptor Alk5 in heart development. *Dev. Biol.* **322**, 208–218.

Stenvers, K. L., Tursky, M. L., Harder, K. W., Kountouri, N., Amatayakul-Chantler, S., Grail, D., Small, C., Weinberg, R. A., Sizeland, A. M. and Zhu, H.-J. (2003). Heart and liver defects and reduced transforming growth factor beta2 sensitivity in transforming growth factor beta type III receptor-deficient embryos. *Mol. Cell. Biol.* **23**, 4371–4385.

Stenzel, D., Lundkvist, A., Sauvaget, D., Busse, M., Graupera, M., van der Flier, A., Wijelath, E. S., Murray, J., Sobel, M., Costell, M., et al. (2011). Integrin-dependent and -independent functions of astrocytic fibronectin in retinal angiogenesis. *Dev. Camb. Engl.* **138**, 4451–4463.

Stephens, L. E., Sutherland, A. E., Klimanskaya, I. V., Andrieux, A., Meneses, J., Pedersen, R. A. and Damsky, C. H. (1995). Deletion of beta 1 integrins in mice results in inner cell mass failure and peri-implantation lethality. *Genes Dev.* **9**, 1883–1895.

Stone, J., Itin, A., Alon, T., Pe'er, J., Gnessin, H., Chan-Ling, T. and Keshet, E. (1995). Development of retinal vasculature is mediated by hypoxia-induced vascular endothelial growth factor (VEGF) expression by neuroglia. *J. Neurosci. Off. J. Soc. Neurosci.* **15**, 4738–4747.

Stratman, A. N., Malotte, K. M., Mahan, R. D., Davis, M. J. and Davis, G. E. (2009). Pericyte recruitment during vasculogenic tube assembly stimulates endothelial basement membrane matrix formation. *Blood* **114**, 5091–5101.

Stricker, J., Beckham, Y., Davidson, M. W. and Gardel, M. L. (2013). Myosin II-mediated focal adhesion maturation is tension insensitive. *PloS One* **8**, e70652.

Strilić, B., Kucera, T., Eglinger, J., Hughes, M. R., McNagny, K. M., Tsukita, S., Dejana, E., Ferrara, N. and Lammert, E. (2009). The molecular basis of vascular lumen formation in the developing mouse aorta. *Dev. Cell* **17**, 505–515.

Strilić, B., Eglinger, J., Krieg, M., Zeeb, M., Axnick, J., Babál, P., Müller, D. J. and Lammert, E. (2010). Electrostatic cell-surface repulsion initiates lumen formation in developing blood vessels. *Curr. Biol. CB* **20**, 2003–2009.

Strömblad, S., Becker, J. C., Yebra, M., Brooks, P. C. and Cheresh, D. A. (1996). Suppression of p53 activity and p21WAF1/CIP1 expression by vascular cell integrin alphaVbeta3 during angiogenesis. *J. Clin. Invest.* **98**, 426–433.

Suchting, S., Freitas, C., le Noble, F., Benedito, R., Bréant, C., Duarte, A. and Eichmann, A. (2007). The Notch ligand Delta-like 4 negatively regulates endothelial tip cell formation and vessel branching. *Proc. Natl. Acad. Sci. U. S. A.* **104**, 3225–3230.

Sundberg, C. and Rubin, K. (1996). Stimulation of beta1 integrins on fibroblasts induces PDGF independent tyrosine phosphorylation of PDGF beta-receptors. *J. Cell Biol.* **132**, 741–752.

Suzuki, A. and Ohno, S. (2006). The PAR-aPKC system: lessons in polarity. *J. Cell Sci.* **119**, 979–987.

Taber, L. A., Voronov, D. A. and Ramasubramanian, A. (2010). The role of mechanical forces in the torsional component of cardiac looping. *Ann. N. Y. Acad. Sci.* **1188**, 103–110.

Taipale, J. and Keski-Oja, J. (1997). Growth factors in the extracellular matrix. *FASEB J. Off. Publ. Fed. Am. Soc. Exp. Biol.* **11**, 51–59.

Taipale, J., Keski-Oja, J., Miyazono, K. and Heldin, C. H. (1994). Latent transforming growth factor-beta 1 associates to fibroblast extracellular matrix via latent TGF-beta binding protein. *J. Cell Biol.* **124**, 171–181.

Taipale, J., Saharinen, J., Hedman, K. and Keski-Oja, J. (1996). Latent transforming growth factor-beta 1 and its binding protein are components of extracellular matrix microfibrils. *J. Histochem. Cytochem. Off. J. Histochem. Soc.* **44**, 875–889.

Taipale, J., Saharinen, J. and Keski-Oja, J. (1998). Extracellular matrix-associated transforming growth factor-beta: role in cancer cell growth and invasion. *Adv. Cancer Res.* **75**, 87–134.

Takagi, J., Strokovich, K., Springer, T. A. and Walz, T. (2003). Structure of integrin alpha5beta1 in complex with fibronectin. *EMBO J.* **22**, 4607–4615.

Takahashi, S., Leiss, M., Moser, M., Ohashi, T., Kitao, T., Heckmann, D., Pfeifer, A., Kessler, H., Takagi, J., Erickson, H. P., et al. (2007). The RGD motif in fibronectin is essential for development but dispensable for fibril assembly. *J. Cell Biol.* **178**, 167–178.

Tam, P. P., Parameswaran, M., Kinder, S. J. and Weinberger, R. P. (1997). The allocation of epiblast cells to the embryonic heart and other mesodermal lineages: the role of ingression and tissue movement during gastrulation. *Dev. Camb. Engl.* **124**, 1631–1642.

Tan, M. H., Sun, Z., Opitz, S. L., Schmidt, T. E., Peters, J. H. and George, E. L. (2004). Deletion of the alternatively spliced fibronectin EIIIA domain in mice reduces atherosclerosis. *Blood* **104**, 11–18.

Tanaka, M., Chen, Z., Bartunkova, S., Yamasaki, N. and Izumo, S. (1999). The cardiac homeobox gene Csx/Nkx2.5 lies genetically upstream of multiple genes essential for heart development. *Dev. Camb. Engl.* **126**, 1269–1280.

Tanjore, H., Zeisberg, E. M., Gerami-Naini, B. and Kalluri, R. (2008). Beta1 integrin expression on endothelial cells is required for angiogenesis but not for vasculogenesis. *Dev. Dyn. Off. Publ. Am. Assoc. Anat.* **237**, 75–82.

Tarui, T., Miles, L. A. and Takada, Y. (2001). Specific interaction of angiostatin with integrin alpha(v)beta(3) in endothelial cells. *J. Biol. Chem.* **276**, 39562–39568.

Ten Dijke, P. and Arthur, H. M. (2007). Extracellular control of TGF[beta] signalling in vascular development and disease. *Nat Rev Mol Cell Biol* **8**, 857–869.

Thibault, G., Lacombe, M. J., Schnapp, L. M., Lacasse, A., Bouzeghrane, F. and Lapalme, G. (2001). Upregulation of alpha(8)beta(1)-integrin in cardiac fibroblast by angiotensin II and transforming growth factor-beta1. *Am. J. Physiol. Cell Physiol.* **281**, C1457–1467.

Thomas, J. W., Ellis, B., Boerner, R. J., Knight, W. B., White, G. C., 2nd and Schaller, M. D. (1998). SH2- and SH3-mediated interactions between focal adhesion kinase and Src. *J. Biol. Chem.* **273**, 577–583.

Tilghman, R. W. and Parsons, J. T. (2008). Focal adhesion kinase as a regulator of cell tension in the progression of cancer. *Semin. Cancer Biol.* **18**, 45–52.

Tomasini-Johansson, B. R., Kaufman, N. R., Ensenberger, M. G., Ozeri, V., Hanski, E. and Mosher, D. F. (2001). A 49-residue peptide from adhesin F1 of Streptococcus pyogenes inhibits fibronectin matrix assembly. *J. Biol. Chem.* **276**, 23430–23439.

Topper, J. N. and Gimbrone, M. A., Jr (1999). Blood flow and vascular gene expression: fluid shear stress as a modulator of endothelial phenotype. *Mol. Med. Today* **5**, 40–46.

Totsukawa, G., Yamakita, Y., Yamashiro, S., Hartshorne, D. J., Sasaki, Y. and Matsumura, F. (2000). Distinct roles of ROCK (Rho-kinase) and MLCK in spatial regulation of MLC phosphorylation for assembly of stress fibers and focal adhesions in 3T3 fibroblasts. *J. Cell Biol.* **150**, 797–806.

Treisman, R. (1996). Regulation of transcription by MAP kinase cascades. *Curr. Opin. Cell Biol.* **8**, 205–215.

Trinh, L. A. and Stainier, D. Y. R. (2004a). Cardiac development. *Methods Cell Biol.* **76**, 455–473.

Trinh, L. A. and Stainier, D. Y. . (2004b). Fibronectin Regulates Epithelial Organization during Myocardial Migration in Zebrafish. *Dev. Cell* **6**, 371–382.

Tronik-Le Roux, D., Roullot, V., Poujol, C., Kortulewski, T., Nurden, P. and Marguerie, G. (2000). Thrombasthenic mice generated by replacement of the integrin alpha(IIb) gene: demonstration that transcriptional activation of this megakaryocytic locus precedes lineage commitment. *Blood* **96**, 1399–1408.

Tsyguelnaia, I. and Doolittle, R. F. (1998). Presence of a fibronectin type III domain in a plant protein. *J. Mol. Evol.* **46**, 612–614.

Tu, Y., Wu, S., Shi, X., Chen, K. and Wu, C. (2003). Migfilin and Mig-2 link focal adhesions to filamin and the actin cytoskeleton and function in cell shape modulation. *Cell* **113**, 37–47.

Turlo, K. A., Noel, O. D. V., Vora, R., LaRussa, M., Fassler, R., Hall-Glenn, F. and Iruela-Arispe, M. L. (2012). An essential requirement for β1 integrin in the assembly of extracellular matrix proteins within the vascular wall. *Dev. Biol.* **365**, 23–35.

Uemura, A., Kusuhara, S., Wiegand, S. J., Yu, R. T. and Nishikawa, S. (2006). Tlx acts as a proangiogenic switch by regulating extracellular assembly of fibronectin matrices in retinal astrocytes. *J. Clin. Invest.* **116**, 369–377.

Unsöld, C., Hyytiäinen, M., Bruckner-Tuderman, L. and Keski-Oja, J. (2001). Latent TGF-beta binding protein LTBP-1 contains three potential extracellular matrix interacting domains. *J. Cell Sci.* **114**, 187–197.

Ussar, S., Moser, M., Widmaier, M., Rognoni, E., Harrer, C., Genzel-Boroviczeny, O. and Fässler, R. (2008). Loss of Kindlin-1 causes skin atrophy and lethal neonatal intestinal epithelial dysfunction. *PLoS Genet.* **4**, e1000289.

Van der Flier, A., Badu-Nkansah, K., Whittaker, C. A., Crowley, D., Bronson, R. T., Lacy-Hulbert, A. and Hynes, R. O. (2010). Endothelial alpha5 and alphav integrins cooperate in remodeling of the vasculature during development. *Dev. Camb. Engl.* **137**, 2439–2449.

Van der Neut, R., Krimpenfort, P., Calafat, J., Niessen, C. M. and Sonnenberg, A. (1996). Epithelial detachment due to absence of hemidesmosomes in integrin beta 4 null mice. *Nat. Genet.* **13**, 366–369.

Van Vliet, A., Baelde, H. J., Vleming, L. J., de Heer, E. and Bruijn, J. A. (2001). Distribution of fibronectin isoforms in human renal disease. *J. Pathol.* **193**, 256–262.

Vanhaesebroeck, B. and Alessi, D. R. (2000). The PI3K-PDK1 connection: more than just a road to PKB. *Biochem. J.* **346 Pt 3**, 561–576.

Vehviläinen, P., Hyytiäinen, M. and Keski-Oja, J. (2009). Matrix association of latent TGF-beta binding protein-2 (LTBP-2) is dependent on fibrillin-1. *J. Cell. Physiol.* **221**, 586–593.

Velling, T., Risteli, J., Wennerberg, K., Mosher, D. F. and Johansson, S. (2002). Polymerization of Type I and III Collagens Is Dependent On Fibronectin and Enhanced By Integrins α11β1and α2β1. *J. Biol. Chem.* **277**, 37377–37381.

Venters, S. J., Thorsteinsdóttir, S. and Duxson, M. J. (1999). Early development of the myotome in the mouse. *Dev. Dyn. Off. Publ. Am. Assoc. Anat.* **216**, 219–232.

Villa, A., Trachsel, E., Kaspar, M., Schliemann, C., Sommavilla, R., Rybak, J.-N., Rösli, C., Borsi, L. and Neri, D. (2008). A high-affinity human monoclonal antibody specific to the alternatively spliced EDA domain of fibronectin efficiently targets tumor neo-vasculature in vivo. *Int. J. Cancer J. Int. Cancer* **122**, 2405–2413.

Vinogradova, O., Haas, T., Plow, E. F. and Qin, J. (2000). A structural basis for integrin activation by the cytoplasmic tail of the alpha IIb-subunit. *Proc. Natl. Acad. Sci. U. S. A.* **97**, 1450–1455.

Vinogradova, O., Velyvis, A., Velyviene, A., Hu, B., Haas, T., Plow, E. and Qin, J. (2002). A structural mechanism of integrin alpha(IIb)beta(3) "inside-out" activation as regulated by its cytoplasmic face. *Cell* **110**, 587–597.

Vlahakis, N. E., Young, B. A., Atakilit, A. and Sheppard, D. (2005). The lymphangiogenic vascular endothelial growth factors VEGF-C and -D are ligands for the integrin alpha9beta1. *J. Biol. Chem.* **280**, 4544–4552.

Vrancken Peeters, M. P., Gittenberger-de Groot, A. C., Mentink, M. M. and Poelmann, R. E. (1999). Smooth muscle cells and fibroblasts of the coronary arteries derive from epithelial-mesenchymal transformation of the epicardium. *Anat. Embryol. (Berl.)* **199**, 367–378.

Wacker, A. and Gerhardt, H. (2011). Endothelial development taking shape. *Curr. Opin. Cell Biol.* **23**, 676–685.

Wagner, N., Löhler, J., Kunkel, E. J., Ley, K., Leung, E., Krissansen, G., Rajewsky, K. and Müller, W. (1996). Critical role for beta7 integrins in formation of the gut-associated lymphoid tissue. *Nature* **382**, 366–370.

Walker, J. L., Fournier, A. K. and Assoian, R. K. (2005). Regulation of growth factor signaling and cell cycle progression by cell adhesion and adhesion-dependent changes in cellular tension. *Cytokine Growth Factor Rev.* **16**, 395–405.

Wang, H. B., Dembo, M., Hanks, S. K. and Wang, Y. (2001a). Focal adhesion kinase is involved in mechanosensing during fibroblast migration. *Proc. Natl. Acad. Sci. U. S. A.* **98**, 11295–11300.

Wang, J. F., Zhang, X. F. and Groopman, J. E. (2001b). Stimulation of beta 1 integrin induces tyrosine phosphorylation of vascular endothelial growth factor receptor-3 and modulates cell migration. *J. Biol. Chem.* **276**, 41950–41957.

Wang, Y., Kaiser, M. S., Larson, J. D., Nasevicius, A., Clark, K. J., Wadman, S. A., Roberg-Perez, S. E., Ekker, S. C., Hackett, P. B., McGrail, M., et al. (2010). Moesin1 and Ve-cadherin are required in endothelial cells during in vivo tubulogenesis. *Dev. Camb. Engl.* **137**, 3119–3128.

Watanabe, N., Kato, T., Fujita, A., Ishizaki, T. and Narumiya, S. (1999). Cooperation between mDia1 and ROCK in Rho-induced actin reorganization. *Nat. Cell Biol.* **1**, 136–143.

Wayner, E. A., Garcia-Pardo, A., Humphries, M. J., McDonald, J. A. and Carter, W. G. (1989). Identification and characterization of the T lymphocyte adhesion receptor for an alternative cell attachment domain (CS-1) in plasma fibronectin. *J. Cell Biol.* **109**, 1321–1330.

Webb, S., Brown, N. A. and Anderson, R. H. (1998). Formation of the atrioventricular septal structures in the normal mouse. *Circ. Res.* **82**, 645–656.

Webb, D. J., Donais, K., Whitmore, L. A., Thomas, S. M., Turner, C. E., Parsons, J. T. and Horwitz, A. F. (2004). FAK-Src signalling through paxillin, ERK and MLCK regulates adhesion disassembly. *Nat. Cell Biol.* **6**, 154–161.

Weinacker, A., Chen, A., Agrez, M., Cone, R. I., Nishimura, S., Wayner, E., Pytela, R. and Sheppard, D. (1994). Role of the integrin alpha v beta 6 in cell attachment to fibronectin. Heterologous expression of intact and secreted forms of the receptor. *J. Biol. Chem.* **269**, 6940–6948.

Wennerberg, K., Lohikangas, L., Gullberg, D., Pfaff, M., Johansson, S. and Fässler, R. (1996). Beta 1 integrin-dependent and -independent polymerization of fibronectin. *J. Cell Biol.* **132**, 227–238.

Wickström, S. A., Lange, A., Montanez, E. and Fässler, R. (2010). The ILK/PINCH/parvin complex: the kinase is dead, long live the pseudokinase! *EMBO J.* **29**, 281–291.

Wierzbicka-Patynowski, I. and Schwarzbauer, J. E. (2002). Regulatory role for SRC and phosphatidylinositol 3-kinase in initiation of fibronectin matrix assembly. *J. Biol. Chem.* **277**, 19703–19708.

Wierzbicka-Patynowski, I., Mao, Y. and Schwarzbauer, J. E. (2007). Continuous requirement for pp60-Src and phospho-paxillin during fibronectin matrix assembly by transformed cells. *J. Cell. Physiol.* **210**, 750–756.

Wijelath, E. S., Murray, J., Rahman, S., Patel, Y., Ishida, A., Strand, K., Aziz, S., Cardona, C., Hammond, W. P., Savidge, G. F., et al. (2002). Novel vascular endothelial growth factor binding domains of fibronectin enhance vascular endothelial growth factor biological activity. *Circ. Res.* **91**, 25–31.

Wijelath, E. S., Rahman, S., Namekata, M., Murray, J., Nishimura, T., Mostafavi-Pour, Z., Patel, Y., Suda, Y., Humphries, M. J. and Sobel, M. (2006). Heparin-II domain of fibronectin is a vascular endothelial growth factor-binding domain: enhancement of VEGF biological activity by a singular growth factor/matrix protein synergism. *Circ. Res.* **99**, 853–860.

Winklbauer, R. and Keller, R. E. (1996). Fibronectin, mesoderm migration, and gastrulation in Xenopus. *Dev. Biol.* **177**, 413–426.

Wipff, P.-J. and Hinz, B. (2008). Integrins and the activation of latent transforming growth factor beta1 - an intimate relationship. *Eur. J. Cell Biol.* **87**, 601–615.

Wipff, P.-J., Rifkin, D. B., Meister, J.-J. and Hinz, B. (2007). Myofibroblast contraction activates latent TGF-beta1 from the extracellular matrix. *J. Cell Biol.* **179**, 1311–1323.

Woods, A. and Couchman, J. R. (1998). Syndecans: synergistic activators of cell adhesion. *Trends Cell Biol.* **8**, 189–192.

Woods, A. and Couchman, J. R. (2001). Syndecan-4 and focal adhesion function. *Curr. Opin. Cell Biol.* **13**, 578–583.

Wozniak, M. A., Desai, R., Solski, P. A., Der, C. J. and Keely, P. J. (2003). ROCK-generated contractility regulates breast epithelial cell differentiation in response to the physical properties of a three-dimensional collagen matrix. *J. Cell Biol.* **163**, 583–595.

Wu, C., Keivens, V. M., O'Toole, T. E., McDonald, J. A. and Ginsberg, M. H. (1995). Integrin activation and cytoskeletal interaction are essential for the assembly of a fibronectin matrix. *Cell* **83**, 715–724.

Wu, C., Hughes, P. E., Ginsberg, M. H. and McDonald, J. A. (1996). Identification of a new biological function for the integrin alpha v beta 3: initiation of fibronectin matrix assembly. *Cell Adhes. Commun.* **4**, 149–158.

Wu, H., Rodgers, J. R., Perrard, X.-Y. D., Perrard, J. L., Prince, J. E., Abe, Y., Davis, B. K., Dietsch, G., Smith, C. W. and Ballantyne, C. M. (2004). Deficiency of CD11b or CD11d results in reduced staphylococcal enterotoxin-induced T cell response and T cell phenotypic changes. *J. Immunol. Baltim. Md 1950* **173**, 297–306.

Wu, H., Gower, R. M., Wang, H., Perrard, X.-Y. D., Ma, R., Bullard, D. C., Burns, A. R., Paul, A., Smith, C. W., Simon, S. I., et al. (2009). Functional Role of CD11c+ Monocytes in Atherogenesis Associated With Hypercholesterolemia. *Circulation* **119**, 2708–2717.

Wurdak, H., Ittner, L. M., Lang, K. S., Leveen, P., Suter, U., Fischer, J. A., Karlsson, S., Born, W. and Sommer, L. (2005). Inactivation of TGFbeta signaling in neural crest stem cells leads to multiple defects reminiscent of DiGeorge syndrome. *Genes Dev.* **19**, 530–535.

Xiao, T., Takagi, J., Coller, B. S., Wang, J.-H. and Springer, T. A. (2004). Structural basis for allostery in integrins and binding to fibrinogen-mimetic therapeutics. *Nature* **432**, 59–67.

Xiong, J. P., Stehle, T., Diefenbach, B., Zhang, R., Dunker, R., Scott, D. L., Joachimiak, A., Goodman, S. L. and Arnaout, M. A. (2001). Crystal structure of the extracellular segment of integrin alpha Vbeta3. *Science* **294**, 339–345.

Xu, K., Sacharidou, A., Fu, S., Chong, D. C., Skaug, B., Chen, Z. J., Davis, G. E. and Cleaver, O. (2011). Blood vessel tubulogenesis requires Rasip1 regulation of GTPase signaling. *Dev. Cell* **20**, 526–539.

Yamada, K. M., Pankov, R. and Cukierman, E. (2003). Dimensions and dynamics in integrin function. *Braz. J. Med. Biol. Res. Rev. Bras. Pesqui. Médicas E Biológicas Soc. Bras. Biofísica Al* **36**, 959–966.

Yang, J. T. and Hynes, R. O. (1996). Fibronectin receptor functions in embryonic cells deficient in alpha 5 beta 1 integrin can be replaced by alpha V integrins. *Mol. Biol. Cell* **7**, 1737–1748.

Yang, J. T., Rayburn, H. and Hynes, R. O. (1993). Embryonic mesodermal defects in alpha 5 integrin-deficient mice. *Dev. Camb. Engl.* **119**, 1093–1105.

Yang, J. T., Rayburn, H. and Hynes, R. O. (1995). Cell adhesion events mediated by alpha 4 integrins are essential in placental and cardiac development. *Dev. Camb. Engl.* **121**, 549–560.

Yang, J. T., Bader, B. L., Kreidberg, J. A., Ullman-Culleré, M., Trevithick, J. E. and Hynes, R. O. (1999). Overlapping and independent functions of fibronectin receptor integrins in early mesodermal development. *Dev. Biol.* **215**, 264–277.

Yang, Z., Mu, Z., Dabovic, B., Jurukovski, V., Yu, D., Sung, J., Xiong, X. and Munger, J. S. (2007). Absence of integrin-mediated TGFbeta1 activation in vivo recapitulates the phenotype of TGFbeta1-null mice. *J. Cell Biol.* **176**, 787–793.

Yeh, Y.-T., Hur, S. S., Chang, J., Wang, K.-C., Chiu, J.-J., Li, Y.-S. and Chien, S. (2012). Matrix stiffness regulates endothelial cell proliferation through septin 9. *PloS One* **7**, e46889.

Yeung, T., Georges, P. C., Flanagan, L. A., Marg, B., Ortiz, M., Funaki, M., Zahir, N., Ming, W., Weaver, V. and Janmey, P. A. (2005). Effects of substrate stiffness on cell morphology, cytoskeletal structure, and adhesion. *Cell Motil. Cytoskeleton* **60**, 24–34.

Yoneda, A., Multhaupt, H. A. B. and Couchman, J. R. (2005). The Rho kinases I and II regulate different aspects of myosin II activity. *J. Cell Biol.* **170**, 443–453.

Yoneda, A., Ushakov, D., Multhaupt, H. A. B. and Couchman, J. R. (2007). Fibronectin matrix assembly requires distinct contributions from Rho kinases I and -II. *Mol. Biol. Cell* **18**, 66–75.

Yoshinaga, K., Obata, H., Jurukovski, V., Mazzieri, R., Chen, Y., Zilberberg, L., Huso, D., Melamed, J., Prijatelj, P., Todorovic, V., et al. (2008). Perturbation of transforming growth factor (TGF)-beta1 association with latent TGF-beta binding protein yields inflammation and tumors. *Proc. Natl. Acad. Sci. U. S. A.* **105**, 18758–18763.

Yu, Q. and Stamenkovic, I. (2000). Cell surface-localized matrix metalloproteinase-9 proteolytically activates TGF-beta and promotes tumor invasion and angiogenesis. *Genes Dev.* **14**, 163–176.

Zaidel-Bar, R., Ballestrem, C., Kam, Z. and Geiger, B. (2003). Early molecular events in the assembly of matrix adhesions at the leading edge of migrating cells. *J. Cell Sci.* **116**, 4605–4613.

Zaidel-Bar, R., Cohen, M., Addadi, L. and Geiger, B. (2004). Hierarchical assembly of cell-matrix adhesion complexes. *Biochem. Soc. Trans.* **32**, 416–420.

Zaidel-Bar, R., Itzkovitz, S., Ma'ayan, A., Iyengar, R. and Geiger, B. (2007). Functional atlas of the integrin adhesome. *Nat. Cell Biol.* **9**, 858–867.

Zamir, E., Katz, M., Posen, Y., Erez, N., Yamada, K. M., Katz, B. Z., Lin, S., Lin, D. C., Bershadsky, A., Kam, Z., et al. (2000). Dynamics and segregation of cell-matrix adhesions in cultured fibroblasts. *Nat. Cell Biol.* **2**, 191–196.

Zamir, E. A., Srinivasan, V., Perucchio, R. and Taber, L. A. (2003). Mechanical asymmetry in the embryonic chick heart during looping. *Ann. Biomed. Eng.* **31**, 1327–1336.

Zeeb, M., Strilic, B. and Lammert, E. (2010). Resolving cell-cell junctions: lumen formation in blood vessels. *Curr. Opin. Cell Biol.* **22**, 626–632.

Zhai, J., Lin, H., Nie, Z., Wu, J., Cañete-Soler, R., Schlaepfer, W. W. and Schlaepfer, D. D. (2003). Direct interaction of focal adhesion kinase with p190RhoGEF. *J. Biol. Chem.* **278**, 24865–24873.

Zhang, Z., Morla, A. O., Vuori, K., Bauer, J. S., Juliano, R. L. and Ruoslahti, E. (1993). The alpha v beta 1 integrin functions as a fibronectin receptor but does not support fibronectin matrix assembly and cell migration on fibronectin. *J. Cell Biol.* **122**, 235–242.

Zhao, Q., Liu, X. and Collodi, P. (2001). Identification and characterization of a novel fibronectin in zebrafish. *Exp. Cell Res.* **268**, 211–219.

Zhou, X., Rowe, R. G., Hiraoka, N., George, J. P., Wirtz, D., Mosher, D. F., Virtanen, I., Chernousov, M. A. and Weiss, S. J. (2008). Fibronectin fibrillogenesis regulates three-dimensional neovessel formation. *Genes Dev.* **22**, 1231–1243.

Zhu, J., Motejlek, K., Wang, D., Zang, K., Schmidt, A. and Reichardt, L. F. (2002). beta8 integrins are required for vascular morphogenesis in mouse embryos. *Dev. Camb. Engl.* **129**, 2891–2903.

Zhu, J., Boylan, B., Luo, B.-H., Newman, P. J. and Springer, T. A. (2007). Tests of the extension and deadbolt models of integrin activation. *J. Biol. Chem.* **282**, 11914–11920.

Zilberberg, L., Todorovic, V., Dabovic, B., Horiguchi, M., Couroussé, T., Sakai, L. Y. and Rifkin, D. B. (2012). Specificity of latent TGF-ß binding protein (LTBP) incorporation into matrix: role of fibrillins and fibronectin. *J. Cell. Physiol.*

Zou, L., Cao, S., Kang, N., Huebert, R. C. and Shah, V. H. (2012). Fibronectin Induces Endothelial Cell Migration through 1 Integrin and Src-dependent Phosphorylation of Fibroblast Growth Factor Receptor-1 at Tyrosines 653/654 and 766. *J. Biol. Chem.* **287**, 7190–7202.

Zovein, A. C., Luque, A., Turlo, K. A., Hofmann, J. J., Yee, K. M., Becker, M. S., Fassler, R., Mellman, I., Lane, T. F. and Iruela-Arispe, M. L. (2010). Beta1 integrin establishes endothelial cell polarity and arteriolar lumen formation via a Par3-dependent mechanism. *Dev. Cell* **18**, 39–51.

11 ACKNOWLEDGEMENTS

I am deeply grateful to the following people:

Prof. Dr. Reinhard Fässler, for supervising and mentoring me through the world of integrins and extracellular matrix.

My Thesis Advisory Committee members, **Prof. Dr. Hellmut Augustin** and **Prof. Dr. Cord Brakebusch**, for attending annual meetings with me and providing their constructive critisism of my work within the TAC framework.

Prof. Dr. Angelika Vollmar, for her willingness to stand as my second Gutachter and **Prof. Dr. Stefan Zahler**, **Prof. Dr. Martin Biel**, **Prof. Dr. Christian Wahl-Schott** and **Prof. Dr. Karl-Peter Hopfner** for making the time and effort to join my examination board.

Dr. Michael Leiss, for his support in transitioning me into this project and providing data.

Dr. Eloi Montañez Miralles, for guiding me through my first steps in embryo stainings.

Prof. Dr. An Zwijsen and Michael Staring, for hosting me at the VIB in Leuven, teaching me the art of embryo histology and sharing valuable protocols.

Dr. Julian Polleux and **Dr. Kyle Legate**, for support in preparing for and performing AFM.

Dr. Armin Lambacher, for his brilliant touch with computers and microscopes.

Mrs. Ines Lach-Kusevic, for her openness and her kindness in assistance with paperwork and translations.

Mr. Klaus Weber, for rapidly managing every chemical order and lending his help to keep the lab running, always with a smile.

Lab members of the Department of Molecular Medicine.

Animal house staff, **Jens, Florian and Bianca**, for taking care of my mouse colonies.

IMPRS, for the academic and social network, and the IMPRS head-coordinator, **Dr. Hans-Joerg Schäffer**, for his outstanding capacity to offer answers, guidance and solutions to any difficulty.

My auntie Jenny and uncle Anthony, as well as all my dear cousins, for believing in me the most.

Both of my grandmothers, none of which could live to see me graduate, but who have guided me in spirit and been my greatest source of strength, courage and inspiration.